Common Characteristics of Good and Poorly Performing PCC Pavements

PUBLICATION NO. FHWA-RD-97-131

JANUARY 1998

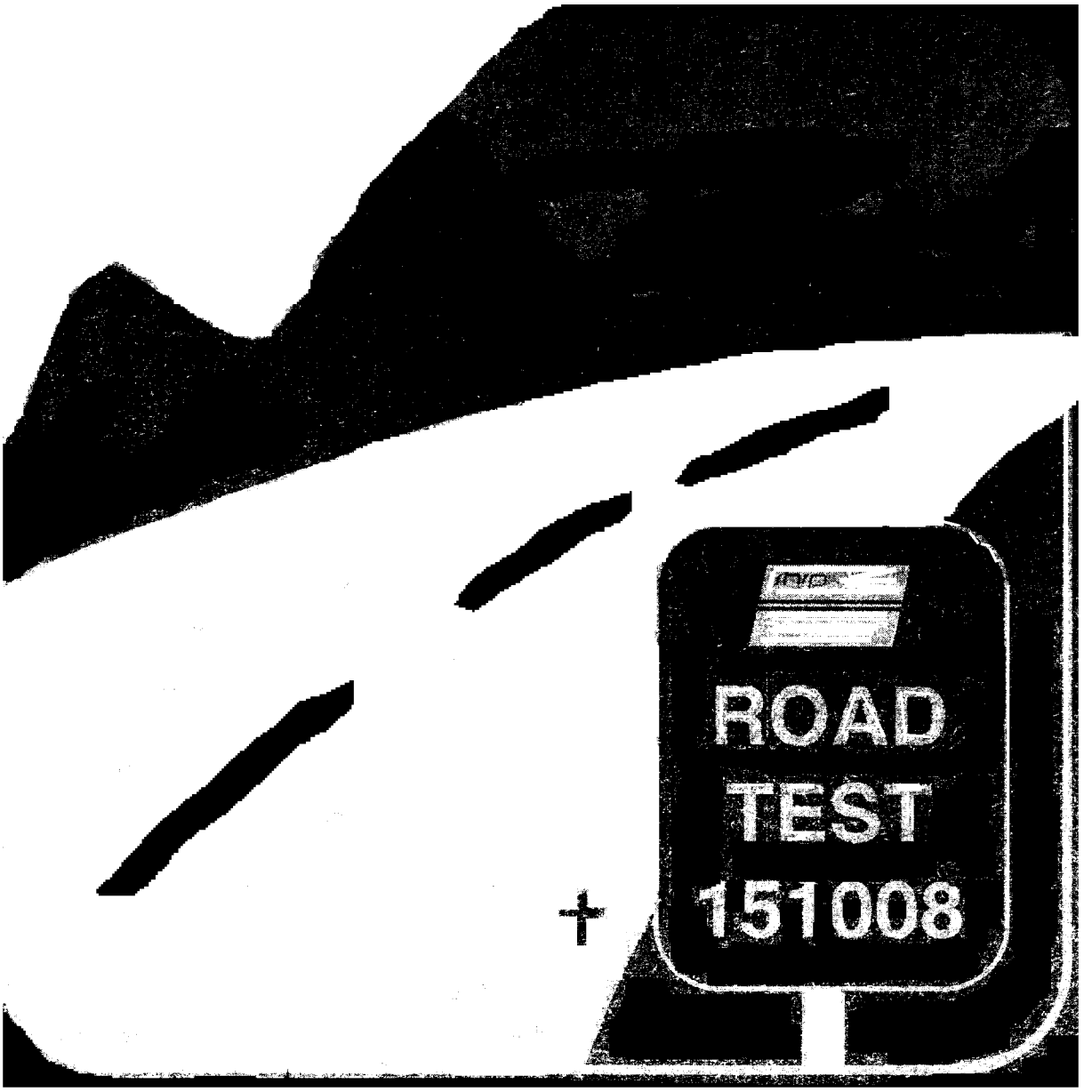

U.S. Department of Transportation
Federal Highway Administration

Research and Development
Turner-Fairbank Highway Research Center
6300 Georgetown Pike
McLean, VA 22101-2296

LTPP

FOREWORD

The request was simple: "Tell us what works." This report documents Long Term Pavement Performance (LTPP) analysis conducted to answer that question for Portland cement concrete (PCC) pavements. Both jointed (plain and reinforced) and continuously reinforced concrete (CRC) pavements are addressed. Performance measures considered included roughness, joint faulting, transverse cracking, and localized failures (CRC only).

This report will be of interest to anyone concerned with the design and construction of PCC pavements that work.

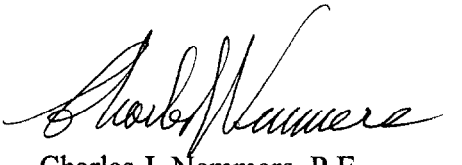

Charles J. Nemmers, P.E.
Director
Office of Engineering
Research and Development

NOTICE

Technical Report Documentation Page

1. Report No.	2. Government Accession No.	3. Recipient's Catalog No.
FHWA-RD-97-131		

4. Title and Subtitle	5. Report Date
COMMON CHARACTERISTICS OF GOOD AND POORLY PERFORMING PCC PAVEMENTS	January 1998
	6. Performing Organization Code

7. Author(s)	8. Performing Organization Report No.
L. Khazanovich, M. Darter, R. Bartlett, and T. McPeak	

9. Performing Organization Name and Address	10. Work Unit No. (TRAIS)
ERES Consultants, Inc. 505 West University Avenue Champaign, IL 61820-3915	C6B
	11. Contract or Grant No. DTFH61-96-C-00003

12. Sponsoring Agency Name and Address	13. Type of Report and Period Covered
Office of Engineering Research and Development Federal Highway Administration 6300 Georgetown Pike McLean, Virginia 22101-2296	Final Report Oct 1996 to Nov 1997
	14. Sponsoring Agency Code

15. Supplementary Notes

FHWA Contracting Officer's Technical Representative (COTR): Cheryl Allen Richter, P.E., HNR-30
Principal Investigator for the Contract: Shiraz D. Tayabji, Ph.D., P.E., ERES Consultants, Inc.

16. Abstract

This report documents the analysis and findings of a study to identify the site conditions and design/construction features of concrete pavements (JPCP, JRCP, CRCP) that lead to good performance and those that lead to poor performance. Data from Long-Term Pavement Performance (LTPP)test sections were used along with findings from previous and ongoing analyses of LTPP data. As there were no known criteria for identifying performance expectations over time as good, normal, or poor; a group of experts was convened to establish criteria. Separate criteria were developed for performance in roughness (IRI), joint faulting, transverse cracking, and localized failures (CRCP).

Many significant site conditions and design/construction features were identified that lead to good and poor performance. The site conditions (traffic, climate, and subgrade) cannot be controlled by the designer, however, steps can be taken to mitigate their effects. Several design and construction features can be controlled or specified by the highway agency and these should be given careful consideration. Knowledge about the design features identified as being critical to concrete pavement performance will contribute to improved guidelines for the design and construction of long-lived PCC pavements.

17. Key Words	18. Distribution Statement
Concrete pavement, performance, design, roughness, distress.	No restrictions. This document is available to the public through the National Technical Information Service, Springfield, VA 22161.

19. Security Classification (of this report)	20. Security Classification (of this page)	21. No. of Pages	22. Price
Unclassified	Unclassified	204	

Form DOT F 1700.7 (8-72) Reproduction of completed page authorized

SI* (MODERN METRIC) CONVERSION FACTORS

APPROXIMATE CONVERSIONS TO SI UNITS

Symbol	When You Know	Multiply By	To Find	Symbol
	LENGTH			
in	inches	25.4	millimeters	mm
ft	feet	0.305	meters	m
yd	yards	0.914	meters	m
mi	miles	1.61	kilometers	km
	AREA			
in^2	square inches	645.2	square millimeters	mm^2
ft^2	square feet	0.093	square meters	m^2
yd^2	square yards	0.836	square meters	m^2
ac	acres	0.405	hectares	ha
mi^2	square miles	2.59	square kilometers	km^2
	VOLUME			
fl oz	fluid ounces	29.57	milliliters	mL
gal	gallons	3.785	liters	L
ft^3	cubic feet	0.028	cubic meters	m^3
yd^3	cubic yards	0.765	cubic meters	m^3
NOTE: Volumes greater than 1000 l shall be shown in m^3.				
	MASS			
oz	ounces	28.35	grams	g
lb	pounds	0.454	kilograms	kg
T	short tons (2000 lb)	0.907	megagrams (or "metric ton")	Mg (or "t")
	TEMPERATURE (exact)			
°F	Fahrenheit temperature	5(F-32)/9 or (F-32)/1.8	Celcius temperature	°C
	ILLUMINATION			
fc	foot-candles	10.76	lux	lx
fl	foot-Lamberts	3.426	candela/m^2	cd/m^2
	FORCE and PRESSURE or STRESS			
lbf	poundforce	4.45	newtons	N
lbf/in^2	poundforce per square inch	6.89	kilopascals	kPa

APPROXIMATE CONVERSIONS FROM SI UNITS

Symbol	When You Know	Multiply By	To Find	Symbol
	LENGTH			
mm	millimeters	0.039	inches	in
m	meters	3.28	feet	ft
m	meters	1.09	yards	yd
km	kilometers	0.621	miles	mi
	AREA			
mm^2	square millimeters	0.0016	square inches	in^2
m^2	square meters	10.764	square feet	ft^2
m^2	square meters	1.195	square yards	yd^2
ha	hectares	2.47	acres	ac
km^2	square kilometers	0.386	square miles	mi^2
	VOLUME			
mL	milliliters	0.034	fluid ounces	fl oz
L	liters	0.264	gallons	gal
m^3	cubic meters	35.71	cubic feet	ft^3
m^3	cubic meters	1.307	cubic yards	yd^3
	MASS			
g	grams	0.035	ounces	oz
kg	kilograms	2.202	pounds	lb
Mg (or "t")	megagrams (or "metric ton")	1.103	short tons (2000 lb)	T
	TEMPERATURE (exact)			
°C	Celcius temperature	1.8C + 32	Fahrenheit temperature	°F
	ILLUMINATION			
lx	lux	0.0929	foot-candles	fc
cd/m^2	candela/m^2	0.2919	foot-Lamberts	fl
	FORCE and PRESSURE or STRESS			
N	newtons	0.225	poundforce	lbf
kPa	kilopascals	0.145	poundforce per square inch	lbf/in^2

* SI is the symbol for the International System of Units. Appropriate rounding should be made to comply with Section 4 of ASTM E380.

(Revised September 1993)

TABLE OF CONTENTS

TABLE OF CONTENTS (continued)

TABLE OF CONTENTS (continued)

LIST OF FIGURES

LIST OF FIGURES (continued)

LIST OF FIGURES (continued)

LIST OF TABLES

LIST OF TABLES (continued)

CHAPTER 1. INTRODUCTION

Research Objective

The objective of the research reported herein was to identify the design features of specific pavement types that lead to good performance and those that lead to poor performance, using data from the Long-Term Pavement Performance (LTPP) test sections. Research results from other analyses of LTPP data were also to be considered in these studies. Knowledge about the design features identified as being critical to pavement performance will contribute to improved guidelines for the design and construction of long-lived Portland Cement Concrete (PCC) pavements.

Research Approach

The LTPP Program includes over 269 PCC General Pavement Studies (GPS) sections for which data have been collected since 1989. Many of these sections are exhibiting very little distress. However, lack of distress is not necessarily an indicator of good performance, because lack of distress may possibly be due to young age, mild climate, an over-designed pavement section, or low traffic. As a simple example, transverse joint faulting of 2 mm might indicate poor performance for a jointed concrete pavement 2 years old, but 3 mm or more might be considered good for a jointed concrete pavement 20 years old. Therefore, it was necessary to establish appropriate criteria to identify if certain pavement sections are exhibiting exceptionally good performance. Similarly, it was necessary to establish criteria to identify if certain pavement sections are exhibiting poor performance.

Since these criteria did not exist, the approach adopted was to convene a panel of selected experts to decide what expectations should apply over a period of 20 years; that is, what should be considered good, normal, and poor performance for specific distress types associated with each pavement type. This approach and the resulting criteria are discussed in chapter 2.

Once the criteria were established, the sections were divided into data sets containing good, normal, and poor performers for each pavement type—jointed plain concrete pavement (JPCP), jointed reinforced concrete pavement (JRCP), and continuously reinforced concrete pavement (CRCP)—and key distress type. For some of the analyses, the normal performers were combined with either the poor or good sections because there were not an adequate number of sections in a particular performance group. As an example, for the t-test comparisons, there were good and normal/poor performing pavement data sets for each of three distress types for JPCP, two for JRCP

(faulting combined with JPCP), and two for CRCP. This amounted to seven data sets available for analysis.

The analyses conducted to identify the common characteristics of good and poor performing pavements are described in chapter 3, and the results are described in chapters 4 through 9 by distress type and pavement type.

In summary, the research effort consisted of the following tasks:

- Establish criteria.
- Identify test sections.
- Perform analysis.
- Document results in a technical report.

Specific site conditions and design/construction features leading to good and poor performance of each pavement type are discussed in chapter 10. A summary of the results and recommendations for continued study appear in chapter 11.

CHAPTER 2. PERFORMANCE CLASSIFICATION CRITERIA

The concrete pavement test sections in the LTPP GPS vary widely in age since construction and in traffic experienced. The classification of these test sections as good, normal, or poor performers required criteria for establishing boundaries with time as to expectations for different distress types and types of pavements. As mentioned in chapter 1, the approach for developing these criteria or boundaries was to convene a panel of experts and arrive at consensus decisions. This expert panel was convened December 16-17, 1996, and consisted of four experts from State highway agencies (Florida, Arizona, Kentucky, Illinois), four FHWA pavement experts, and one consultant that had retired from the Virginia DOT. The range of years of experience in pavement engineering of this group was 5 to 35, with a mean of 15 years.

Approach for Developing Performance Classification Criteria

A proposed procedure for establishing the criteria had been developed and was furnished to the group of experts for their consideration. This approach centered around a graphical approach involving plotting the boundaries between the three levels of performance (good, normal, poor) for each distress type versus age since construction. Although pavements are designed for some level of cumulative equivalent single axle loads (ESALs) at a given reliability over a given design period (or "age"), age since construction was selected as the primary scaling variable for the following reasons:

- It appeared too difficult to ask engineers to think in terms of both ESALs (at a given reliability level) and design life or age.

- The cumulative ESAL estimate in the current LTPP data base is approximate, but age is very accurate.

- Since pavements are designed for a certain number of load repetitions over a design period, it appears more straightforward and understandable to ask an engineer to rate performance only over a design period. The performance of a pavement then can be rated either good, normal, or poor over a time period of 20 years. Three rating groups were used based on the preference of the panel.

Blank graphs were provided on paper and transparencies for the use of the panel in their deliberations. Other plots were furnished for each distress type that included the actual LTPP data available. These plots provided some guidance as to the ranges of distress existing in the LTPP test sections.

After considerable discussion for an individual distress type and the functional shape of a graph of distress versus time, each individual drew in the two boundaries for the three types of concrete pavements. These boundaries were then plotted on a transparency, projected, and discussed in detail. The panel then reached a consensus on the specific boundaries for each of the three types of pavements for an individual distress. There appeared to be reasonable agreement, with no seriously divergent opinions.

Performance Classification Criteria

The consensus good and poor boundary conditions for the three PCC pavement types and key PCC distress types appear in figures 1 to 4. These plots, superimposed with actual LTPP data points, are presented and discussed in subsequent chapters. It should be noted that the data points represent individual observations rather than overall performance of individual test sections. Stated differently, time-sequence information is included such that a single test section can have several observations over a period of time. This appeared to the research team to be by far the most logical manner to include the time-sequence information.

It should be noted that the expectations of the panel for concrete pavements resulted in only one set of criteria and did not separate interstate pavements and non-interstate pavements as was done for Asphalt Concrete (AC) pavements, since there were not enough PCC pavement sections. In fact, for all t-test comparisons given in chapters 4 to 9, the sections are divided into two groups by combining either poor and normal or good and normal sections so that a sufficient number of sections exist in each group.

The primary input by the panel (their choice) was magnitudes of distress at 20 years; initial roughness levels were also considered. The shape of the curves was discussed, but the panel elected to leave the connection of the selected points to the experience of the research team.

The review of the spalling data indicated that very few sections exhibited more than 5 percent of joint length spalled. On the basis of this finding, the expert panel recommended that analysis of joint spalling data not be pursued as it was not considered significant.

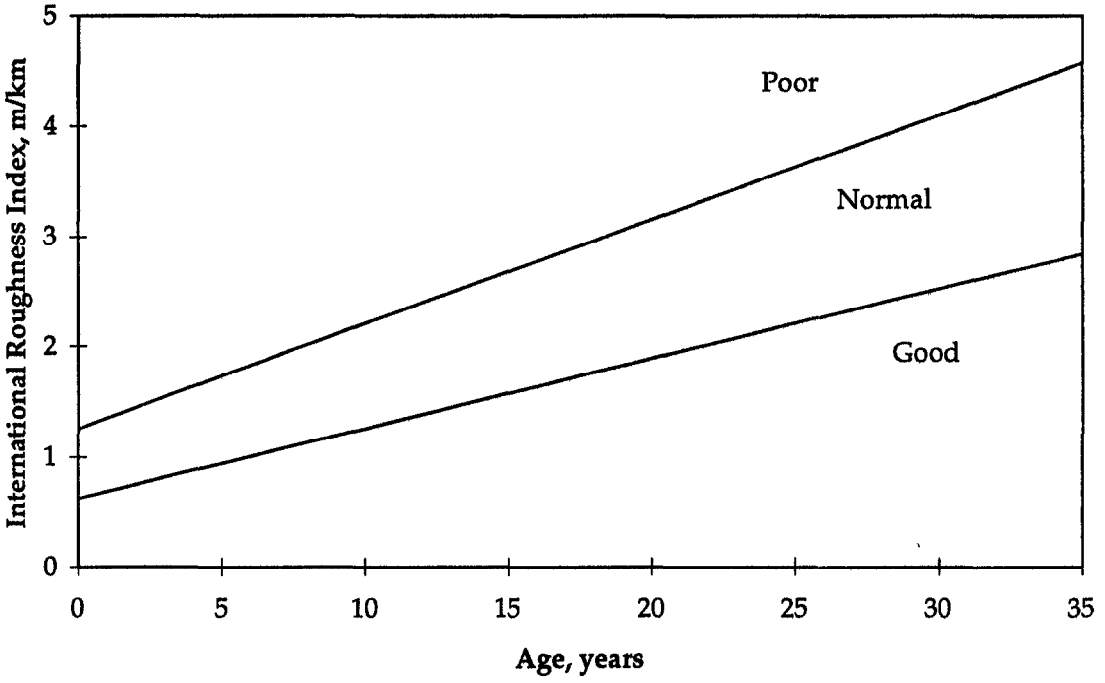

Figure 1. Performance criteria for IRI of PCC pavements.

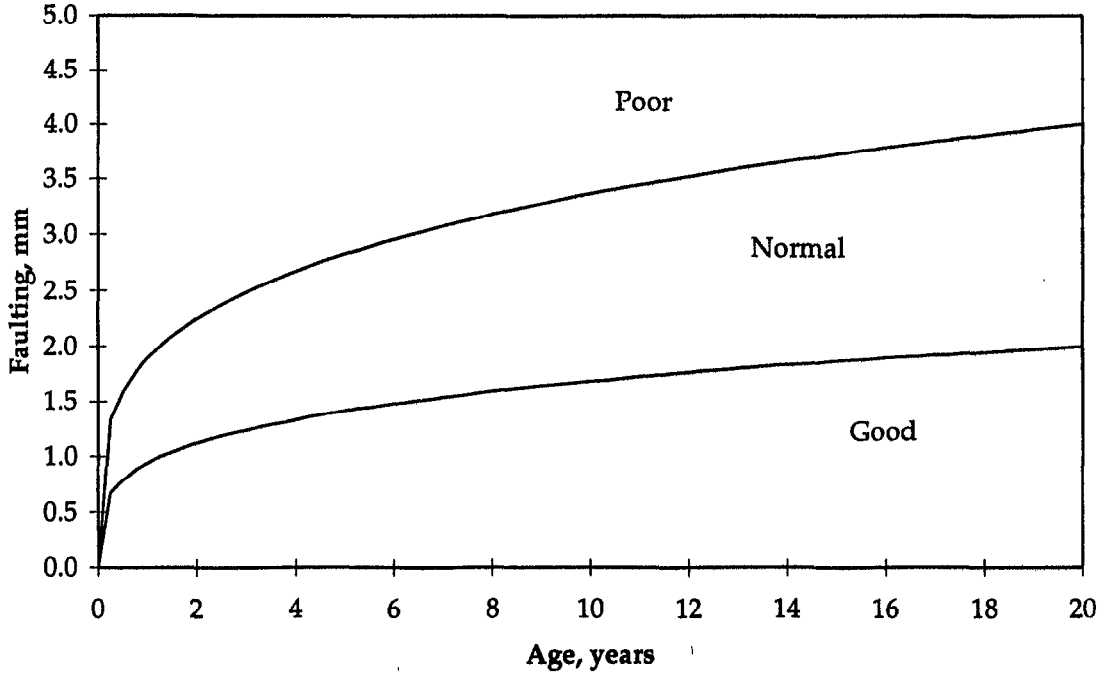

Figure 2. Performance criteria for faulting of jointed concrete pavements.

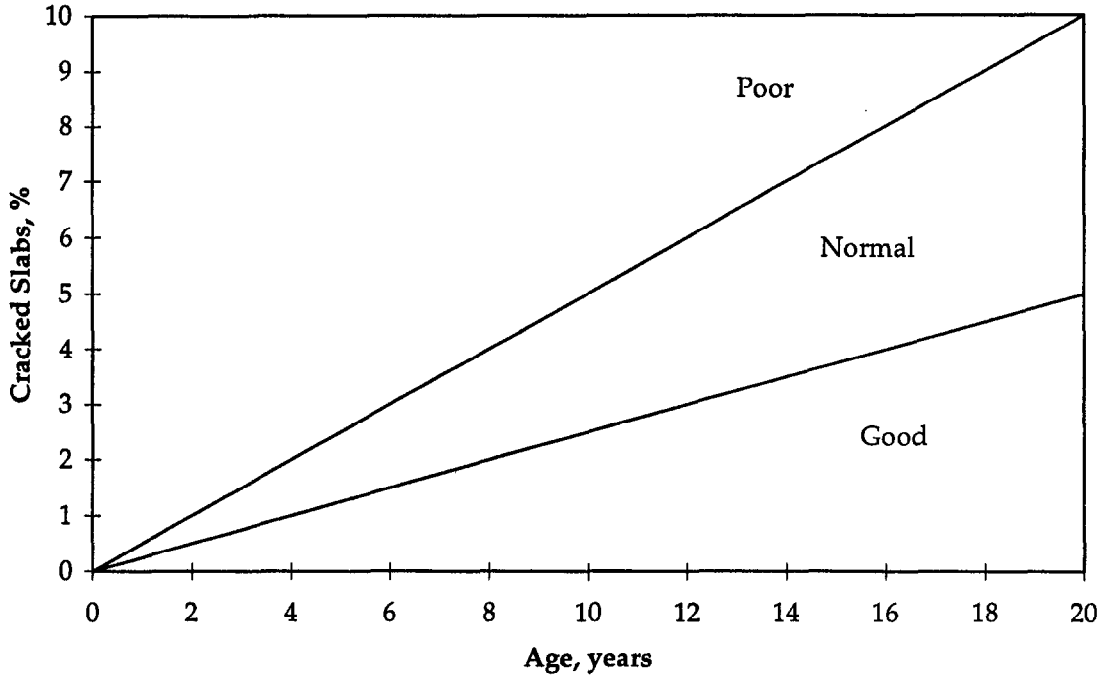

Figure 3. Performance criteria for cracking of JPCP.

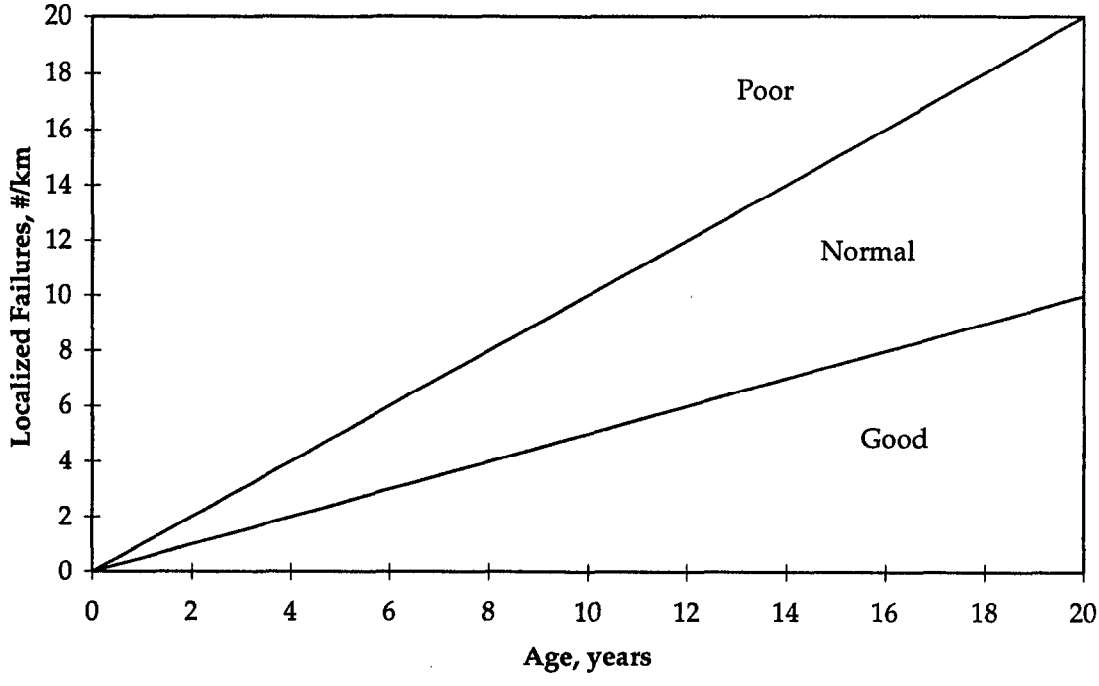

Figure 4. Performance criteria for localized failures on CRCP.

CHAPTER 3. SELECTION OF ANALYTICAL TECHNIQUES

Various statistical approaches are available to study the characteristics unique to good and poorly performing pavements. In addition, considerable value was found from visually examining the data to observe a variety of patterns and trends. The statistical techniques included bivariate tools such as t-tests, F-tests, Fisher's exact tests, chi-square tests, and maximum-likelihood chi-square tests, as well as multivariate tools like regression, principle component analysis, factor analysis, and discriminate analysis. Results from other studies were considered and brought into the overall summary of findings to help ensure that any characteristics identified as contributing to good or poor performance had strong support.

Performance Classification of Observation Points

Before the examination of the characteristics of the variables, each LTPP test section had to be classified according to its performance: good, normal, or poor. This was done with respect to the boundaries defined by the panel of experts as described in chapter 2. The performance classification was carried out for each observation and distress type/pavement type. It should be noted that observations for a test section could fall in one data set at one point in time and another at some other point in time. However, the latest point in time was selected for the analysis. Similarly, observations for a test section could fall in one performance class for one distress and another for a different distress.

Selection of Statistical Methods

Following the performance classification of each observation point, the data bases were examined to decide whether characteristics existed that differentiate good from poor performance. Again, since there were limited PCC sections, the normal group was not excluded from the analysis, but combined with either the good pavements or the poor pavements, depending on the number of data points available, to balance the number of sections in both groups.

Bivariate Analysis

The following tests were used for the bivariate analysis: t-tests, F-tests, Fisher's exact tests, chi-square tests, and maximum-likelihood chi-square tests. These tests (except for the F-test) compared the mean of each variable in the good group to its mean in the poor group. Those variables with significant differences, relative to the number of

points and the variation of the data available, might be indicative of good and poor pavement performance.[4]

The t-tests used an estimate of the standard deviation based on separate group estimates. This allows for differences in the group variances. A necessary assumption for the t-test is that the sample means are approximately normally distributed. Hence, this test was used for those independent variables that were reasonably well behaved. It was not used for discrete (0,1) variables such as base type or subgrade type. The test works by taking the ratio of the difference between the two group means to an appropriate estimate of standard deviation of this difference. If this ratio is large, then the group means differ a great deal for data with this much variability. Hence, it is concluded that this difference is due to something other than chance. If the ratio is small, then it is concluded that the difference could be due to chance—we cannot be confident that the difference is a real one.

The F-tests compare the variabilities of the two groups and are considered significant for p-values less than 0.05 or greater than 0.95.

For the discrete (0,1) variables, the Fisher's exact tests, chi-square tests, and maximum likelihood chi-square tests were used to compare the proportions of the two groups. The Fisher's exact test calculates the exact probability of observing this realization or something more extreme under the assumption that the proportions are equal. If the test is significant, the observed difference in the sample proportions is not due to chance. This probability is the ratio of combinatorics, so it is not available for large sample sizes. For large sample sizes, the chi-square and maximum likelihood chi-square tests provide approximate probabilities under the assumption that the proportions are equal.

The main downside of bivariate tests is that they do not take into account the effects of other variables. The confounding effects of other factors can inflate or deflate the results. This was a significant problem with some of the analyses and led to the necessity of conducting multivariate tests. For example, if those JPCP sections identified as performing good in roughness had a significantly thicker slab than those JPCP sections identified as performing poorly, then it would be tentatively concluded that a thicker PCC slab contributed to good performance of JPCP roughness. Of course, this conclusion is filled with potential risks because of other variables that may be correlated with thickness. Thus, the results of other studies, particularly mechanistic studies that explain why a thicker slab might result in smoother JPCP, must be considered in the analysis.

Multivariate Tools

The t-tests and other bivariate analyses mentioned above do not take into account the interactions of the different variables and their effects on performance. For example, it could be that joint load transfer design together with thick slabs is the cause of the good performance of JPCP. The t-tests will not isolate the effect of either of these variables on performance. The only way this can be accomplished is through multivariate analyses to learn more about the interrelationships of the variables. This study considered regression, principle component analysis, factor analysis, and discriminate function analysis.

Regression and stepwise regression were used in an exploratory manner to identify promising combinations of variables. For the standard regression models, the adjusted R-square indicates the amount of variability in the response that is explained by the model after adjusting for the number of parameters. The F-test indicates if the model is useful for estimating the response. Efforts were made to find regression models that had the least amount of collinearity. Cook's distance was also used to identify influential points. If any observations significantly altered the parameter estimates, then the model was refit without the points and the two models were compared.

In chapters 4 through 6, a stepwise regression with F-In = 2 and F-Out = 1.9 was used to provide a starting point. The technique suggested one possible model and compared the other variables to this model. The redundancy tables provide R-squares, partial correlations, and semipartial correlations for the variables in and not in the model. These statistics are based on regressing each variable onto the variables in the model. Those variables in the model are regressed on the remaining variables in the model. The R-square is a measure of the fit of this regression. The semipartial correlation is found by a second regression of the residuals from these regressions on the raw y values. The partial correlation is found by regressing these first residuals onto the residuals created by regressing y onto the variables in the model. A small semipartial correlation with a relatively large partial correlation is indicative of a promising variable.

Another guide for selecting variables is the correlation matrix. This matrix contains estimates of the pairwise correlations for two groups of variables. Also included is the p-value, which indicates if the estimate is significantly different from zero.

One common issue with data collected from a sample is collinearity, which refers to strong correlation among some independent variables. This can be thought of in two ways: one group of variables is nearly a linear function of another group, or as a restricted sample space containing only certain combinations of values of the variables. Models based on collinear variables have a few drawbacks. Collinearity inflates the

variance of the regression coefficients, the coefficients are not valid outside the sample space, and the coefficients might not be interpretable. Usually it takes very strong correlation before the effects of collinearity are harmful.

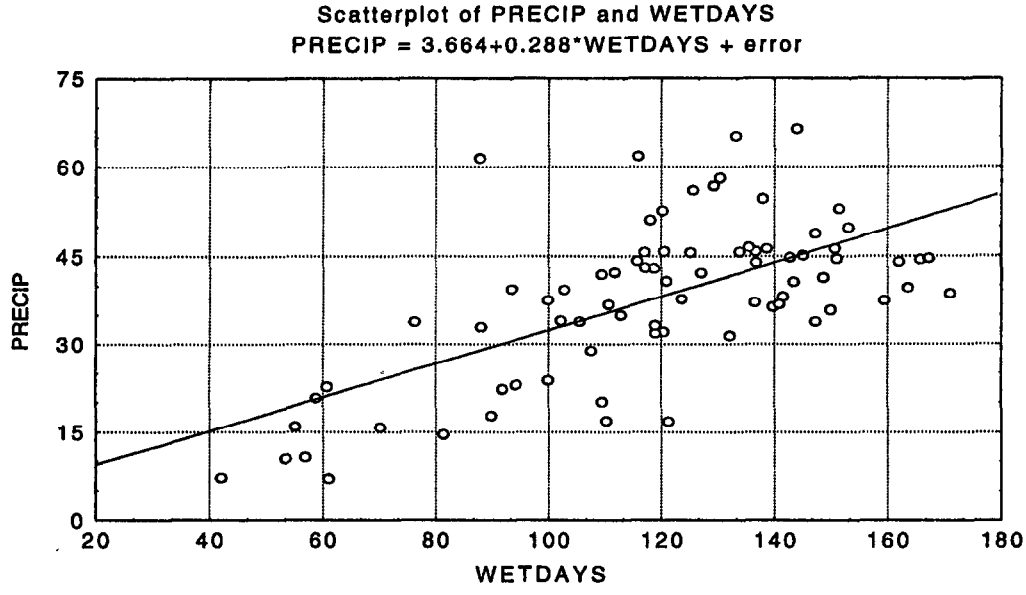

Figure 5. IRI as a function of PRECIP and WETDAYS.

As an example, consider modeling IRI as a function of PRECIP and WETDAYS (in the GPS 5 data set). Figure 5 shows that PRECIP and WETDAYS are highly correlated.

The estimated pairwise correlation for these two variables is 0.6416, and this is significantly different from zero. As you can see in the graph, some combinations of these variables were not observed. Large values of PRECIP with small values of WETDAYS and small values of PRECIP with large values of WETDAYS are not present. Hence, a regression model using both of these variables will be extrapolating for any new sections that have an unobserved combination of PRECIP and WETDAYS. For this situation it is unlikely to observe new sections that do not fall into this sample space.

Principal components analysis was used to address the collinearity problem when analyzing the faulting data. This tool is useful for decomposing a set of k variables into k orthogonal components that capture the cumulative variability of these variables in k dimensions. Each principal component (factor) is a linear combination of the variables that is independent of the other factors. Factor 1 is the linear combination with the most

variability; factor 2 is the linear combination that has the most variability of those linear combinations that are orthogonal to factor 1. Factor 3 is the next linear combination with the most variability of those linear combinations that are independent of factors 1 and 2. The later factors explain less and less of the variability. From these principal components, the variables that are correlated with the same components and how much variability these components explain can be noted.

Once the number of variables is narrowed down, a small set of variables can be put into a regression model. This type of model is helpful for thinking about the way the variables interrelate. All the models were developed from the data, so the statistics can only be interpreted in a descriptive or exploratory manner.

Principal components were used from a factor-analysis perspective as well. In this case, the principal components represent underlying sources of variability. Then these components are used to imitate the underlying effects within regression models.

Discriminate function analysis is a technique for finding functions of the explanatory variables that fit the groupings provided. Given two or more observed groups, this technique finds a function of the explanatory variables which nearly partitions the most extreme group from the rest. Then the algorithm continues finding functions that partition the remaining groups. By looking at the resulting classification functions, we can try to understand the basis for group membership.

Summary

Results from the visual observations, the bivariate tests, the multivariate analysis, and previous studies were combined to identify site conditions and design/construction features that may be expected to lead to good or poor performance of concrete pavements. Chapters 4 through 9 show the results of these analyses.

CHAPTER 4. PERFORMANCE OF JPCP IN ROUGHNESS

Roughness is an extremely important characteristic of a pavement's performance. Pavement roughness greatly affects ride quality, safety, and vehicle operation costs, which are very important to the traveling public. Sayers and Gillespie define road roughness as "the variation in surface elevation that induces vibrations in traversing vehicles."[6] Roughness is caused by two general sources: surface irregularities that are built into a pavement during construction and surface irregularities that develop after construction due to traffic, climatic, and other factors.

One measure of pavement roughness provided in the LTPP data base is the International Roughness Index (IRI), established in 1986 by the World Bank. A pavement's IRI is calculated from the longitudinal road profile and is reported in units of inches/mile or meters/kilometer. IRI has been shown to correlate with the present serviceability rating (PSR), which is a subjective user rating of the existing ride quality of the pavement.[5] As such, IRI can be used as an approximate user response to pavement condition. The objective of this analysis was to examine in a practical way the LTPP data base and identify the site conditions and design/construction features that significantly affect JPCP roughness as measured by IRI.

Previous Studies

Performance of JPCP with respect to roughness has been investigated in several studies. Two IRI models were developed in the early LTPP Data Analysis Study.[1] The model developed for doweled JPCP is as follows:

$$IRI = 1.671 + 0.683\left[\frac{AGE}{KSTATIC}\right] + 0.114\ JTSPACE + 0.00443\ HPCC + 0.213\ EDGESUP \qquad (1)$$

where

IRI	=	International Roughness Index, m/km
AGE	=	pavement age, years
KSTATIC	=	FWD backcalculated modulus of subgrade reaction (divided by 2), kPa/mm
JTSPACE	=	joint spacing, m
HPCC	=	PCC slab thickness, mm
EDGESUP	=	edge support (=1 if tied PCC shoulder; =0 otherwise)

This model predicts IRI as a function of site conditions and pavement design features. Age is positively correlated to IRI; that is, an increase in age corresponds to an increase in IRI. This is reasonable because pavement distresses that increase the roughness of the pavement generally tend to increase with age. Also, pavement features such as subgrade k-value, joint spacing, and PCC slab thickness have a logical influence on the IRI. Note that the apparent effect of PCC tied shoulders may not be correct in that there may have been errors in the early data base regarding shoulder type.

The model developed for non-doweled JPCP is as follows:

$$IRI = 0.613 + 0.203\ CESAL + 0.00350\ FT + 9.32 * 10^{-4}\ PRECIP - 0.173\ BASE - 0.216\ SUBGR \quad (2)$$

where

IRI	=	International Roughness Index, mm/km
CESAL	=	cumulative 80-kN equivalent single axle loads (ESALs), millions
FT	=	mean annual air freeze-thaw cycles
PRECIP	=	mean annual precipitation, mm
BASE	=	1 = stabilized material, 0 = unbound granular material
SUBGR	=	1 = coarse-grained (AASHTO A-1, A-2, or A-3) 0 = fine-grained (AASHTO A-4, A-5, A-6, or A-7)

IRI is predicted as a function of site conditions and pavement design features. CESAL is positively correlated to IRI; that is, an increase in the number of 80-kN ESAL applications corresponds to increased IRI. This is reasonable because distresses that increase the pavement roughness generally increase as more axle loads are applied to the pavement. The pavement foundation conditions, base and subgrade type, and climatic variables such as the number of freeze-thaw cycles and precipitation also have a logical influence on predicted IRI.

A recent study utilizing the LTPP data base developed the following IRI model for doweled and non-doweled JPCP as a function of site conditions and design features:[3]

$$IRI = 1.303 + 0.0158\ KESAL^{0.4}(0.01\ WETDAYS + 0.72\ FREEZE) + 0.0158\ AGE^{0.4}(0.0091\ FI + 2.27*10^{-7}\ EPCC - 3.5\ SUBGR - 0.121\ DOWDIAM) \quad (3)$$

where

IRI	=	International Roughness Index, m/km
KESAL	=	cumulative number of ESALs, thousands

AGE	=	pavement age, years
FI	=	freezing index, degree days below freezing
EPCC	=	PCC slab elastic modulus, kPa
DOWDIAM	=	dowel diameter, mm
SUBGR	=	subgrade type; 1=coarse-grained, 0=fine-grained
WETDAYS	=	number of days on which precipitation is greater than 12.7 mm
FREEZE	=	LTPP climatic zone, 1=freezing climate, 0=nonfreezing climate

In a recent study utilizing the FHWA data base, a prediction model for IRI of JPCP indicated that IRI could be predicted as a function of visible distress, including joint faulting, spalling, and transverse cracking.[2] The model is shown below:

$$IRI^2 = (24805 + 41.2 * FaultTT + 458.5 * Spall + 0.00233* T\text{-}crack^3)/10^6 \quad (4)$$

where

IRI	=	International Roughness Index, m/km
FaultTT	=	total joint faulting per km, mm/km
T-crack	=	amount of transverse cracking, number of cracks/km
Spall	=	percentage of the joints spalled medium-high severity

This model permits indirect investigation of the effect of the design features and site conditions on IRI through their effect on the individual distresses characterized by the corresponding prediction models.

Table 1 summarizes the site conditions and design features that were included in these prediction models. With one exception, all of the design/construction features and site conditions from the multivariate studies agree in the direction of their effect on IRI (such as precipitation, where IRI is higher on those JPCP subjected to higher amounts of annual precipitation). The only disagreement is in the effect of slab thickness. The early analysis of LTPP data and the FHWA study show that the IRI is lower for those JPCP with thicker slabs, as it should logically be due to faulting and cracking impacts. The recent LTPP model indicates the opposite. It is possible that thicker slabs are built rougher; however, a subsequent analysis of the initial roughness in initial IRI did not verify this.

Note that the effect of the initial IRI after construction was not directly included in these studies. A major research study was just completed that determined that the future roughness of a pavement was highly dependent on its initial, as-constructed roughness. Prediction models for many projects, including JPCP, were developed for future IRI.[4]

Table 1. Summary of the effects of site conditions and design features on IRI.

Site Condition/ Design Feature	Effect on IRI Over Life (given an increase in site condition/design feature)	References
Pavement age	Increases *	1, 2, 3
Subgrade k-value	Decreases	1
Joint spacing	Increases	1
PCC slab thickness	Decreases Increases	1, 2, 3
Tied shoulder	Increases	1 (data problem on shoulder type)
Widened lane	Decreases	2
Traffic (ESAL)	Increases	1, 2
Stabilized base	Decreases	1, 2
Coarse subgrade	Decreases	1
Precipitation	Increases	1, 2, 3
Number of freeze-thaw cycles	Increases	1
PCC Flexural strength	Decreases	2
PCC Modulus of Elasticity	Increases	3
Freezing Index	Increases	2, 3
Initial Roughness	Increases	4

* For example, as pavement age increases, IRI increases. As k-value increases, IRI decreases.

Performance Criteria for IRI

This section presents an analysis of the site conditions and design/construction features that lead to roughness of JPCP based on the IRI measurements from the LTPP data base. The version of the LTPP data base analyzed in this study contains IRI data for 121 JPCP sections. The total number of observations is 485. For some sections, time series data contain up to 10 observations made over 5 years. Other sections have only one performance record in the data base.

The data was divided into three performance categories, poor, normal, and good, based on IRI and pavement age as previously described. This grouping was done to facilitate the analysis of identifying features that contribute to good and poor roughness. This grouping was established based on the experience of a group of State highway engineers. The limits that were set are shown in figure 6. The pavement section was considered to be performing good (i.e., better than expected) if its IRI satisfies the following condition:

$$IRI < 0.631 + 0.0631 * AGE \quad (5)$$

where

IRI = International Roughness Index, m/km
AGE = pavement age at the time of the observation, years.

The pavement section was considered to be performing poor if its IRI satisfies the following condition:

$$IRI < 1.263 + 0.0947 * AGE \quad (6)$$

where

IRI = International Roughness Index, m/km
AGE = pavement age at the time of the observation, years.

Figure 6 presents a plot of all IRI observations for the LTPP JPCP sections and shows designation of those sections by their performance at the time of observation. Because the number of observations differs among the sections, the use of all these observations in the subsequent analysis may make it biased toward the sections with a higher number of observations. To avoid this, only the last observation for each section was considered in the analysis if not stated otherwise. Figure 7 presents a plot of all JPCP sections with respect to IRI at the time of the last available observation.

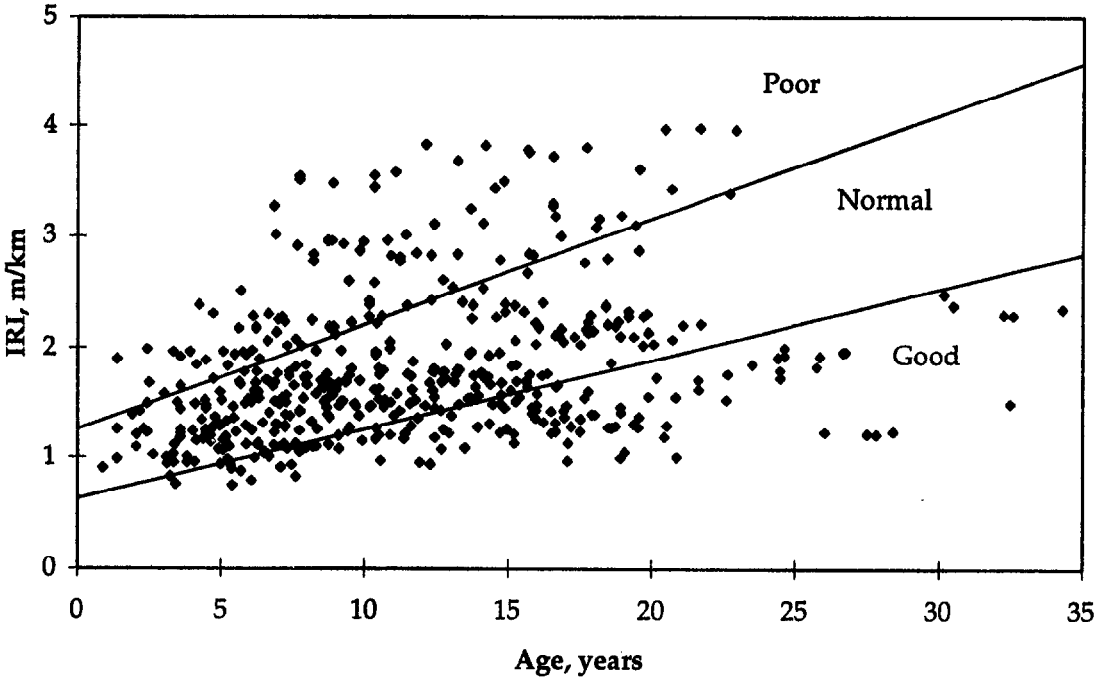

Figure 6. IRI for JPCP including all time-series data.

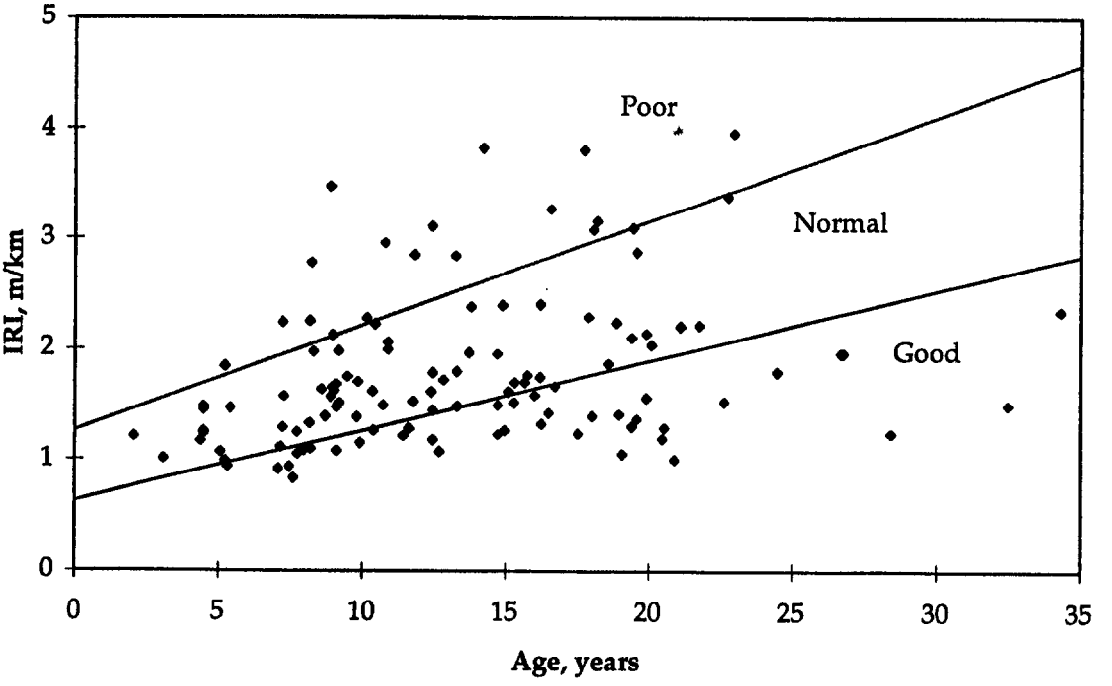

Figure 7. IRI for JPCP (last IRI observations only).

Factors Considered for IRI

The general types of factors affecting the IRI of JPCP include site conditions and design and construction features. The factors studied in this analysis include those found to be significant from previous studies and others based on engineering experience:

- **Site Conditions**
  - o Geographic/climatic location
    - Latitude
    - Longitude
  - o Temperature factors
    - Freezing index
    - Freeze-thaw cycles
    - Mean annual temperature
    - Minimum annual temperature
    - Maximum annual temperature
    - Number of days warmer than 32°C per year
    - Number of days colder than 0°C per year
  - o Precipitation factors
    - Average annual precipitation
    - Average number of wet days per year
  - o Subgrade soil
  - o Traffic (ESAL)

- **Design and Construction Features**
  - o Slab thickness
  - o Concrete properties
    - Modulus of elasticity
    - Modulus of rupture
  - o Joint spacing
  - o Base type
  - o Dowels
  - o Drainage coefficient
  - o Initial as-constructed roughness

Comparative and Statistical Analysis of IRI

Two general types of analyses were performed: a visual comparative analysis and a statistical analysis. Comparative analysis includes visual trend analysis of plots with a distribution of pavement sections by their performance as a function of those factors,

and a comparison of average values of those factors for different groups of pavement sections. The reader can observe the plots and evaluate the graphical results.

Statistical analyses conducted include the bivariate t-test and, in some cases, multivariate analyses to identify those site conditions and design features that contribute to good and poor roughness performance. The JPCP section data were partitioned into two groups based on IRI: those that fell into the good/normal group and those that fell into the poor group (note that the good/normal group will subsequently be called the good group for convenience). The normal group had to be used in the analysis due to the limited number of sections.

The t-test was then used to compare the mean of each variable in the good group to its mean in the poor group. The test works by taking the ratio of the difference between the two group means to an appropriate estimate of standard deviation of this difference. If this ratio is large, then the group means differ a great deal for data with this much variability. Hence, it would be concluded that this difference is due to something other than chance. If the ratio is small, then we conclude that the difference could be due to chance—the analysis cannot be confident that the difference is a real one.

As an example, JPCP performing good with respect to IRI had a significantly higher elastic modulus base than for JPCP performing poor.

E(base) for good IRI group = 3,784,381 kPa, n = 101
E(base) for poor IRI group = 1,343,550 kPa, n = 18
t-value = -2.60, df = 117
Level of significance = 0.010 (the probability is less than 0.01 that this has occurred due to chance). Note that a level of significance of 0.05 was considered to be significant in the discussion below.

Figure 8 show the means of base modulus. Based on these results, it was concluded that JPCP with higher modulus of the base had a lower IRI. However, note that the t-tests are one-dimensional tests that do not adjust for the effects of other variables—collinearity. Other variables could possibly be causing the above effect, a variable that correlates strongly with base modulus. This collinearity can only be considered through further rigorous statistical analysis, which is not within the scope of this study.

Table 2 provides a summary of all the t-values for each comparison made for continuous variables. Table 3 provides a summary of chi-squared tests for discrete (0,1) variables for IRI (JPCP). These will be referred to during the following presentation.

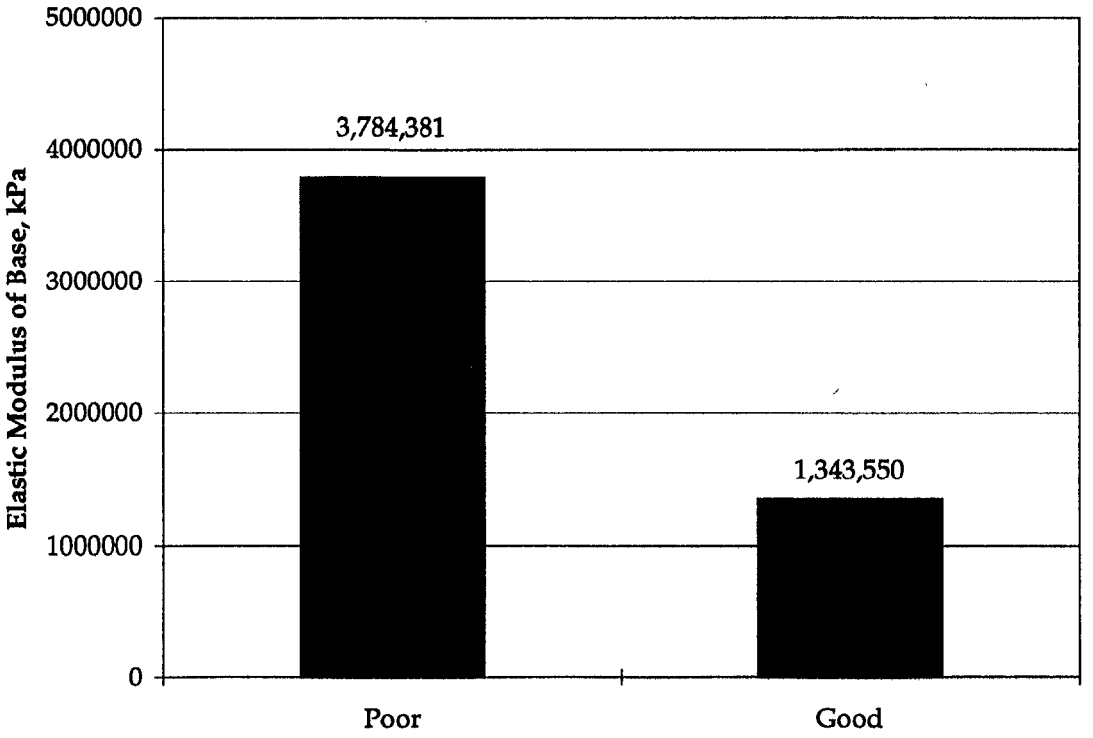

Figure 8. Effect of average elastic modulus of base on JPCP IRI performance

In addition, two-dimensional plots of IRI with respect to different parameters were analyzed, and a comparison of mean values of those variables for good, normal, and poor sections was performed. Although the results of this analysis are of great interest because they highlight the most significant trends in pavement roughness, they must be considered with caution because of the possibility of misleading conclusions as a result of confounding effects of other factors.

Table 2. Results of t-tests for JPCP IRI performance (continuous variables).

	Poor	Good/Normal	t separ. var. est.	df	p 2-sided	Valid N Poor	Valid N Good	Std. Dev. Poor	Std. Dev. Good	F-ratio variance	p variance
FI	716.536	313.324	3.492	19.471	0.002	17	101	453.111	356.333	1.617	0.156
FT	91.556	75.911	1.842	26.652	0.077	17	101	30.700	41.000	1.782	0.189
PRECIP	854.964	805.866	0.634	27.702	0.531	17	101	276.860	386.080	1.943	0.132
WETDAYS	136.790	110.125	3.286	24.183	0.003	17	101	30.100	35.600	1.395	0.458
LONG	86.611	96.777	-3.313	27.981	0.003	18	103	11.500	14.800	1.671	0.227
LAT	42.167	38.330	3.275	26.208	0.003	18	103	4.400	5.300	1.419	0.417
TMAX	14.251	19.450	-4.481	23.784	0.000	17	101	4.333	5.000	1.331	0.529
TMIN	2.604	6.309	-3.188	22.877	0.004	17	101	4.389	4.778	1.186	0.732
TMEAN	8.428	12.879	-3.901	23.202	0.001	17	101	4.278	4.778	1.238	0.652
DAYS32	12.347	40.859	-5.624	42.101	0.000	17	101	16.100	32.400	4.048	0.003
DAYS0	142.437	94.055	3.873	25.848	0.001	17	101	45.500	58.600	1.657	0.251
JTSPACE	4.861	5.108	-1.347	40.670	0.185	18	103	0.610	1.128	3.383	0.006
SKEW	0.432	0.437	-0.064	25.680	0.949	18	103	0.274	0.336	1.343	0.500
DOWDIAM	8.661	11.760	-0.822	23.415	0.420	18	103	15.240	15.240	1.011	1.000
KESAL	3911.600	5776.195	-1.555	31.815	0.130	15	87	3738.000	6635.300	3.151	0.019
HPCC	240.741	239.370	0.171	22.899	0.866	18	103	30.480	30.480	1.071	0.784
MR28	4826.631	4667.741	1.478	28.517	0.150	18	103	399.620	527.774	1.746	0.190
EPCC	27419.106	27158.873	0.590	43.564	0.559	18	103	1454.655	2821.498	3.762	0.003
EBASE	1343.550	3784.384	-3.427	32.388	0.002	18	101	2554.962	3822.030	2.238	0.061
C_d	0.872	0.996	-3.314	24.344	0.003	18	103	0.100	0.200	1.148	0.782
KSTATIC	36.672	45.738	-1.216	21.127	0.238	18	103	29.947	24.413	1.506	0.215
JTWIDTH	8.585	9.169	-0.571	18.744	0.574	16	74	5.080	2.540	1.809	0.099

where

FI:	= Freezing Index, °C-days	JTSPACE	= Distance between slab joints, m
FT	= Annual air freeze-thaw cycles	SKEW	= Joint skewness, m
PRECIP	= Mean annual precipitation, mm	DOWDIAM	= Dowel diameter, mm
WETDAYS	= Mean number of wet days	KESAL	= 80-kN equivalent single axle load, thousand
LONG	= Longitude location, °	HPCC	= Thickness of PCC slab, mm
LAT	= Latitude location, °	MR28	= Mean 28-day modulus of rupture, kPa
TMIN	= Minimum annual temperature, °C	EPCC	= Mean PCC elastic modulus, MPa
TMAX	= Maximum annual temperature, °C	EBASE	= Estimated base-layer modulus of elasticity, MPa
TMEAN	= Mean annual temperature, °C	C_d	= AASHTO drainage coefficient
DAYS32	= Annual number of days with temperature higher than 32°C	KSTATIC	= Static elastic modulus of subgrade reaction, kPa/mm
DAYS0	= Annual number of days with temperature lower than 0°C	JTWIDTH	= Joint width, mm

Table 3. Results of chi-square tests for JPCP IRI performance.

Variable	Pearson Chi-square		Maximum Likelihood Chi-square	
	Chi-square	p	Chi-square	p
Dowels	0.941	0.332	0.976	0.323
GRANBAS	11.590	0.001	11.697	0.001
ACBASE	3.676	0.055	4.683	0.030
CEMBASE	0.206	0.650	0.215	0.643
LEAN	2.992	0.084	5.189	0.023
SUBGR	1.092	0.296	1.115	0.291
WW	4.318	0.038	5.052	0.025
WD	2.328	0.127	4.090	0.043
CW	8.945	0.003	8.550	0.003
COLDDRY	0.000	0.992	0.000	0.992
TEXT1	3.052	0.081	2.900	0.089
TEXT2	0.002	0.965	0.002	0.965
TEXT3	0.109	0.741	0.117	0.732
TEXT5	4.665	0.031	3.505	0.061
TEXT7	6.232	0.013	4.476	0.034
DRTYP1	0.019	0.890	0.019	0.890
DRTYP2	0.586	0.444	0.554	0.457
SEAL1	6.260	0.012	5.518	0.019
SEAL2	0.003	0.958	0.003	0.958
SEAL3	1.019	0.313	1.126	0.289
SEAL4	0.711	0.399	0.736	0.391
SEAL5	1.003	0.317	1.789	0.181

where

Dowels	= 1, if dowels present = 0, if no dowels	TEXT2	=1, if broom is used to texture concrete surface =0, otherwise
GRANBAS	=1, if granular base present =0, otherwise	TEXT3	=1, if burlap drag is used to texture concrete surface =0, otherwise
ACBASE	=1, if asphalt stabilized base present =0, otherwise	TEXT5	=1, if grooved float is used to texture concrete surface =0, otherwise
CEMBASE	=1, if cement treated base present =0, otherwise	TEXT7	=1, if astro turf and tine are used to texture concrete surface =0, otherwise
LEAN	=1, if lean concrete base present =0, otherwise	DRTYP1	=1, if no subsurface drainage is placed =0, otherwise
SUBGR	=1, if subgrade is coarse-grained soil =0, otherwise	DRTYP2	=1, if longitudinal drainage is placed =0, otherwise
WW	=1, if a climate is warm-wet =0, otherwise	SEAL1	=1, if a cold application sealant type =0, otherwise
WD	=1, if a climate is warm-dry =0, otherwise	SEAL2	=1, if an M123 (AASHTO) hot poured elastic sealant type =0, otherwise
CW	=1, if a climate is cold-wet =0, otherwise	SEAL3	=1, if an M282 (AASHTO) hot poured for PCC sealant type =0, otherwise
COLDDRY	=1, if a climate is cold-dry =0, otherwise	SEAL4	=1, if an M301 (AASHTO) hot poured for concrete and AC sealant type =0, otherwise
TEXT1	=1, if tine is used to texture concrete =0, otherwise	SEAL5	=1, if a preformed sealant type

Climatic Site Conditions

Geographic/climatic location. Figures 9 and 10 show distribution of good, normal, and poor sections with respect to longitude and latitude of their location, respectively. Latitude and longitude are correlated with climatic factors such as precipitation and air temperature. No poor section (with respect to roughness) is located west of 110° longitude and south of 37° latitude, which corresponds to the warm-dry climate in the southwest United States. The t-test confirmed the significance of both latitude and longitude on IRI performance of JPCP, as shown in table 2. Specific climatic variables that were also significant are discussed below.

Temperature factors. The following temperature parameters were considered in this study: freezing index (FI), number of air freeze-thaw cycles (FT), mean annual temperature (T_{mean}), minimum annual temperature (T_{min}), maximum annual temperature (T_{max}), number of days per year with a temperature higher than 32°C (DAYS32), and number of days per year with a temperature lower than 0°C (DAYS0).

The distribution of IRI vs. freezing index, FI, for each performance category is shown in figure 11. It is observed that the majority of poor performing sections are located in the areas with a freezing index of 280°C-days and higher, which corresponds to a cold climate. Figure 12 shows the average annual FI for good, normal, and poor sections. It shows that the average FI for poor performing sections is much higher than for normal and good sections. The mean FI for poor sections was 717°C-days, whereas normal and good performing sections have mean FIs of 327 and 293°C-days, respectively. The result of the t-test (table 2) confirms the significance of this difference.

Figure 13 illustrates the effects of the annual number of air freeze-thaw cycles on IRI. There is a clear trend showing that more annual air freeze-thaw cycles leads to higher IRI values (rougher pavements). Figure 14 presents the mean of the mean annual freeze-thaw cycles for good, normal, and poor sections. This plot shows the same trend: fewer annual freeze-thaw cycles is associated with smoother pavements. The mean number of annual air freeze-thaw cycles for poor performing sections was 92. The mean values for normal and good performing sections were 80 and 70 cycles, respectively. This is logical, since freezing and thawing cause or accelerate JPCP deterioration in many ways.

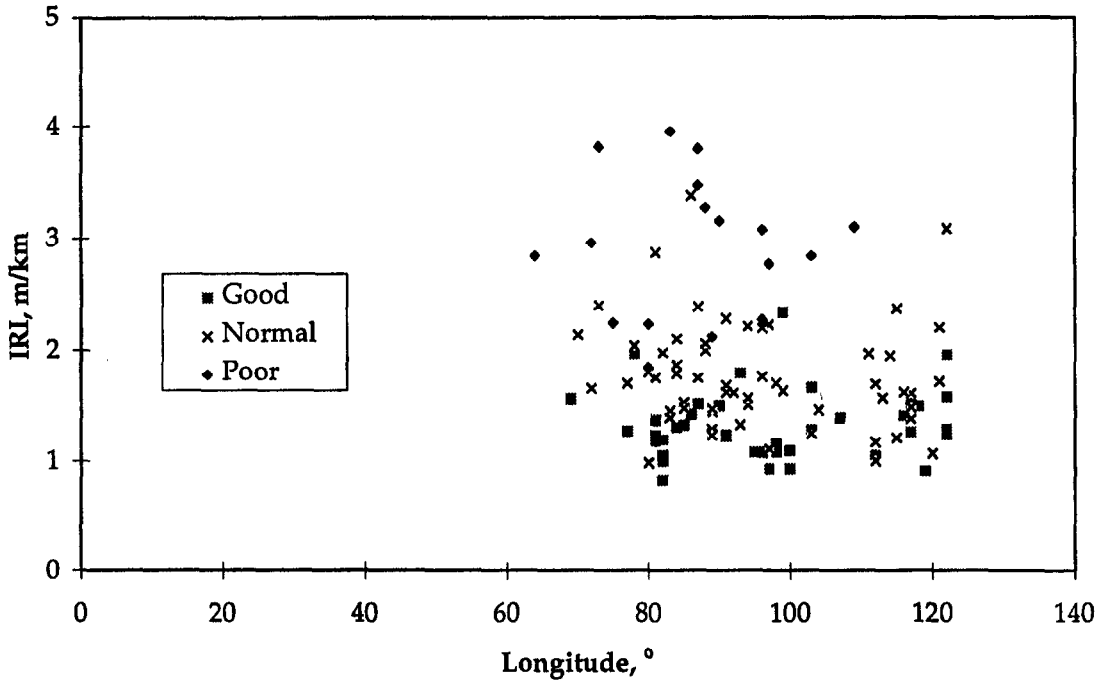

Figure 9. Longitude versus IRI for JPCP.

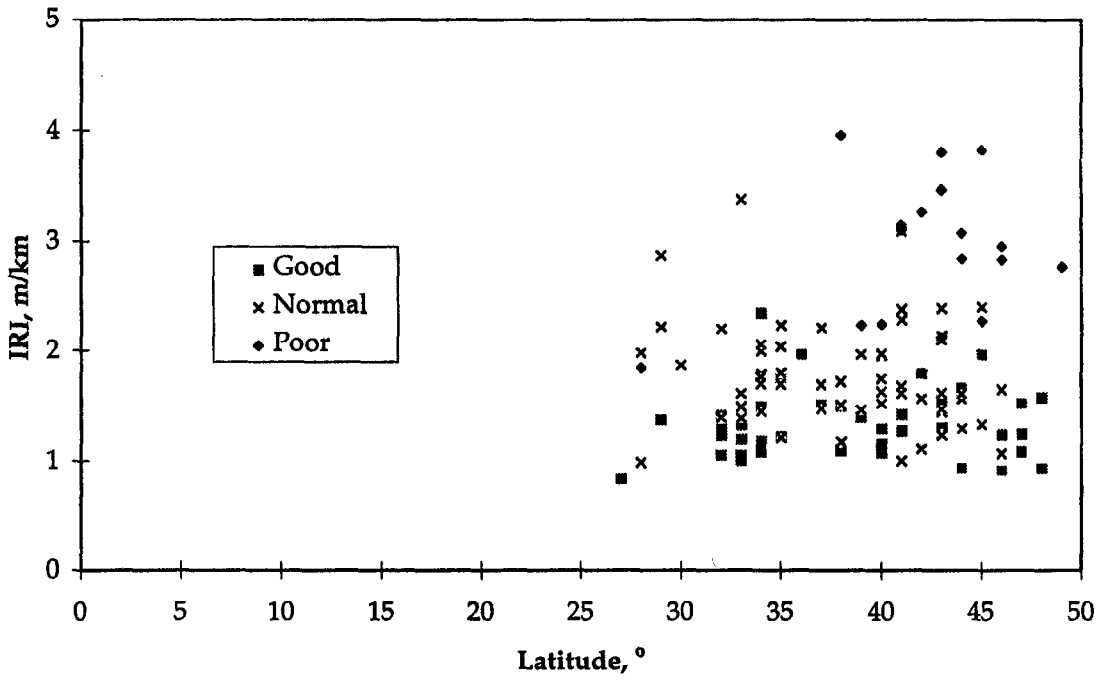

Figure 10. Latitude versus IRI for JPCP.

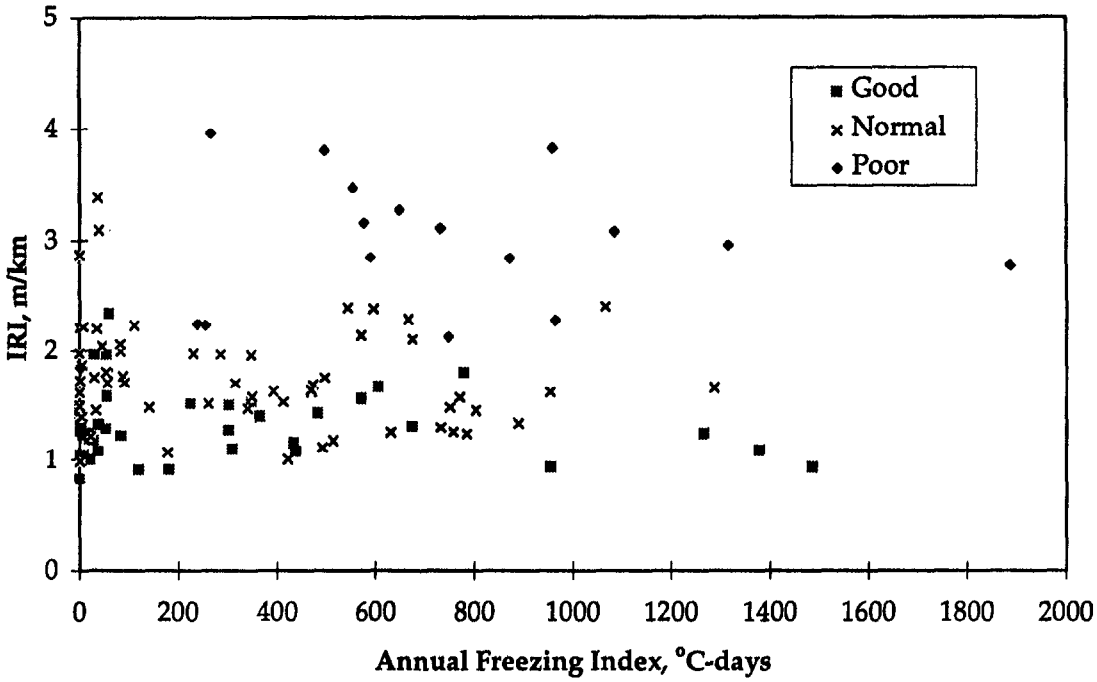

Figure 11. Freezing index versus IRI for JPCP.

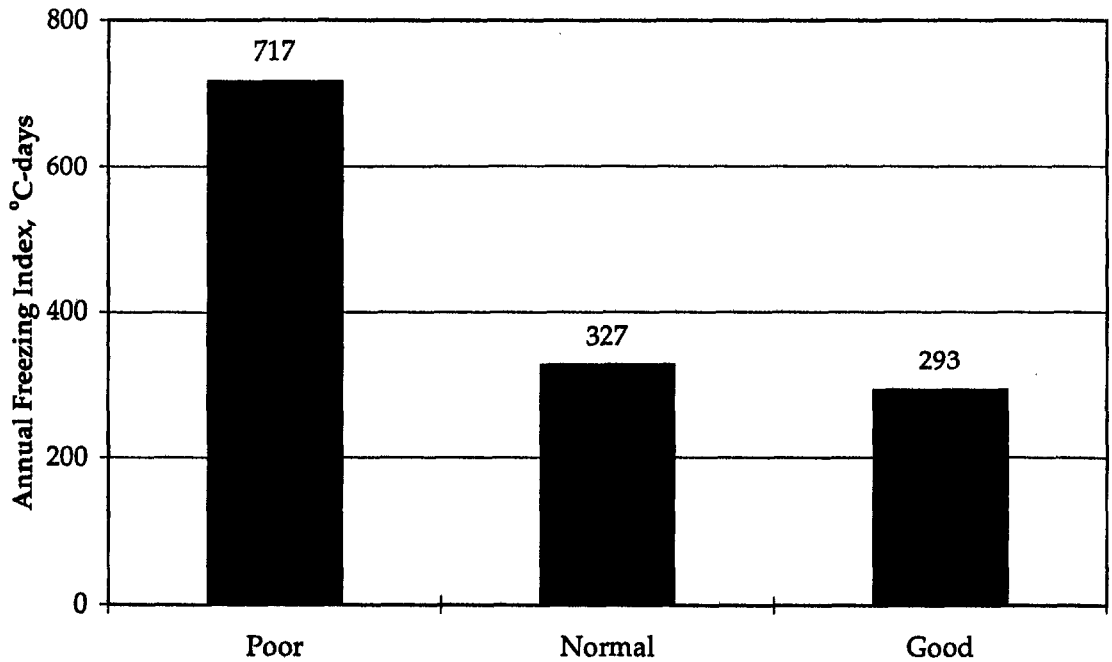

Figure 12. Effect of freezing index on JPCP IRI performance.

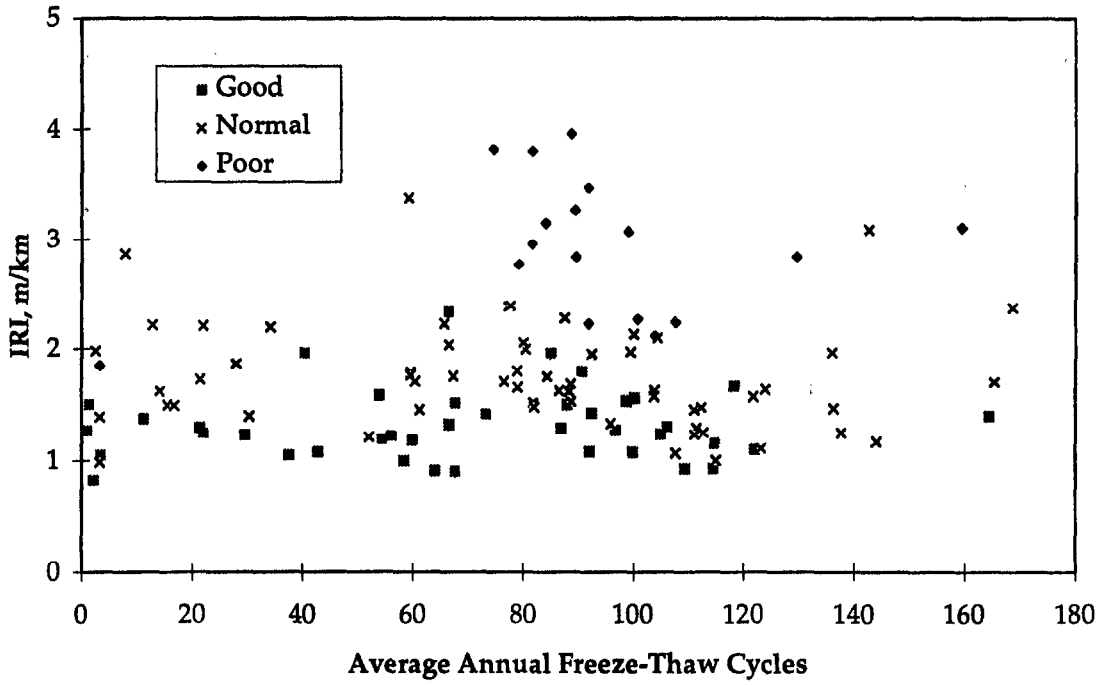

Figure 13. Average annual air freeze-thaw cycles versus IRI for JPCP.

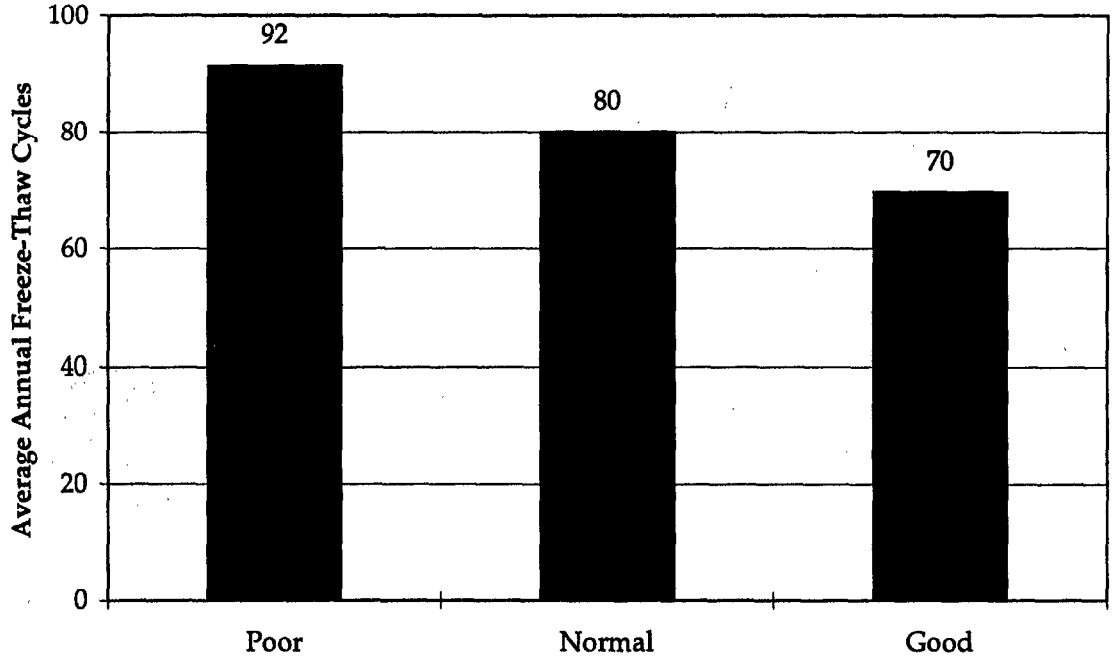

Figure 14. Effect of annual air freeze-thaw cycles on JPCP IRI performance.

Figure 15 shows the distribution of IRI vs. DAYS32. It is observed that only one poor performing section has DAYS32 greater than 20 days, whereas DAYS32 for good and normal sections are almost uniformly distributed from 0 to 120 days. Figure 16 compares mean values of DAYS32 for good, normal, and poor sections. This index is much lower for poor sections than for good and normal sections. The mean DAYS32 for good, normal, and poor performing sections were 42, 40, and 12 days, respectively. The result of the t-test (table 2) confirms the significance of this difference.

Figure 17 shows the distribution of IRI vs. DAYS0. As expected, poor sections have high values for DAYS0, but normal and good sections exhibit a wide variety of this index. Also, the average DAYS0 for poor sections was 142 days, which is much higher than for good and normal sections, as shown in figure 18. Good and normal performing sections had mean DAYS0 of 86 and 99 days, respectively. The result of the t-test (table 2) confirms the significance of this difference.

Figures 19 and 20 present the distributions of IRI vs T_{mean} and the trends for good, normal, and poor. The mean T_{mean} for poor, normal, and good sections were 8.4, 12.7 and 13.2°C, respectively. The result of the t-test (table 2) confirms the significance of the differences for T_{mean}.

The findings show that a large majority of poor performing sections (with respect to IRI) are located in colder climates.

Precipitation factors. Two precipitation factors were analyzed in this study: average annual precipitation and average number of wet days per year. No clear trend was observed relating annual precipitation levels to IRI performance. The result of the t-test (table 2) did not confirm the significance of this difference.

Figures 21 and 22 show trends for the average number of wet days vs. IRI. All poor sections have an average number of wet days per year greater than 70, but several good and normal performing pavements are located in drier zones. The average number of Wet Days for poor pavements is also higher than those for good and normal sections. The mean value for wet days for poor sections was 137 days, whereas the mean values for normal and good sections were 109 and 112 days, respectively. The result of the t-test (table 2) confirms the significance of this difference. These results indicate that the presence of increased moisture over an extended percent of time advances JPCP deterioration and roughness.

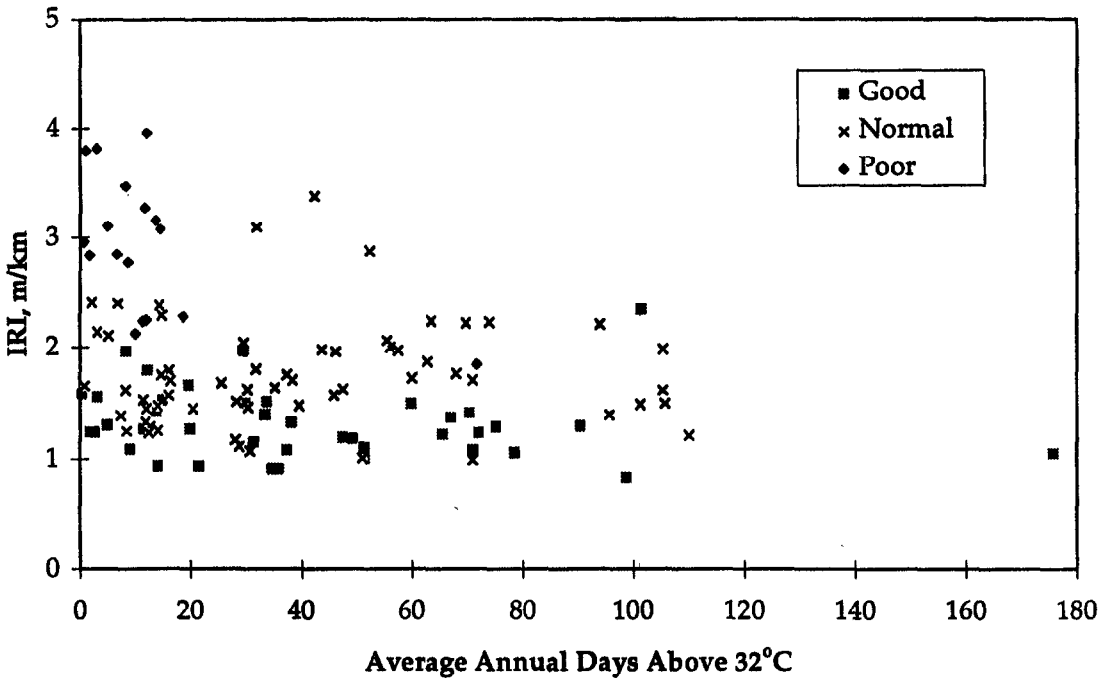

Figure 15. Average annual days above 32°C versus IRI for JPCP.

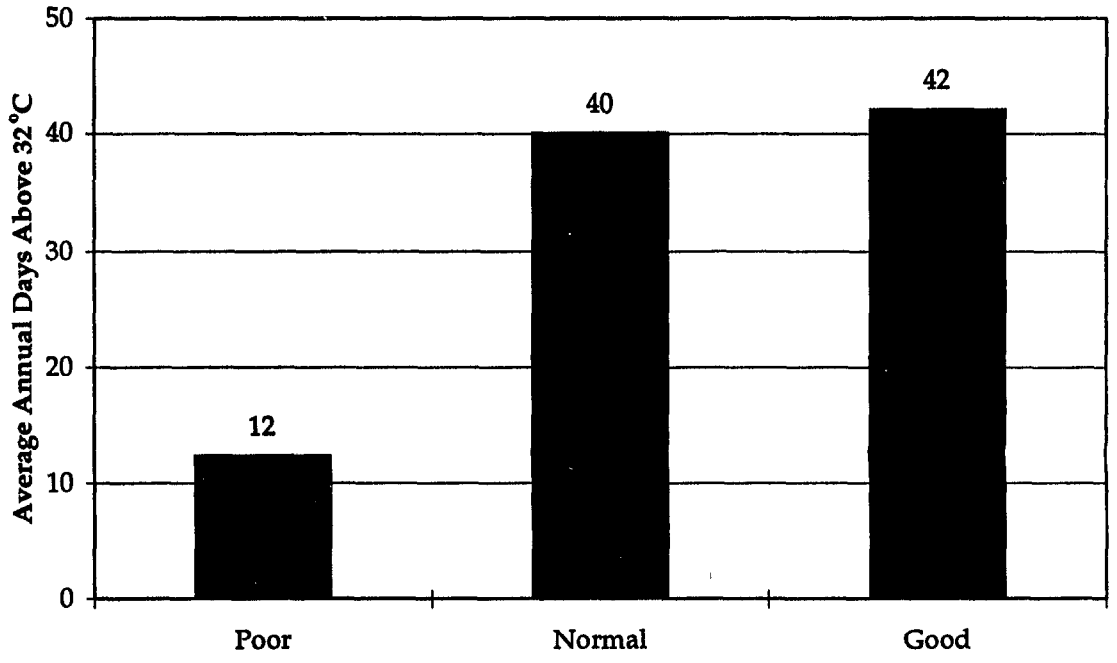

Figure 16. Effect of annual days above 32°C on JPCP IRI performance.

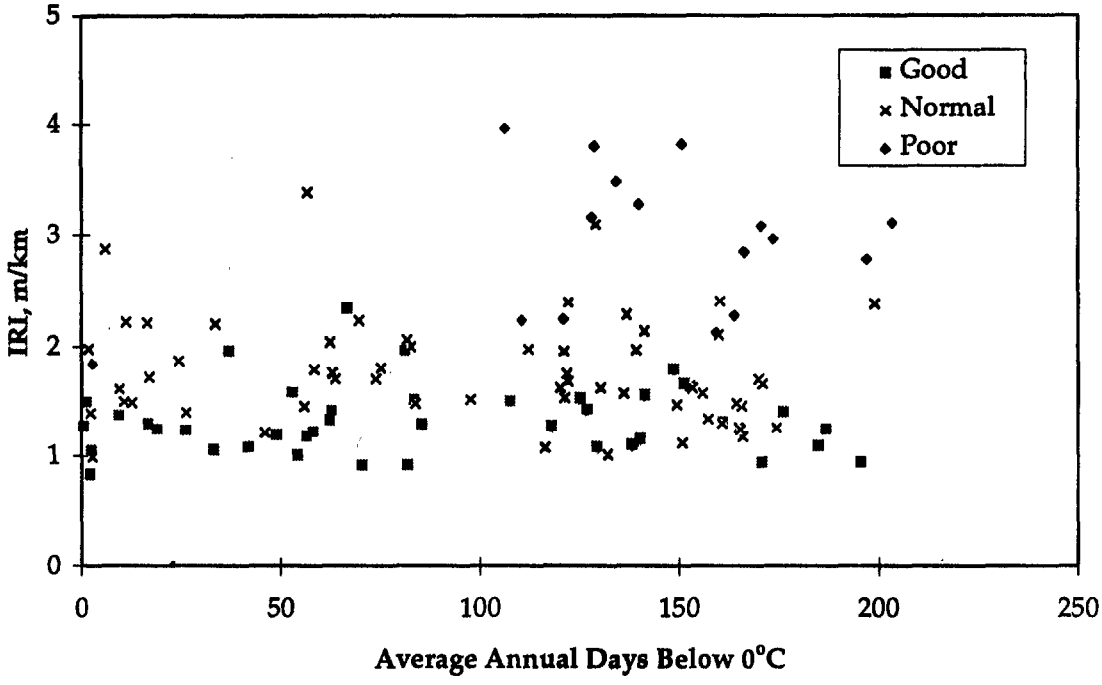

Figure 17. Average annual days below 0°C versus IRI for JPCP.

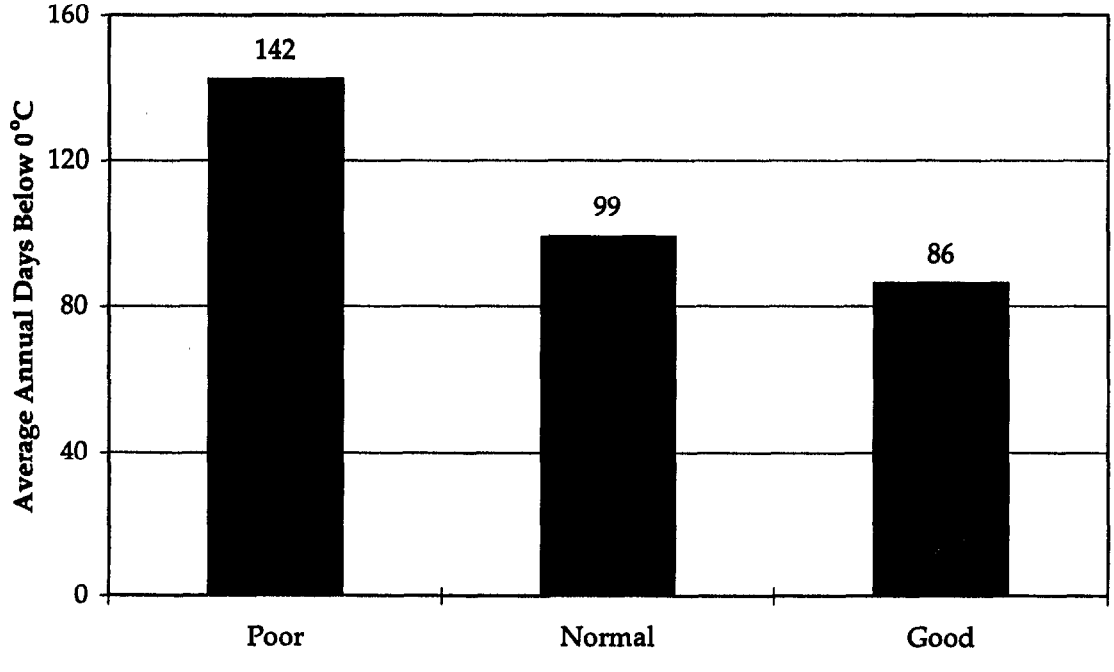

Figure 18. Effect of average annual days below 0°C on JPCP IRI performance.

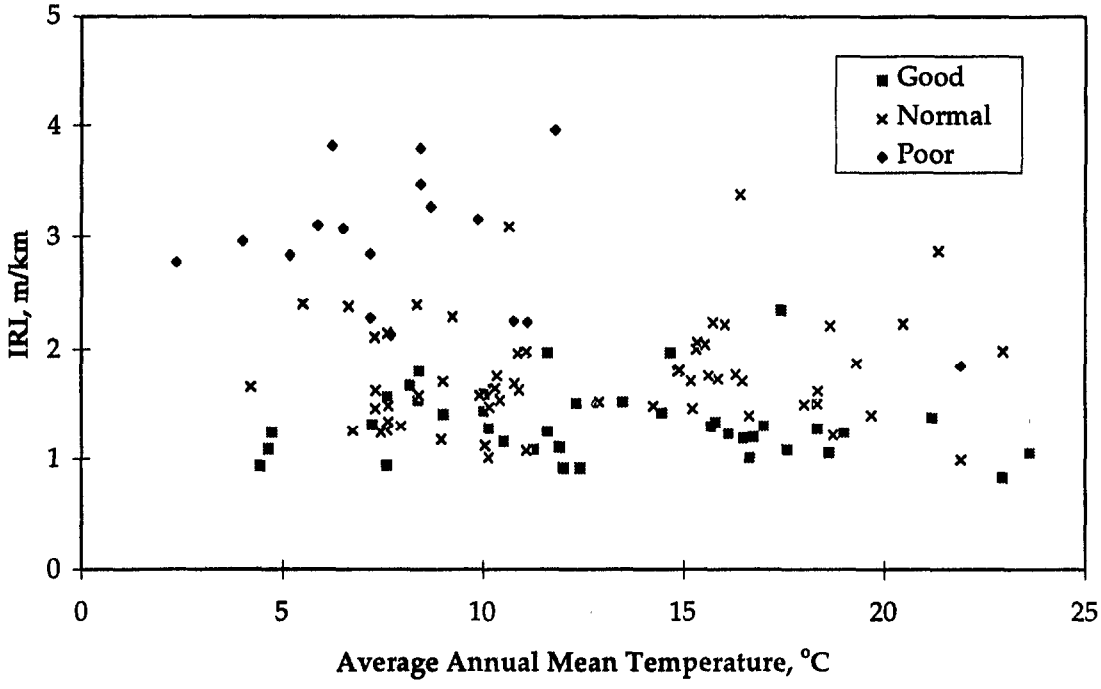

Figure 19. Average annual mean temperature versus IRI for JPCP.

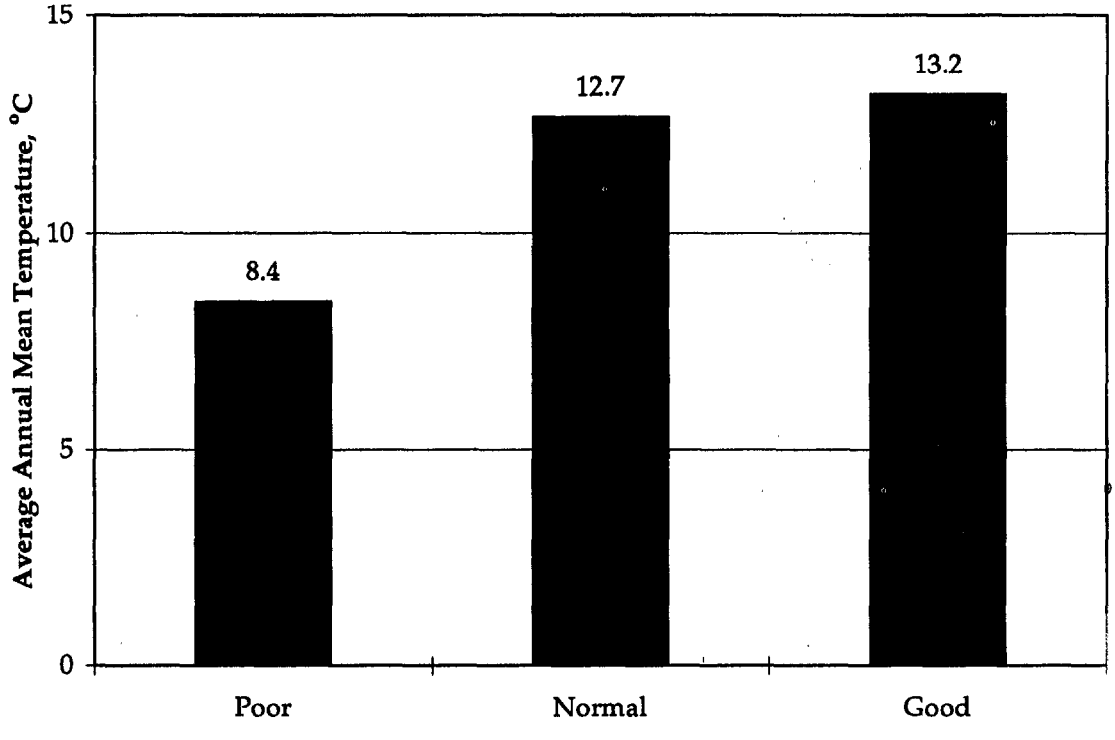

Figure 20. Effect of average annual mean temperature on JPCP IRI performance.

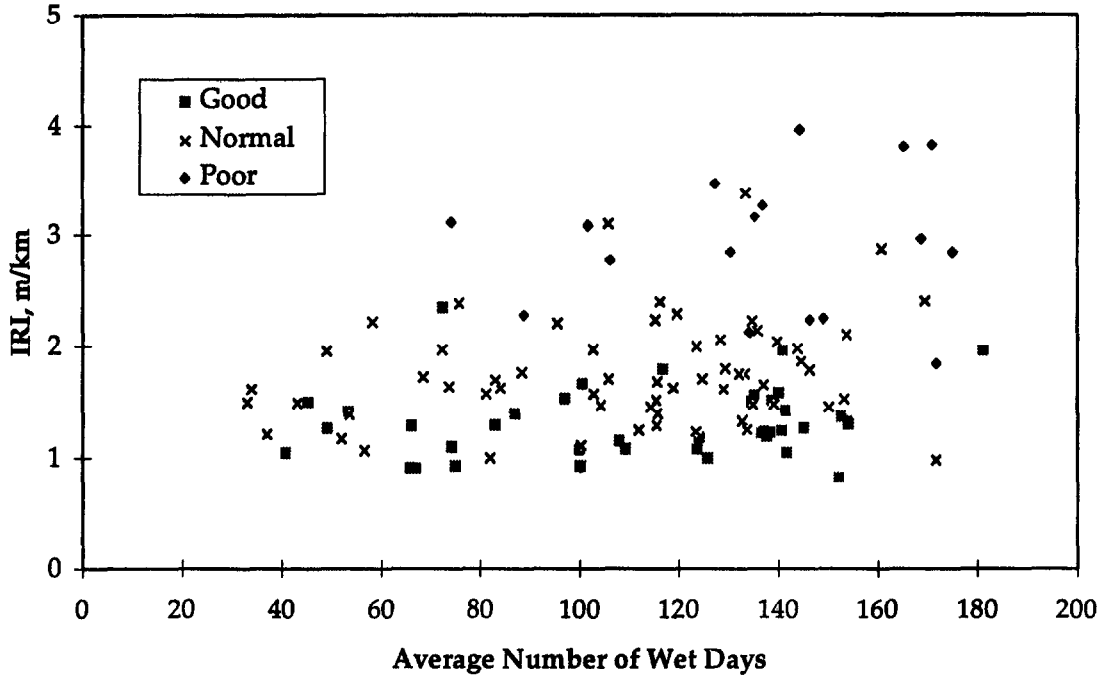

Figure 21. Average number of wet days versus IRI for JPCP.

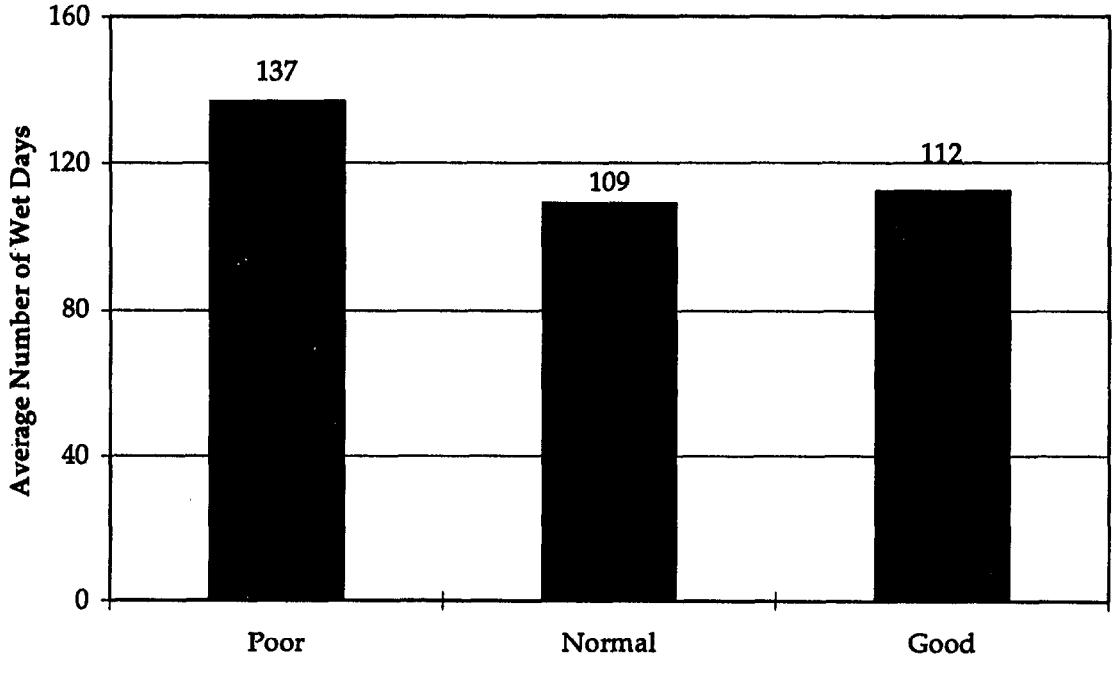

Figure 22. Effect of average number of wet days on JPCP IRI performance.

Figure 23 shows overall trends that were noted previously. Approximately 71 percent of all sections rated as poor are located in cold-wet regions. This may be due to the wet freeze-thaw and moisture considerations discussed earlier. Approximately 24 percent of poor sections are located in cold-dry regions, 6 percent in warm-wet regions, and none in any warm-dry area. These results indicate the strong effect of climate on pavement roughness over time.

Subgrade Site Conditions

The subgrade can be separated into fine-grained soils and coarse-grained soils. The percent of sections rated poor, normal, and good for each soil type were computed. Figure 24 shows that 67 percent of sections constructed over fine-grained soils had poor IRI performance, while only 33 percent constructed over coarse soils had poor IRI performance. The result of the chi-square test (table 3) comparing poor vs. normal/good, however, did not show any significance.

Traffic Site Conditions

Figures 25 and 26 show the relationship between applied ESALs and IRI. It is expected that increased levels of traffic would clearly lead to an increase in IRI. However, perhaps due to the confounding effects of other design parameters (e.g., slab thickness), the result of the t-test (table 2) did not confirm the significance of this difference. Other variables are likely confounded with ESAL level (such as structural design of the pavement).

Design and Construction Features

Thickness. Figure 27 shows a plot of the thickness vs. IRI data. No clear trend was observed relating slab thickness to IRI in this data base, and the t-test did not show any significance difference either (table 2). Initial roughness has a large effect on future roughness, and any true effect of slab thickness may have been confounded with initial roughness. The mean estimated initial IRI was approximately the same for thinner slabs as for thicker slabs.

Concrete properties. Plots of IRI versus the concrete modulus of elasticity and estimated modulus of rupture at 28 days show no direct correlation between these parameters and IRI. The result of the t-test (table 2) did not confirm the significance of any difference between the two data sets.

Joint spacing. Plots of IRI with respect to joint spacing show no trend in the data. The t-test did not show a statistical significance for this design feature. Increasing joint spacing has been shown in past studies to somewhat increase joint faulting and greatly increase transverse cracking, but these data show no effect on IRI.[2]

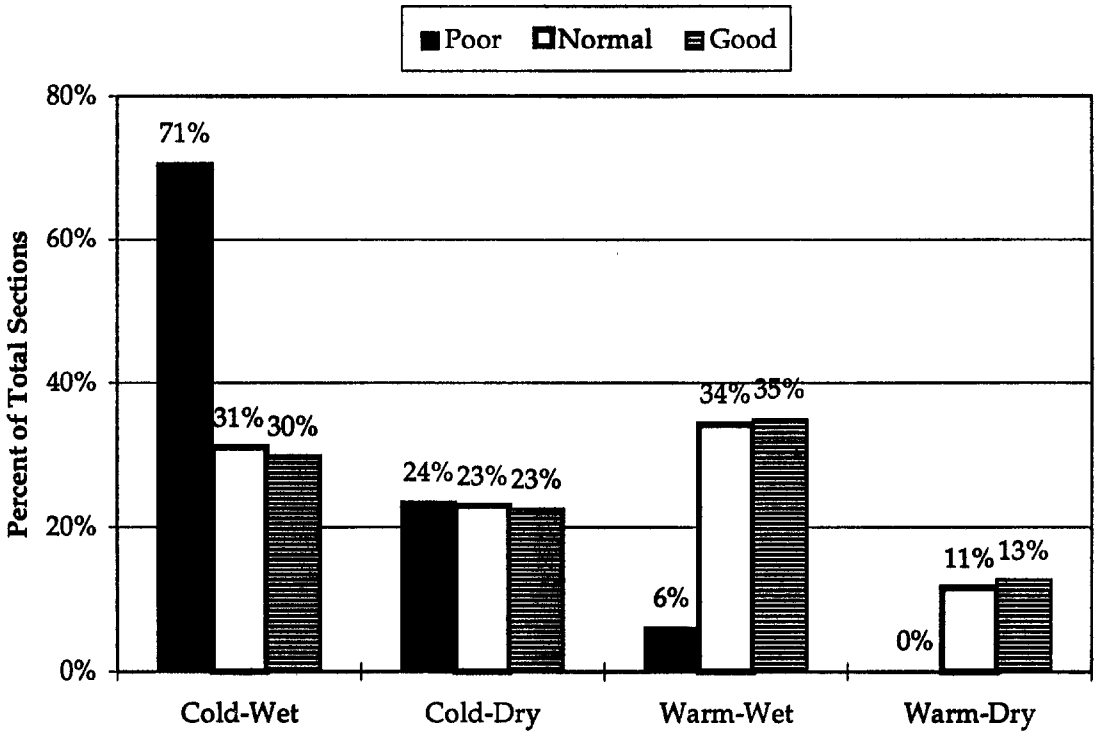

Figure 23. Effect of climatic region on JPCP IRI performance.

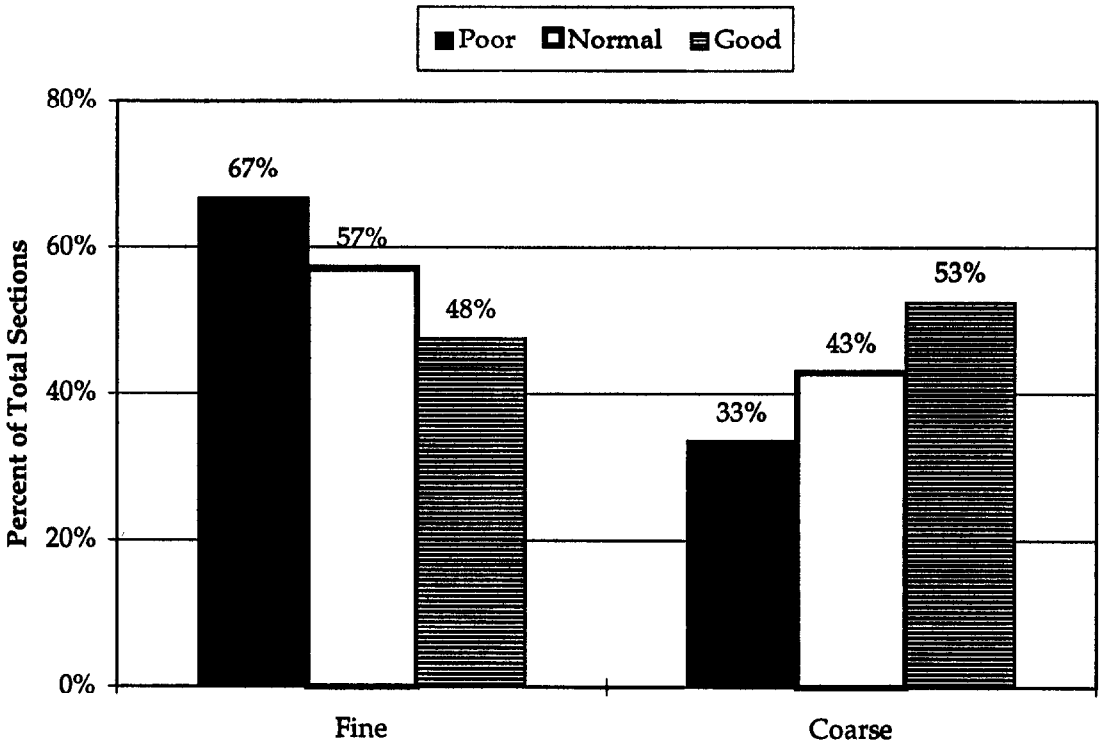

Figure 24. Effect of subgrade soil on JPCP IRI performance.

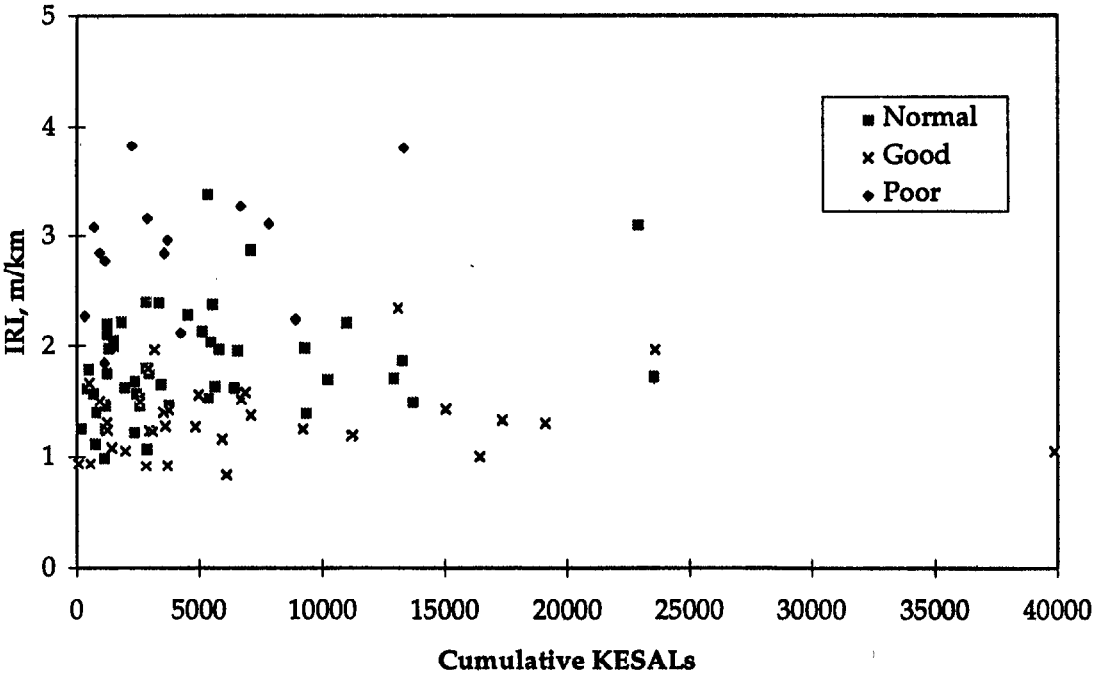

Figure 25. Cumulative KESALs versus IRI for JPCP.

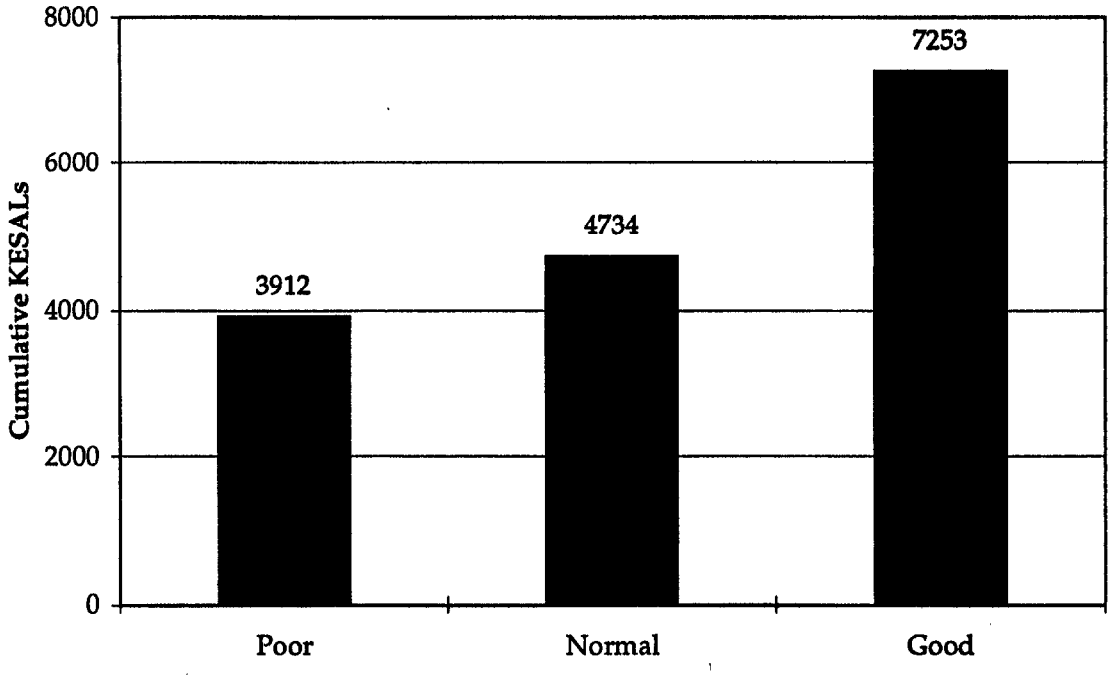

Figure 26. Effect of cumulative traffic on JPCP IRI performance (values shown are in 1,000s of ESALs, 7253 = 7,253,000 ESALs).

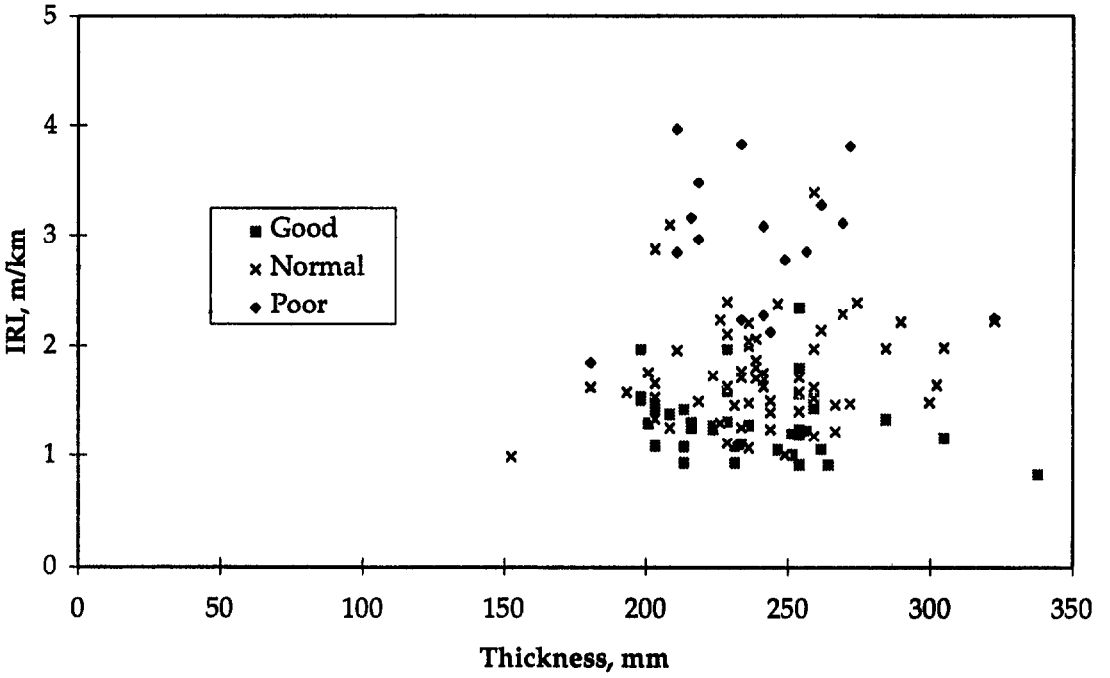

Figure 27. PCC slab thickness versus IRI for JPCP.

Base modulus and type. Figure 28 shows that JPCP with a stabilized base layer has a lower IRI than JPCP with a granular base layer (82 percent of poor sections had granular base). The elastic modulus of the base was used to test the effect of the base type. Results for base modulus were previously shown on page 17 and in figure 8. JPCP with higher modulus base layers on average had lower IRI than JPCP with a lower modulus. The base modulus result of the t-test (table 2) confirms the significance of this difference.

Additional chi-square tests were conducted to compare various base types. The results in table 3 show that significant difference occurred between granular base and stabilized base (stabilized base lower IRI), asphalt stabilized base and all other bases (asphalt stabilized base lower IRI), and lean concrete and all other bases (lean concrete lower IRI). Cement-treated base did not show a significant difference with other bases.

Dowels. To investigate the effect of dowels on roughness, all JPCP sections were divided into two groups: the sections that are younger than 10 years and the sections that are older than 10 years. Figure 29 shows percentages of doweled sections for good, normal, and poor performing sections for these two groups. It was observed that the percentage of doweled sections is the same for poor, normal, and good young sections. It suggests that dowels have little effect on roughness of young pavements. The fraction of doweled old poor sections (18 percent) is lower than for old normal and

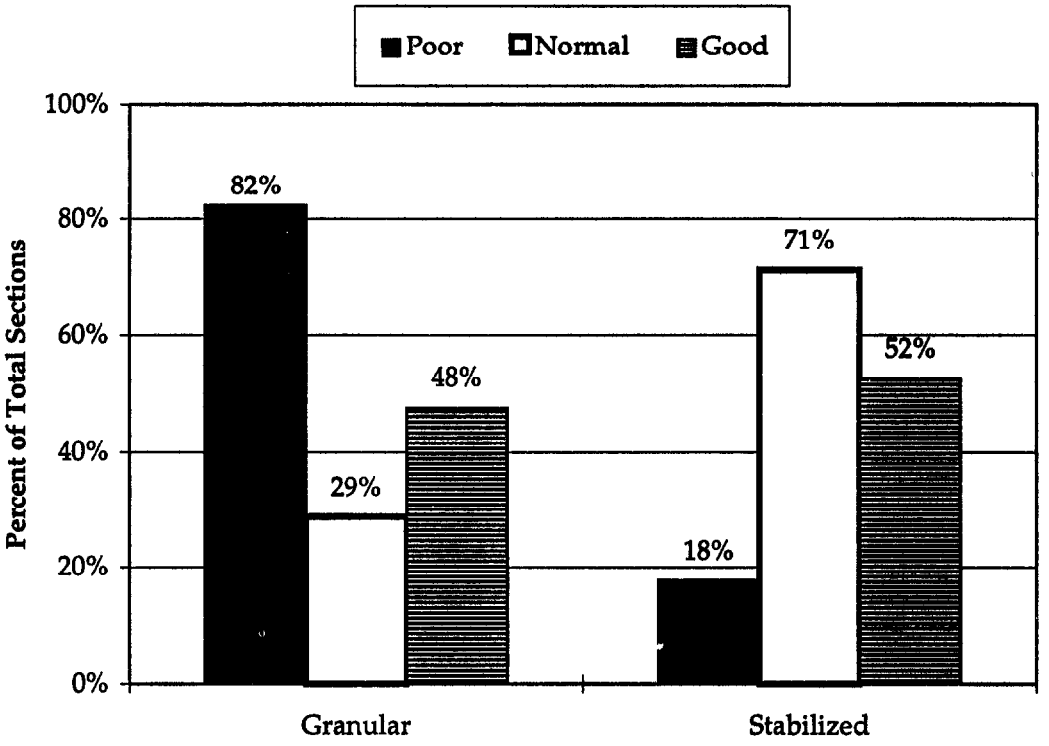

Figure 28. Effect of base-layer type on JPCP IRI performance.

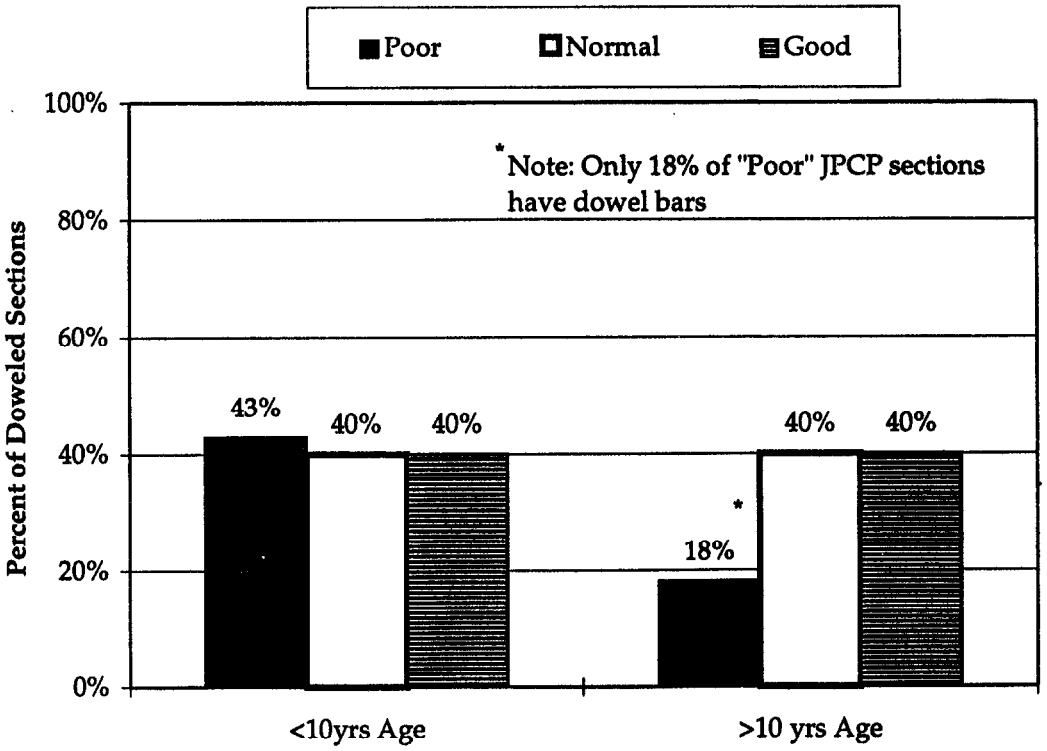

Figure 29. Effect of pavement age and dowels on JPCP IRI performance.

poor sections (40 percent). This suggests that non-doweled sections increase in IRI faster than doweled sections, likely due to increased rate of faulting of joints. The result of the chi-square (table 3) did not show the significance of the difference in performance of doweled and non-doweled JPCP sections of all ages. However, an additional chi-square test for JPCP sections older than 10 years showed that the difference has a moderate level of significance (p=0.10).

Drainage. Subdrainage was characterized using the modified AASHTO drainage coefficient, C_d, which reflects the pavement's ability to drain excessive moisture from the structure. Higher C_d corresponds to better drainage.[2] Table 4 shows the criteria used to estimate C_d for each LTPP section. Figure 30 shows the distribution of IRI vs. C_d. It is observed that only two poor performing sections have C_d greater than 0.95, whereas a significant number of good and normal sections have C_d from 1 to 1.3 (which corresponds to good drainage). There is also a clear trend in the data showing lower IRI with higher C_d (or better drainage).

Figure 31 compares mean values of C_d for good, normal, and poor sections. This index is much lower for poor sections than for good and normal sections. The mean value of C_d for poor sections was 0.87, whereas normal and good performing sections had mean values of 0.99 and 1.00. The result of the t-test (table 2) confirms the significance of this difference.

Table 4. Matrix for selection of the overall drainage coefficient, C_d.[2]

Edge Drains	Precipitation Level	Fine-Grained Soils		Coarse-Grained Soils	
		Nonpermeable Base	Permeable Base	Nonpermeable Base	Permeable Base
No	Wet	0.70-0.80	0.70-0.80	0.80-0.90	0.90-1.00
	Dry	0.80-0.90	0.80-0.90	0.90-1.00	0.80-0.90
Yes	Wet	0.85-0.95	0.80-0.90	0.95-1.05	1.05-1.15
	Dry	0.95-1.05	1.10-1.20	1.05-1.15	1.15-1.20

Notes
1. Fine grained = A-1 through A-3 classes
2. Coarse grained = A-4 through A-7 classes
3. Permeable base = k = 300 m/day or CU ≤ 6
4. Wet climate = Precipitation > 635 mm/year
5. Dry climate = Precipitation ≤ 635 mm/year
6. Select midpoint of range and use other drainage features to adjust upward or downward.

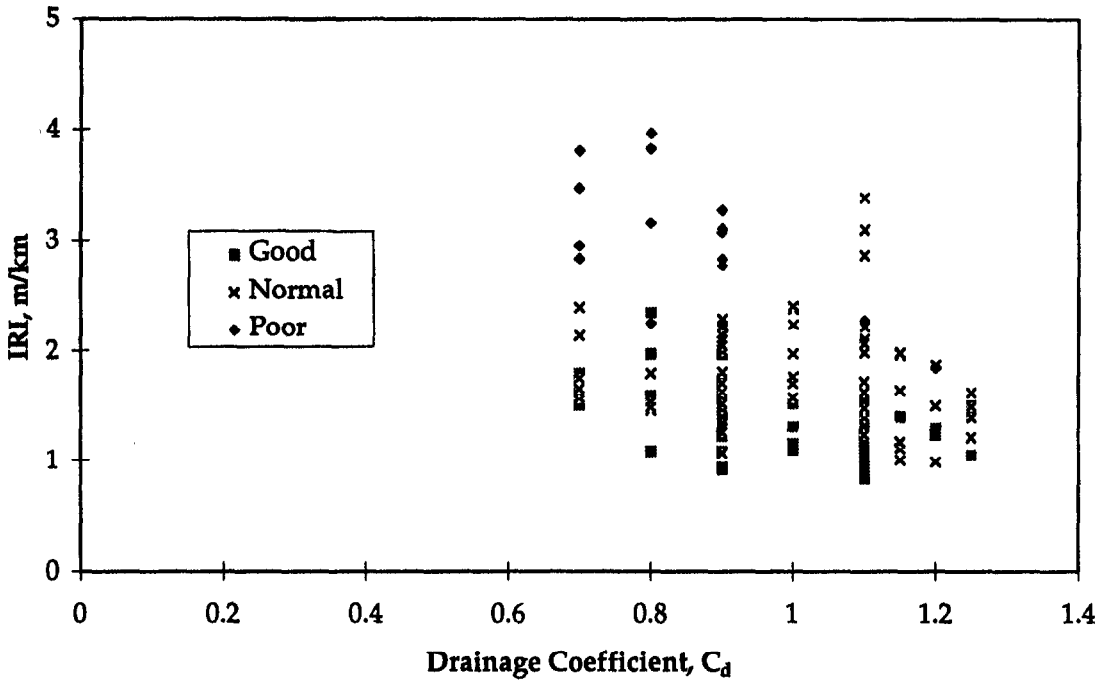

Figure 30. Drainage coefficient (C_d) versus IRI for JPCP.

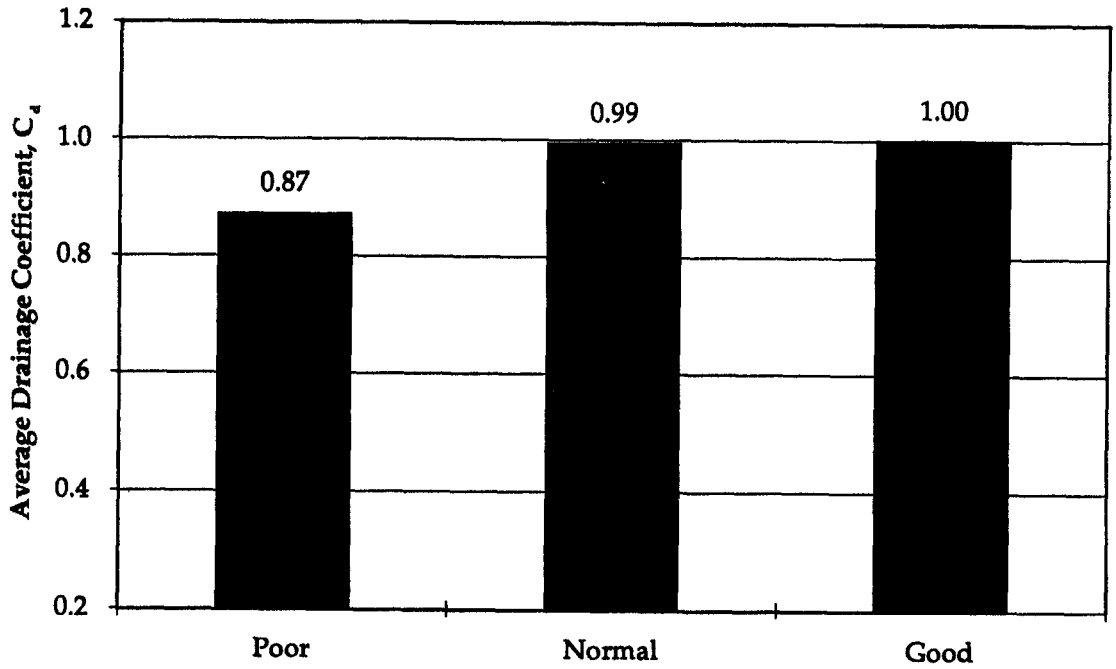

Figure 31. Effect of drainage coefficient (C_d) on JPCP IRI performance.

Initial as-constructed roughness. A recently completed study concluded that the initial roughness has significant influence on future pavement roughness.[4] In this study, an attempt was made to evaluate this conclusion using the LTPP data base. Because the LTPP data base does not contain as-constructed initial roughness data, linear regression was used to "backcast" an estimate of the initial as-constructed roughness. This estimated value is called an initial roughness factor (IRF), which attempts to estimate the initial IRI from the available time series IRI data. The following procedure, as illustrated in figure 32, was used to determine the IRF and α (the rate of IRI increase per year):

1. Plot IRI versus Age for each section.
2. Identify questionable observation and questionable sections (sections where IRI decreases with time).
3. Eliminate sections with IRI data over a period of less than 2 years.
4. Run linear regression for each section to compute an initial roughness factor, IRF, and deterioration rate, α:

$$IRI = IRF + \alpha * AGE \tag{7}$$

where AGE is the pavement age.

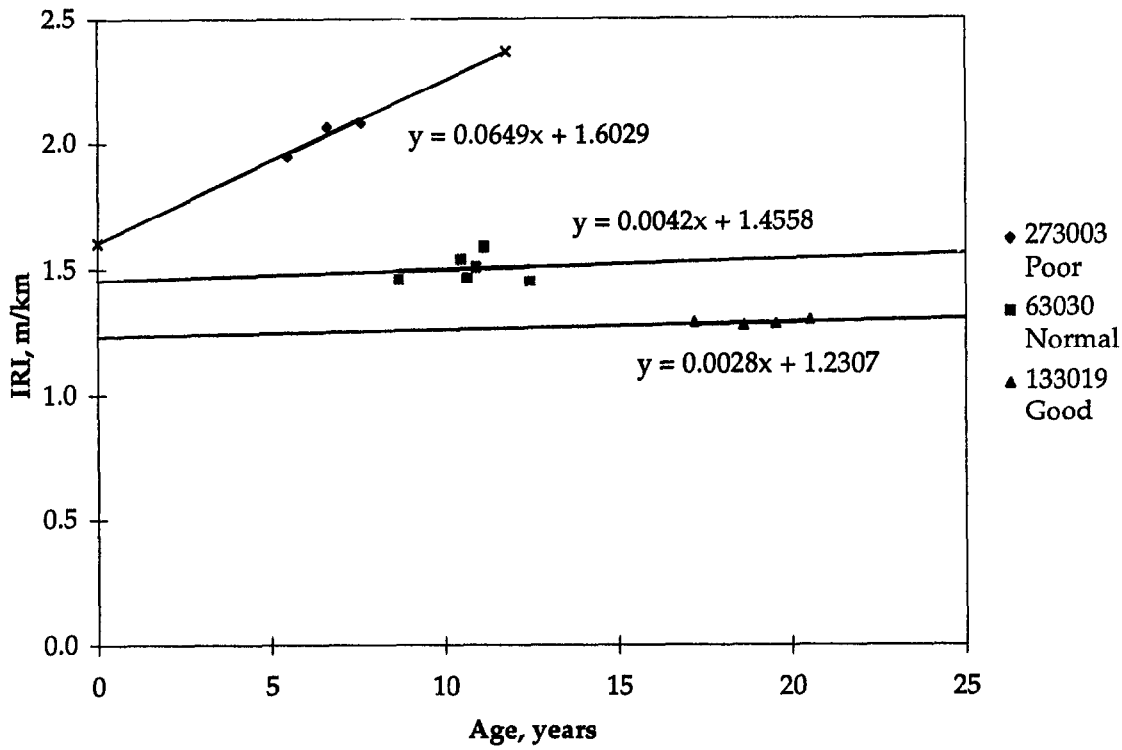

Figure 32. Illustration of IRF and α prediction procedure.

The IRF for a JPCP section may not be exactly equal to the initial as-constructed IRI for a pavement at time zero, IRI_0. A typical pavement section experiences a short-term period of rapid increase when first subjected to traffic loadings and environmental conditions. The rate of increase then decreases, and data collected during this time is used in the linear analysis.

Although IRI_0 and IRF may not be equal, it is believed that they are closely correlated. Therefore, a study to determine the effects of initial pavement roughness on future roughness was conducted using the IRF and α terms. Table 5 presents the resulting IRF and α for 150 pavement sections from GPS-3, GPS-4, and GPS-5 experiments and represents the rate of increase in IRI per year. All types are combined here since there are only limited number of sections from each type of pavement. The JPCP is separated out afterward for illustration.

Figure 33 presents average IRFs for poor, normal, and good LTPP test sections of all ages and pavement types. Poor sections had a mean IRF of 2.09 m/km, whereas normal and good performing sections had mean IRFs of 1.32 and 1.15 m/km, respectively.

The same general trends are seen for the rate of IRI increase, as shown in figure 34. Poor sections have the highest average rate of increase, 0.063 m/km/year, and good sections have the lowest rate, 0.015 m/km/year. Normal performing sections had a mean rate of deterioration of 0.038 m/km/year. This suggests that initial roughness has a very strong effect on future roughness: sections built smooth on average remain smoother, whereas sections built rougher on average will remain rough. If further validated with additional analyses, this is an extremely important finding relative to the justification of construction specifications, including smoothness incentives.

The rate of increase in IRI/yr. ranges widely, probably depending on site conditions and design features. Table 5 shows examples of JPCP built very smooth but having a rapid increase in roughness. Examples also exist of JPCP built rougher but having a low rate of IRI increase.

This analysis was conducted using a very simplified approach to determine initial roughness and deterioration rate characteristics. Because the accuracy of this "backcasting" is higher for newer sections, the analysis was repeated for 70 sections that are less than 15 years in age. Figures 35 and 36 present comparisons of average values of IRF and deterioration slope, respectively, for all pavement types rated as young sections as well as all sections. This comparison of young versus all sections yields similar values of IRF and α values. These results appear to indicate that "backcasting" the IRF may provide, on average, reasonably good estimates for both younger and older pavements. Table 6 summarizes the results of this analysis.

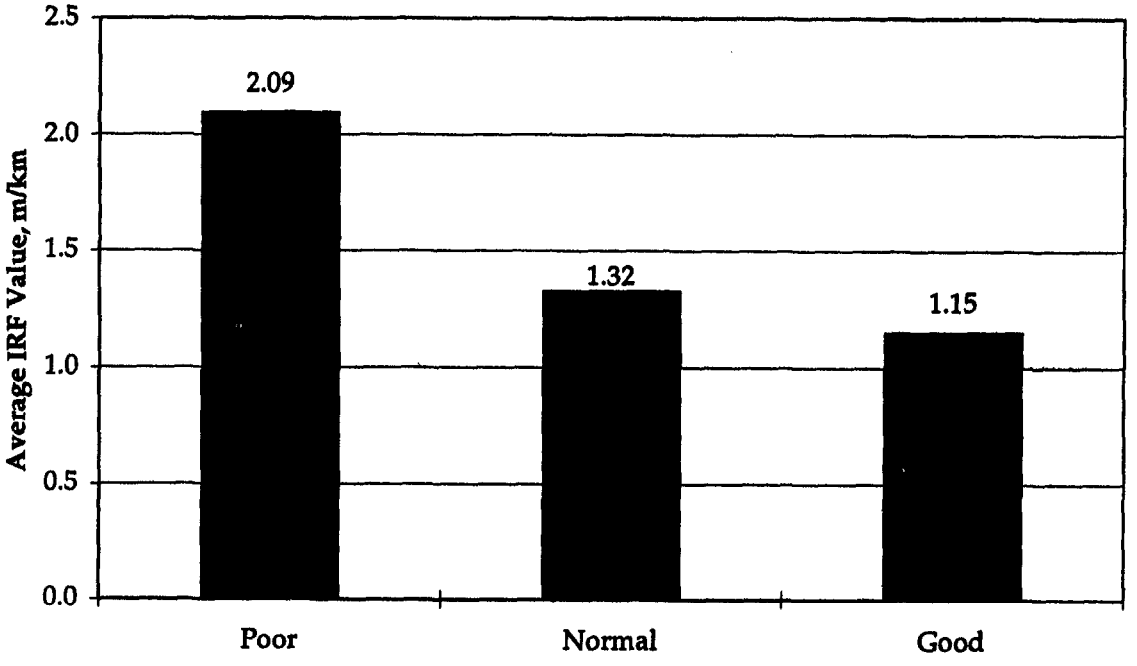

Figure 33. Average IRF (estimate of initial IRI) values for all PCC types and ages.

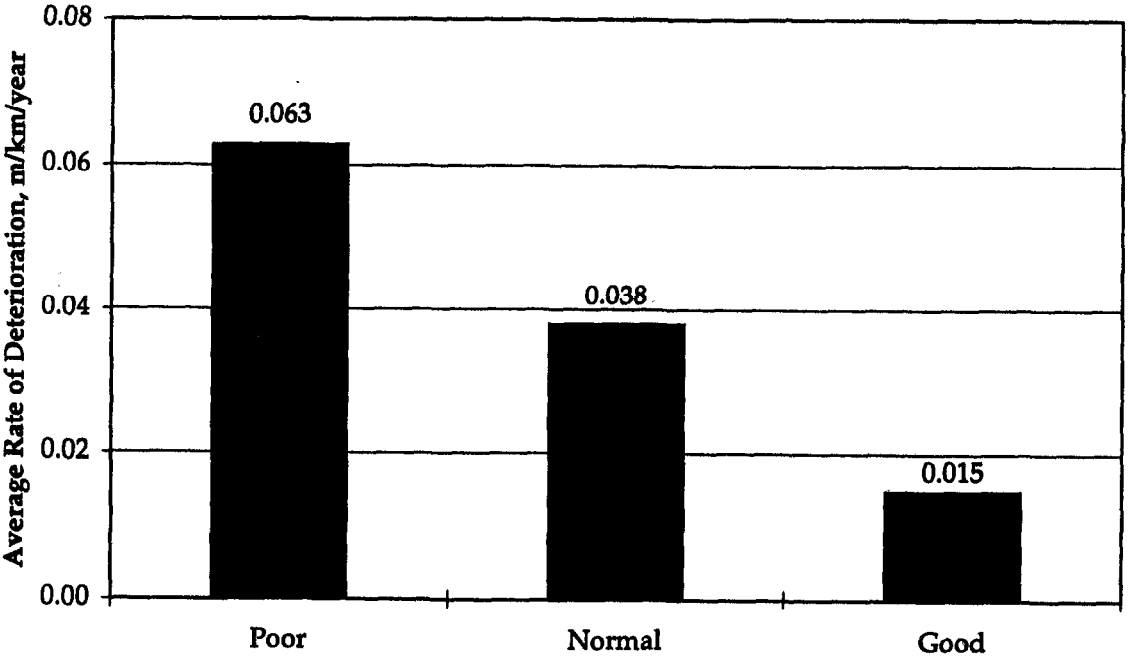

Figure 34. Average rate deterioration, α, for all PCC types and ages.

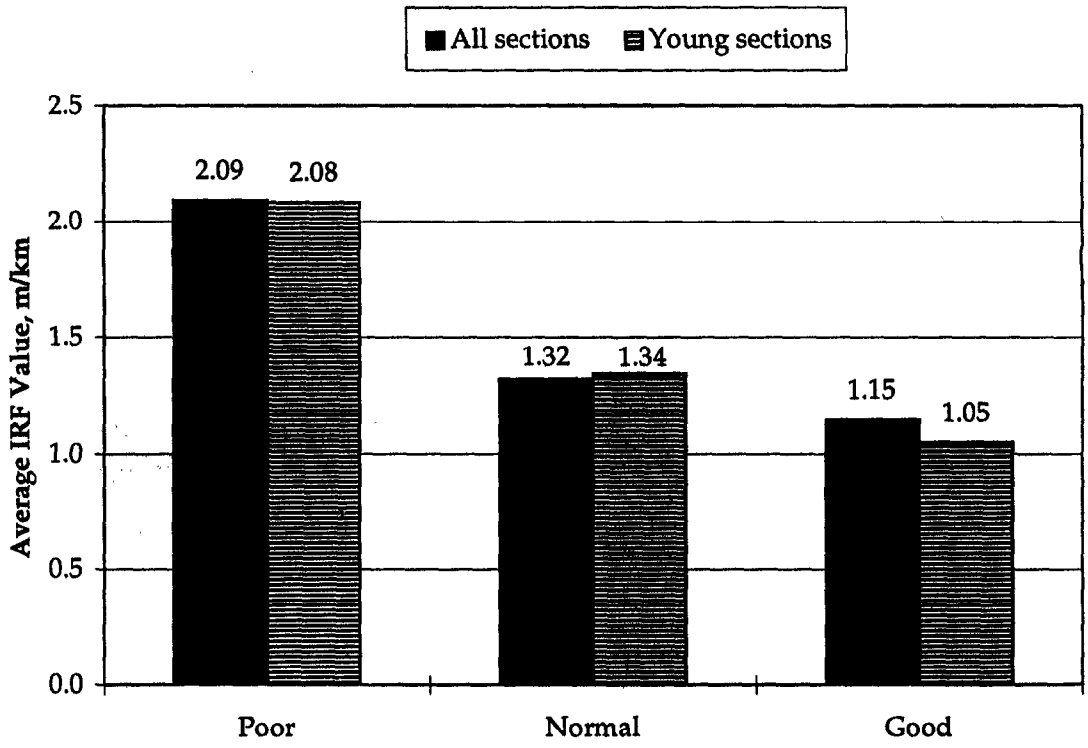

Figure 35. Comparison of average IRF values for all PCC pavement types.

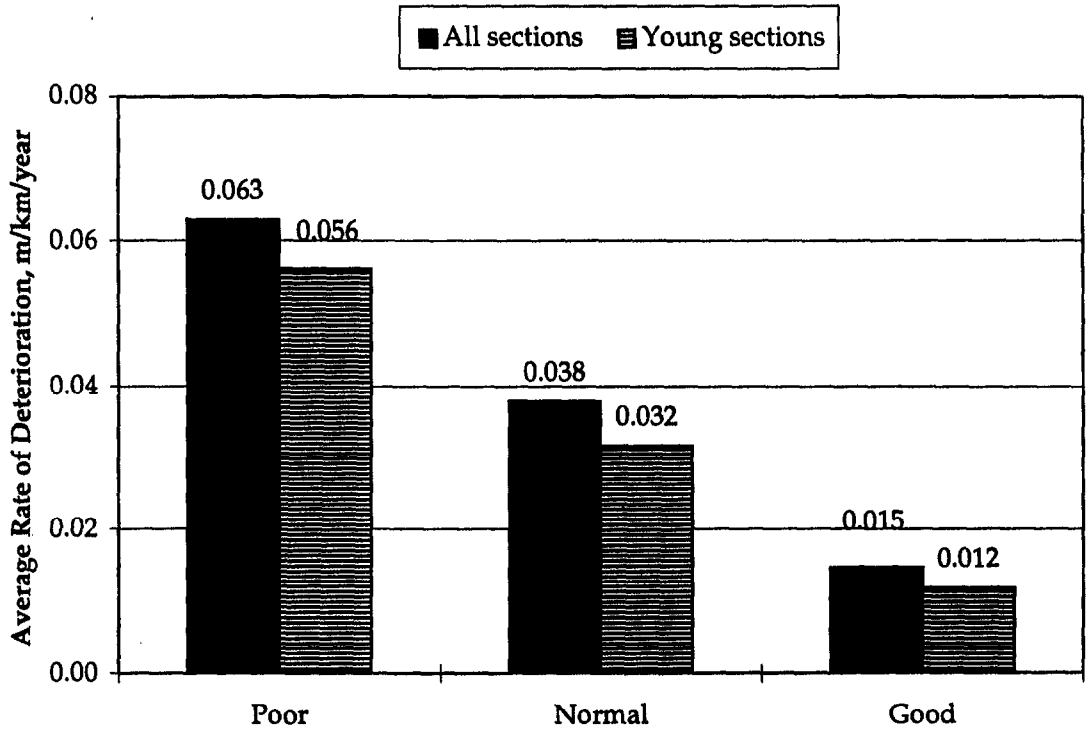

Figure 36. Comparison of average rate of deterioration, α, for all PCC pavement types.

Table 5. Summary of all IRF and rate of IRI increase for all JPCP, JRCP, and CRCP.

State ID	SHRPID	GPS	Performance	IRF m/km	ALPHA m/km/year
1	3028	3	bad	2.278	0.051
5	3011	3	good	0.906	0.027
6	3010	3	good	0.982	0.020
6	3017	3	good	1.354	0.011
6	3019	3	normal	1.344	0.010
6	3021	3	good	1.317	0.005
6	3024	3	normal	1.415	0.002
6	3030	3	good	1.231	0.003
8	7776	3	normal	1.376	0.025
12	3804	3	normal	0.987	0.109
12	3811	3	normal	1.218	0.035
12	4057	3	good	0.686	0.018
12	4138	3	normal	1.843	0.052
13	3007	3	normal	1.722	0.007
13	3015	3	good	1.157	0.006
13	3018	3	good	0.817	0.009
13	3019	3	normal	1.456	0.004
13	3020	3	normal	1.322	0.005
16	3017	3	normal	1.529	0.008
16	3023	3	normal	1.367	0.023
18	3002	3	normal	1.738	0.003
19	3006	3	bad	1.011	0.121
19	3009	3	normal	2.287	0.000
19	3055	3	good	1.107	0.028
23	3013	3	normal	1.693	0.023
23	3014	3	good	1.026	0.026
27	3003	3	bad	1.602	0.065
27	3013	3	normal	1.232	0.008
28	3018	3	normal	1.359	0.051
28	3019	3	normal	1.065	0.083
31	3018	3	normal	0.909	0.086
31	3023	3	good	1.098	0.006

Table 5. Summary of all IRF and rate of IRI increase for all JPCP, JRCP, and CRCP (continued).

State ID	SHRPID	GPS	Performance	IRF m/km	ALPHA m/km/year
31	3033	3	normal	0.568	0.072
32	3010	3	normal	1.694	0.058
32	3013	3	normal	1.144	0.056
35	3010	3	good	1.233	0.005
37	3008	3	normal	1.482	0.022
37	3044	3	good	1.345	0.024
37	3816	3	normal	2.006	0.010
39	3013	3	bad	1.980	0.090
40	3018	3	normal	1.140	0.057
40	4160	3	normal	1.586	0.011
45	3012	3	good	0.993	0.017
46	3010	3	normal	1.993	0.018
46	3012	3	bad	2.823	0.001
46	3053	3	normal	1.090	0.013
46	6600	3	normal	0.873	0.081
48	3003	3	normal	1.904	0.011
49	3010	3	normal	0.519	0.084
49	3011	3	normal	0.420	0.110
49	3015	3	normal	1.942	0.006
49	7082	3	normal	0.912	0.046
53	3011	3	good	1.323	0.016
53	7409	3	normal	0.846	0.057
55	3008	3	bad	2.024	0.103
55	3010	3	normal	0.128	0.150
55	3014	3	bad	3.264	0.010
55	3015	3	bad	1.787	0.037
55	3016	3	normal	1.245	0.006
55	3019	3	good	0.625	0.036
55	6352	3	normal	1.208	0.009
84	3803	3	bad	1.004	0.147
89	3002	3	bad	2.685	0.081

Table 5. Summary of all IRF and rate of IRI increase for all JPCP, JRCP, and CRCP (continued).

State ID	SHRPID	GPS	Performance	IRF m/km	ALPHA m/km/year
89	3015	3	normal	0.669	0.122
1	4084	4	normal	0.827	0.109
5	3059	4	normal	1.142	0.043
5	3073	4	good	1.821	0.006
5	4021	4	good	1.808	0.003
5	4046	4	normal	0.859	0.065
10	4002	4	normal	2.131	0.001
20	4016	4	good	1.321	0.008
20	4052	4	normal	1.656	0.006
20	4053	4	normal	1.155	0.071
20	4054	4	normal	1.295	0.064
20	4063	4	normal	1.899	0.010
21	4025	4	normal	1.135	0.083
22	4001	4	good	0.029	0.086
26	4015	4	normal	1.621	0.000
27	4033	4	normal	0.721	0.057
27	4034	4	good	1.365	0.020
27	4037	4	normal	1.049	0.040
27	4040	4	normal	1.646	0.012
27	4054	4	normal	0.269	0.083
27	4055	4	good	1.144	0.000
28	4024	4	good	0.793	0.041
29	4036	4	normal	0.959	0.047
29	5000	4	normal	1.722	0.022
29	5058	4	good	1.438	0.011
29	5081	4	normal	0.845	0.073
29	5091	4	good	1.481	0.006
29	5503	4	normal	0.929	0.044
31	4019	4	normal	0.460	0.090
36	4017	4	normal	1.829	0.011
36	4018	4	good	1.719	0.002
39	4031	4	good	1.602	0.017

Table 5. Summary of all IRF and rate of IRI increase for all JPCP, JRCP, and CRCP (continued).

State ID	SHRPID	GPS	Performance	IRF m/km	ALPHA m/km/year
42	1606	4	good	1.206	0.018
48	3699	4	good	0.950	0.037
48	4142	4	normal	1.691	0.017
48	4143	4	normal	1.954	0.014
48	4146	4	normal	2.103	0.005
48	4152	4	bad	2.539	0.013
54	4003	4	normal	1.404	0.022
54	4004	4	bad	2.214	0.063
5	5805	5	good	1.191	0.006
9	5001	5	normal	1.859	0.000
10	5004	5	good	1.080	0.007
10	5005	5	good	1.034	0.002
17	5843	5	normal	0.238	0.114
17	5854	5	normal	1.586	0.055
17	5869	5	normal	1.527	0.009
17	5908	5	good	1.975	0.002
17	9267	5	good	0.587	0.021
18	5043	5	normal	0.473	0.081
19	5046	5	good	1.450	0.006
26	5363	5	normal	1.555	0.016
27	5076	5	good	0.410	0.021
28	5006	5	good	0.855	0.048
28	5025	5	good	0.345	0.057
28	5803	5	normal	0.707	0.074
28	5805	5	good	1.303	0.001
31	5052	5	good	0.996	0.004
37	5037	5	good	1.066	0.003
39	5003	5	normal	1.037	0.012
40	4158	5	normal	0.909	0.028
40	4166	5	good	0.870	0.010
41	5006	5	good	1.219	0.008
41	5008	5	good	0.735	0.010

Table 5. Summary of all IRF and rate of IRI increase for all JPCP, JRCP, and CRCP (continued).

State ID	SHRPID	GPS	Performance	IRF m/km	ALPHA m/km/year
41	5021	5	normal	0.862	0.031
41	5022	5	good	0.961	0.004
42	1598	5	good	1.584	0.006
45	5017	5	normal	1.795	0.017
46	5025	5	good	1.276	0.000
46	5040	5	good	1.409	0.024
48	3779	5	normal	1.968	0.013
48	5024	5	bad	2.315	0.021
48	5035	5	normal	1.710	0.007
48	5154	5	good	1.427	0.008
48	5274	5	good	1.523	0.006
48	5278	5	good	1.655	0.000
48	5283	5	normal	1.127	0.007
48	5284	5	bad	1.765	0.076
48	5287	5	normal	1.391	0.028
48	5301	5	normal	1.557	0.009
48	5317	5	normal	1.930	0.032
48	5323	5	normal	1.738	0.003
48	5336	5	normal	1.423	0.002
51	2564	5	good	0.925	0.002
51	5010	5	normal	1.482	0.024
54	5007	5	normal	1.312	0.081
55	5040	5	normal	2.272	0.006

Table 6. Comparison of IRF and deterioration rate for JPCP, JRCP, and CRCP pavement types combined.

Parameter	Category	All Sections	Young Sections
Initial Roughness IRF, mm/km	Poor	2.09	2.08
	Normal	1.32	1.34
	Good	1.15	1.05
Rate of IRI Increase α, mm/km/year	Poor	0.063	0.056
	Normal	0.038	0.032
	Good	0.015	0.012

A comparison between young and all sections for JPCP is presented in figures 37 and 38 for IRF and rate of deterioration, respectively. These values are not significantly different either. All results are summarized in table 7 for the JPCP sections. The rate of deterioration of JPCP is a little higher than the mean of all concrete pavement types.

Table 7. Comparison of IRF and deterioration rate for JPCP.

Parameter	Category	All Sections	Young Sections
Initial Roughness IRF, mm/km	Poor	2.05	1.98
	Normal	1.30	1.28
	Good	1.08	1.05
Rate of IRI increase α, mm/km/year	Poor	0.071	0.066
	Normal	0.041	0.036
	Good	0.016	0.013

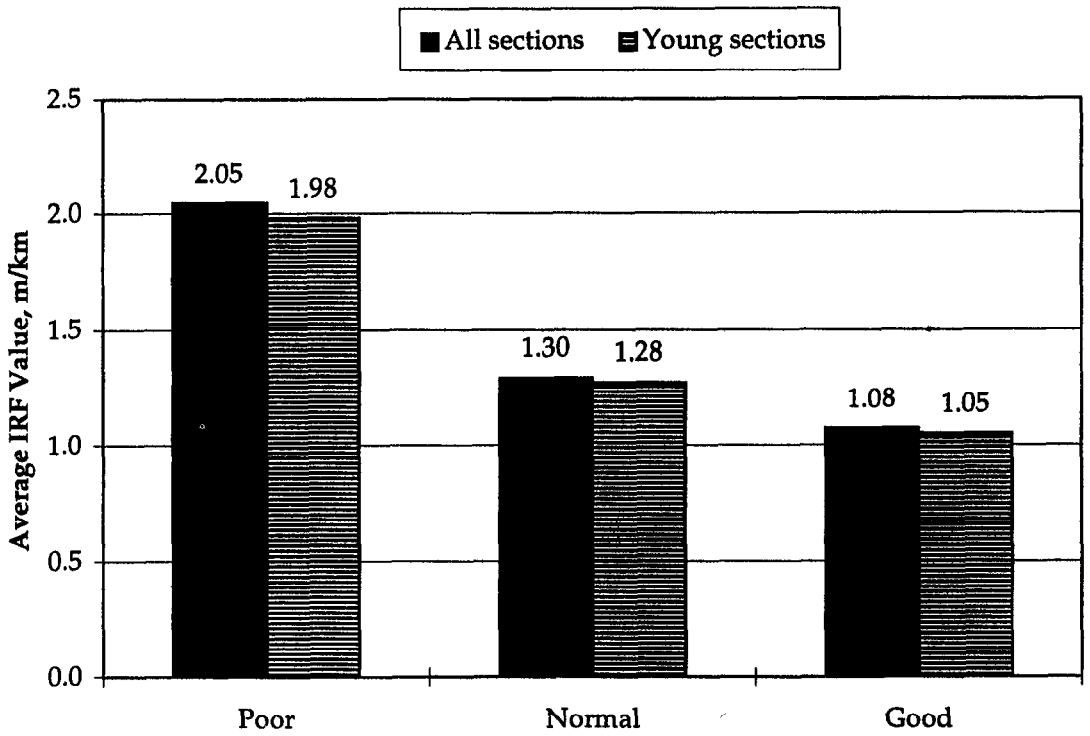

Figure 37. Comparison of average IRF values for JPCP.

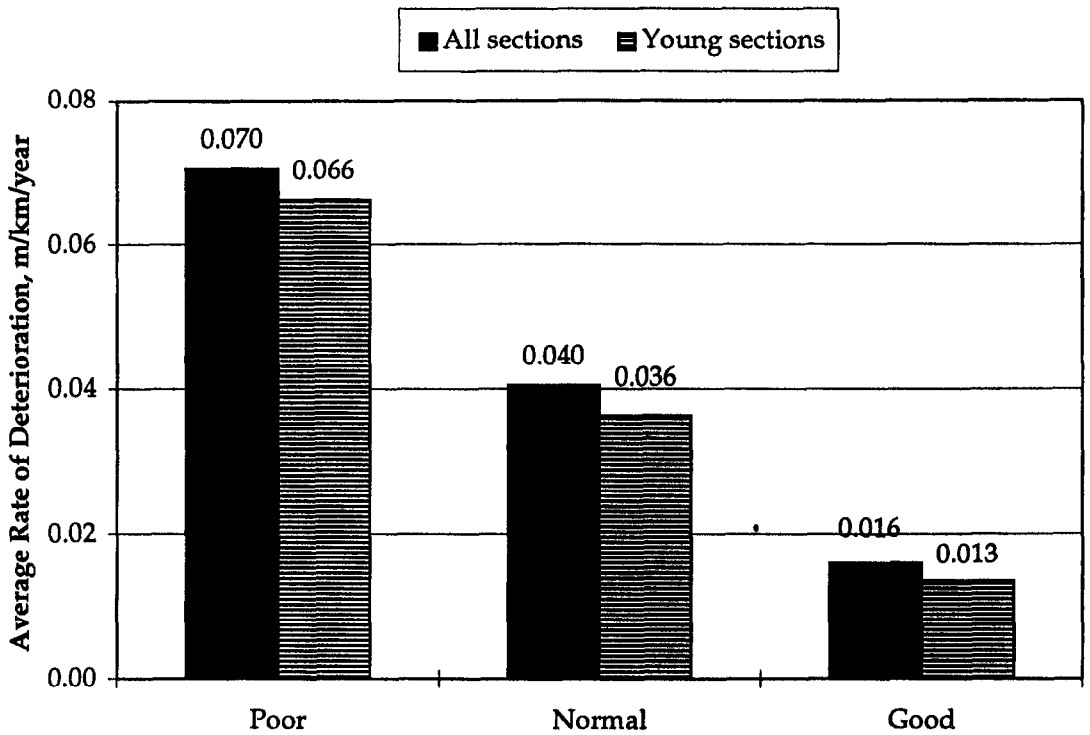

Figure 38. Comparison of average rate of deterioration, α, for JPCP.

Summary of IRI for JPCP

This analysis showed that there are several site conditions and design and construction features that affect the IRI of JPCP over time and traffic. IRI is an extremely important performance characteristic of any type of pavement because of its impact on the traveling public.

The following site conditions were found to have either a significant effect on the IRI of JPCP, or to show a strong trend in affecting IRI of JPCP.

- **Climate:** Several temperature variables and one moisture variable were found to be related to roughness of JPCP.
    - Latitude and longitude: JPCP located in the southwestern United States were smoother.
    - Freezing index: JPCP located in colder climates were rougher.
    - Mean air freeze-thaw (F-T) cycles: JPCP subjected to increased F-T cycles were rougher.
    - Mean annual temperatures (minimum, mean, maximum): warmer climates show smoother JPCP.
    - Mean number of days above 32°C: JPCP in warmer climates were smoother.
    - Mean number of days below 0°C: JPCP in colder climates, were rougher.
    - Mean number of wet days per year: JPCP with increased number of rain days were rougher.

- **Traffic:** JPCP in the good IRI performance category carried much higher ESALs than those classified as poor or normal. There was too much collinearity between key variables to show other significance (e.g., JPCP with higher traffic were designed to carry heavier traffic). However, ESALs are included in several previous multivariate models that show increased ESALs increase IRI.

- **Subgrade:** JPCP constructed on coarse-grained subgrades were smoother than JPCP on fine-grained subgrades. Seventy-one percent of poor JPCP had a fine-grained subgrade, but only 29 percent of JPCP constructed on course grained soils had poor IRI performance.

The following design and construction features were found to be either statistically significant or to have a strong trend in keeping a JPCP smoother over time:

- **Base type and elastic modulus of the base course:** Sections with higher base modulus have a lower mean IRI.

  JPCP with a granular base had a significantly higher IRI than JPCP with a stabilized base.

  JPCP with granular base had much larger percentage of sections in the poor IRI performance group (82 percent) than JPCP with stabilized base (18 percent).

  JPCP with asphalt stabilized base had significantly lower IRI than all other bases. JPCP with a lean concrete base also had significantly lower IRI than other bases. The same was not true for cement-treated bases.

- **Subdrainage coefficient** (precipitation, permeability of base, edge drains, coarse-grained subgrade): JPCP with higher drainage coefficients all had low IRIs (smoother pavement). Higher drainage coefficients were the result of lower precipitation, permeable base, edge drains, and coarse-grained subgrades.

- **Dowel bars at transverse joints:** This design feature affects the IRI much more after 10 years than during the first 10 years. After 10 years, JPCP with dowels were smoother than those without dowels.

- **Initial roughness/smoothness of JPCP:** The data analysis showed that the average roughness of a JPCP over time depends greatly on its initial IRI. The analysis also showed that the average rate of increase in IRI over time is higher for those JPCP that are rated poor than for those rated good. Thus, smoother construction results in smoother JPCP over time and traffic.

  For example, a JPCP rated poor would have an initial IRI of approximately 2.09 m/km as contrasted to a JPCP rated good would have an initial IRI of approximately 1.15m/km. The average rate of increase in IRI for poor sections is five times higher than good sections.

CHAPTER 5. PERFORMANCE OF JRCP IN ROUGHNESS

Previous Studies

The performance of JRCP with respect to roughness has been investigated in several studies. The IRI predictive model developed for JRCP in the early LTPP Data Analysis Study is as follows:[1]

$$IRI = -2.225 + 0.0134 * AGE + 0.000216 * PRECIP + 5.967 * [1/KSTATIC] + 0.0132\ HPCC + 0.2383 * EDGESUP \quad (8)$$

where

IRI	=	International Roughness Index, m/km
AGE	=	pavement age, years
PRECIP	=	mean annual precipitation, mm
KSTATIC	=	FWD backcalculated modulus of subgrade reaction (divided by 2), kPA/mm
HPCC	=	PCC slab thickness, mm
EDGESUP	=	edge support (=1 if tied PCC shoulder; =0 otherwise)

This model predicts IRI as a function of site conditions and JRCP design features. Age (and, of course, the associated accumulated traffic loadings) is positively correlated to IRI; that is, an increase in age corresponds to an increase in IRI. Pavement distress that results in increased roughness increases with aging and traffic. This model indicates that increasing JRCP slab thickness results in increased IRI. Pavement features such as the modulus of subgrade reaction, precipitation, and the PCC slab edge support conditions have an influence on the IRI, although not as pronounced.

One prediction model exists for the mean panel present serviceability rating (PSR) for JRCP. Although PSR is not the same as IRI, Al Omari and Darter showed an approximate correlation between the two.[5] The following model was developed for PSR of JRCP but did not use the LTPP data base.[7] Data from four States were used.

$$PSR = 4.5 - CESAL^{0.424}(-1.88*10^{-3} + 14.417\ RATIO^{3.58} + 0.0399\ PUMP + 0.00718\ JTSPACE + 0.1146\ DCRACK + 0.05903\ REACTAG + 7.48*10^{-5}\ FI + 6.42*10^{-5}\ PRECIP - 0.070535\ BASE) \quad (9)$$

where

PSR	=	present serviceability rating (mean panel rating of ride quality)
CESAL	=	accumulated 80-kN ESALs, millions
RATIO	=	Westergaard's edge stress/modulus of rupture
PUMP	=	pumping (=1 if medium or high pumping exists; 0 if no or low-severity pumping exists)
JTSPACE	=	transverse joint spacing, m
DCRACK	=	D-cracking (=1 if D-cracking exists; =0 for no D-cracking)
REACTAG	=	reactive aggregate (=1 if reactive aggregates exist; 0 if no reactive aggregate exists)
FI	=	Freezing index
PRECIP	=	average annual precipitation, mm
BASE	=	base type (=1 if stabilized base; =0 if granular base)

This study showed that traffic level, stress ratio, transverse joint spacing, the presence of aggregate durability problems, freezing index, precipitation, slab thickness, and pumping all have an effect on the roughness characteristics of JRCP.

A recent study utilizing the LTPP data base resulted in developing of the following IRI model for JRCP.[3]

$$IRI = 1.2721 + 0.00836\ KESAL^{0.4}*PSTEEL + 0.0074\ AGE^{0.7}\ (5.78 + 0.0106\ PRECIP - 1.95\ DRAIN - 3.73\ SUBGTYP) \quad (10)$$

where

IRI	=	International Roughness Index, m/km
KESAL	=	cumulative 80-kN ESALs, thousands
PSTEEL	=	percent steel
AGE	=	pavement age, years
PRECIP	=	average annual precipitation, mm
DRAIN	=	presence of edgedrain, 1 = edgedrain, 0 = no edgedrains
SUBGTYP	=	subgrade type, 1=coarse-grained, 0=fine-grained

This model indicates that pavement age, annual precipitation, slab thickness, and subdrainage all have an effect on the roughness characteristics of JRCP. Increased slab thickness also results in increased IRI, as in the first model derived from LTPP data.

Table 8 summarizes the design and site condition variables that were found to be significant. Note that none of the models considered the initial IRI immediately after construction. However, the initial IRI has been shown to be an important factor for JRCP.[4]

Table 8. Summary of the effects of site conditions and design features on IRI of JRCP.

Design Feature	Effect on IRI	Reference
Pavement age	Increases *	1, 3
Subgrade k-value	Decreases	1
Joint spacing	Increases	7
PCC thickness	Increases	1, 3
Percent reinforcement	Increase	3
Traffic	Increases	7
Stabilized base	Decreases	7
Tied PCC shoulder	Increases	1
Precipitation	Increases	1,3,7
Drainage, C_d	Decreases	3
FI	Increases	7
Initial Roughness	Increases	4

*For example, as pavement age increases, IRI or roughness increases. As the k-value increases, IRI decreases.

Performance Criteria for IRI

The following analysis evaluates site conditions and design/construction features that may effect roughness of JRCP as measured by the IRI extracted from the LTPP data base. The LTPP data base contains IRI data for 65 JRCP sections and 265 observations. The number of observations per section varied from 1 to 10.

The data was divided into three performance categories: poor, normal, and good, based on the IRI value corresponding to a specific pavement age. This grouping facilitated selection of factors that contribute to good and poor performance in terms of roughness. The differentiation between the groups was based on recommendations of an expert panel of State highway engineers and researchers. The established limits are shown in figure 39. A pavement was considered to be good performing (i.e., performing better than expected) if its IRI satisfied the following condition:

$$IRI < 0.631 + 0.0631 * AGE \tag{11}$$

where

IRI = International Roughness Index, m/km
AGE = pavement age at the time of the IRI observation, years

The pavement section was considered to be performing poor if its IRI satisfied the following condition:

$$IRI > 1.262 + 0.0947 * AGE \tag{12}$$

where

IRI = International Roughness Index, m/km
AGE = pavement age at the time of the IRI observation, years

Figure 39 shows the IRI values and corresponding time of observation for the JRCP sections evaluated. Since the number of observations differs among the sections, the use of all observations in the analysis may bias the results toward sections with a higher number of observations. To avoid this, only the last observation for each section was considered in the analysis unless stated otherwise. Figure 40 presents a plot of all JRCP (GPS-4) sections with respect to IRI at the time of the last available observation.

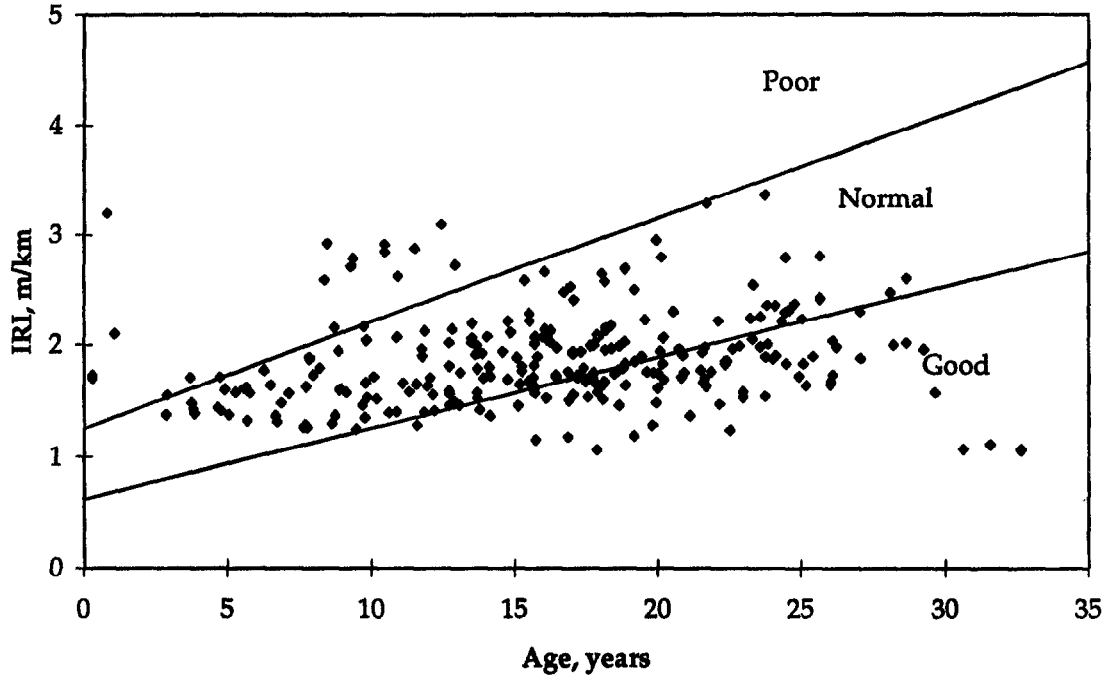

Figure 39. IRI for JRCP including all time-series data.

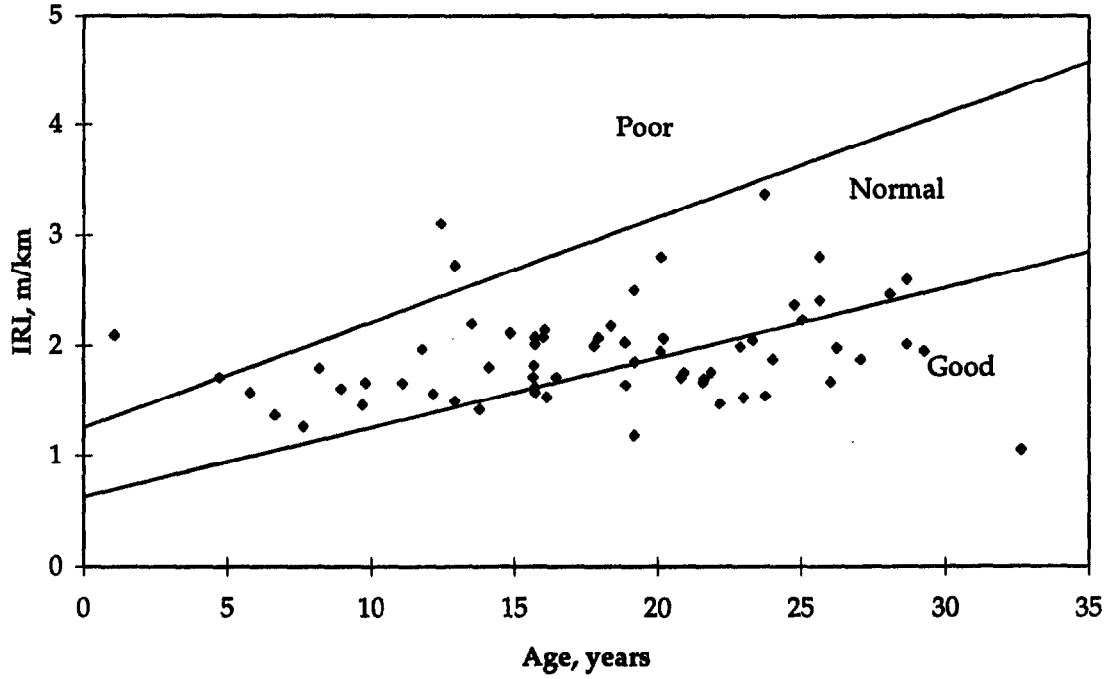

Figure 40. IRI for JRCP (last IRI observation only).

Factors Considered for IRI

Factors affecting the IRI of JRCP may be categorized as either site conditions or design and construction features. The factors evaluated in this study include those found to be significant in previous studies and based on engineering experience:

- **Site Conditions**
  - o Geographic location
    - Latitude
    - Longitude
  - o Temperature factors
    - Freezing Index
    - Freeze-thaw cycles
    - Mean annual temperature
    - Minimum annual temperature
    - Maximum annual temperature
    - Number of days warmer than 32 °C
    - Number of days colder than 0 °C
  - o Precipitation factors
    - Average annual precipitation
    - Average number of wet days/year
  - o Subgrade soil type
  - o Traffic (ESAL)

- **Design and Construction Features**
  - o Slab thickness
  - o Concrete properties
    - Modulus of elasticity
    - Modulus of rupture
  - o Joint spacing
  - o Base type
  - o Dowels
  - o Drainage coefficient
  - o Design steel content
  - o Initial as-constructed roughness
  - o Method used to texture concrete

Comparative and Statistical Analysis of IRI

Two general types of analyses were performed: a visual comparative analysis and a statistical analysis. Comparative analysis includes visual analysis of plots with a

distribution of pavement sections by their performance as a function of those factors, and a comparison of average values of those factors for different groups of pavement sections. The plots can be observed and the graphical results evaluated as to significance.

Statistical analyses conducted include the bivariate t-test and in some cases multivariate analyses to identify those site conditions and design features that contribute to good and poor roughness performance. The JRCP section data were partitioned into two groups based on IRI: those that fell into the good group and those that fell into the poor/normal group (note that the poor/normal group will subsequently be called the poor group for convenience). The normal group had to be used in the analysis due to the limited number of sections available.

Table 9 provides a summary of all the t-values for each comparison made for continuous variables. Table 10 provides a summary of Fisher's exact tests for discrete variables for IRI of JRCP. These will be referred to during the following presentation. The significant variables at the 90 or 95 percent confidence level consist of KESAL, AGE, HPCC, and EBASE. However, t-tests and Fisher's exact tests are one-dimensional and do not consider collinearity with other variables. Stated differently, the interrelationship with other variables could be masking a variable's true relationship with IRI. This collinearity can only be considered through further rigorous statistical analyses.

In this study, two-dimensional plots of IRI with respect to various parameters were analyzed. A comparison of the mean values of those parameters and good, normal, and poor sections was performed. Although the results of this analysis are of great interest because they highlight the most significant visual trends in pavement roughness, they must be viewed with caution since the interrelationship of the variables may have a significant influence on the observed trends.

Table 9. Results of t-tests for JRCP IRI performance.

	Mean Poor*	Mean Good	t separ. var. est	df	p 2-sided	Valid N Poor	Valid N Good	Std. dev. Poor	Std. dev. Good	F-ratio variance	p variance
FI	388.712	372.209	0.167	36.375	0.868	22	42	397.778	329.222	1.460	0.295
FT	76.329	79.319	-0.500	49.786	0.619	22	42	21.200	25.300	1.422	0.390
PRECIP	1050.214	1055.268	-0.081	44.899	0.936	22	42	233.680	246.380	1.117	0.805
WETDAYS	125.772	131.148	-1.009	58.078	0.317	22	42	17.000	25.300	2.226	0.052
LONG	87.273	89.000	-0.848	34.184	0.402	22	43	8.400	6.500	1.676	0.153
LAT	38.727	38.233	0.443	39.443	0.660	22	43	4.400	4.000	1.181	0.630
TMAX	17.941	17.250	0.504	60.765	0.616	22	42	4.111	6.833	2.791	0.014
TMIN	6.224	5.285	0.687	61.340	0.495	22	42	4.000	6.944	3.014	0.009
TMEAN	12.082	11.268	0.597	61.128	0.553	22	42	4.000	6.889	2.921	0.010
DAYS32	30.126	32.123	-0.305	41.481	0.762	22	42	25.200	24.300	1.071	0.825
DAYS0	102.435	102.368	0.006	42.138	0.995	22	42	42.800	42.100	1.033	0.899
JTSPACE	14.795	15.126	-0.277	52.572	0.783	22	43	4.118	5.307	1.643	0.222
SKEW	0.083	0.074	0.156	41.471	0.877	22	43	0.214	0.214	1.053	0.859
DOWDIAM	27.711	28.651	-0.465	43.648	0.644	22	43	7.620	7.620	1.065	0.902
PSTEEL	0.158	0.140	0.434	15.083	0.671	12	21	0.100	0.100	3.147	0.025
KESAL	10063.810	6992.381	1.175	30.821	0.249	21	42	10659.400	7716.100	1.908	0.079
HPCC	234.823	245.313	-2.084	43.810	0.043	22	43	17.780	20.320	1.074	0.885
MR28	4719.064	4801.124	-0.713	56.568	0.479	22	43	378.950	538.109	2.016	0.086
EPCC	28102.893	27919.973	0.380	51.605	0.705	22	43	1679.774	2103.472	1.568	0.269
EBASE	1298.139	2146.563	-1.250	48.146	0.217	22	42	2450.126	2807.060	1.313	0.510
C_d	0.859	0.860	-0.040	39.727	0.968	22	43	0.100	0.100	1.161	0.662
KSTATIC	41.478	38.450	0.480	35.482	0.634	20	33	23.464	20.100	1.363	0.428

* Poor group combines poor and normal sections.

where

FI	= Freezing Index, °C-days	JTSPACE	= Distance between slab joints, m
FT	= Annual air freeze-thaw cycles	SKEW	= Joint skewness, m
PRECIP	= Mean annual precipitation, mm	PSTEEL	= Percentage of reinforcement of cross-section area
WETDAYS	= Mean number of wet days	KESAL	= 80-kN equivalent single axle load, thousands
LONG	= Longitude location, degrees	HPCC	= Thickness of PCC slab, mm
LAT	= Latitude location, degrees	MR28	= Mean 28-day modulus of rupture, kPa
TMIN	= Minimum annual temperature, °C	EPCC	= Mean 28-day elastic modulus, MPa
TMAX	= Maximum annual temperature, °C	EBASE	= Mean base-layer modulus of elasticity, MPa
TMEAN	= Mean annual temperature, °C	C_d	= AASHTO drainage coefficient
DAYS32	= Annual number of days with temperature higher than 32°C	KSTATIC	= Static elastic modulus of subgrade reaction, kPa/mm
DAYS0	= Annual number of days with temperature lower than 0°C	DOWDIAM	= Dowel diameter, mm

Table 10. Results of Fisher Exact Tests for JRCP IRI performance.

	Fisher Exact		
	One-tailed p	Two-tailed p	Description of variable
DOWELS	0.737	1.000	= 1, if dowels present = 0, if no dowels
GRANBAS	0.010	0.017	=1, if granular base present =0, otherwise
ACBASE	0.169	0.248	=1, if asphalt stabilized base present =0, otherwise
CEMBASE	0.361	0.737	=1, if cement-treated base present =0, otherwise
BASE	0.009	0.015	=1, if stabilized base present =0, otherwise
SUBGR	0.401	0.770	=1, if subgrade is coarse-grained soil =0, otherwise
WW	0.439	0.791	=1, if a climate is warm-wet =0, otherwise
CW	0.578	1.000	=1, if a climate is cold-wet =0, otherwise
TEXT1	0.003	0.004	=1, if tine is used to texture concrete =0, otherwise
TEXT3	0.001	0.001	=1, if burlap drag is used to texture concrete surface =0, otherwise
SEAL1	0.385	0.701	=1, cold application sealant type =0, otherwise
SEAL3	0.347	0.536	=1, hot poured for PCC sealant type =0, otherwise

Site Conditions

Geographic Location. Latitude and longitude are closely related to climatic factors such as precipitation and air temperature. No clear trend relating latitude and longitude to IRI was found for the JRCP sections evaluated. The results of the t-test, shown in table 9, do not show latitude and longitude to be significant in affecting IRI. There were no JRCP located in the southwestern United States, as with the JPCP sections that showed location to be significant. Specific climatic variables that may influence IRI are discussed below.

Temperature Factors. The following temperature parameters were considered in this study: freezing index (FI), number of air freeze-thaw cycles (FT), mean annual temperature (T_{mean}), minimum annual temperature (T_{min}), maximum annual temperature (T_{max}), number of days per year with a temperature higher than 32°C (DAYS32), and number of days per year with a temperature lower than 0°C (DAYS0). No clearly defined trends relating IRI with the temperature factors were observed. In addition, none of these parameters was found to be significant in the t-test analysis (table 9).

Precipitation Factors. Two precipitation factors were analyzed in this study: average annual precipitation and average number of wet days per year. No clear trend was observed relating annual precipitation levels to IRI. The results of the t-test (table 9) also fail to show significance of this variable. However, the multivariate analysis shown later clearly indicated that precipitation is positively correlated with IRI.
Figures 41 and 42 show the average number of wet days versus IRI. The average number of wet days for poor pavements is higher than for good and normal sections. The mean value of wet days for poor sections was 144 days, whereas the mean values for normal and good sections were 130 and 126 days, respectively. This confirms the findings and trends of previous studies which showed that the increased presence of moisture advances pavement deterioration. The t-test, however, did not verify significance of this difference (see table 9) because poor sections were combined with normal. The results would be different if poor sections were analyzed versus combined normal and good. An insufficient number of poor sections did not permit this comparison. It should be noted that increased precipitation effects might be reduced by pavement drainage provisions and thus the effect negated for JRCP.

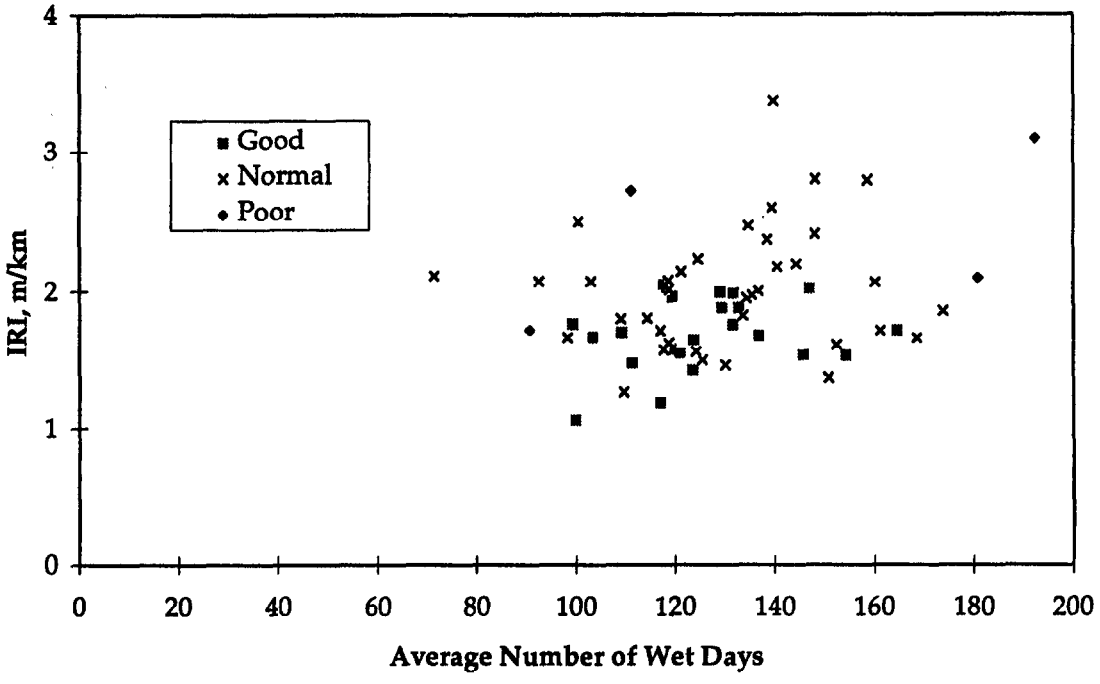

Figure 41. Average number of wet days versus IRI for JRCP.

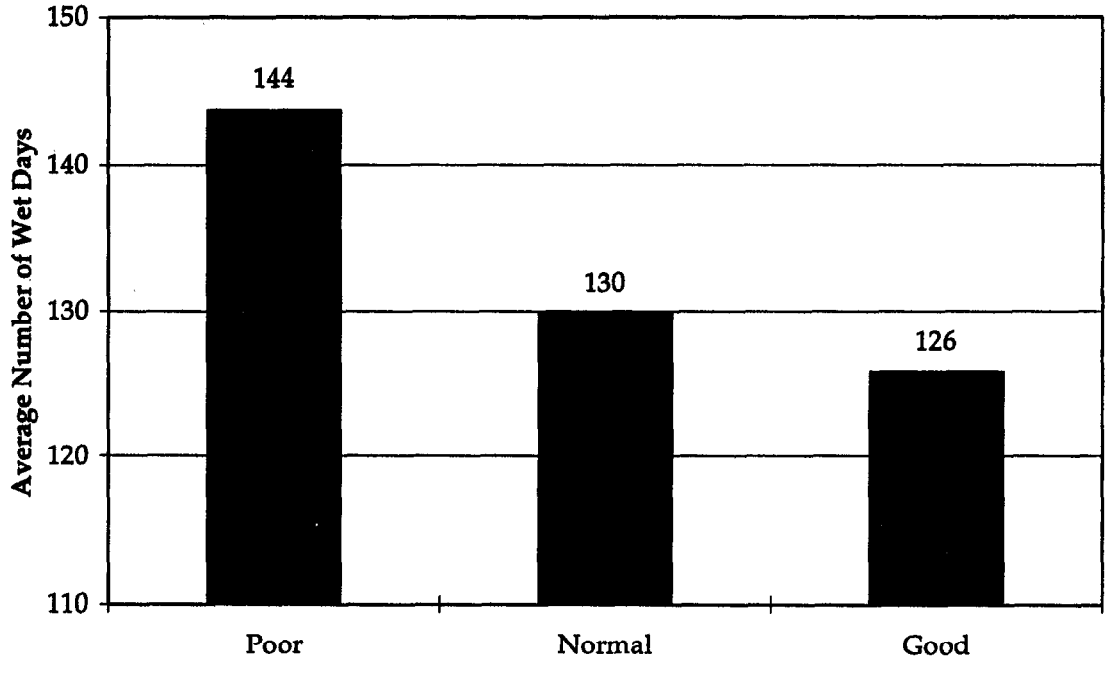

Figure 42. Effect of average number of wet days on JRCP performance.

Subgrade Soils. The subgrade soils are differentiated as fine-grained and coarse-grained based on AASHTO classification criteria. Figure 43 illustrates that, in general, JRCP constructed on coarse-grained soils perform better than those constructed on fine-grained soils. Every one of the poor performing JRCP sections evaluated was constructed on fine-grained subgrade soil. Seventy-one percent of the normal sections and 68 percent of the good sections were constructed on fine-grained subgrade soils. However, the Fisher's exact test (table 10) did not confirm the statistical significance of subgrade soil because poor and normal sections were combined.

Traffic. Figure 44 shows the relationship between applied KESALs and IRI. It is expected that increased levels of traffic would lead to an increase in IRI. Figure 45 shows that the good pavements received more ESALs than the poor pavements. However, due to the apparent influence of other design parameters, the t-test found no statistical significance of this difference.

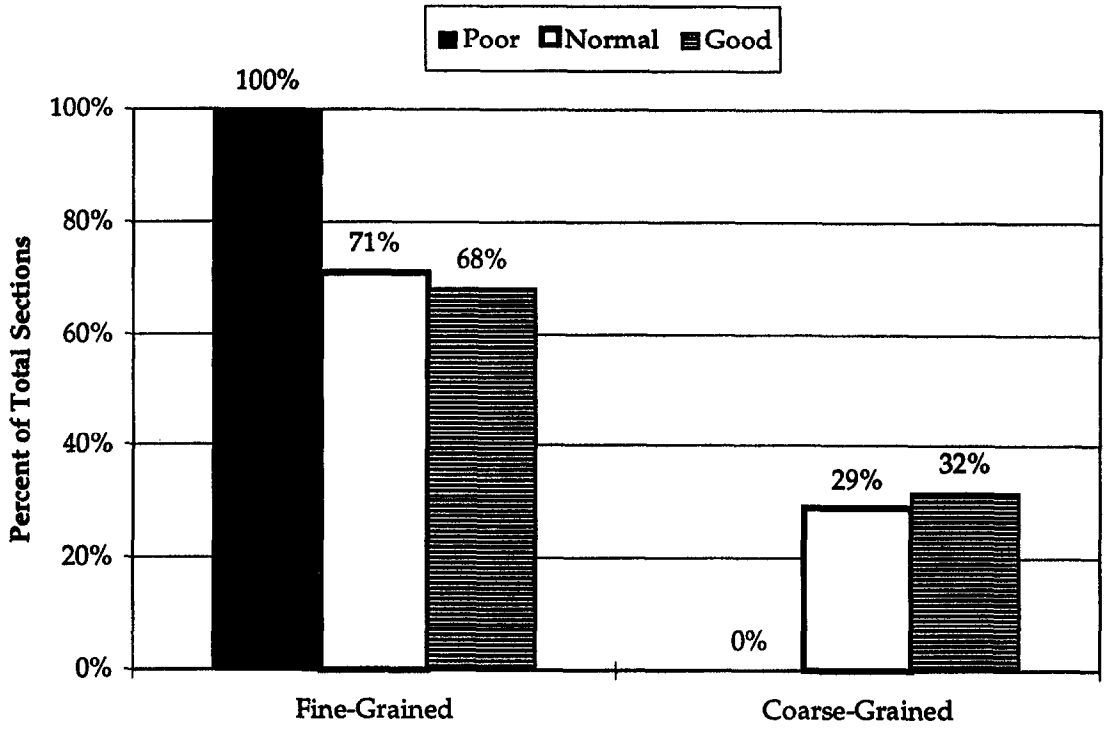

Figure 43. Effect of subgrade soil on JRCP performance.

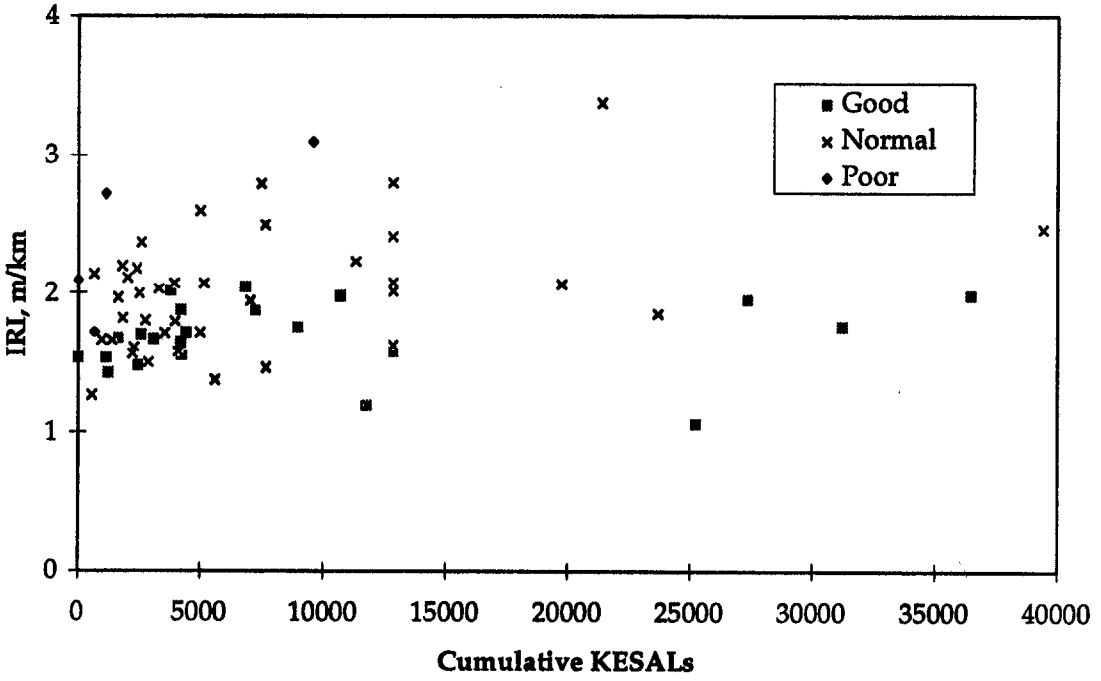

Figure 44. Cumulative KESALs versus IRI for JRCP.

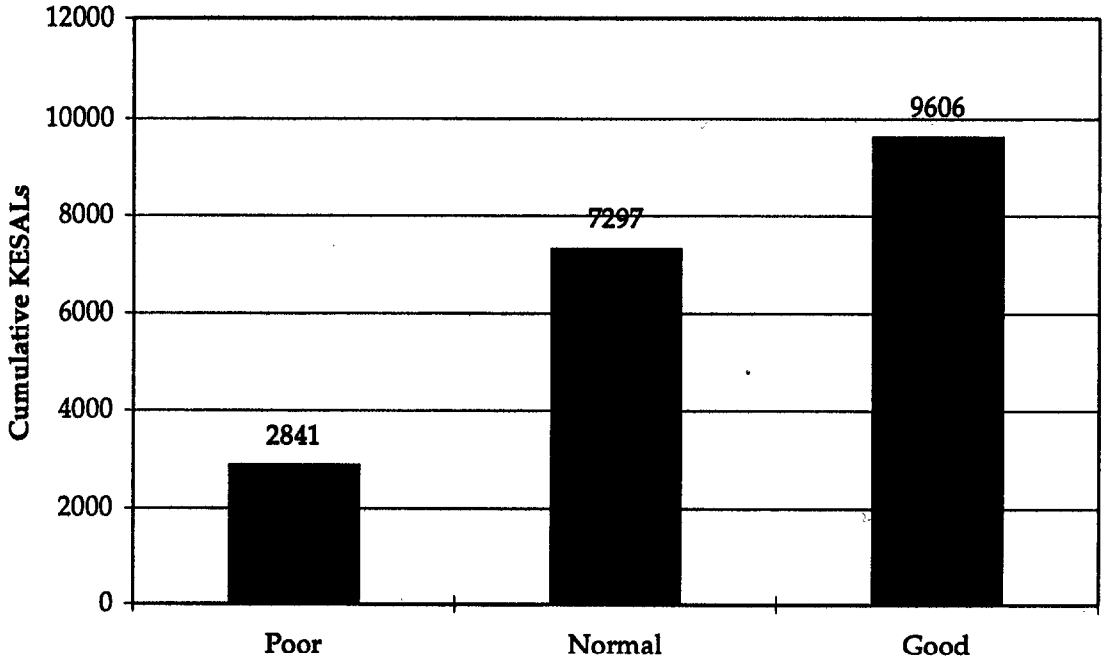

Figure 45. Effect of cumulative traffic on JRCP performance (values shown are in 1,000s of ESALs, 2841 = 2,841,000 ESALs).

Design and Construction Features

Thickness. The relationship between PCC slab thickness and IRI is shown in figure 46. A trend exists showing increased IRI with increased JRCP slab thickness. This agrees with the multivariate analysis that showed that PCC thickness is positively correlated with IRI as shown by the trend in figure 46. The reason for this positive correlation is that thicker slabs were constructed rougher than thinner slabs, as shown in the summary. The t-test (table 9) between those sections rated good and those rated poor did not show statistical significance for slab thickness, indicating that slab thickness for the good group was about the same as for the poor group. Thus the trend shown in figure 46 was caused by constructing thicker JRCP at a higher roughness.

Concrete Properties. The effect of the PCC modulus of elasticity and estimated modulus of rupture at 28 days on IRI values were investigated in this study. No direct correlation between these parameters and IRI was observed. The t-test (table 9) showed no statistical significance of either of these variables.

Design Steel Content. The effect of the longitudinal reinforcing steel content versus IRI for the JRCP sections was evaluated in this study. Comparative analysis did not show a clear trend relating good, normal, and poor performing sections and design steel content. The majority of the JRCP sections evaluated in this study had no data for design steel content; therefore, a detailed statistical analysis was not possible.

Joint Spacing. No trend was observed relating joint spacing to IRI performance. The t-test (table 9) did not confirm a statistical significance for this parameter.

Base Type. The relationship between base-layer type and poor, normal, and good performing sections is presented in figure 47. It is observed that the poor and normal pavement sections show no significant effect of base type. However, 82 percent of the good performing sections (based on IRI) were constructed on granular rather than stabilized bases. The Fisher's exact test results, shown in table 10, did not confirm the statistical significance of this parameter.

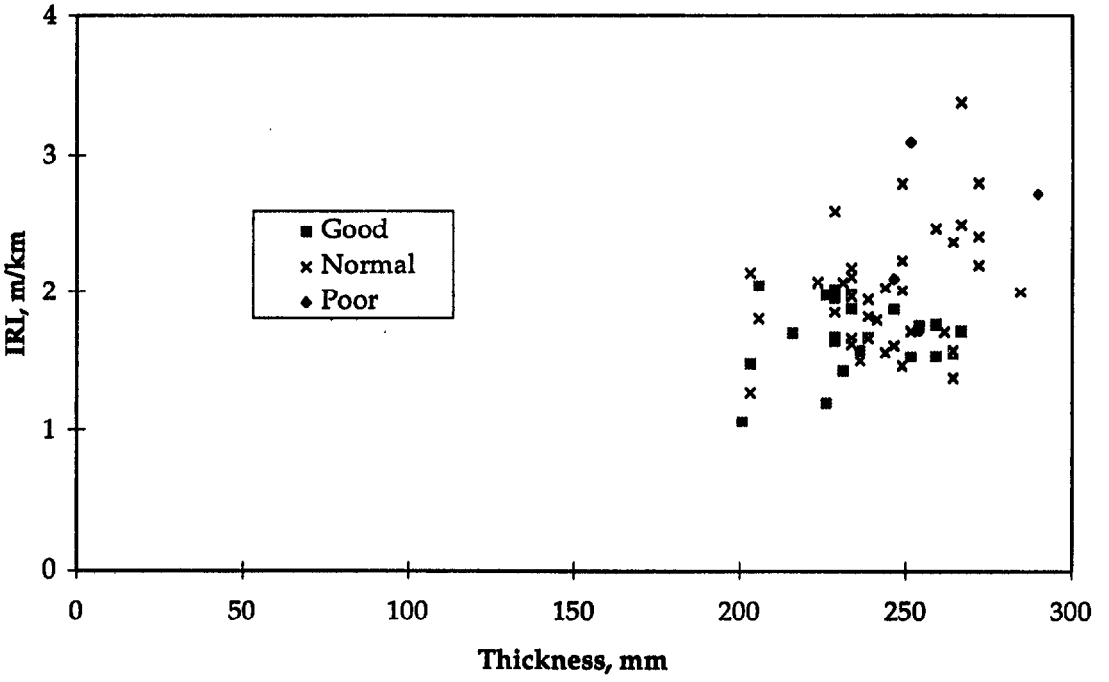

Figure 46. PCC slab thickness versus IRI for JRCP.

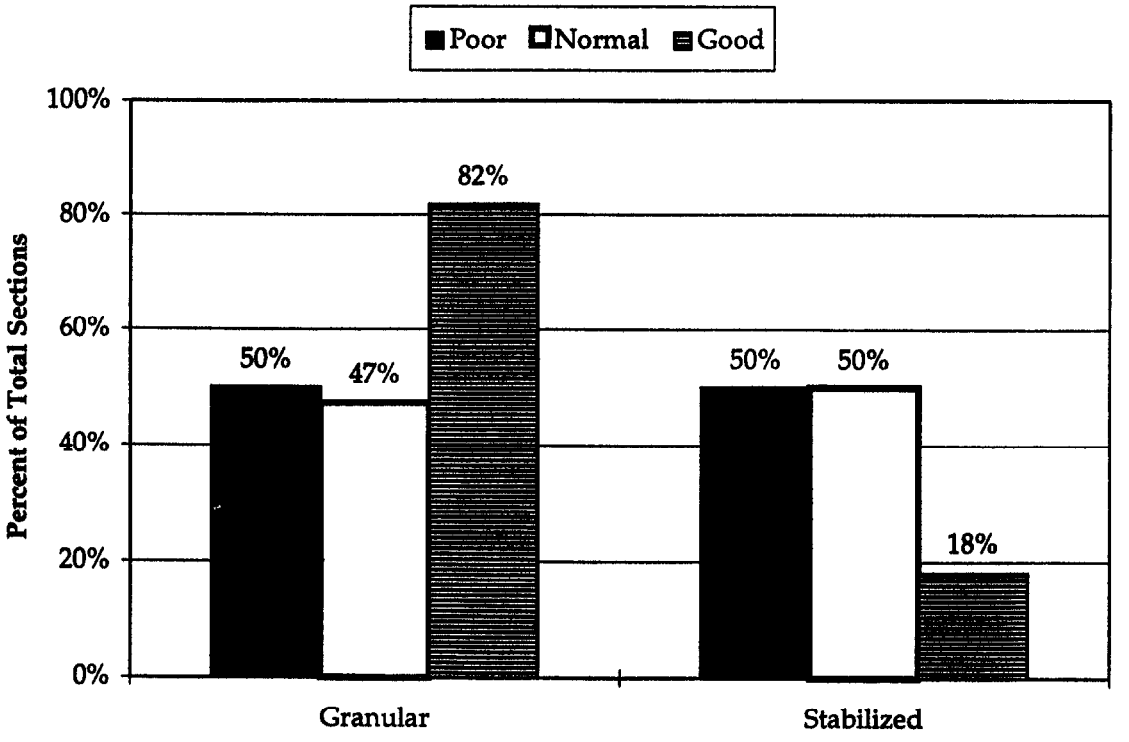

Figure 47. Effect of base-layer type on JRCP performance.

Drainage. Subdrainage has previously been shown to have a significant effect on pavement performance. In this study, the overall subdrainage of a pavement was characterized by the drainage coefficient, C_d. The drainage coefficient reflects the pavement's ability to drain excessive moisture from the structure and the amount of precipitation available, with a higher C_d corresponding to better drainage. Figure 48 shows the relationship between IRI and C_d for the JRCP sections evaluated. There appears to be a trend showing that high C_d is associated with lower IRI.

Figure 49 presents the mean values of C_d for good, normal, and poor sections. The value of C_d is significantly lower for poor sections than for good and normal sections. The mean value of C_d for poor sections was 0.80, whereas normal and good performing sections had mean values of 0.87 and 0.86, respectively. However, the t-test (table 9) did not indicate a strong statistical significance of this variable when evaluating the good and poor ratings. The multivariate analysis shown on pages 74 through 79 indicated that better drainage improves the pavement performance with respect to IRI as illustrated by the trend in figure 48.

Initial, As-Constructed Roughness. As discussed in chapter 4, a recently completed study concluded that the initial, as-constructed roughness has significant influence on future pavement roughness.[4] An attempt was made, as part of the current study, to validate this conclusion using the LTPP data base. Since the LTPP GPS data base does not contain as-constructed initial roughness data, linear regression was used to "backcast" an initial roughness factor (IRF). This value was used to estimate an initial IRI based on the available time series IRI data. It was shown that backcasting of the IRF values provides similar estimates for younger and older pavements. Young pavements in this case are those less than 15 years old at the time of the IRI observation.

The linear analysis procedure discussed earlier was used to predict the effects of initial IRI, as modeled with IRF, and the rate of IRI increase, α, for JRCP sections. A comparison between young and all sections and IRF and the rate of increase of IRI are presented in figures 50 and 51, respectively. These results are summarized in table 11 for the JRCP sections evaluated. These results show that both the initial IRF (estimate of initial IRI) and the rate of increase of IRI over time are greater for those JRCP rated poor. These results are very important and have far-reaching effects. They are similar to that found for JPCP.

For example, a representative JRCP rated poor for roughness had an initial constructed IRI of 2.38 m/km as opposed to a JRCP rated good which had an initial IRI of 1.10 m/km. The rate of increase in IRI per year was twice as high for those JRCP rated poor as those rated good.

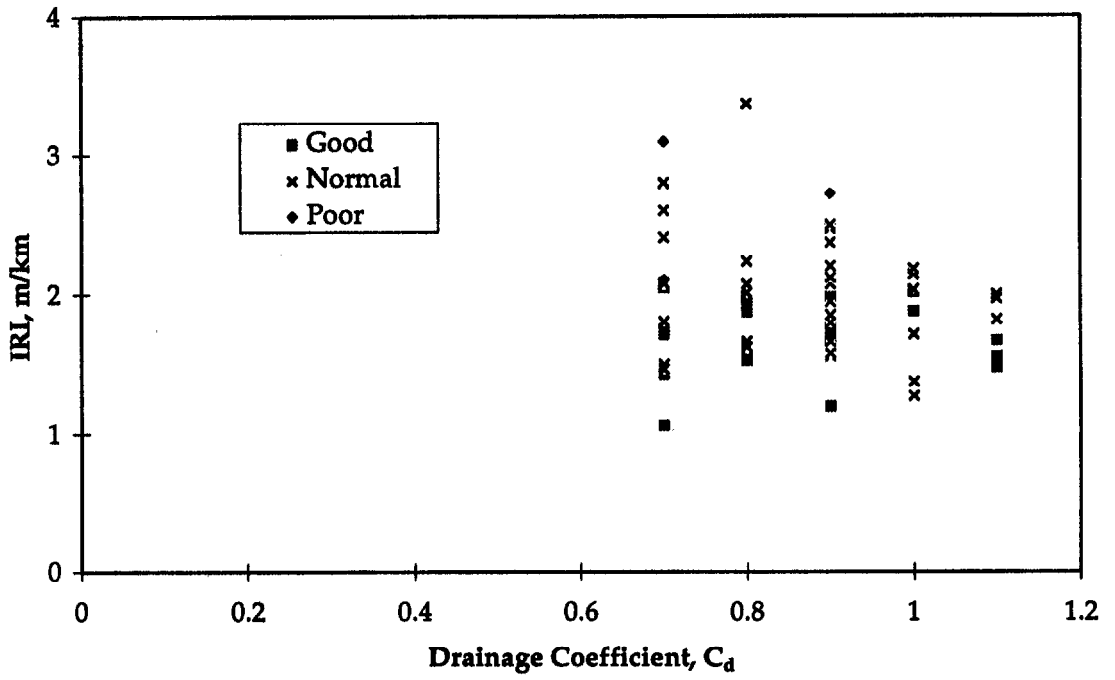

Figure 48. Drainage coefficient (C_d) versus IRI for JRCP.

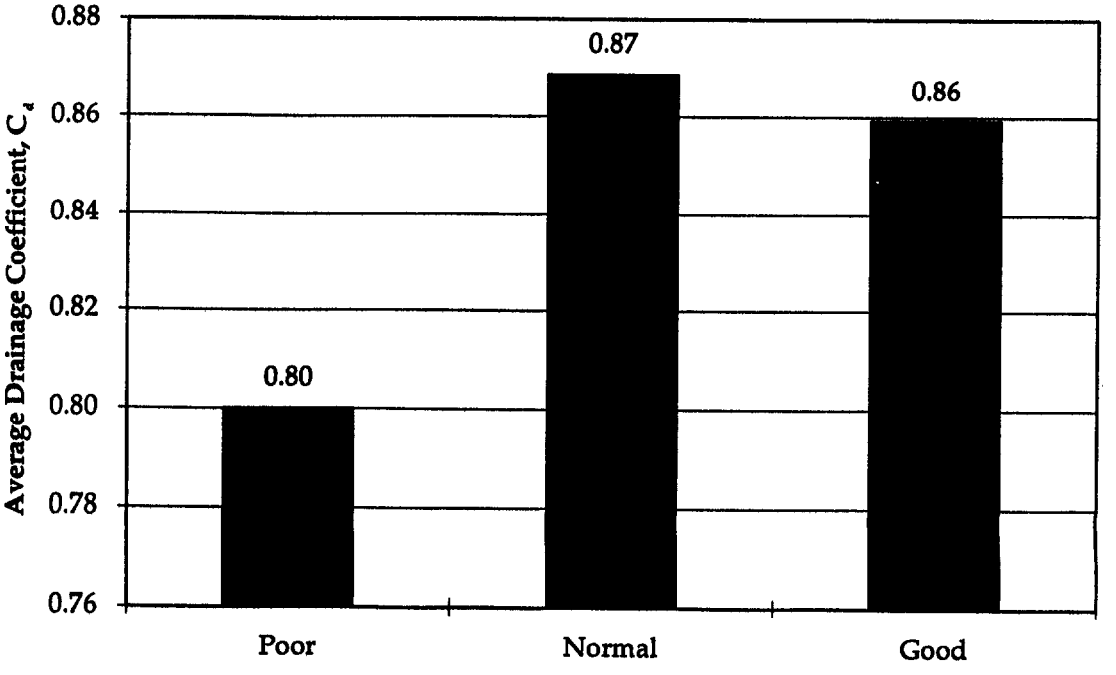

Figure 49. Effect of drainage coefficient (C_d) on JRCP performance.

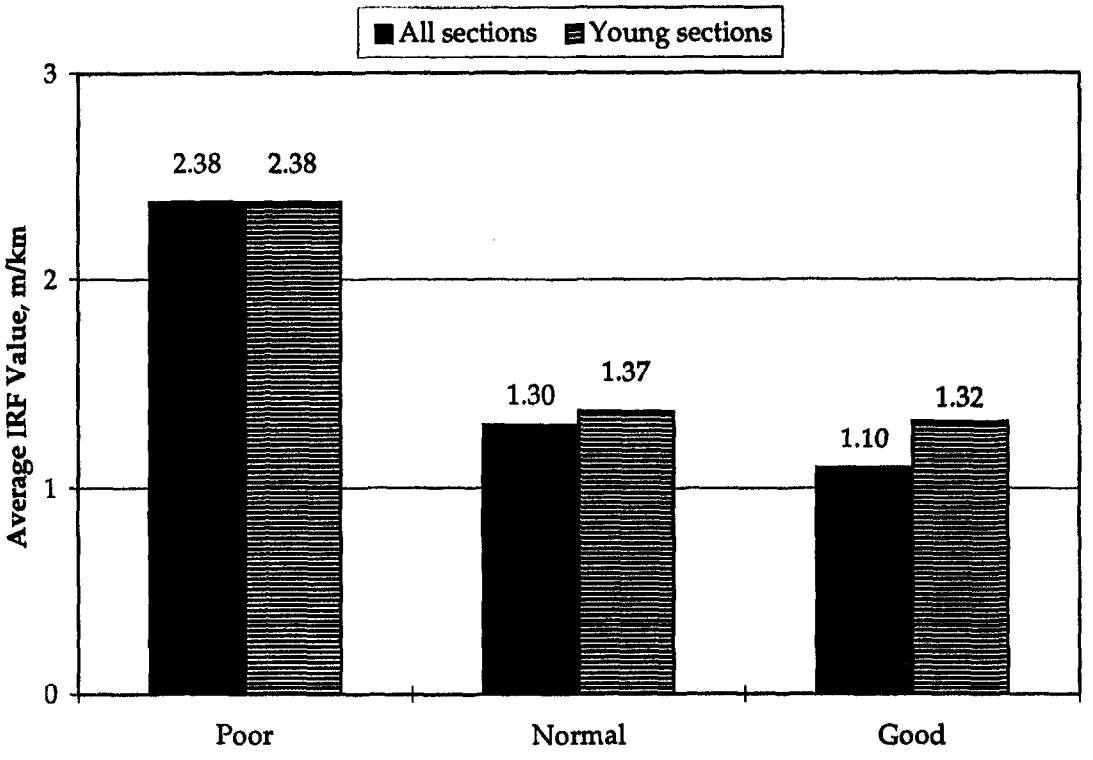

Figure 50. Comparison of average IRF values for JRCP.

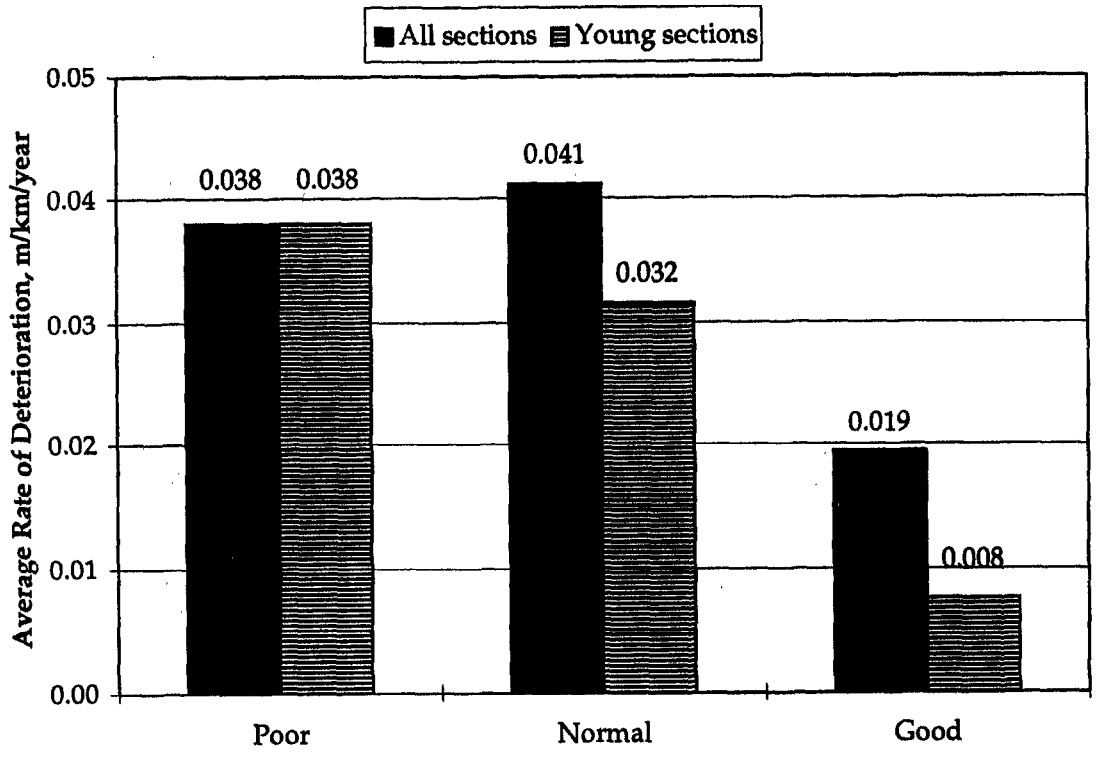

Figure 51. Comparison of average rate of deterioration, α, for JRCP.

Table 11. Comparison of IRF (estimate of initial IRI) and deterioration rate for JRCP.

Parameter	Category	All sections	Young sections
IRF, m/km	Poor	2.38	2.38
	Normal	1.30	1.37
	Good	1.10	1.32
α, m/km/year	Poor	0.038	0.038
	Normal	0.041	0.032
	Good	0.019	0.008

Multivariate Analysis

A multivariate analysis was conducted due to the perceived large number of interactions between design and construction features and site conditions. The overall objective of the multivariate analysis was to identify key factors from the 29 independent variables evaluated and gain an understanding of the interrelationship of these variables. Specific objectives included reducing the number of variables for further evaluation and determining which combinations of variables are the most descriptive.

Table 12 includes all of the 29 variables that were considered in the JRCP analysis. The first seven rows were selected by a stepwise regression. The second column shows the R-square value for the variables when regressed on these first seven variables. DOWELS, DOWDIAM, and EPCC have small R-square values because they are not well explained by the first seven variables. The partial correlation and the semi-partial correlation (columns 3 and 4, respectively) are also found by regressing each variable on the first seven variables. The residuals from this regression are regressed on the corresponding residuals from IRI (using the seven variables) and the raw IRI observations. A relatively large partial correlation with a small semi-partial correlation indicates that the variable explains a unique part of the variability in IRI.

Table 12. Redundancies, First iteration.

Variable	R-square	Partial correlation	Semipart correlation
HPCC	0.203	0.340	0.263
AGE	0.112	0.324	0.248
KSTATIC	0.115	-0.326	-0.250
C_d	0.390	-0.446	-0.361
CW	0.418	-0.340	-0.262
WETDAYS	0.384	0.415	0.331
GRAN_BAS	0.516	-0.288	-0.218
FI	0.464	0.063	0.046
FT	0.651	0.032	0.023
PRECIP	0.505	-0.026	-0.019
TMEAN	0.350	-0.089	-0.065
JTSPACE	0.302	-0.110	-0.079
SKEW	0.241	0.040	0.029
DOWDIAM	0.096	0.040	0.029
DOWELS	0.091	0.053	0.039
PSTEEL	0.231	-0.077	-0.056
KESAL	0.311	-0.089	-0.065
MR28	0.098	0.068	0.049
EPCC	0.064	-0.045	-0.032
EBASE	0.510	-0.017	-0.013
ACBASE	0.231	-0.022	-0.016
CEMBASE	0.324	0.036	0.026
BASE	0.847	-0.068	-0.049
SUBGR	0.636	0.008	0.006
WW	0.951	-0.141	-0.102
TEXT1	0.376	-0.077	-0.055
TEXT3	0.338	0.130	0.095
SEAL1	0.154	0.032	0.023
SEAL3	0.290	-0.071	-0.052

Redundancy of independent variables; DV: IRI; n = 27

Based on these initial results, nine variables were eliminated from further consideration. For example, PSTEEL, SEAL1, and SEAL3 were missing data for many sections, had small partial correlations, and little bivariate correlation with IRI. This resulted in n = 42. The stepwise regression was then run again on the new set of variables. The second analysis resulted in a different set of seven primary variables (CW was replaced by PRECIP). Table 13 shows the results of the second analysis using the 20 variables selected.

Table 13. Redundancies, second iteration.

Variable	R-square	Partial correlation	Semipartial correlation
HPCC	0.278	0.287	0.230
AGE	0.266	0.272	0.217
KSTATIC	0.106	-0.256	-0.203
C_d	0.281	-0.353	-0.289
PRECIP	0.386	0.128	0.099
WETDAYS	0.391	0.305	0.245
GRANBAS	0.542	-0.292	-0.234
FI	0.660	-0.015	-0.011
FT	0.653	-0.152	-0.117
TMEAN	0.122	0.091	0.070
JTSPACE	0.294	-0.061	-0.047
DOWDIAM	0.074	-0.014	-0.011
DOWELS	0.091	0.044	0.033
KESAL	0.307	-0.058	-0.045
MR28	0.102	0.037	0.028
EPCC	0.073	-0.046	-0.035
CEMBASE	0.321	0.057	0.044
BASE	0.846	0.006	0.005
TEXT1	0.367	-0.024	-0.018
TEXT3	0.304	0.049	0.038

Redundancy of independent variables; DV: IRI
R-square column contains R-square of respective variable with all other independent variables; n = 42

The correlations between these 20 variables and IRI were examined. Table 14 shows that FI, FT, PRECIP, TMEAN, KESAL, AGE, HPCC, KSTATIC, and GRANBAS are all strongly correlated with IRI. A p value less than 0.05 indicates a strong correlation based on the established criteria.

Table 14. Correlation matrix.

Variable	IRI
FI	-0.4590 p=0.003
FT	-0.5107 p=0.001
PRECIP	0.5307 p=0.001
WETDAYS	-0.0481 p=0.771
TMEAN	0.5486 p=0.000
JTSPACE	0.1892 p=0.249
DOWDIAM	-0.0994 p=0.547
DOWELS	-0.1382 p=0.402
KESAL	0.3357 p=0.037
AGE	0.3081 p=0.056
HPCC	0.3041 p=0.060
MR28	0.4008 p=0.011
EPCC	0.1546 p=0.347
C_d	-0.0414 p=0.803
KSTATIC	-0.1960 p=0.232
GRANBAS	-0.2678 p=0.099
CEMBASE	0.1721 p=0.295

Table 14. Correlation matrix (continued).

Variable	IRI
GRAN	-0.2580 p=0.113
TEXT1	0.1799 p=0.273
TEXT3	-0.1558 p=0.344

n=39 (Casewise deletion of missing data)

Based on a lack of correlation with IRI and the relatively small partial correlations, FI, TMEAN, JTSPACE, DOWELDIA, DOWELS, KESAL, MR28, EPCC, CEMBASE, BASE, and TEXT3 were eliminated from further analysis. The remaining nine variables were analyzed again using a stepwise regression to compare the corresponding partial and semi-partial correlations.

The results of the third stepwise regression analysis are shown in table 15. These results indicate that a predictive model based on stepwise regression is reasonable.

Table 15. Redundancies, third iteration.

Variable	Toleran.	R-square	Partial Correlation	Semipart Correlation
HPCC	0.818	0.182	0.330	0.288
KSTATIC	0.925	0.075	-0.260	-0.222
C_d	0.935	0.065	-0.316	-0.275
PRECIP	0.796	0.204	0.309	0.268
FT	0.464	0.536	-0.102	-0.084
WETDAYS	0.863	0.137	0.168	0.138
AGE	0.826	0.174	0.176	0.145
GRANBAS	0.704	0.296	-0.091	-0.075
TEXT1	0.922	0.078	-0.022	-0.018

Redundancy of independent variables; DV: IRI
R-square column contains R-square of respective variable with all other independent variables; n = 42

The regression summary presented in table 16 provides insight into the interrelations of the variables analyzed (regressors). The Cook's distances were relatively small for all residuals. The coefficients for HPCC, KSTATIC, and C_d appeared as though they would not be affected by influential points.

Table 16. Regression summary.

	BETA	St. Err. of BETA	B	St. Err. of B	t(47)	p-level	Valid N
Intercpt			0.67100	0.73183	0.918	0.364	
HPCC	0.319	0.133	0.00706	0.00295	2.397	0.021	65
KSTATIC	-0.231	0.125	-0.00477	2.61800	-1.845	0.071	53
C_d	-0.284	0.124	-0.99420	0.43500	-2.284	0.027	65
PRECIP	0.300	0.135	0.00055	0.00025	2.227	0.031	64

Regression summary for dependent variable: IRI; n = 52
$R = 0.56514641$ $R^2 = 0.31939047$ Adjusted $R^2 = 0.26146626$
$F(4,47)=5.5139$ $p<0.00101$ Std. Error of estimate: 24.046

The model presented in table 16 is useful for examining the way in which the variables interrelate. However, this is not a validated model obtained from a previous data set or a hypothesis. This model was developed solely from the data analyzed in this study; therefore, the statistics can only be interpreted in a descriptive or exploratory manner. The model has an adjusted R-square value of 0.261 and a highly significant F-ratio. The significant F-ratio indicates that the model is far more useful for estimating IRI than the sample mean of IRI.

The model coefficients estimate the effects of the four designated variables on IRI averaged over changes in the other regressors. An increase in HPCC or PRECIP is associated with an average increase in IRI. Increases in C_d or KSTATIC are associated with decreases in IRI. All of these average effects make sense physically except the slab thickness, HPCC. This can only be explained by the possibility that thicker slabs were constructed with a higher IRI. A regression was made between the IRF (estimated initial IRI) and JRCP slab thickness. A positive significant correlation was obtained, indicating that thicker JRCP were built rougher than thinner JRCP.

Summary of IRI Findings for JRCP

The JRCP sections were evaluated both comparatively and statistically using the t-test and multivariate linear regression. The results of the comparative analysis and t-test comparisons were misleading in some instances due to the influence of other variables on the variable being analyzed. One factor undoubtedly causing significant problems in the data analysis is the initial IRI after construction. This value appears to vary widely and has a long-term effect on IRI. Another example is the drainage coefficient, which is highly influenced by many variables, including material characteristics, precipitation, pavement structure, subgrade soil type, and edge drains.

All JRCP rated as poor were constructed on a fine-grained subgrade. No JRCP rated as poor was constructed on a course-grained subgrade. Although the designer usually does not select the type of subgrade, where poor subgrade soils exist, the specification of a thick granular layer may be beneficial.

Given all of the analysis performed, the following factors were found to have the greatest influence on IRI:

- **Initial roughness/smoothness of JRCP:** The data analysis showed that the roughness of a JRCP over time depends greatly on its initial IRI. The analysis also showed that the rate of increase in IRI over time is higher for those JRCP that are rated poor as compared to those rated good. These are very important findings for JRCP.

- **Traffic:** JRCP in good IRI performance category carried much higher ESALs than those in the poor or normal groups. Too much collinearity existed between key variables to show other significance (i.e., JRCP with higher traffic were designed to carry heavier traffic). Previous multivariate models have shown, however, that increased ESALs increase IRI.

- **Multivariate analysis:** The effect of these variables (except initial roughness, which could not be backcasted for all sections and thus is not included here) is shown in the following equation:

  $$IRI = 0.671 + 0.00706 * HPCC - 0.00477 * KSTATIC - 0.9942 * C_d + 0.000551 * PRECIP \quad (13)$$

  This model for IRI (m/km) has a relatively low R-squared value, which would be expected given the nonconsideration of the initial IRI value and the interrelationship of the parameters evaluated. The variables contained in the IRI model substantially agree with other studies conducted with the LTPP data base.

- **AASHTO drainage coefficient (C_d).** The drainage coefficient reflects the pavement's ability to drain excessive moisture from the structure, with a higher C_d corresponding to better drainage. JRCP having a high C_d are smoother over time than those with a low C_d.

- **Modulus of subgrade reaction (KSTATIC).** JRCP with higher k-value on average have lower IRI, as shown by the multivariate analysis. The subgrade k-value may be correlated with soil type in that granular soils typically have a higher k-value. The comparative analysis indicated that JRCP constructed on coarse-grained soils perform better than those constructed on fine-grained soils, since every one of the poor performing JRCP sections was constructed on a fine-grained subgrade soil.

- **PCC slab thickness (HPCC).** The thicker the JRCP slab, the rougher the pavement. This of course goes against mechanistic theory. However, the reason for this was determined to be that thicker JRCP slabs were built to a much higher initial roughness level. The mean IRF (estimated initial IRI) for 200- to 230-mm JRCP slabs was 1.23 m/km, but the mean IRF for 250- to 300-mm JRCP was 1.56 m/km. The initial roughness strongly affects the future IRI over many years to come.

- **Average annual precipitation (PRECIP).** JRCP located in areas having a greater annual precipitation or number of wet days have a higher IRI. The C_d also includes some effects of precipitation. Therefore, precipitation has quite a strong influence on IRI of JRCP.

CHAPTER 6. PERFORMANCE OF CRCP IN ROUGHNESS

Previous Studies

Performance of CRCP with respect to roughness has been investigated in several studies. An IRI model was developed in the early LTPP Data Analysis Study.[1] The model developed for CRCP is as follows:

$$IRI = 4.135 + 0.0232\ CESAL - 0.00182\ HPCC - 3.666\ PSTEEL - 0.4703\ WIDENED - 0.2652\ SUBGRADE \quad (14)$$

where

IRI	=	International Roughness Index, m/km
CESAL	=	cumulative ESALs, millions
PSTEEL	=	percentage of longitudinal reinforcement steel
HPCC	=	PCC slab thickness, mm
WIDENED	=	1 = widened traffic lane, 0 = normal width traffic lane
SUBGRADE	=	1 = coarse-grained (AASHTO A-1, A-2, or A-3) 0 = fine-grained (AASHTO A-4, A-5, A-6, or A-7)

This model predicts IRI as a function of site conditions and pavement design features. No climatic variables were found to be sufficiently significant to be included in this model. PSTEEL is inversely correlated to IRI; that is, an increase in the amount of steel reinforcement corresponds to a decrease in IRI. This is explainable because the function of reinforcing steel is to hold transverse cracks tightly together which reduces the number of punchouts and deterioration of the cracks. Also, pavement features such as CESAL, slab thickness, widened vs. normal-width lane, and the subgrade type have an influence on the predicted IRI. Also, the form of the model provides for an increase in IRI with time (age and cumulative traffic loadings).

A recent study utilizing the LTPP data base developed the following IRI model for CRCP as a function of site conditions and design features:[3]

$$IRI = 1.118 + 0.0158\ KESAL^{0.3}(0.9 - 0.62PSTEEL) + 0.0158\ AGE^{0.4}(0.2\ DAYS32 - 3.45\ DRY + 18.6\ FREEZE - 0.0294\ KSTATIC+7.62) \quad (15)$$

where

IRI	=	International Roughness Index, m/km
KESAL	=	cumulative 80-kN equivalent single axle loads, thousands
PSTEEL	=	percent steel
AGE	=	pavement age, years

DRY = LTPP climatic zone, 1 = dry climate, 0 = wet climate
FREEZE = LTPP climatic zone, 1 = freezing climate, 0 = nonfreezing climate
KSTATIC = modulus of subgrade reaction, kPa/mm
DAYS32 = annual number of days with temperature higher than 32°C

A national pooled-fund study administered by the Federal Highway Administration was conducted on 23 inservice CRCPs to study the effects of various design and construction features on the performance of CRCPs.[15] The attributes studied included:

- Design thickness - ranging from 200 to 330 mm
- Epoxy coated reinforcement - three sections
- Permeable base - two sections
- Age - ranging from 0.3 to 22 years
- Subgrade - both coarse- and fine-grained soils
- Base - lean concrete, cement treated, asphalt treated, and granular
- Steel amount - 0.45 to 0.7 percent
- Steel placement - tube-fed and chairs
- Shoulder type - asphalt and tied concrete
- Climatic region - wet-freeze and wet-no freeze

This study determined that there was a trend of increasing IRI with increasing age. This is expected because pavements become rougher as they get older.

Studies on CRCP performance on the Illinois Interstate highway system for localized failures (punchouts) has shown that steel percentage, slab thickness, and ESALs were the most significant variables. Increased steel percentage and increased slab thickness reduced the development of localized failures.[10] Localized failures of course cause serious roughness problems if they are not repaired immediately.

Table 17 summarizes the site conditions and design features that were included in these studies. The general effect of each parameter on roughness is shown. Note that the effects of initial IRI after construction were not directly included in these studies. A recent major research study determined that the future roughness of a pavement was highly dependent on its initial as-constructed roughness. Prediction models for many projects, including CRCP, were developed relating initial IRI to future IRI.[4]

Table 17. Summary of the effects of CRCP site conditions and design features on IRI.

Design Feature	Effect on IRI	Reference
Pavement age	Increases *	1,3,15
Traffic	Increases	1, 10 (localized failures)
Wet days	Increases	3
Days above 32°C	Increases	3
Coarse subgrade	Decreases	1
Widened lane	Decreases	1
Amount of steel	Decreases	1, 10 (localized failures)
PCC thickness	Decreases	1, 10 (localized failures)
k-value	Decreases	1
Drainage, C_d	Decreases	3
Initial roughness	Increases	4

* For example, as pavement age increases, IRI or roughness increase. As amount of reinforcing steel increases, IRI decreases.

Performance Criteria for IRI

This section presents an analysis of the factors that lead to roughness of CRCP based on the IRI measurements from the LTPP data base. The version of the LTPP data base analyzed in this study contains IRI data for 83 CRCP sections. The total number of observations is 345. For some sections, time series data contain up to 10 observations made over 5 years. Other sections have only one performance record in the data base.

The data was divided into three performance categories: poor, normal, and good, based on IRI and pavement age as previously described. This grouping was done to facilitate the analysis of identifying features that contribute to good and poor roughness performance. This grouping was established based on the experience of a group of

State highway engineers. The limits that were set are shown in figure 52. The pavement section was considered good (i.e., performing better than expected) if its IRI satisfied the following condition:

$$IRI > 0.631 + 0.0631 * AGE \quad (16)$$

where

IRI = International Roughness Index, m/km
AGE = pavement age at the time of the IRI observation, years

The pavement section was considered poor if its IRI satisfied the following condition:

$$IRI > 1.262 + 0.094.7 * AGE \quad (17)$$

where

IRI = International Roughness Index, m/km
AGE = pavement age at the time of the IRI observation, years

Figure 52 presents a plot of all IRI observations for the LTPP CRCP sections and shows designation of those sections by their performance at the time of observations. Because the number of observations differs among the sections, the use of all these observation in the subsequent analysis may make it biased toward the sections with a higher number of observations. To avoid this, only the last observation for each section was considered in the analysis if not stated otherwise. Figure 53 presents a plot of all CRCP (GPS-5) sections with respect to IRI at the time of the last available observation.

Only two of the CRCP sections studied fall into the poor performance category. Because this is not enough data for a comprehensive analysis, the poor and normal performing sections were combined. For convenience, this group will be referred to as the poor group. The distribution of percent CRCP sections with respect to performance category is shown in figure 54. Most sections in this study fell into the category good. The good performing sections account for 54 percent of all sections, and poor and normal sections combined make up the remaining 46 percent of the sections.

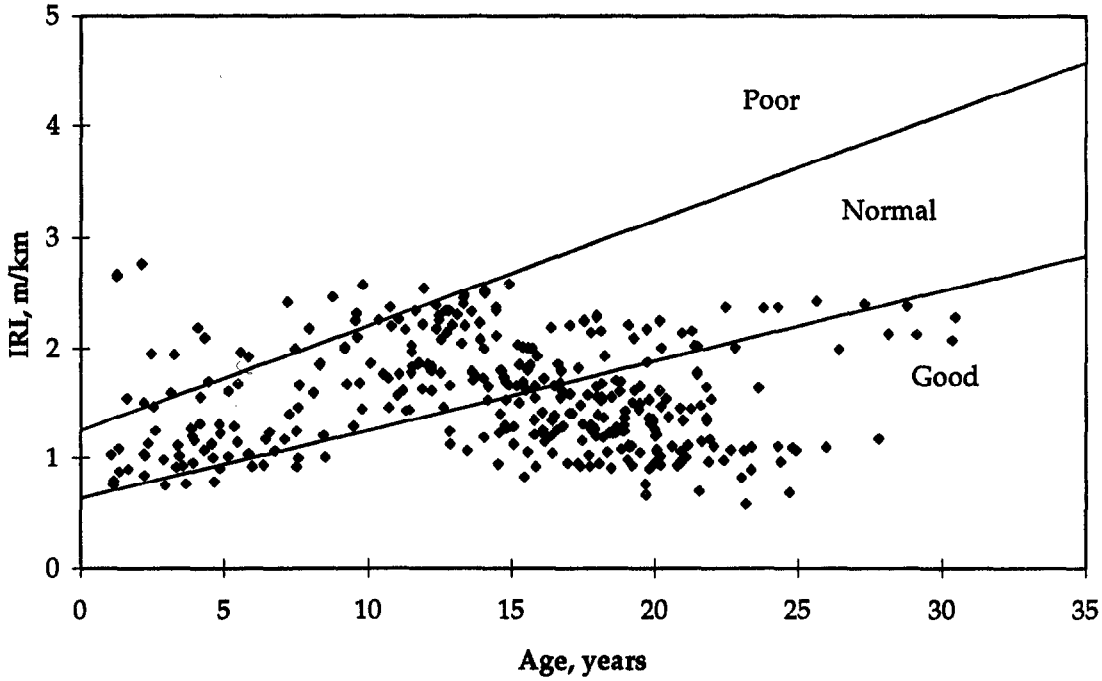

Figure 52. IRI for CRCP including all time-series data.

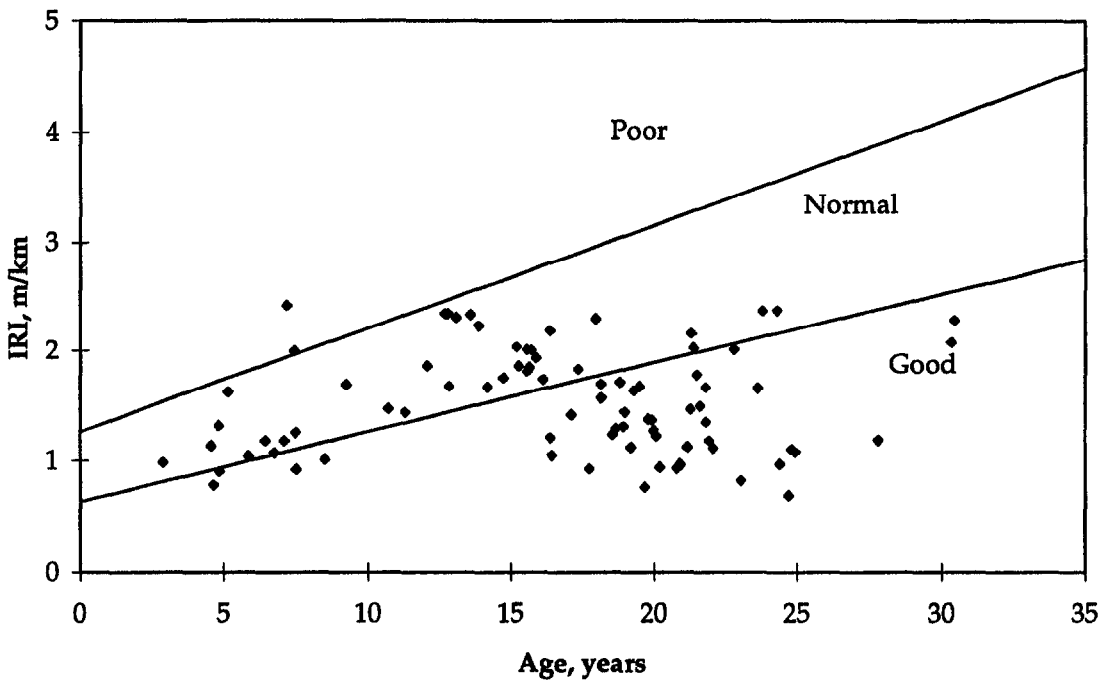

Figure 53. IRI for CRCP (last IRI observation only).

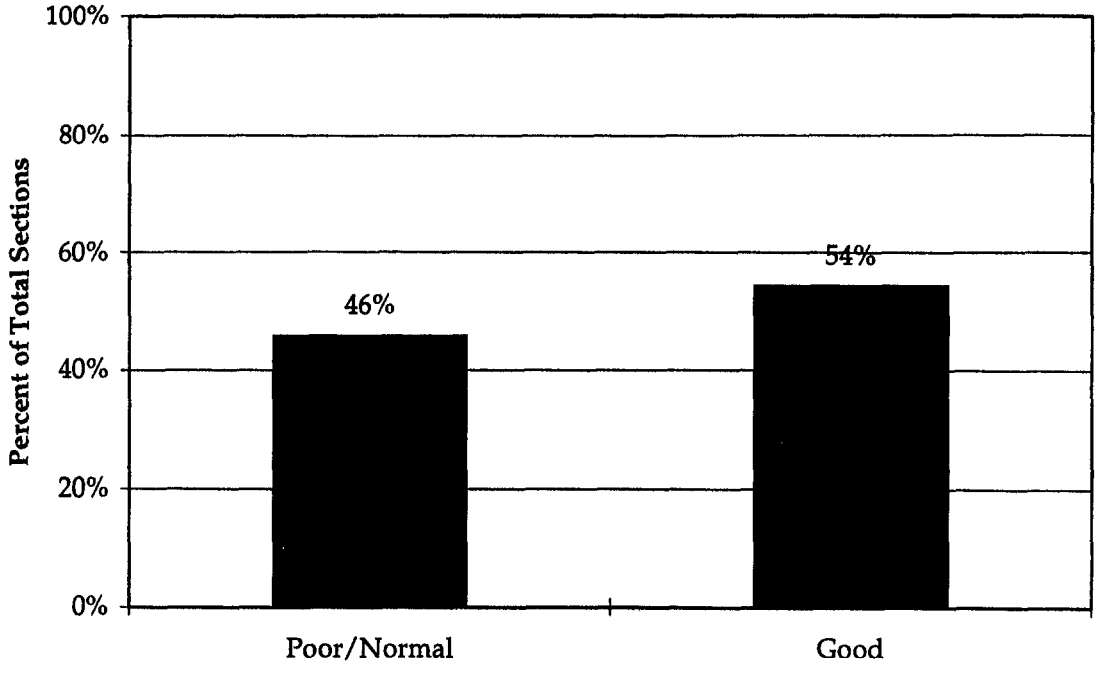

Figure 54. Distribution of sections for CRCP.

Factors Considered for IRI

The general types of factors affecting the IRI of CRCP include site conditions, design features, and construction quality. The factors studied in this analysis include those found to be significant from previous studies and engineering judgment:

- **Site Conditions**
  - o Geographic/climatic location
    - Latitude
    - Longitude
  - o Temperature factors
    - Freezing index
    - Freeze-thaw cycles
    - Mean annual temperature
    - Minimum annual temperature
    - Maximum annual temperature
    - Number of days warmer than 32°C
    - Number of days colder than 0°C

- Precipitation factors
  - Average annual precipitation
  - Average number of wet days per year
- Subgrade soil
- Traffic (ESAL)

- **Design and Construction Features**
  - Slab thickness
  - Concrete properties
    - Modulus of elasticity
    - Modulus of rupture
  - Steel content
  - Base type
  - Drainage
  - Initial as-constructed roughness
  - Method used to texture concrete

Comparative and Statistical Analysis of IRI

Two general types of analysis were performed: a visual comparative analysis and a statistical analysis. Comparative analysis includes visual analysis of plots with a distribution of pavement sections by their performance as a function of those factors, and a comparison of average values of those factors for different groups of pavement sections. The plots can be studied for trends.

Statistical analyses conducted include the t-test and, in some cases, multiple regression analyses to identify those site conditions and design features that contribute to good and poor roughness performance. The t-test was used to compare the mean of each variable in the good group to its mean in the poor group. The test works by taking the ratio of the difference between two group means relative to an appropriate estimate of the standard deviation for this difference. If this ratio is large, then the group means differ a great deal for data with this much variability. Hence, it would be concluded that this difference is due to something other than chance. If this ratio is small, then we conclude that the difference could be due to chance—the analysis cannot be confident that the difference is a real one. Table 18 provides a summary of all the t-values for each comparison made for continuous variables. Table 19 provides a summary of Fisher's exact tests for discrete variables for IRI of JRCP.

Table 18. Results of t-tests for CRCP IRI performance.

	Mean Poor*	Mean Good	t separ. var. est	df	p 2-sided	Valid N Poor	Valid N Good	Std. dev. Poor	Std. dev. Good	F-ratio variance	p variance
FI	276.877	187.924	1.499	73	0.138	45	38	334.788	197.904	2.862	0.001
FT	70.828	69.551	0.193	77	0.847	45	38	29.022	30.788	1.125	0.702
PRECIP	976.579	939.343	0.520	79	0.605	45	38	377.647	272.999	1.914	0.046
WETDAYS	117.536	119.732	-0.338	77	0.736	45	38	28.488	30.316	1.132	0.688
LONG	92.778	91.921	0.314	78	0.754	45	38	12.124	12.611	1.082	0.797
LAT	37.533	36.658	0.856	81	0.394	45	38	5.021	4.295	1.367	0.333
TMAX	19.639	20.358	-0.760	76	0.450	45	37	4.193	4.318	1.061	0.846
TMIN	7.178	7.808	-0.710	79	0.480	45	37	4.183	3.838	1.187	0.600
TMEAN	13.408	14.083	-0.751	78	0.455	45	37	4.129	3.978	1.078	0.824
DAYS32	38.621	48.427	-1.315	63	0.193	45	38	26.465	39.026	2.174	0.014
DAYS0	86.693	79.982	0.677	81	0.500	45	38	47.572	42.697	1.241	0.503
STEEL	0.608	0.622	-0.663	52	0.510	44	38	0.060	0.124	4.281	0.000
ESAL	11873.670	5640.214	2.321	57	0.024	43	28	16107.590	5752.585	7.840	0.000
HPCC	213.131	234.493	-3.784	75	0.000	45	38	24.155	26.772	1.231	0.506
MR28	4750.634	4729.606	0.126	64	0.901	45	38	599.313	873.583	2.125	0.017
EPCC	27742.771	28481.234	-0.936	71	0.352	45	38	3147.256	3907.551	1.542	0.169
EBASE	3092.845	4114.056	-1.697	78	0.094	45	38	2717.849	2743.631	1.019	0.945
C_d	0.978	0.983	-0.171	79	0.865	45	38	0.138	0.134	1.065	0.850
KSTATIC	47.539	56.882	-1.167	56	0.248	43	35	26.762	40.736	2.317	0.010

* Poor group combines poor and normal sections.

where

FI	= Freezing index, °C-days	DAYS0	= Annual number of days with temperature lower than 0°C
FT	= Annual air freeze-thaw cycles	STEEL	= Percentage of reinforcement of cross-section area
PRECIP	= Mean annual precipitation, mm	KSTATIC	= Static elastic modulus of subgrade reaction, kPa/mm
WETDAYS	= Mean number of wet days	ESAL	= 80-kN equivalent single axle load, thousands
LONG	= Longitude location, degrees	HPCC	= Thickness of PCC slab, mm
LAT	= Latitude location, degrees	MR28	= Mean 28-day modulus of rupture, kPa
TMIN	= Minimum annual temperature, °C	EPCC	= Mean 28-day elastic modulus, MPa
TMAX	= Maximum annual temperature, °C	EBASE	= Mean base-layer modulus of elasticity, MPa
TMEAN	= Mean annual temperature, °C	C_d	= AASHTO drainage coefficient
DAYS32	= Annual number of days with temperature higher than 32°C		

Table 19. Results of Fisher exact tests for CRCP IRI performance.

	Fisher Exact		
	One-tailed p	Two-tailed p	Description of variable
GRANBAS	0.441	0.787	=1, if granular base presents =0, otherwise
ACBASE	0.300	0.513	=1, if asphalt stabilized base presents =0, otherwise
CEMBASE	0.114	0.184	=1, if cement-treated base presents =0, otherwise
BASE	0.441	0.787	=1, if stabilized base presents =0, otherwise
SUBGR	0.317	0.510	=1, if subgrade is coarse-grained soil =0, otherwise
WW	0.388	0.663	=1, if a climate is warm-wet =0, otherwise
CW	0.266	0.460	=1, if a climate is cold-wet =0, otherwise
COLDDRY	0.049	0.065	=1, if a climate is cold-dry =0, otherwise
TEXT1	0.002	0.002	=1, if tine is used to texture concrete =0, otherwise
TEXT3	0.017	0.025	=1, if burlap drag is used to texture concrete surface =0, otherwise

In this study, two-dimensional plots of IRI with respect to different parameters were analyzed and a comparison of the mean values of those parameters for good, normal, and poor sections was performed. Although the results of this analysis are of great interest because they highlight the most significant trends in pavement roughness, they must be considered with caution because of the possibility of misleading conclusions as a result of confounding effects of other factors.

Climatic Site Conditions

Geographic/Climatic Location. Latitude and longitude are correlated with climatic factors such as precipitation and air temperature. However, no clear trend relating latitude and longitude to roughness performance was found for CRCPs. The t-test

found no significance of latitude and longitude on IRI performance of CRCP, as shown in table 18. Specific climatic variables that may cause IRI variations are discussed below.

Temperature Factors. The following temperature parameters were considered in this study: freezing index (FI), number of air freeze-thaw cycles (FT), mean annual temperature (T_{mean}), minimum annual temperature (T_{min}), maximum annual temperature (T_{max}), number of day per year with a temperature higher than 32°C (DAYS32), and number of days per year with a temperature lower than 0°C (DAYS0). However, no clear trend relating performance with temperature factors was observed. None of these parameters was found to be significant as a result of the t-test.

Precipitation Factors. Two precipitation factors were analyzed in this study: average annual precipitation and average number of wet days per year. No clear trend was observed relating annual precipitation levels to IRI. The results of the t-test (table 18) did not confirm the significance of this difference.

The good and poor performing sections are also randomly distributed according to number of wet days. The mean value for WetDays for poor sections was 120 days, whereas the mean value for good sections was 118 days. The statistical t-test (table 18) verified no significance of this difference.

Subgrade Site Conditions

The subgrade can be separated into fine-grained soils and coarse-grained soils. Figure 55 shows that, in general, pavements constructed over coarse-grained soils perform better than those constructed on fine-grained soils. Of all poor performing sections, 63 percent had fine-grained subgrade soil and only 37 percent were built in areas where the subgrade soil was coarse-grained. The results of the Fisher's exact test (table 19) did not confirm the significance of this difference, however.

Traffic Site Conditions

Figures 56 and 57 show the relationship between applied ESALs and IRI. It is expected that increased levels of traffic would lead to an increase in IRI. However, perhaps due to the confounding effects of other design parameters (i.e., slab thickness), the results of the t-test did not confirm the significance of this difference. Other variables are likely confounded with ESAL level (such as structural design of the pavement). The mean value for ESALs for good sections was 11.8 million, whereas the mean value for poor sections was only 5.6 million. This can be explained by the presence in the data base of many old CRCP sections performing exceptionally well with respect to roughness.

Design and Construction Features

Thickness. No clear trend was observed relating slab thickness to IRI in this data base. The t-test (table 18) found that this difference was of no statistical significance. Figure 58 shows a plot of the PCC thickness vs. IRI data.

Concrete Properties. The effect of concrete modulus of elasticity and estimated modulus of rupture at 28 days on IRI was investigated. The t-test found that this difference was of no statistical significance. However, the multivariate analysis led to the model which contains modulus of rupture as a significant parameter. According to that model, an increase in modulus of rupture increases IRI of CRCP. This may be explained by a higher water/cement ratio of higher strength concrete mixes which make them less workable. This may make more difficult proper finishing of the concrete surface and can lead to a rougher built pavement.

Design Steel Content. Figure 59 shows the designed longitudinal reinforcing steel content vs. IRI for the CRCP sections in this study. Comparative analysis did not discover a clear trend relating good and poor performing sections and design steel content. Figure 60 presents the average values of steel content. Good sections had a mean steel content of 0.61 percent, whereas poor performing sections had a mean steel content of 0.62 percent. The multivariate analysis, however, clearly indicates that an increase in steel content is associated with smoother CRCP.

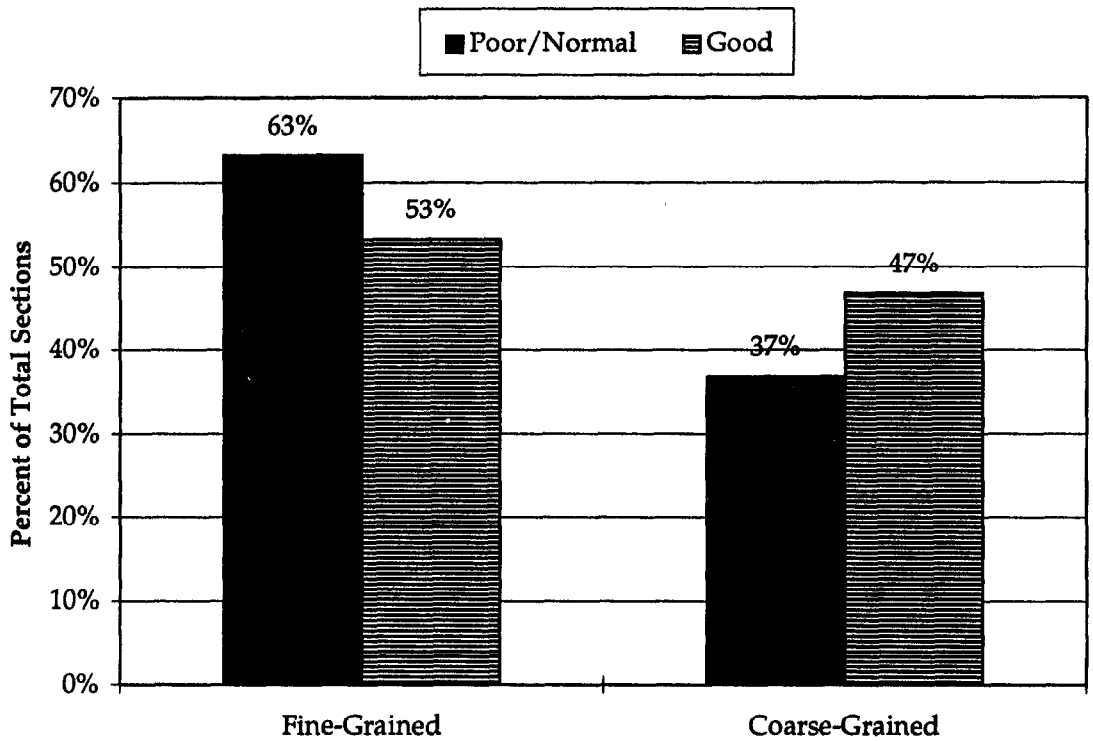

Figure 55. Effect of subgrade soil on CRCP performance.

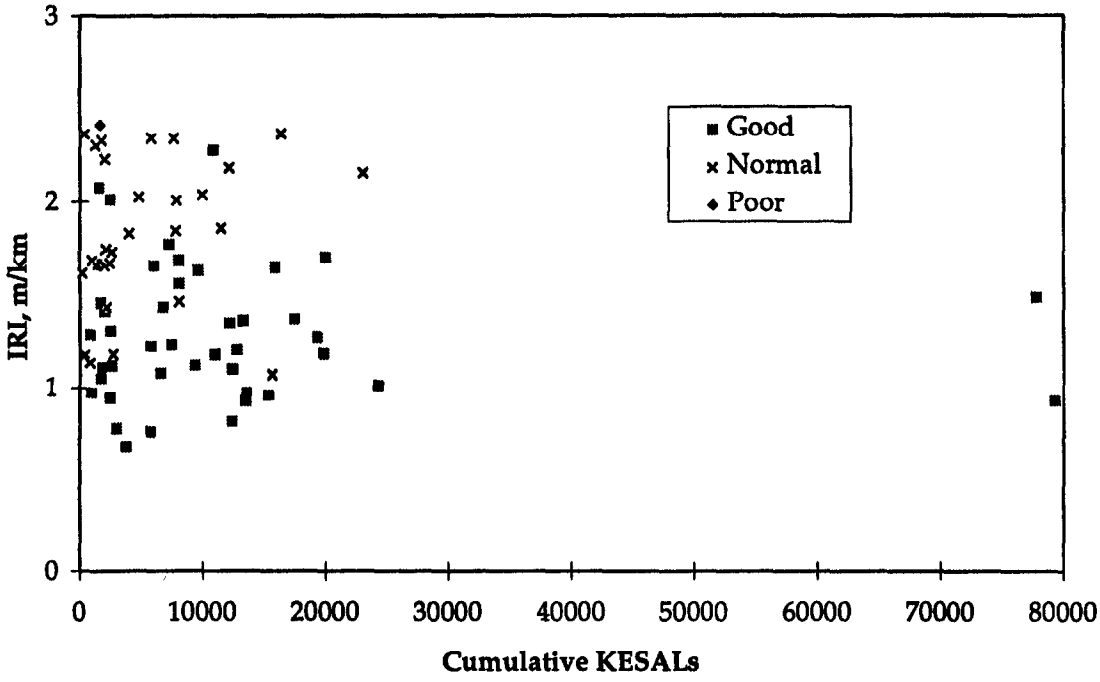

Figure 56. Cumulative KESALs versus IRI for CRCP.

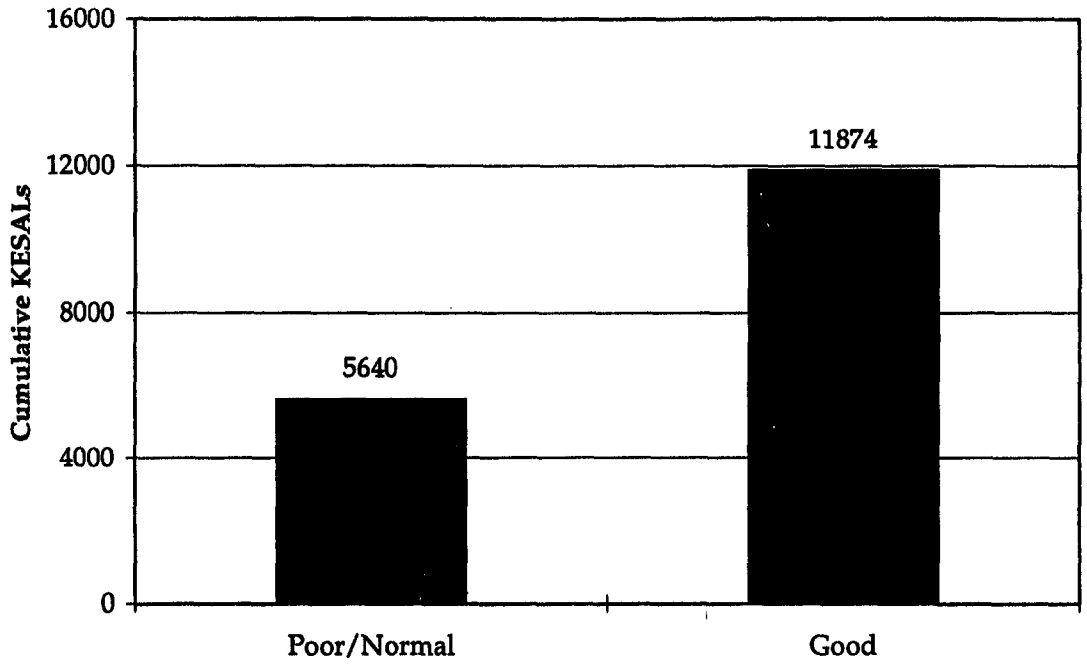

Figure 57. Effect of cumulative traffic for CRCP performance (values shown are in 1,000s of ESALs, 5640 = 5,640,000 ESALs).

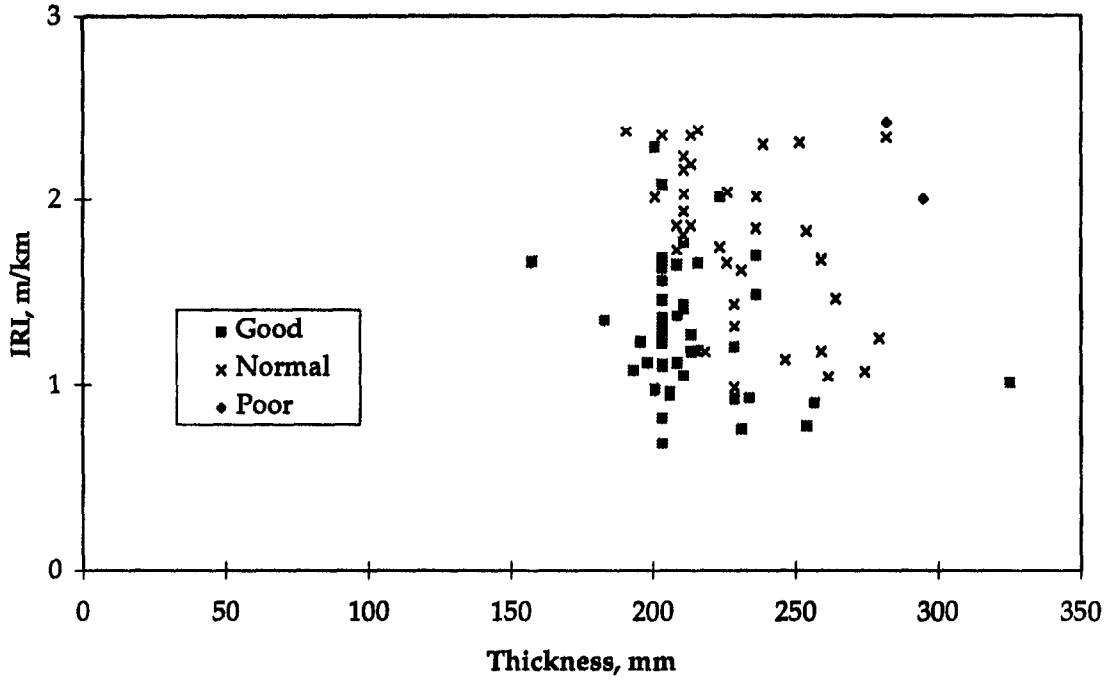

Figure 58. PCC slab thickness versus IRI for CRCP.

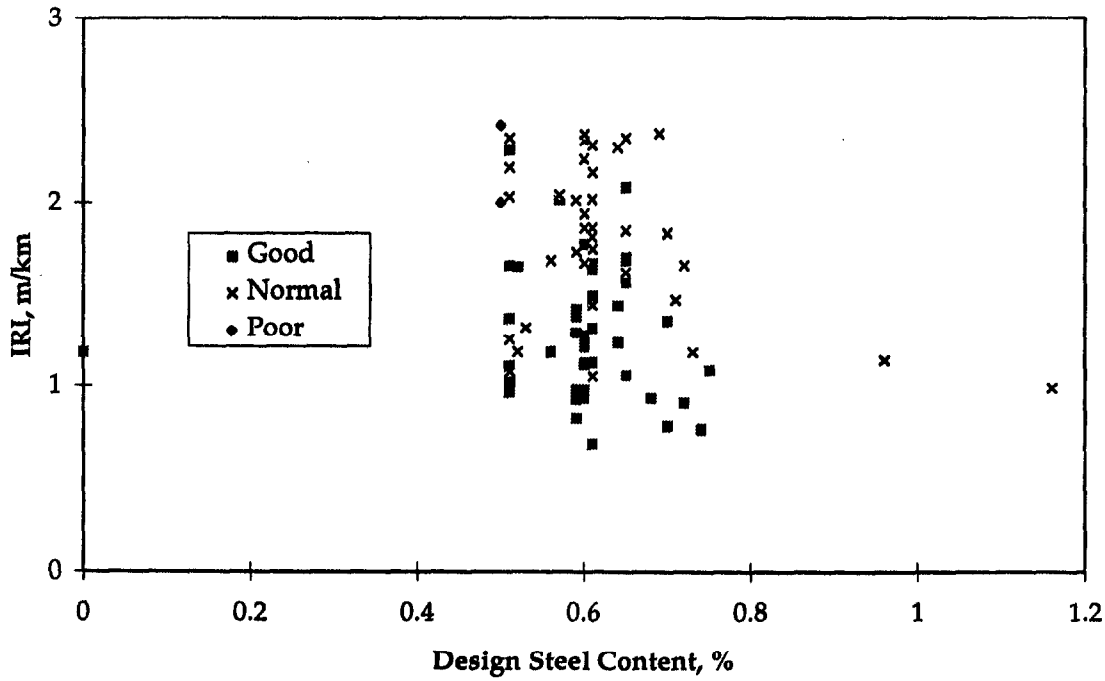

Figure 59. Design steel content versus IRI for CRCP.

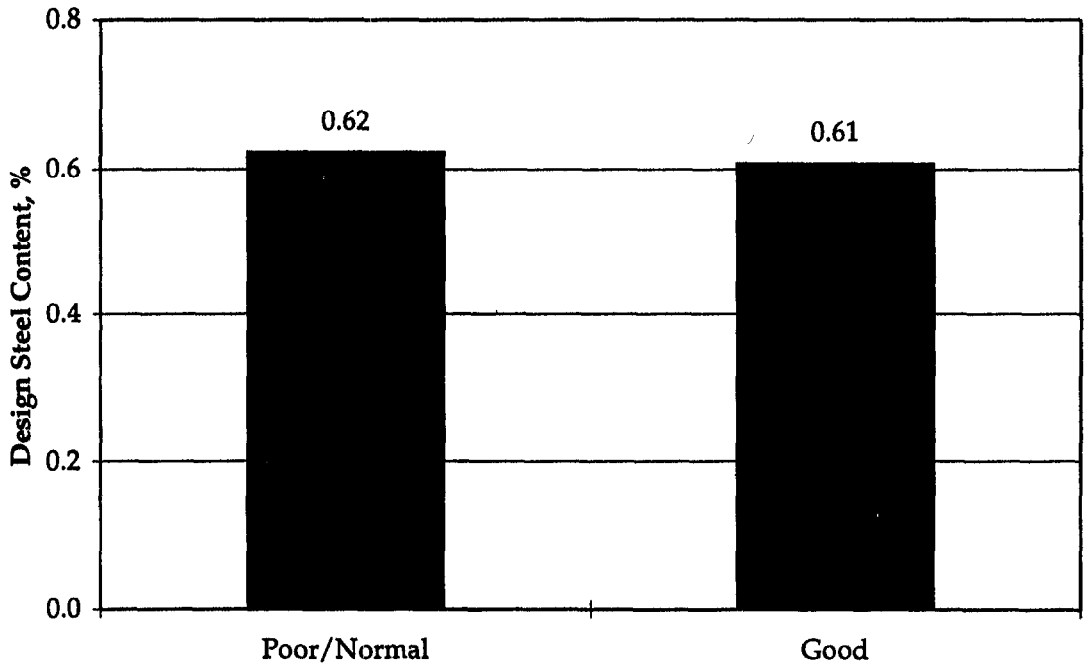

Figure 60. Effect of design steel content on CRCP performance.

Base Type. Only 20 percent of CRCP sections have a non-stabilized base, which is a much lower percentage compared to JPCP and JRCP sections (43 and 59 percent, respectively). This might be one of the factors contributing to the lowest percentage of poor sections and the highest percentage of good sections with respect to IRI for CRCP sections. Figure 61 shows that good performing CRCP sections have higher average modulus of elasticity than normal and poor performing sections. The Fisher's exact test (table 19) shows that this difference is of moderate significance.

Drainage. Unlike JPCP and JRCP, comparative analysis did not discover a clear trend relating good and poor performing sections and subdrainage. Figure 62 shows the distribution of IRI vs. C_d. Nevertheless, the multivariate analysis has found the drainage coefficient to be an important parameter that decreases IRI for CRCP.

Initial As-Constructed Roughness. As discussed in the JPCP section, a recently completed study concluded that the initial roughness has a significant influence on future pavement roughness (CRCP was included in the study).[4] Plots from the LTPP data base of IRI versus age for CRCP show a large majority of sections with very flat curves, which makes it obvious that the initial IRI of the CRCP projects would likely have a large effect on future IRI.

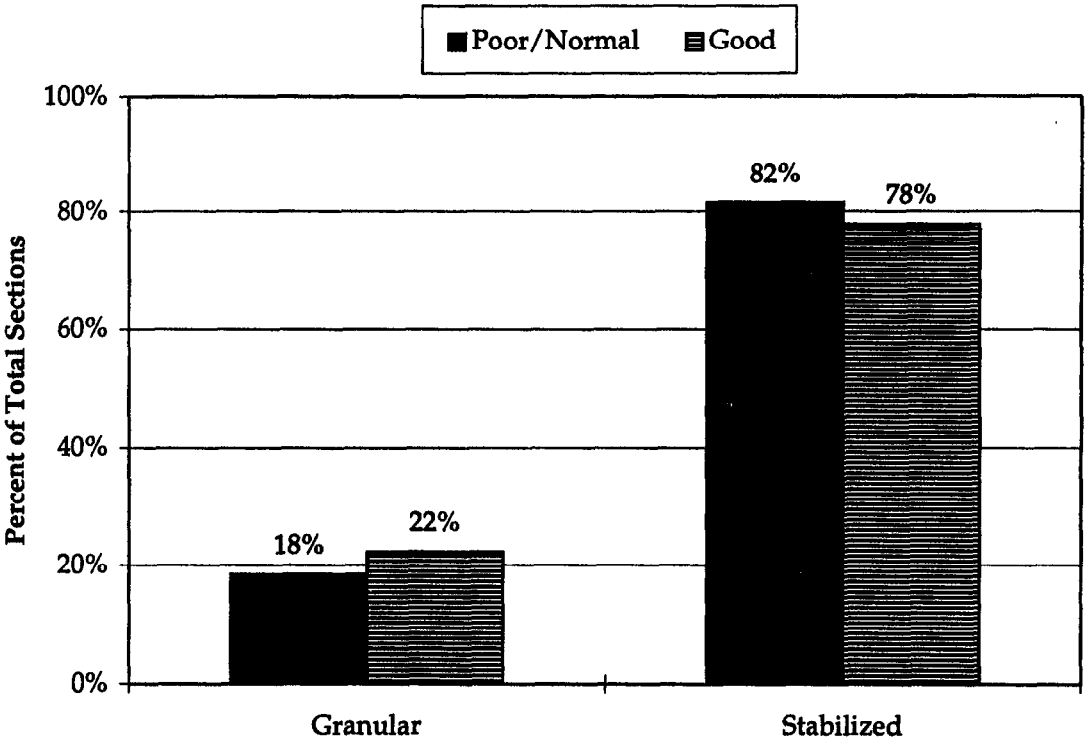

Figure 61. Effect of base-layer type on CRCP performance.

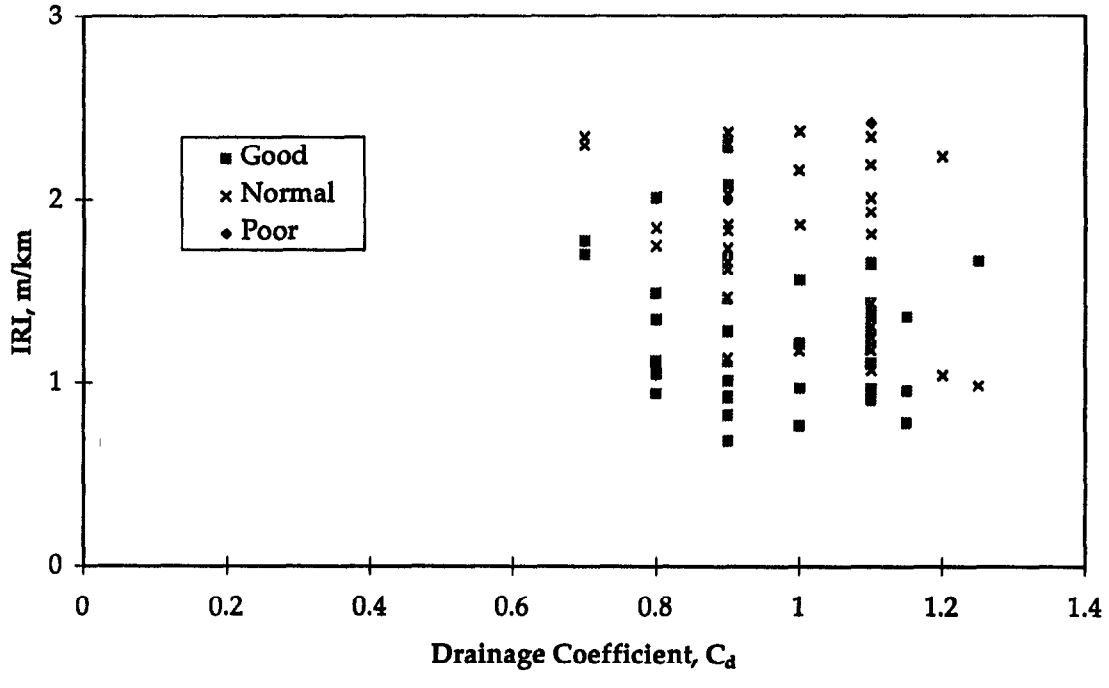

Figure 62. Drainage coefficient (C_d) versus IRI for CRCP.

In this study, an attempt was made to evaluate this conclusion using the LTPP data base. Because the LTPP data base does not contain as-constructed initial roughness data, a simple linear technique was used to "backcast" an initial roughness factor (IRF), which attempts to estimate initial IRI from the available time series IRI data. It was shown that backcasting of IRF values provides reasonably good estimates for younger and older pavements.

Results also showed that the mean initial roughness for thicker CRCP was approximately the same as thinner CRCP. This was also true for JPCP, but not for JRCP, as previously documented.

The linear analysis procedure discussed earlier was used to predict the effects of initial IRI, as modeled with IRF, and the rate of IRI increase, α, for CRCP sections. A comparison between young and all sections for CRCP is presented in figures 63 and 64 for IRF and rate of deterioration, respectively. All results are summarized in table 20 for the CRCP sections. The values for young and all CRCP are approximately the same, indicating that the backcasting process is reasonable, even for older pavements.

Two important trends are shown in figures 63 and 64. The mean IRF (estimate of initial IRI) is 1.1m/km for all good CRCP, whereas the mean IRF for all poor CRCP is 1.4 m/km. The mean rate of increase in IRI over time is 0.01 m/km/year for all good CRCP, whereas the mean IRI increase over time for all poor CRCP is 0.03 m/km/year.

Table 20. Comparison of IRF (estimate of initial IRI) and deterioration rate for CRCP.

Parameter	Category	All sections	Young sections
Initial Roughness IRF, m/km	Poor/Normal	1.44	1.53
	Good	1.14	0.92
Rate of IRI Increase α, m/km/year	Poor/Normal	0.031	0.026
	Good	0.011	0.007

The rate of increase in IRI over time for pavements rated as good is much lower than for those rated poor. This finding is similar to that determined for JPCP and JRCP.

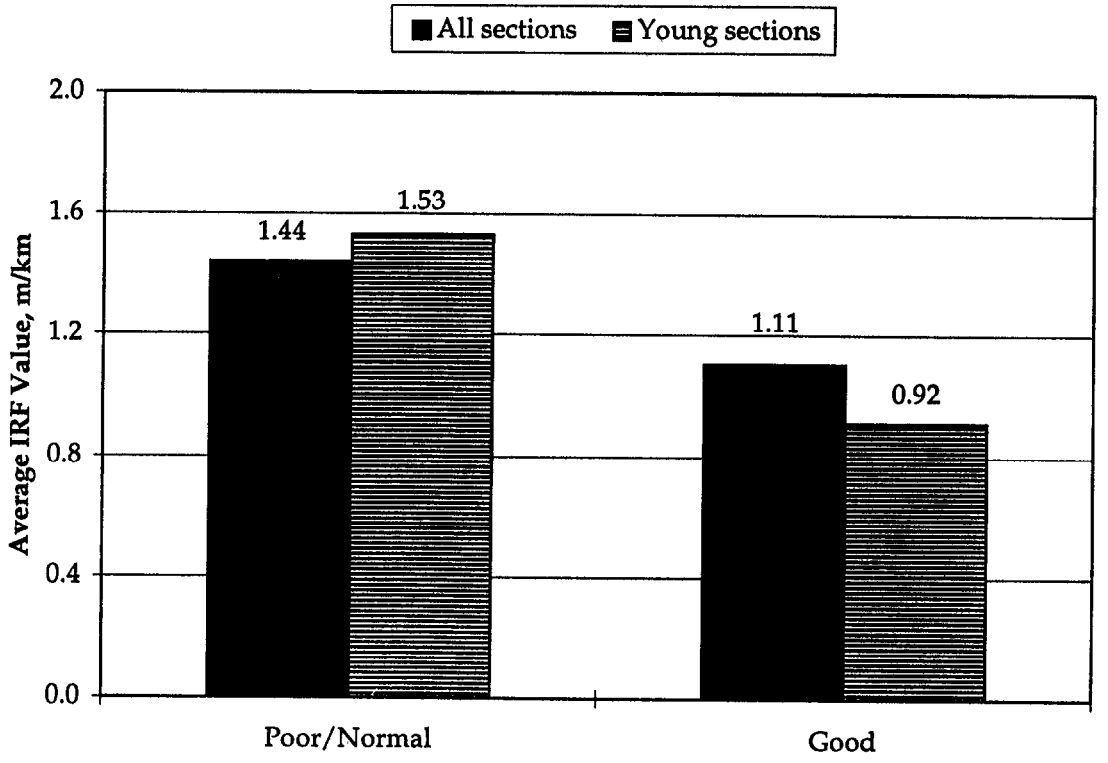

Figure 63. Comparison of average IRF values for CRCP.

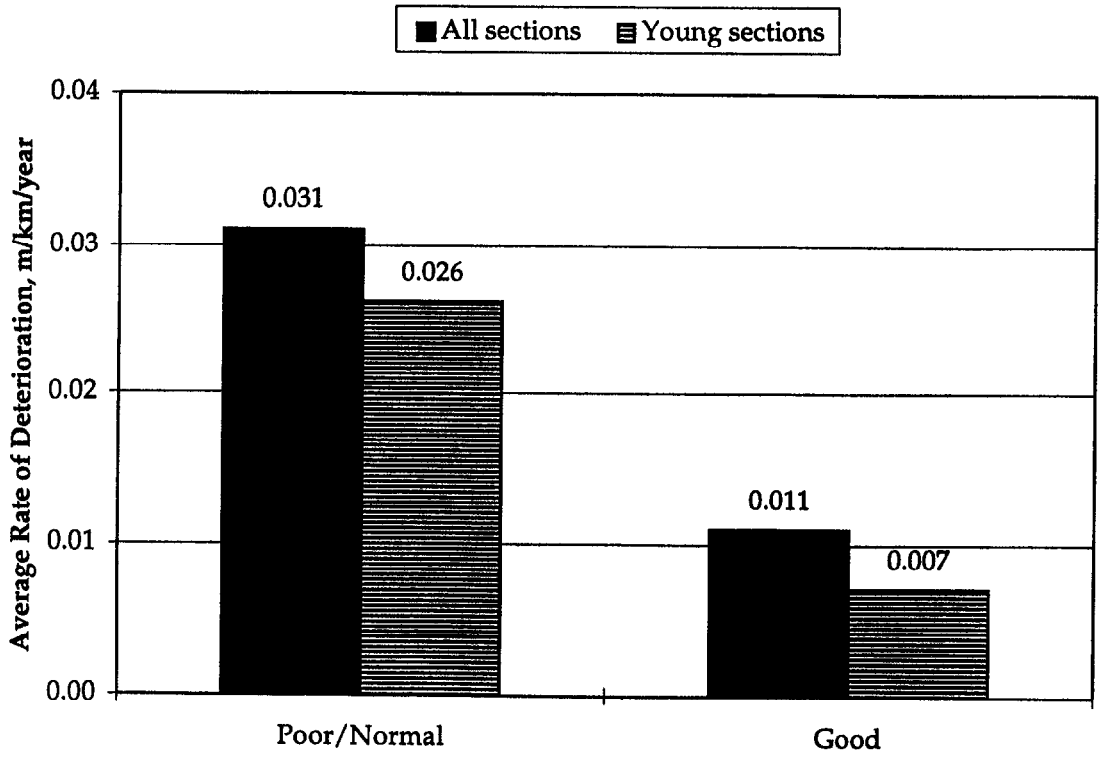

Figure 64. Comparison of average rate of deterioration, α, for CRCP.

Multivariate Analysis

Because the visual and graphical comparisons and the t-tests did not show any significant variables were contributing to good and poor IRI performance, the following multivariate analysis approach was used to attempt to identify site conditions or design features that contribute to IRI of CRCP. The objective of this analysis is to study the interrelationships of the variables. The first part is to select the most significant regressors from the 23 available variables. The second, and somewhat overlapping, part is to find a combination of variables that is efficient at modeling IRI. The initial IRI was not included in this analysis because it was not available for every section.

Variable Selection. The first step in conducting the regression analysis was to select the most significant independent variables. The explanation of the variables can be found from tables 18 and 19. Table 21 is the result of a stepwise regression. It contains the 23 variables that were available to model IRI. The second column contains the R-square for the variables when regressed on the first five variables in the table. KESAL and HPCC have small R-squares because they are not well explained by the first five variables. The partial correlation and the semi-partial correlation are also found by regressing each variable on the first five variables. The residuals from this regression are regressed on the corresponding residuals from IRI (using the 22 variables) and the raw IRI observations. For example, the residuals from PSTEEL are correlated with the corresponding residuals for IRI (-0.249). These residuals are also correlated with the raw IRI observations (-0.229). A large partial correlation followed by a relatively small semi-partial correlation indicates that the variable makes a unique contribution toward modeling IRI. The first five variables have the largest differences.

BASE and GRANBAS are identical. This is why the R-square for GRANBAS equals 1. They are subsequently combined and denoted GRANS. There are up to 58 observations depending on each variable's missing data.

Table 21. Redundancy of independent variables. (R-square column contains R-square of respective variable with all other independent variables n = 58)

	R-square	Partial cor.	Semi-part cor.
PSTEEL	0.008	-0.249	-0.229
C_d	0.307	-0.181	-0.164
TEXT1	0.191	0.273	0.253
MR28	0.041	0.247	0.227
BASE	0.358	-0.183	-0.166
FI	0.238	-0.031	-0.028
FT	0.135	-0.062	-0.056
PRECIP	0.145	-0.056	-0.050
WETDAYS	0.208	-0.055	-0.049
TMEAN	0.217	0.154	0.137
ESAL	0.099	-0.120	-0.107
AGE	0.271	0.088	0.078
HPCC	0.061	-0.091	-0.081
EPCC	0.720	-0.112	-0.100
EBASE	0.402	0.141	0.125
KSTATIC	0.236	0.042	0.037
GRANBAS	1.000		
ACBASE	0.327	-0.116	-0.104
CEMBASE	0.128	0.149	0.132
COARSE	0.542	-0.121	-0.108
WW	0.185	-0.034	-0.031
CW	0.308	-0.002	-0.002
TEXT3	0.442	-0.080	-0.071

Table 22 contains the correlations between the raw values of the 23 variables and the raw values of IRI. The second value for each variable indicates if this correlation is significantly different from zero. If the p-value is less than 0.10, then this result was considered to be too strong to be due to chance. There are 53 observations because the entire case was deleted if there were any missing values.

Table 22. Correlations between 23 variables and IRI.
n=53 (Casewise deletion of missing data)

	IRI
FI	-0.126 p=0.368
FT	-0.223 p=0.108
PRECIP	-0.029 p=0.838
WETDAYS	-0.105 p=0.454
TMEAN	0.247 p=0.074
PSTEEL	-0.240 p=0.084
ESAL	-0.141 p=0.313
AGE	-0.159 p=0.254
HPCC	0.057 p=0.685
MR28	0.281 p=0.041
EPCC	0.223 p=0.109
EBASE	0.204 p=0.143
C_d	-0.104 p=0.459
KSTATIC	-0.004 p=0.975
GRANBAS	-0.007 p=0.962
ACBASE	-0.069 p=0.621
CEMBASE	0.089 p=0.525
EBASE	0.007 p=0.962
COARSE	-0.100 p=0.477
WW	0.101 p=0.472
CW	0.023 p=0.872
TEXT1	0.259 P=0.061
TEXT3	-0.203 p=0.144

At this point, PSTEEL and MR28 are the most significant variables because they appear to be singly correlated with a unique piece of the variability in IRI. The other variables overlap—explaining the same variability.

Studying of variables was further continued by breaking them into groups. Since C_d is a variable based directly on COARSE, WW, and CW, one of those variables must be chosen to avoid accounting for the same input twice. C_d was chosen because of its strong performance. The remaining variables were put into four families: the weather group, the pavement measurements, the AGE/ESAL group, and pavement classification variables. The first three families were studied.

The weather group consists of FI, FT, PRECIP, WETDAYS, and TMEAN. Table 23 contains all the correlations between the weather variables and IRI. The top value is the correlation and the bottom value indicates if the correlation is significantly different from zero. None of the variables appear to be correlated with IRI. WETDAYS is not correlated with FI or FT; all the other weather variables are pair-wise connected.

Table 23. Correlations between climatic variables and IRI.
n=82 (Casewise deletion of missing data)

	IRI	FI	FT	PRECIP	WETDAYS	TMEAN
IRI	1.000	-0.025	-0.063	-0.024	-0.034	0.108
	p= ---	p=0.822	p=0.576	p=0.832	p=0.763	p=0.335
FI	-0.025	1.000	0.605	-0.326	0.088	-0.823
	p=0.822	p= ---	p=0.000	p=0.003	p=0.431	p=0.000
FT	-0.063	0.605	1.000	-0.316	0.112	-0.845
	p=0.576	p=0.000	p= ---	p=0.004	p=0.316	p=0.000
PRECIP	-0.024	-0.326	-0.316	1.000	0.643	0.296
	p=0.832	p=0.003	p=0.004	p= ---	p=0.000	p=0.007
WETDAYS	-0.034	0.088	0.112	0.643	1.000	-0.276
	p=0.763	p=0.431	p=0.316	p=0.000	p= ---	p=0.012
TMEAN	0.108	-0.823	-0.845	0.296	-0.276	1.000
	p=0.335	p=0.000	p=0.000	p=0.007	p=0.012	p= ---

Table 24 contains the principal components of IRI with the weather variables. Each factor is one linear combination of the variables which is independent of the other factors. Factor 1 is the linear combination with the most variability; factor 2 is the linear combination that has the most variability of those linear combinations which are orthogonal to factor 1. The values in the first six rows of the table are the correlations between the variable and the factors. The seventh row contains the eigen values for these factors, and the final row is the proportion of variability from the six variables that is explained by the factor. This table leads us to think of the six variables as three groups: factor 1 is highly correlated with FI, FT, and TMEAN; factor 2 is correlated with PRECIP and WETDAYS; and factor 3 is correlated with IRI. The remaining three factors contain only 10 percent of the variability. Because IRI is not correlated with the same factors that are correlated with the weather variables, it appears that the weather variables are not very useful for modeling IRI.

Table 24. Factor loadings for IRI and climatic variables (unrotated).
Extraction: Principal components
(Marked loadings are >0.700000)

	Factor 1	Factor 2	Factor 3	Factor 4	Factor 5	Factor 6
IRI	-0.102	0.124	-0.987	0.027	0.005	0.011
FI	0.874	-0.039	-0.082	-0.456	0.118	-0.080
FT	0.883	-0.072	-0.025	0.430	0.148	-0.087
PRECIP	-0.465	-0.821	-0.030	-0.022	0.328	0.043
WETDAYS	0.086	-0.947	-0.096	0.007	-0.287	-0.064
TMEAN	-0.962	0.198	0.013	-0.011	0.058	-0.180
Eigen Value	2.703	1.631	0.991	0.394	0.229	0.052
Princip. Var.	0.450	0.272	0.165	0.066	0.038	0.009

The second family of six variables relate to pavement measurements. Table 25 shows the correlations between the pavement measurements and IRI. These correlations reveal the pair-wise relationships of the variables. PSTEEL and MR28 are significantly correlated with IRI. The remaining variables are correlated with each other and with PSTEEL and MR28. This gives the impression that these other variables are weaker copies of PSTEEL and MR28. However, the true relationships might be reversed.

Table 25. Correlations between pavement design parameters and IRI.
n=77 (Casewise deletion of missing data)

	IRI	PSTEEL	HPCC	MR28	EPCC	EBASE	KSTATIC
IRI	1.000	-0.239	0.042	0.236	0.164	0.102	0.003
	p= ---	p=0.036	p=0.715	p=0.039	p=0.155	p=0.375	p=0.982
PSTEEL	-0.239	1.000	-0.058	-0.019	-0.065	-0.163	0.277
	p=0.036	p= ---	p=0.614	p=0.873	p=0.577	p=0.157	p=0.015
HPCC	0.042	-0.058	1.000	0.042	0.147	0.211	0.010
	p=0.715	p=0.614	p= ---	p=0.715	p=0.204	p=0.066	p=0.931
MR28	0.236	-0.019	0.042	1.000	0.845	0.124	0.110
	p=0.039	p=0.873	p=0.715	p= ---	p=0.000	p=0.284	p=0.342
EPCC	0.164	-0.065	0.147	0.845	1.000	0.200	0.124
	p=0.155	p=0.577	p=0.204	p=0.000	p= ---	p=0.082	p=0.284
EBASE	0.102	-0.163	0.211	0.124	0.200	1.000	0.190
	p=0.375	p=0.157	p=0.066	p=0.284	p=0.082	p= ---	p=0.098
KSTATIC	0.003	0.277	0.010	0.110	0.124	0.190	1.000
	p=0.982	p=0.015	p=0.931	p=0.342	p=0.284	p=0.098	p= ---

Table 26 contains the principal components for IRI and this family of variables. The results are less definitive than those in table 24—the variables overlap much more. Factor 1 is highly correlated with MR28 and EPCC and somewhat correlated with IRI. Factor 2 is highly correlated with PSTEEL and KSTATIC and somewhat correlated with IRI. IRI is not correlated with factor 3, which is correlated with HPCC and EBASE. Overall, it appears that HPCC and EBASE are less important for explaining IRI.

Table 26. Factor loadings for IRI and pavement design parameters (unrotated).
Extraction: Principal components
(Marked loadings are > 0.700000)

	Factor 1	Factor 2	Factor 3	Factor 4	Factor 5	Factor 6	Factor 7
IRI	0.418	0.420	0.080	-0.561	-0.545	-0.174	-0.031
PSTEEL	-0.182	-0.820	0.041	0.097	-0.281	-0.451	-0.020
HPCC	0.266	0.146	-0.617	0.555	-0.456	0.102	0.028
MR28	0.877	-0.153	0.351	0.114	0.046	-0.017	0.262
EPCC	0.898	-0.136	0.223	0.208	0.104	0.041	-0.263
EBASE	0.424	0.097	-0.683	-0.195	0.425	-0.355	0.015
KSTATIC	0.223	-0.663	-0.363	-0.450	-0.068	0.414	0.007
Eigen Val	2.083	1.362	1.161	0.928	0.782	0.544	0.141
Princ Var	0.298	0.195	0.166	0.133	0.112	0.078	0.020

The third family is the AGE/ESAL group. Table 27 shows the correlations for IRI, AGE, and ESAL. IRI does not appear to be correlated with either AGE or KESAL, but AGE and KESAL are correlated.

Table 27. Correlations between AGE /ESAL and IRI.
Marked correlations are significant at p < 0.05000
N=71 (Casewise deletion of missing data)

	IRI	ESAL	AGE
IRI	1.000	-0.149	-0.036
	p= ---	p=0.215	p=0.768
ESAL	-0.149	1.000	0.209
	p=0.215	p= ---	p=0.081
AGE	-0.036	0.209	1.000
	p=0.768	p=0.081	p= ---

Table 28 contains the principal components of IRI with AGE and ESAL. It shows that there is some overlap between IRI and ESAL/AGE--these principal components do not partition the variability neatly.

Table 28. Factor loadings for IRI and AGE/ESAL (unrotated).
Extraction: Principal components

	Factor 1	Factor 2	Factor 3
IRI	-0.504	-0.803	-0.319
ESAL	0.771	-0.046	-0.635
AGE	0.653	-0.565	0.504
Expl. Var.	1.274	0.966	0.760
Principal Total	0.425	0.322	0.253

Based on the above analyses, a strong regression model should be based on PSTEEL and MR28. These variables make unique contributions and are uncorrelated. Some of the other variables will be useful for completing a model. For the selection of the remaining variables, preference should be given to regressors that are not highly correlated with each other. The remaining variables to consider are C_d; the weather family; ESAL/AGE; and BASE, ACBASE, CEMBASE, and TEXT1. C_d, BASE, and TEXT1 are the next most significant because of their larger partial and semi-partial correlations. It appears that two of the five weather variables will represent that family adequately. AGE is favored over ESAL because of ESAL's missing values. The remaining three variables might also be helpful: ACBASE, CEMBASE, and TEXT3.

The second step is to find a combination of these variables that will efficiently explain the variability in IRI. To find the variables that will best compliment PSTEEL and MR28, stepwise regression was used to find the model in table 29. The second and third columns of table 29 are the standardized regression coefficients and the corresponding standard deviations. The fourth and fifth columns are the raw coefficients. The remaining columns are for the t-tests comparing the raw coefficients to zero. Pair-wise deletion of missing data was used so these t-tests have different degrees of freedom.

Table 29. Regression summary for dependent variable; step 1.
R^2= 0.20728522 Adjusted R^2= 0.14437135
F(5,63)=3.2947 p<0.01048 Std. Error of estimate: 27.967

	BETA	St. Err. of BETA	B	St. Err. of B	t(63)	p-level	Valid N
Intercpt			1.996	0.731	2.729	0.008	
PSTEEL	-0.230	0.113	-1.154	0.566	-2.041	0.045	82
C_d	-0.197	0.135	-0.696	0.475	-1.465	0.148	83
TEXT1	0.281	0.125	0.269	0.119	2.253	0.028	70
MR28	0.232	0.115	$0.151*10^{-3}$	$0.07*10^{-3}$	2.025	0.047	83
BASE	-0.207	0.140	-0.243	164.362	1.478	0.145	83

Table 30 shows the standardized coefficients in the second column and the partial and semi-partial correlations in the third and fourth columns. The standardized coefficients are indicative of the influence of these variables after considering the first five regressors. These coefficients are sensitive to correlations between the regressors. AGE and TEXT3 were eliminated because of their small partial and semi-partial correlations. FI and WETDAYS were also dropped to remove some redundancy.

Table 30. Redundancy of regressor variables.

	Beta in	Partial corr.	Semi-partial corr.
PSTEEL	-0.230	-0.249	-0.229
C_d	-0.197	-0.181	-0.164
TEXT1	0.281	0.273	0.253
MR28	0.232	0.247	0.227
BASE	-0.207	-0.183	-0.166
FI	-0.032	-0.031	-0.028
FT	-0.060	-0.062	-0.056
PRECIP	-0.054	-0.056	-0.050
WETDAYS	-0.055	-0.055	-0.049
TMEAN	0.155	0.154	0.137
AGE	0.092	0.088	0.078
ACBASE	-0.126	-0.116	-0.104
CEMBASE	0.142	0.149	0.132
TEXT3	-0.095	-0.080	-0.071

Table 31 shows the pair-wise correlations for the remaining variables, and table 32 shows their factor loadings.

Table 31. Correlations between remaining variables and IRI.
n=69 (Casewise deletion of missing data)

	IRI	FT	PRECIP	TMEAN	PSTEEL	MR28	C_d	ACBASE	CEMBASE	BASE	TEXT1
IRI	1.000	-0.046	-0.017	0.131	-0.261	0.232	-0.214	-0.030	0.056	-0.056	0.149
	p= —	p=0.706	p=0.889	p=0.284	p=0.030	p=0.055	p=0.077	p=0.806	p=0.646	p=0.650	p=0.223
FT	-0.046	1.000	-0.285	-0.838	0.022	-0.107	-0.224	-0.249	0.066	-0.275	-0.245
	p=0.706	p= —	p=0.018	p=0.000	p=0.858	p=0.381	p=0.065	p=0.039	p=0.593	p=0.022	p=0.043
PRECIP	-0.017	-0.285	1.000	0.260	-0.129	-0.157	-0.296	-0.020	0.005	-0.100	-0.044
	p=0.889	p=0.018	p= —	p=0.031	p=0.289	p=0.196	p=0.014	p=0.869	p=0.969	p=0.413	p=0.720
TMEAN	0.131	-0.838	0.260	1.000	-0.045	0.145	0.289	0.437	-0.106	0.398	0.293
	p=0.284	p=0.000	p=0.031	p= —	p=0.717	p=0.233	p=0.016	p=0.000	p=0.385	p=0.001	p=0.014
PSTEEL	-0.261	0.022	-0.129	-0.045	1.000	0.010	-0.005	0.046	-0.103	-0.058	-0.045
	p=0.030	p=0.858	p=0.289	p=0.717	p= —	p=0.933	p=0.966	p=0.708	p=0.399	p=0.637	p=0.711
MR28	0.232	-0.107	-0.157	0.145	0.010	1.000	-0.026	0.313	-0.165	0.187	-0.031
	p=0.055	p=0.381	p=0.196	p=0.233	p=0.933	p= —	p=0.834	p=0.009	p=0.175	p=0.123	p=0.798
C_d	-0.214	-0.224	-0.296	0.289	-0.005	-0.026	1.000	0.310	0.113	0.595	0.340
	p=0.077	p=0.065	p=0.014	p=0.016	p=0.966	p=0.834	p= —	p=0.009	p=0.357	p=0.000	p=0.004
ACBASE	-0.030	-0.249	-0.020	0.437	0.046	0.313	0.310	1.000	-0.615	0.518	0.181
	p=0.806	p=0.039	p=0.869	p=0.000	p=0.708	p=0.009	p=0.009	p= —	p=0.000	p=0.000	p=0.137
CEMBASE	0.056	0.066	0.005	-0.106	-0.103	-0.165	0.113	-0.615	1.000	0.276	0.162
	p=0.646	p=0.593	p=0.969	p=0.385	p=0.399	p=0.175	p=0.357	p=0.000	p= —	p=0.022	p=0.183
GRAN	-0.056	-0.275	-0.100	0.398	-0.058	0.187	0.595	0.518	0.276	1.000	0.400
	p=0.650	p=0.022	p=0.413	p=0.001	p=0.637	p=0.123	p=0.000	p=0.000	p=0.022	p= —	p=0.001
TEXT1	0.149	-0.245	-0.044	0.293	-0.045	-0.031	0.340	0.181	0.162	0.400	1.000
	p=0.223	p=0.043	p=0.720	p=0.014	p=0.711	p=0.798	p=0.004	p=0.137	p=0.183	p=0.001	p= —

Table 32. Factor loadings for IRI and remaining variables (unrotated).
Extraction: Principal components
(Marked loadings are > 0.700000)

	Factor 1	Factor 2	Factor 3	Factor 4	Factor 5	Factor 6	Factor 7	Factor 8	Factor 9	Factor 10	Factor 11
IRI	-0.048	-0.168	-0.382	-0.758	0.133	-0.284	-0.052	0.360	-0.126	0.046	-0.004
FT	0.706	0.235	0.413	-0.237	-0.231	-0.048	0.306	0.107	-0.077	-0.228	-0.030
PRECIP	-0.042	-0.375	-0.636	0.378	-0.140	0.141	0.454	0.032	-0.252	0.013	-0.008
TMEAN	-0.816	-0.244	-0.335	0.137	0.145	0.012	-0.203	0.061	0.075	-0.266	-0.029
PSTEEL	0.047	-0.050	0.439	0.422	0.718	-0.200	0.171	0.186	-0.071	0.008	-0.003
MR28	-0.279	-0.322	0.257	-0.578	0.345	0.412	0.134	-0.311	-0.124	-0.019	-0.002
C_d	-0.609	0.525	0.290	0.119	-0.156	0.044	-0.254	0.041	-0.404	0.001	0.008
ACBASE	-0.697	-0.382	0.451	-0.041	-0.265	-0.053	0.212	0.155	0.081	-0.007	0.124
CEMBASE	0.123	0.770	-0.455	-0.071	0.263	0.279	0.106	0.068	0.060	-0.051	0.105
BASE	-0.749	0.423	0.126	-0.085	-0.065	0.254	0.282	0.210	0.166	0.083	-0.098
TEXT1	-0.523	0.382	-0.158	-0.127	0.031	-0.586	0.276	-0.344	0.009	-0.010	-0.002
Eigen Vals	2.956	1.728	1.626	1.349	0.915	0.803	0.667	0.470	0.312	0.135	0.038
Prp. Var.	0.269	0.157	0.148	0.123	0.083	0.073	0.061	0.043	0.028	0.012	0.003

Carefully studying these tables indicates that it is necessary to choose between TEXT1, and ACBASE or CEMBASE. ACBASE is heavily correlated with many other variables, so CEMBASE was retained. In addition, FT, PRECIP, and TMEAN were also dropped. Table 33 shows a model that uses CEMBASE. Influential points using Cook's distance were identified. One of these affected the coefficients for PSTEEL and C_d. After deleting it, the following model is obtained:

Table 33. Regression summary for dependent variable; step 2.
R= 0.40104476 R^2= 0.16083690 Adjusted R^2= 0.10489269
F(5,75)=2.8750 p<0.01984 Std. Error of estimate: 28.521

	BETA	St. Err. of BETA	B	St. Err. of B	t(75)	p-level	Valid N
Intercpt			2.226	0.831	2.678	0.009	
PSTEEL	-0.238	0.111	-1.546	0.722	-2.140	0.036	81
MR28	0.250	0.110	$0.16*10^{-3}$	$0.071*10^{-3}$	2.270	0.026	82
C_d	-0.171	0.130	-0.615	0.465	-1.322	0.190	82
CEMBASE	0.153	0.113	0.175	0.129	1.357	0.179	82
BASE	-0.164	0.132	-0.191	0.154	1.239	0.219	82

Exchanging CEMBASE for TEXT1 produces the model shown in table 34.

Table 34. Regression summary for dependent variable; step 3.
R^2= 0.20728522 Adjusted R^2= 0.14535438
F(5,64)=3.3470 p<0.00952 Std. Error of estimate: 27.948

	BETA	St. Err. of BETA	B	St. Err. of B	t(64)	p-level	Valid N
Intercpt			1.997	725.426	2.751	0.008	
PSTEEL	-0.230	0.112	-1.154	561.222	-2.057	0.044	82
C_d	-0.197	0.134	-0.696	471.259	-1.476	0.145	83
TEXT1	0.281	0.124	0.269	118.450	2.271	0.027	70
MR28	0.232	0.114	$0.151*10^{-3}$	$0.07*10^{-3}$	2.041	0.045	83
BASE	-0.207	0.139	-0.243	0.163	1.489	0.141	83

This final simple model was obtained by dropping BASE, and eliminating three influential points.

Table 35. Regression summary for dependent variable; step 4.
R^2= 0.17981495 Adjusted R^2= 0.12934203
F(4,65)=3.5626 p<0.01090 Std. Error of estimate: 28.209

	BETA	St. Err. of BETA	B	St. Err. of B	t(65)	p-level	Valid N
Intercpt			2.473	0.656	3.764	0.000	
PSTEEL	-0.223	0.113	-1.122	0.566	-1.983	0.052	82
C_d	-0.289	0.120	-1.017	0.422	-2.405	0.019	83
TEXT1	0.229	0.120	0.219	0.114	1.911	0.060	70
MR28	0.198	0.112	$0.128*10^{-3}$	$0.07*10^{-3}$	1.764	0.082	83

These simplified regression analyses lead to the conclusion that higher steel content and improved drainage decreases roughness in CRCP, whereas an increase in modulus of rupture or tined texture increases roughness in CRCP.

The usefulness of these models is to discover the way the variables interrelate. However, they do not include interaction effects, and we are not in a position to validate models obtained from previous data sets or hypotheses. These models were found from the data, so the statistics can only be interpreted in a descriptive or exploratory manner.

The adjusted R-squares are small, but F-ratios are significant. A small adjusted R-square indicates that much of the variability in IRI is not explained by the model. A significant F-ratio indicates that the model is useful for explaining part of the variability. These groups of variables are better at estimating IRI than the sample mean of IRI. The strength of this model is that the independent variables are not pairwise correlated.

Summary of IRI Findings for CRCP

The CRCP sections were evaluated both comparatively and statistically using the t-test and multivariate linear regression. The results of the comparative analysis and t-test comparisons were misleading in some instances due to the influence of other variables on the variable being analyzed. One factor undoubtedly causing significant problems in the data analysis is the initial IRI after construction. This value appears to vary

widely and has a long-term effect on IRI. Another example is the drainage coefficient which is highly influenced by many variables including material characteristics, precipitation, pavement structure, subgrade soil type, and edge drains.

Given all of the analysis performed, the following factors were found to have the greatest influence on IRI of CRCP:

- **Initial roughness/smoothness of CRCP:** The data analysis showed that the roughness of a CRCP over time depends greatly on its initial IRI. The analysis also showed that the rate of increase in IRI over time is higher for those CRCP rated poor as opposed to those rated good. Thus, smoother construction results in smoother CRCP over time and traffic.

- **Climatic variables.** None of the location, temperature, or moisture variables showed much significance. However, the drainage coefficient indicates that dry climates show smoother CRCP than wet climates. This agrees with reference 3 findings where a drier climate showed lower IRI for CRCP. Reference 3 also showed that cold climates showed rougher CRCP than warm climates. The small number of poorly performing CRCP sections in the LTPP data base did not permit a comprehensive investigation of the effect of climatic variables on CRCP IRI.

- **Multivariate analysis:** The effect of these variables (except initial roughness which could not be backcasted for all sections and thus not included here) is shown in the following equation:

$$IRI = 2.473 - 1.122\ STEEL - 1.017\ C_d + 0.219\ TEXT1 + 0.000128\ MR28 \qquad (18)$$

  This model for IRI (m/km) has a relatively low R-squared value, which would be expected given the range of values of the variables and the interrelationship of the parameters evaluated. The variables contained in the IRI model substantially agree with other studies conducted with the LTPP data base and the Illinois study. [1, 3, 10]

- **Steel percentage (longitudinal).** The higher the amount of steel reinforcement in CRCP, the smoother the pavement over time. This result must be interpreted within the inference scope of the amount of steel included in LTPP sections. This ranged from 0.51 to 0.75 percent with a mean of about 0.61 percent. This certainly agrees with the Illinois study for localized failures.[10]

- **Surface texture.** CRCP finished with a tined texture on average have higher IRI's. The IRI is apparently picking up some extra roughness from the tined surface.

- **AASHTO drainage coefficient (C_d).** The drainage coefficient reflects the level of precipitation and the pavement's ability to drain excessive moisture from the structure, with a higher C_d corresponding to better drainage. CRCP having a high C_d are smoother over time than those with a low C_d (poor subdrainage).

- **Modulus of rupture (flexural strength) of concrete.** This is the estimated 28-day flexural strength. This was estimated from construction inventory data and cores taken and tested in indirect tensile strength. The higher the modulus of rupture the rougher the CRCP. This relationship does not make sense from a mechanistic view, however, there may be some construction process that has resulted in a higher IRI. Indeed, higher strength concrete mixes have a lower water/cement ratio which makes them less workable. This may make more difficult proper finishing of the concrete surface and can lead to a rougher built pavement.

CHAPTER 7. PERFORMANCE OF JCP WITH RESPECT TO TRANSVERSE JOINT FAULTING

Transverse joint faulting is an important deterioration mechanism of jointed concrete pavements (JCP) because of the negative effect on ride quality. Transverse joint faulting is a differential elevation across the joint and is the result of a combination of heavy axle loads, insufficient load transfer between adjacent slabs, free moisture beneath the pavement, and erosion of the supporting base or subgrade material from beneath the slab.

Erosion occurs when excess moisture is ejected from beneath the leave slab corner as it is loaded by a vehicle. The moisture that is ejected carries base and subgrade fines with it, resulting in a void beneath the pavement at the leave slab corner. In addition, there is a corresponding deposition of this material under the approach slab corner. Due to the build-up of material beneath the approach corner and the loss of support under the leave corner, faulting and corner cracking can develop.[1] Significant joint faulting has a major impact on the life-cycle costs of pavement in terms of rehabilitation and vehicle operating costs.

Faulting is not considered directly in the pavement design process, but rather implicitly through joint design standards. This approach has proven to be inadequate, as many pavements require early rehabilitation due to excessive faulting.

Previous Studies

Transverse joint faulting has been the focus of various field and laboratory investigations. Two faulting models were developed in the early LTPP Data Analysis Study.[1] The model developed for doweled JPCP is as follows:

$$FAULTD = 25.4\ CESAL^{0.25} \times [0.0238 + 0.0000666\ JTSPACE^2 + 0.0037 \times \left(\frac{27.2}{KSTATIC}\right)^2 + 0.0039 \times \left(\frac{AGE}{10}\right)^2 - 0.0037 \times EDGESUP - 8.58*10^{-4}\ DOWDIAM] \quad (19)$$

where

FAULTD	=	mean transverse doweled joint faulting, mm
CESAL	=	cumulative 80-kN ESALs in traffic lane, millions
JTSPACE	=	mean transverse joint spacing, m
KSTATIC	=	mean backcalculated static k-value, kPa/mm
AGE	=	age since construction, years
EDGESUP	=	edge support (1=tied concrete shoulder; 0=any other shoulder type)
DOWDIAM	=	diameter of dowels in transverse joints, mm

The model for non-doweled JPCP has the following form:

$$FAULTND = 25.4CESAL^{0.25}\,[-0.07575 + 0.0251\,\sqrt{AGE} + 2.01*10^{-8}\,PRECIP^{2} + 8.50*10^{-5}\left(FI\,\frac{PRECIP}{1000}\right) - 0.0378 \times DRAIN] \quad (20)$$

where

FAULTND	=	mean transverse non-doweled joint faulting, mm
CESAL	=	cumulative 80-kN ESALs in traffic lane, millions
PRECIP	=	mean annual precipitation, mm
FI	=	mean freeze index, °C-days freezing
AGE	=	age since construction, years
DRAIN	=	1=longitudinal subdrainage; 0=otherwise

These models predict faulting as a function of site conditions and pavement design features. The most notable parameter affecting faulting is the presence and configuration of dowels. It was shown that heavy traffic loading is positively correlated to faulting; that is, an increase in the number of heavy axle loads corresponds to an increase in joint faulting. Pavement design features such as drainage, joint spacing, base type, and presence of a widened lane have a significant effect based on these models. Climatic conditions, such as precipitation and freeze-thaw (characterized by the freezing index and precipitation) also influence faulting significantly.

A recently completed FHWA-sponsored project on JCP provides prediction models for faulting of JCP based on a limited data base.[2] These models identified several pavement design features and site conditions affecting transverse joint faulting. The faulting model for non-doweled pavements is as follows:

$$FAULTND = 25.4\ CESAL^{0.25} * [0.2347 - 0.1516*C_d - 2.87*10^{-7}\ HPCC^2/JTSPACE^{0.25} - 0.0115 * BASE + 8.37*10^{-8} * FI^{1.5}*PRECIP^{0.25} - 0.002478 * DAYS32^{0.5} - 0.0415 * WIDENLANE] \quad (21)$$

where

FAULTND	=	mean transverse non-doweled joint faulting, mm
CESAL	=	cumulative 80-kN equivalent single axle loads, millions
JTSPACE	=	mean transverse joint spacing, m
HPCC	=	PCC slab thickness, mm
BASE	=	base type (0 = nonstabilized base; 1 = stabilized base)
WIDENLANE	=	widened lane (0 = not widened, 1 = widened)
C_d	=	modified AASHTO drainage coefficient, calculated from data base
FI	=	mean annual freezing index, °C-days
PRECIP	=	mean annual precipitation, mm
DAYS32	=	annual number of days with temperature higher than 32°C

The following model was developed for doweled pavements:

$$FAULTD = 25.4\ CESAL^{0.25} * [0.0628 - 0.0628 * C_d + 7.73*10^{-5} * BSTRESS^2 + 4.57*10^{-5} * JTSPACE^2 + 0.48*10^{-9} * FI^2 * PRECIP^{0.5} - 0.009503 * BASE - 0.01917 *WIDENLANE + 0.0009217 * AGE] \quad (22)$$

where:

FAULTD	=	mean transverse doweled joint faulting, mm
CESAL	=	cumulative 80-kN equivalent single axle loads, millions
BSTRESS	=	maximum dowel/concrete bearing stress, MPa
JTSPACE	=	mean transverse joint spacing, m
BASE	=	base type (0 = nonstabilized base; 1 = stabilized base)
WIDENLANE	=	widened lane (0 = not widened, 1 = widened)
C_d	=	modified AASHTO drainage coefficient, calculated from data base information
FI	=	mean annual freezing index, °C-days
PRECIP	=	mean annual precipitation, mm
AGE	=	pavement age, years

These models generally agree with the LTPP Early Analysis Models. In addition, they highlight the effectiveness of widened PCC slabs in faulting reduction.

Two mechanistic-empirical faulting models were developed by the American Concrete Pavement Association (ACPA).[8] These models are extensions of the ACPA faulting

models developed by Packard et al. and use erodability as the main factor influencing faulting.[9] Using Miner's linear damage hypothesis, the percent of erosion damage occurring at the slab corner was defined as follows:

$$EROSION = 100*n_1*(C_2/N_i) \quad (23)$$

where

EROSION	=	percent erosion damage
n_1	=	expected number of axle load repetitions for each axle group I
N_i	=	allowable number of repetitions for axle group I
C_2	=	0.06 for pavements without a shoulder and 0.94 for pavements with a tied concrete shoulder

The allowable number of load application was related to the power, or rate of work, of each axle pass at the corner of the slab, P, as follows:

$$\log N = 14.524 - 6.777 * (C_1 * P - 9.0)^{0.103} \quad (24)$$

where

N = allowable load repetitions to end of design period
P = power
$C_1 = 1 - (KSTATIC/292/HPCC)^2$

where

HPCC = slab thickness, mm
KSTATIC = modulus of subgrade reaction, kPa/mm

The following equation was used to calculate the power of each axle pass at the corner of the slab:

$$P = 55.4 * p^2/HPCC/KSTATIC^{0.73} \quad (25)$$

where

P = power (rate of work)
p = pressure at slab-foundation interface, kPa

From regression analyses, the following models were developed for predicting faulting for undoweled and doweled pavements, respectively:

$$FAULTND = 25.4\ EROSION^{0.25}\ [0498*10^{-4}\ (PRECIP)^{0.91907} + 0.0116\ JTSPACE^{0.54428} - 0.016799*DRAIN] \quad (26)$$

$$FAULTD = 25.4\ EROSION^{0.25}\ [9.94*10^{-6}\ (PRECIP/10)^{1.84121} + 0.00916\ JTSPACE^{0.38274}\ ] \quad (27)$$

where

FAULTND	=	faulting at undoweled transverse pavement joints, mm
FAULTD	=	faulting at doweled transverse pavement joints, mm
EROSION	=	calculated accumulated erosion
PRECIP	=	annual precipitation, mm
JTSPACE	=	joint spacing, m
DRAIN	=	dummy variable for the presence of edge drains

These models generally agree with the RIPPER and LTPP Early Analysis faulting models. In addition, they identify the PCC thickness as a significant parameter that is negatively correlated with faulting.

In the recent Nationwide Pavement Cost Model refinement study, the following mechanistic-empirical faulting model was developed:[16]

$$FAULT = 25.4\ DAMAGE^{0.23}\ (\ 0.35\ -\ 0.0277BASE\ -\ 0.25C_d\ +\ 3.91*10^{-5}FI) \quad (28)$$

where

FAULT	=	mean transverse joint faulting, mm
DAMAGE	=	n/N
n_i	=	number of applications for each axle group I
N_i	=	allowable number of load repetitions for each axle group I
C_d	=	drainage coefficient
BASE	=	base type (0 = nonstabilized base; 1 = stabilized base)
FI	=	freezing index

The allowable number of load repetitions is defined as follows:

$$Log\ N = 4.27\ -1.6\ Log(DE\ -\ 1.148*10^{-5}) \quad (29)$$

where

N	=	allowable number of load repetitions
DE	=	differential of subgrade elastic energy density, kPa*mm

The model predicts faulting for doweled and non-doweled pavements and illustrates that the presence of dowels significantly reduces faulting through reduction of DE. In addition, it indicates that a stabilized base, stiff subgrade, and improved drainage are negatively correlated with faulting.

In the recent LTPP study, the NAPCOM faulting model was recalibrated using data from the LTPP data base.[3] The following model was obtained:

$$FAULT = 25.4\ DAMAGE^{0.3}\ [0.05 + 0.00004\ WETDAYS - 9.45*10^{-5}\ DOWDIAM - 0.025\ C_d\ (0.5+BASE)] \quad (30)$$

Where

DAMAGE	=	CESAL/N
CESAL	=	cumulative ESALs
N	=	allowable number of 80-kN load repetitions
C_d	=	drainage coefficient
BASE	=	base type (0 = nonstabilized base; 1 = stabilized base)
WETDAYS	=	average number of wet days per year
DOWDIAM	=	dowel diameter, mm

The main difference in the two latest models is that the LTPP model characterizes traffic in terms of ESALs, whereas the NAPCOM model uses actual axle loads. The NAPCOM model considers the freezing index to be an important climatic parameter, whereas the recent LTPP model identifies the number of wet days per year as positively correlated with faulting. Table 36 summarizes the design and site condition variables that were found to be significant in all models considered.

Performance Criteria for Faulting

This section presents an analysis of the factors that lead to faulting of JCP. The version of the LTPP data base analyzed in this study contains faulting data for 176 JPCP and JRCP sections. The total number of observations is 368. For some sections, time series data contain up to 10 observation made over 5 years. Other sections have only one performance record in the data base.

The data was divided into three performance categories: poor, normal, and good, based on average transverse joint faulting and pavement age as previously described. The grouping was done to facilitate the analysis of identifying features that contribute to good and poor faulting performance. This grouping was established based on the

Table 36. Summary of the effects of site conditions and design features on JCP faulting.

Site Condition/ Design Feature	Effect on Faulting	Reference
Pavement age	Increases*	1, 2
k-value	Decreases	1, 3,8, 9, 16
Joint spacing	Increases	1, 2, 3,8,9, 16
PCC thickness	Decreases	1, 2, 3, 8, 9, 16
PCC modulus of elasticity	Decreases	3, 8, 9, 16
Dowels	Decreases	1, 2, 3, 8, 9, 16
Traffic loads	Increases	1, 2, 3, 8, 9, 16
Stabilized base	Decreases	2, 3, 16
Coarse subgrade	Decreases	1
Tied PCC shoulder	Decreases	1, 2, 8, 9
Precipitation	Increases	1, 2, 8, 9
Number of wet days	Increases	3
Number of freeze-thaw cycles	Increases	1
Drainage	Decreases	1, 3, 8, 9, 16
FI	Increases	1, 2, 16

* For example, as pavement age increases, faulting increases. As k-value increases, faulting decreases.

experience of a group of State highway engineers. The limits that were set, in addition to the time-series data for all observations, are shown in figure 65. The pavement section was considered to be performing good (i.e., performing better than expected) if its faulting satisfied the following condition:

$$FAULT < 2\left(\frac{AGE}{20}\right)^{0.25} \tag{31}$$

where

FAULT = faulting, mm
AGE = pavement age at the time of the observation, years

The pavement section was considered to be performing poor if its average transverse joint faulting satisfied the following condition:

$$FAULT > 4\left(\frac{AGE}{20}\right)^{0.25} \tag{32}$$

where

FAULT = faulting, mm
AGE = pavement age at the time of the observation, years

Figure 65 presents a plot of all faulting observations for the LTPP JPCP and JRCP sections and shows designation of those sections by their performance at the time of observation. Because the number of observations differs among the sections, the use of all the observations in the subsequent analysis may bias the results toward the sections with a higher number of observations. To avoid this, only the last observation for each section was considered in the analysis, unless stated otherwise. Figure 66 presents a plot of all JPCP and JRCP sections with respect to faulting at the time of the last available observation.

Effect of Transverse Joint Faulting on the Ride Quality of JCP

Faulting of transverse joints dramatically affects ride quality. As was shown in the recent RIPPER study, mean transverse joint faulting is highly correlated with the International Roughness Index (IRI).[2] A similar trend was observed in this study.

The LTPP data base contains both IRI and faulting data for JPCP and JRCP. However, measurement of these parameters was not conducted simultaneously. To investigate the influence of transverse joint faulting on ride quality, the following steps were performed:

1. For each faulting measurement, the corresponding IRI data, measured not more than 1 year from the date of the faulting measurement, was identified.
2. The IRI values were averaged for each faulting measurement.
3. The sections with zero faulting and high IRI (greater than 1.8 m/km) were eliminated from the analysis.
4. A simple linear regression of IRI with respect to faulting was performed.

Figure 67 presents IRI versus joint faulting for the LTPP JPCP and JRCP sections, as well as the results of the regression. Sections with higher faulting levels, on average, have higher IRI values. Variation in faulting explains 43 percent of the variation in IRI. Therefore, to ensure good ride quality, design practices that directly control joint faulting must be used.

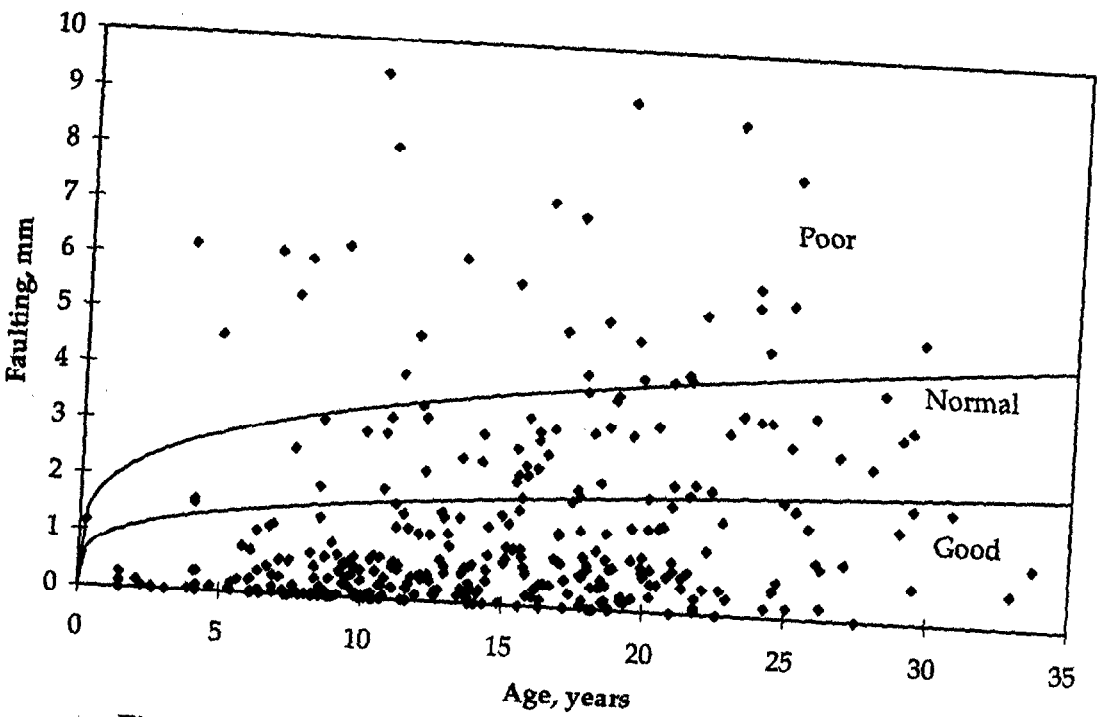

Figure 65. Faulting versus pavement age (all observations).

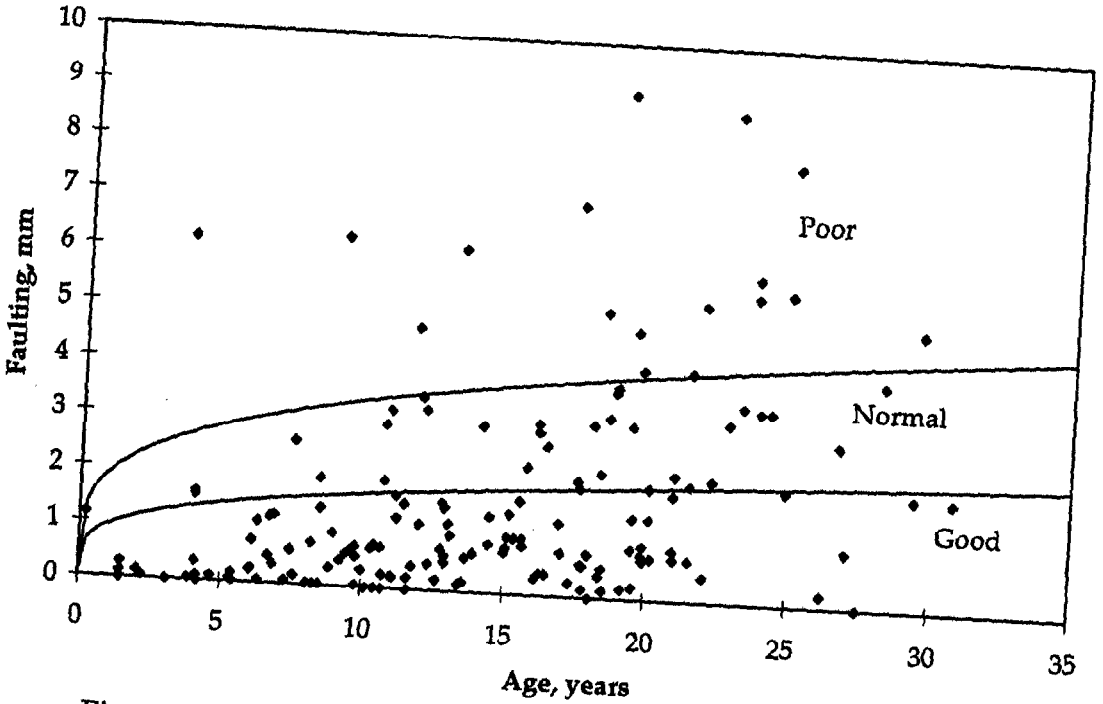

Figure 66. Faulting versus pavement age (last observation only).

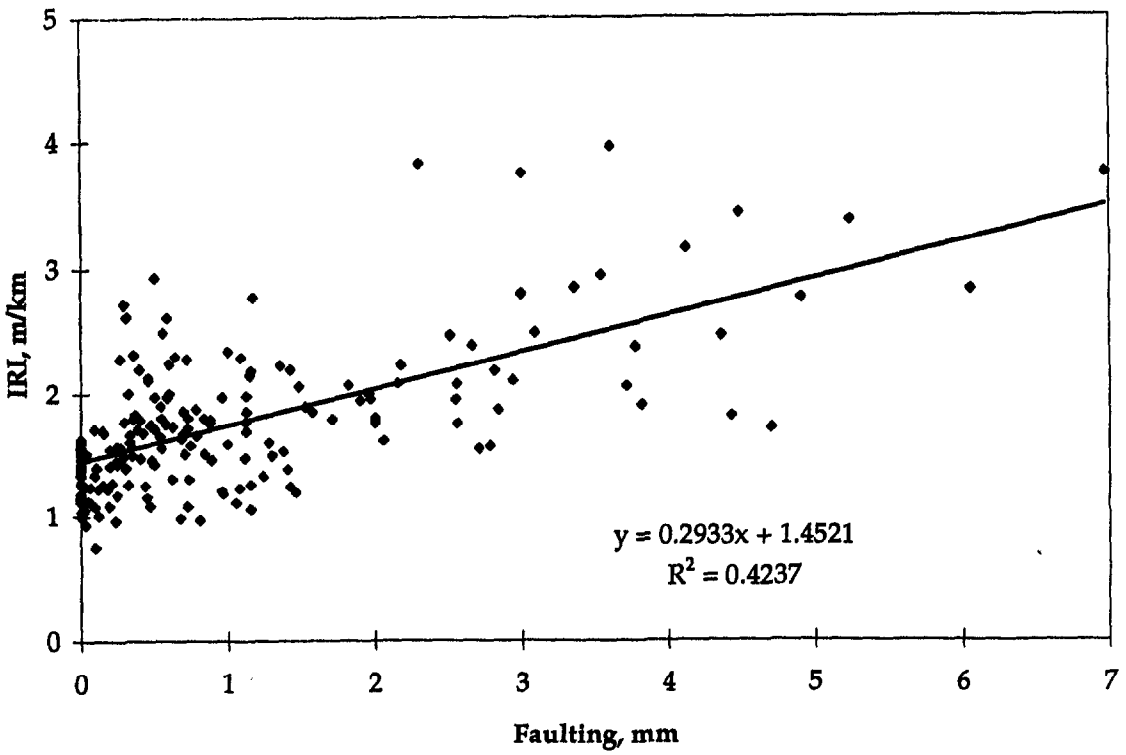

Figure 67. IRI versus joint faulting

Factors Considered for Faulting

The factors affecting transverse joint faulting of JPCP and JRCP include site conditions and design and construction features. The factors evaluated in this study include those found to be significant in previous studies and those based on engineering judgement:

- **Site Conditions**
  - o Geographic location
    - Latitude
    - Longitude
  - o Temperature factors
    - Freezing index
    - Freeze-thaw cycles
    - Mean annual temperature
    - Minimum annual temperature
    - Maximum annual temperature
    - Number of days warmer than 32°C
    - Number of days colder than 0°C

- Precipitation factors
  - Average annual precipitation
  - Average number of wet days
- Subgrade soil
- Traffic (ESAL)

- **Design and Construction Features**
  - Dowels
  - Slab thickness
  - Slab width
  - Concrete properties
    - Modulus of elasticity
    - Modulus of rupture
  - Joint spacing
  - Joint orientation
  - Base type
  - Drainage

Comparative and Statistical Analysis of Transverse Joint Faulting

Two general types of analyses were performed: a visual comparative analysis and a statistical analysis. Comparative analysis includes visual analysis of plots with a distribution of pavement sections by their performance as a function of those factors, and a comparison of average values of those factors for different groups of pavement sections. The reader can observe the plots and evaluate the graphical results.

Statistical analyses conducted include the t-test and, in some cases, multivariate analyses to identify those site conditions and design features that contribute to good and poor faulting performance. The JPCP and JRCP section data were partitioned into two groups based on transverse joint faulting: those that fell into the poor/normal group and those that fell into the good group (note that the poor/normal group will subsequently be called only the poor group for convenience). The normal group had to be used in the analysis due to the limited number of sections. Since an initial analysis indicated that presence of doweled overshadow all other design and site condition factors, t-test was performed separately for doweled and non-doweled sections. Overall results from the t-test for doweled and non-doweled sections are given in tables 37 and 38, respectively.

Table 37. Summary of results from t-tests for doweled JPCP/JRCP joint faulting.

	Mean poor	Mean good	t separ. var. est.	df.	p 2-sided	Valid N poor	Valid N good	Std. Dev. poor	Std. Dev. good	F-ratio variance	p variance
FI	341.018	330.107	0.116	17.214	0.909	12	73	290.091	362.924	1.565	0.421
FT	69.831	74.510	-0.445	14.051	0.663	12	73	34.225	30.637	1.248	0.545
PRECIP	1039.190	1052.652	-0.181	16.419	0.858	12	73	232.207	272.567	1.378	0.579
WETDAYS	143.398	129.624	1.746	14.499	0.103	12	73	25.489	24.354	1.095	0.755
LONG	87.083	86.932	0.081	22.417	0.936	12	73	5.401	8.931	2.734	0.070
LAT	37.083	37.521	-0.271	14.196	0.791	12	73	5.248	4.802	1.194	0.613
TMAX	19.234	19.107	0.083	14.699	0.935	12	73	4.958	4.864	1.039	0.844
TMIN	7.288	6.896	0.265	14.707	0.795	12	73	4.769	4.684	1.037	0.848
TMEAN	13.261	13.002	0.172	14.644	0.865	12	73	4.857	4.731	1.054	0.820
DAYS32	30.690	37.338	-0.847	18.936	0.407	12	73	23.631	33.095	1.961	0.219
DAYS0	93.098	94.597	-0.092	14.357	0.928	12	73	52.503	49.183	1.140	0.689
JTSPACE	14.960	9.678	1.995	12.219	0.069	12	73	8.934	5.129	3.034	0.004
LANEWID	3.660	3.694	-2.043	72.000	0.045	12	73	0.000	0.140	0.000	1.000
SKEW	0.305	0.430	-0.404	1.061	0.756	2	30	0.431	0.291	2.201	0.297
KESAL	8075.182	6195.186	0.895	15.039	0.385	11	70	6279.923	7615.498	1.471	0.522
HPCC	234.315	248.056	-1.225	13.074	0.242	12	73	37.186	27.661	1.809	0.136
MR28	4963.949	4695.253	1.201	12.668	0.251	12	73	747.875	500.352	2.234	0.043
E28	28436.946	27327.239	2.014	21.348	0.057	12	73	1606.960	2540.840	2.500	0.097
EBASE	1400.967	3042.605	-1.935	18.539	0.068	12	72	2570.514	3492.724	1.846	0.264
C_d	0.858	0.905	-0.785	12.755	0.446	12	73	0.198	0.135	2.127	0.058
KSTATIC	36.220	47.037	-1.393	11.102	0.191	9	68	21.439	25.024	1.362	0.678

Table 38. Summary of results from t-tests for non-doweled JPCP joint faulting.

	Mean poor	Mean good	t separ. var. est.	df.	p 2-sided	Valid N poor	Valid N good	Std. Dev. poor	Std. Dev. good	F-ratio variance	p variance
LANEWID	3.660	3.719	-2.080	40.000	0.044	26	41	0.000	0.183	0.000	1.000
FI	371.282	404.268	-0.329	63.130	0.743	26	41	349.834	468.060	1.790	0.126
FT	78.943	77.157	0.179	60.789	0.859	26	41	36.499	44.688	1.499	0.287
PRECIP	916.381	608.254	3.650	51.120	0.001	26	41	343.840	325.145	1.118	0.736
WETDAYS	125.035	93.376	3.587	50.488	0.001	26	41	36.155	33.651	1.154	0.671
LONG	94.538	103.463	-2.331	46.312	0.024	26	41	16.263	13.572	1.436	0.301
LAT	39.500	39.902	-0.292	52.111	0.771	26	41	5.559	5.389	1.064	0.842
TMAX	17.777	18.580	-0.616	51.808	0.541	26	41	5.277	5.077	1.080	0.810
TMIN	5.380	5.121	0.230	54.236	0.819	26	41	4.458	4.558	1.045	0.925
TMEAN	11.579	11.851	-0.230	53.117	0.819	26	41	4.724	4.697	1.012	0.952
DAYS32	30.052	37.950	-1.128	60.679	0.264	26	41	25.603	31.236	1.488	0.295
DAYS0	103.681	100.514	0.214	60.732	0.832	26	41	54.175	66.208	1.494	0.291
JTSPACE	5.197	5.103	0.177	63.361	0.860	26	41	1.836	2.484	1.830	0.113
SKEW	0.572	0.627	-1.273	46.910	0.209	22	35	0.154	0.164	1.135	0.774
KESAL	7575.190	6201.667	0.607	32.765	0.548	21	33	9026.179	6404.280	1.986	0.081
HPCC	237.287	235.356	0.268	40.987	0.790	26	41	32.106	22.835	1.975	0.053
MR28	4562.813	4661.450	-0.440	30.720	0.663	26	41	1083.515	457.241	5.615	0.000
E28	26464.242	27126.182	-0.520	30.369	0.607	26	41	6168.443	2522.157	5.981	0.000
EBASE	2218.580	4167.610	-2.174	59.627	0.034	25	41	3189.557	4035.038	1.600	0.223
C_d	0.956	1.015	-1.396	50.419	0.169	26	41	0.173	0.161	1.158	0.664
KSTATIC	46.279	49.419	-0.500	40.550	0.620	23	39	25.222	21.480	1.379	0.376

Effect of Dowels on Joint Faulting

Load transfer is the mechanism through which wheel loads are conveyed from one slab to the next and is achieved by aggregate interlock between the abutting joint faces or use of mechanical load transfer devices (e.g., dowel bars). Poor load transfer across the transverse joint contributes to the development of joint faulting based on past research. Dowels improve load transfer characteristics between adjacent PCC slabs so greatly that the presence of dowels was found to be the most important design feature affecting joint faulting for JPCP and JRCP. The t-test confirmed the significance of dowels. Level of significance was found to be less than 0.001 (the probability was less than 0.001 that this has occurred due to chance).

Figure 68 presents two faulting frequency curves for doweled and non-doweled JPCP sections. It is shown that over 90 percent of doweled sections exhibit faulting less than 2 mm. This means that the doweled sections showed good performance with respect to faulting. On the other hand, faulting for 40 percent of the non-doweled sections exceeded 2 mm, and 20 percent exceeded 4 mm.

The diameter of the dowels influences the effectiveness in controlling faulting. Figure 69 shows a bar chart of the mean joint faulting for non-doweled and doweled JPCP/JRCP versus dowel diameter. Of course, each section has received different levels of traffic; however, even considering this and other confounding influences, the trend clearly shows that the larger dowel bars perform better with respect to faulting. This phenomenon has been modeled mechanistically and is related to the bearing stress between the dowel and concrete. The steel/concrete bearing stress for a 25-mm-diameter dowel is over 2.5 times that for a 38-mm-diameter dowel bar.

Climatic Site Conditions

LTPP results show that traffic loading, climate (temperature and precipitation), and subgrade all affect faulting. An increased number of heavy axle loads, colder and wetter climate, and fine-grained subgrade soil all contribute to joint faulting. The LTPP data demonstrates that faulting can be controlled through appropriate selection of design features both with and without dowels over a wide range of site conditions. Specific site condition variables that may cause faulting variations are discussed below.

Geographic/climatic location. Figures 70 and 71 show the distribution of good and poor sections with respect to longitude and latitude of their location, respectively. Latitude and longitude are correlated with climatic factors such as precipitation and air temperature. No clear trend relating latitude and longitude to faulting performance was found when doweled and non-doweled pavements are plotted together. However,

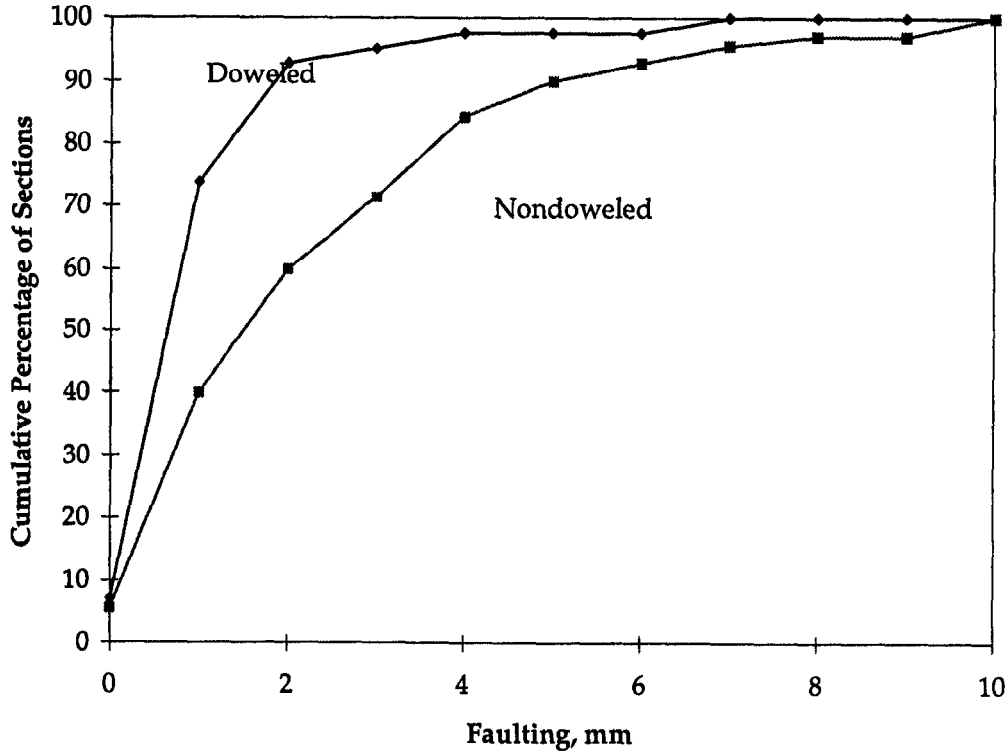

Figure 68. Cumulative frequency curves for doweled and non-doweled JPCP.

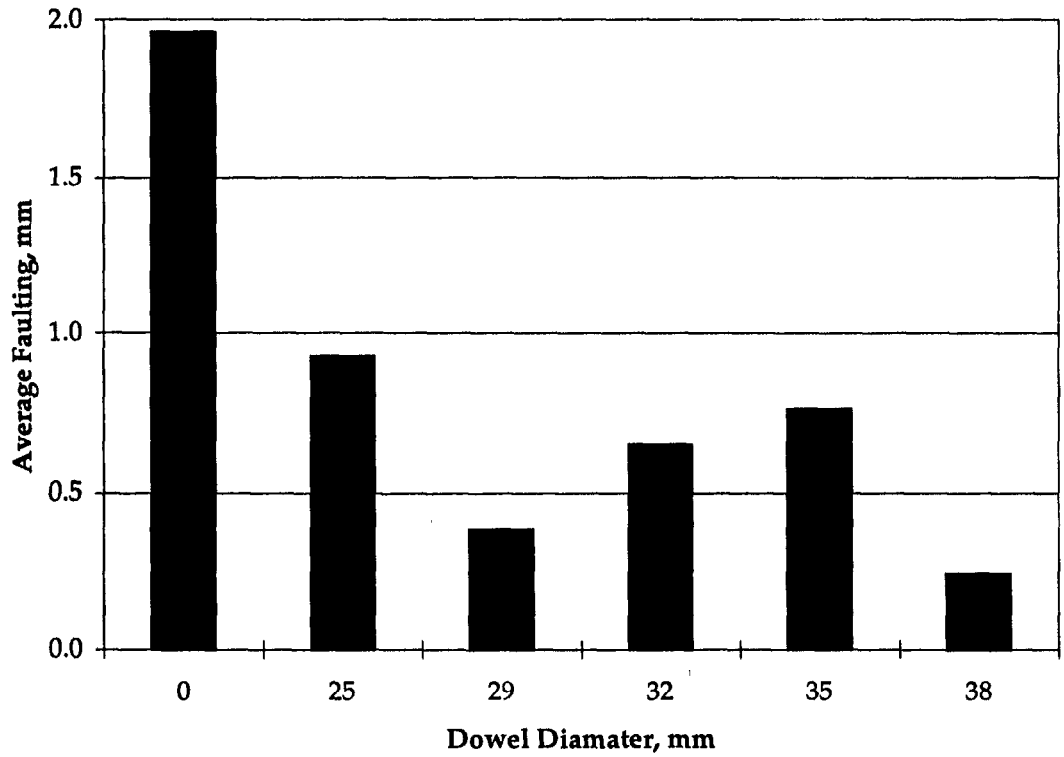

Figure 69. Effect of dowel bar diameter on JPCP/JRCP performance.

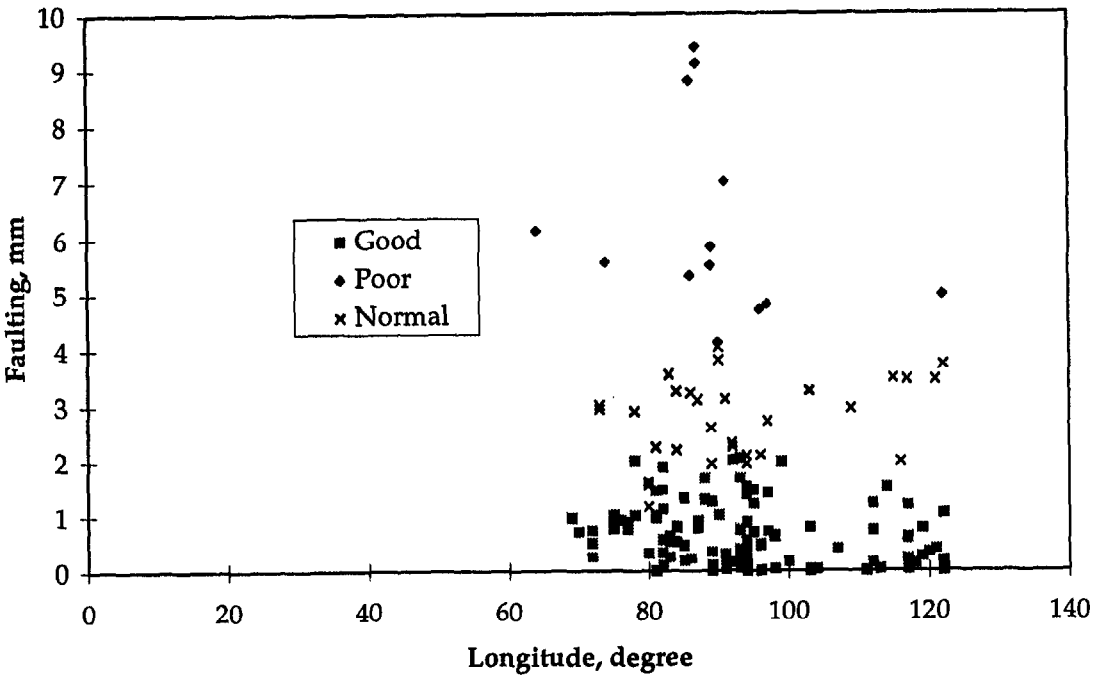

Figure 70. Longitude versus faulting.

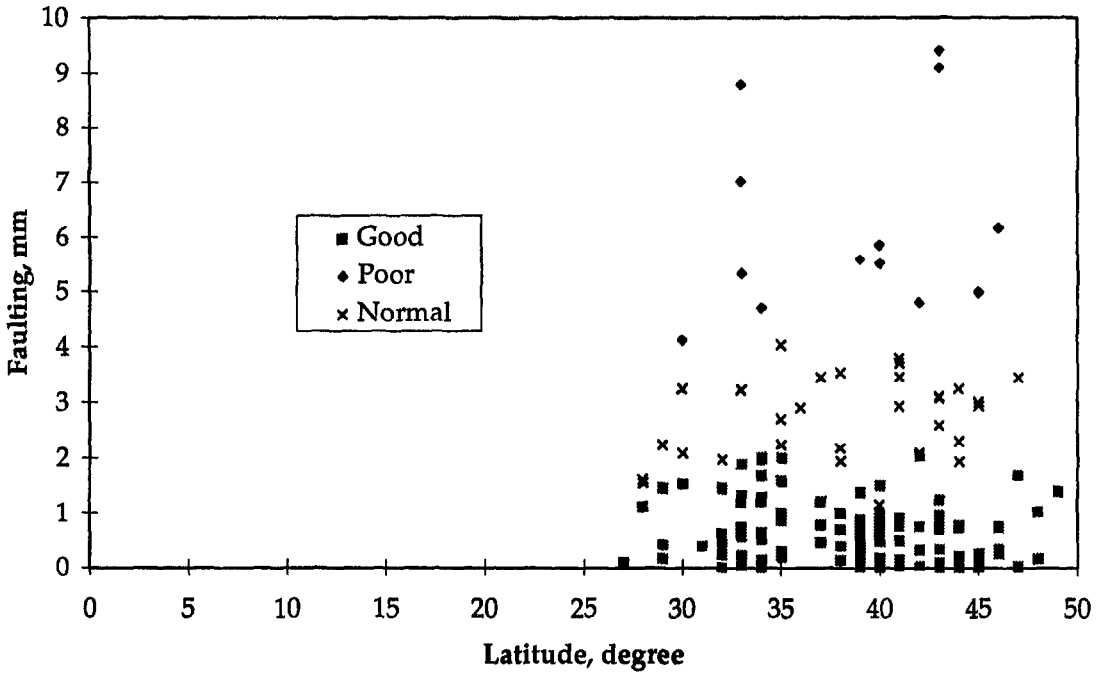

Figure 71. Latitude versus faulting.

the t-test found that average longitude for non-doweled good sections is significantly higher than for poor sections, as shown in table 38. This indicates that non-doweled JPCP in the western part of North America tends to have less faulting than in the east. This could be related to precipitation differences.

Temperature factors. The following temperature parameters were considered in this study: freezing index (FI), number of air freeze-thaw cycles (FT), mean annual temperature (T_{mean}), minimum annual temperature (T_{min}), maximum annual temperature (T_{max}), number of day per year with a temperature higher than 32°C (Days32), and number of days per year with a temperature lower than 0°C (DAYS0). However, no clear trend relating faulting with temperature factors was observed. None of these parameters was found to be significant as a result of the t-test.

Precipitation factors. Two precipitation factors were analyzed in this study: average annual precipitation and average number of wet days per year. The mean value for annual precipitation for poor non-doweled sections was 857 mm, whereas the mean value for good sections was 589 mm, as shown in figure 72. The mean value for WetDays for poor non-doweled JPCP sections was 125 days, whereas the mean value for good sections was 93 days (see figure 73). The results of the t-test (table 38) confirm the significance of this difference for non-doweled sections, but did not confirm it for doweled. No clear trend was observed relating annual precipitation levels and average number of wet days to faulting for doweled pavements.

Subgrade Site Conditions

The subgrade can be categorized into fine and coarse-grained soils. Figure 74 shows that, in general, pavements constructed over coarse-grained soils perform better than those constructed on fine-grained soils. Of all poor performing non-doweled JPCP sections, 58 percent had fine-grained subgrade soil and only 42 percent where built in areas were the subgrade soil was coarse-grained. The same trend is observed for doweled JPCP and JRCP sections: only 23 percent of all poor/normal sections were built on the coarse-grained subgrade.

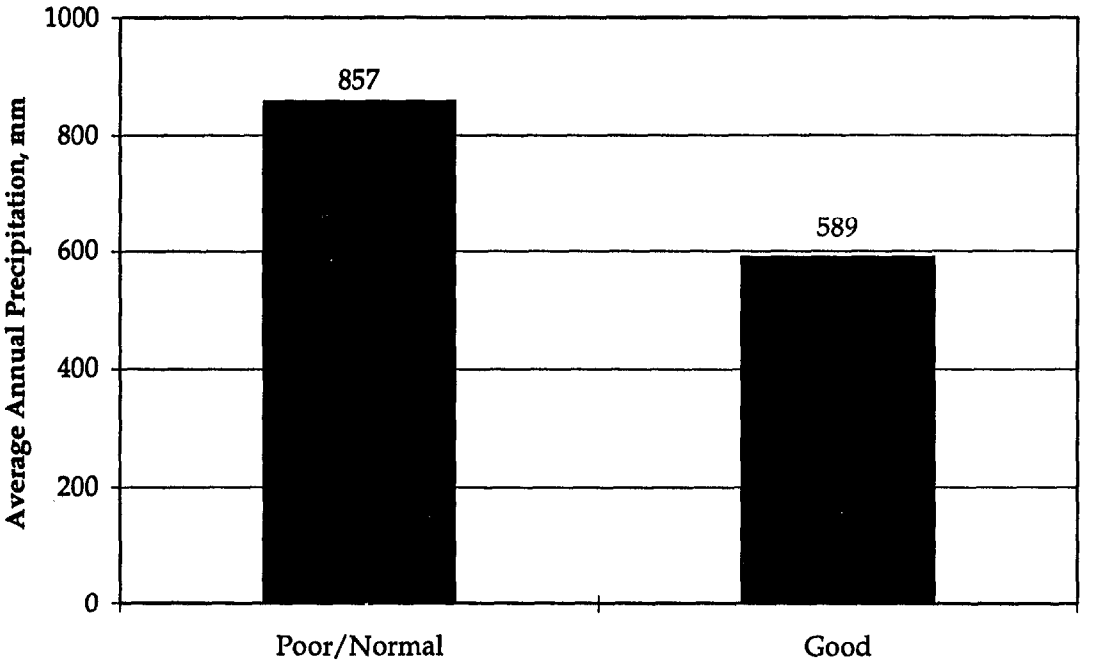

Figure 72. Effect of average annual precipitation on non-doweled JPCP faulting.

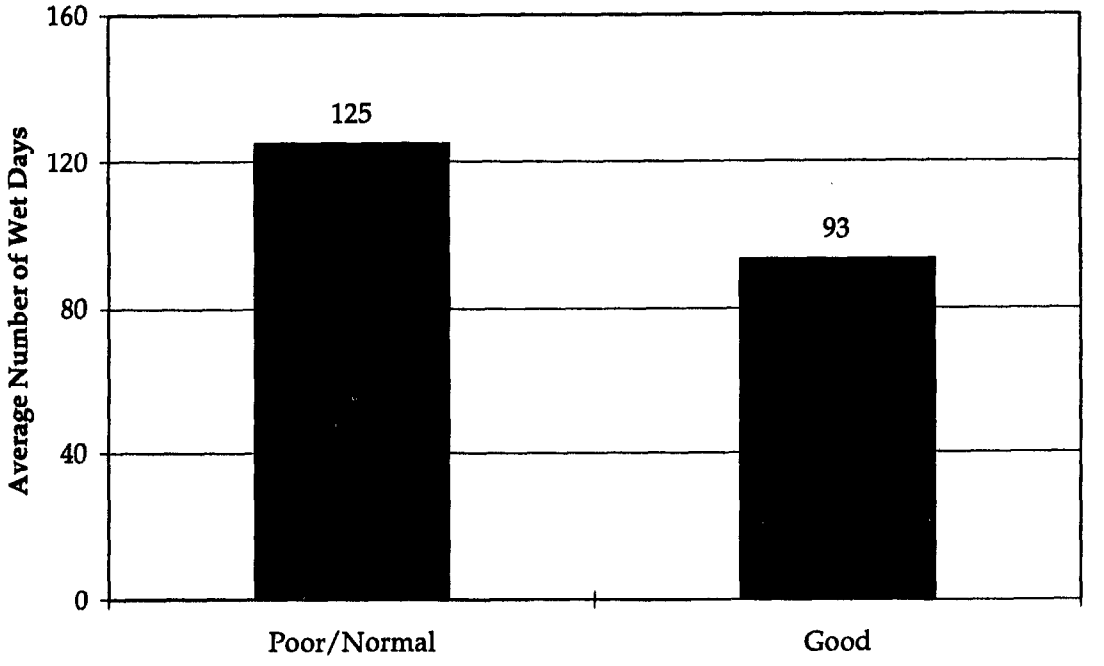

Figure 73. Effect of number of wet days on non-doweled JPCP faulting.

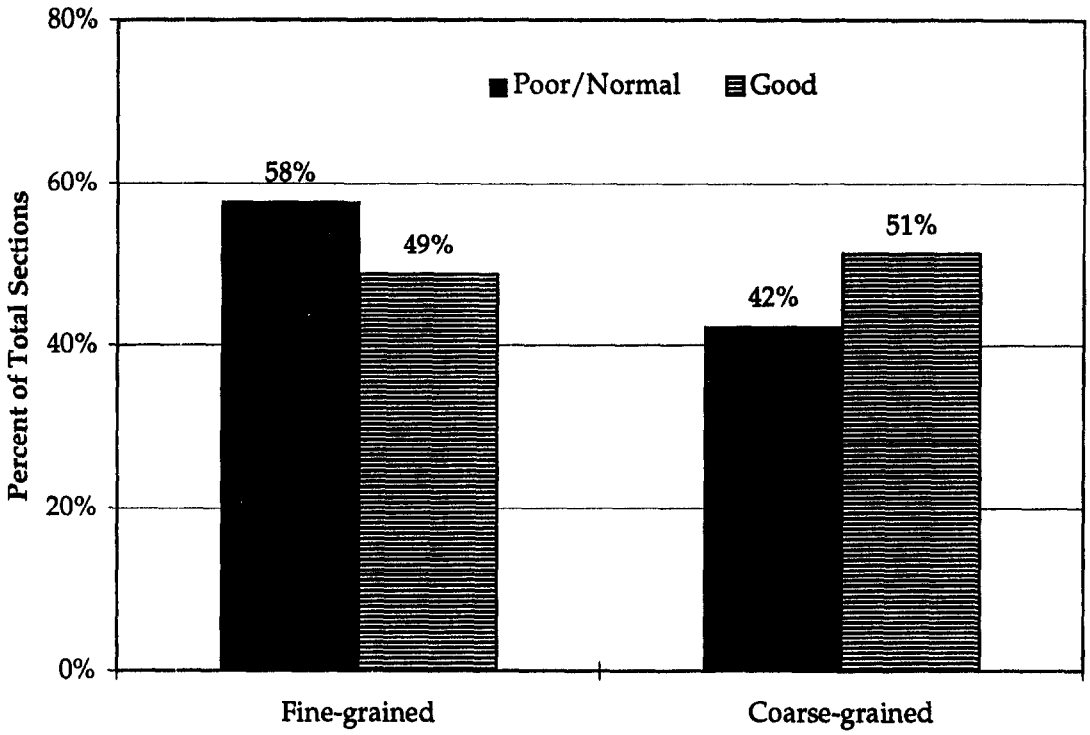

Figure 74. Effect of subgrade soil on non-doweled JPCP faulting.

Traffic Site Conditions

Figures 75 and 76 show the relationship between applied ESALs and faulting of non-doweled JPCP. It is expected that increased levels of traffic would clearly lead to an increase in transverse faulting. The mean value for accumulated ESALs for good sections was 6.2 million, whereas the mean accumulated ESALs for poor sections was 7.5 million. However, the result of the t-test (table 38) did not confirm the significance of this difference.

Design and Construction Factors

Thickness. No clear trend was observed relating slab thickness to transverse joint faulting in this data base. The t-test (table 38) found that this difference was of no significance.

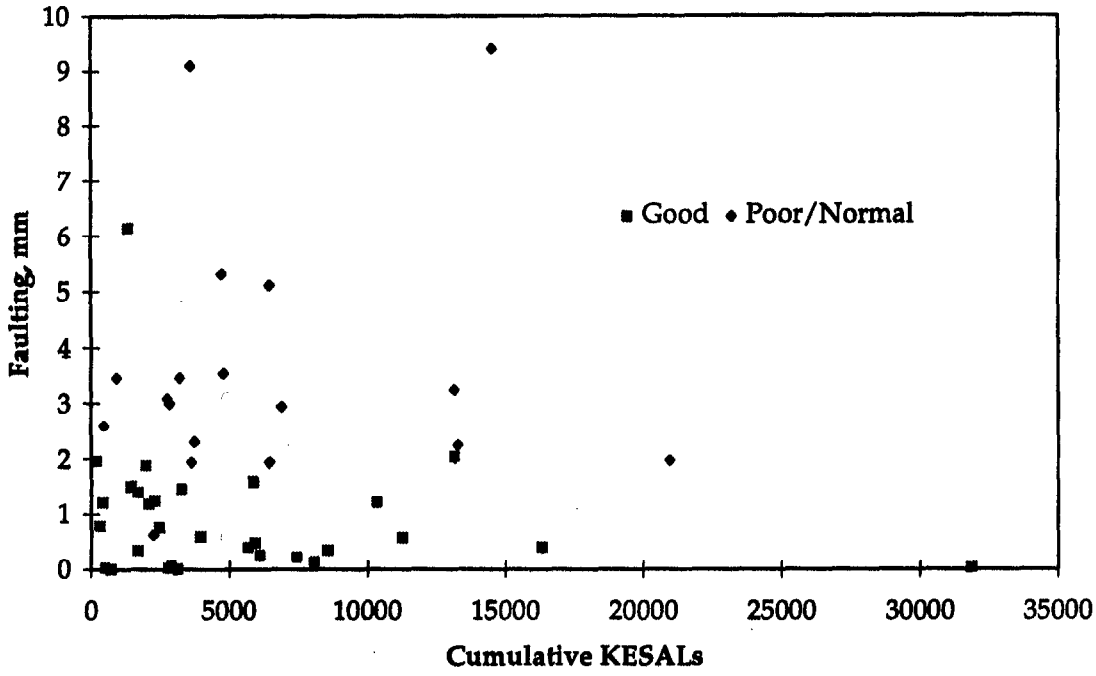

Figure 75. Cumulative traffic versus faulting for non-doweled JPCP.

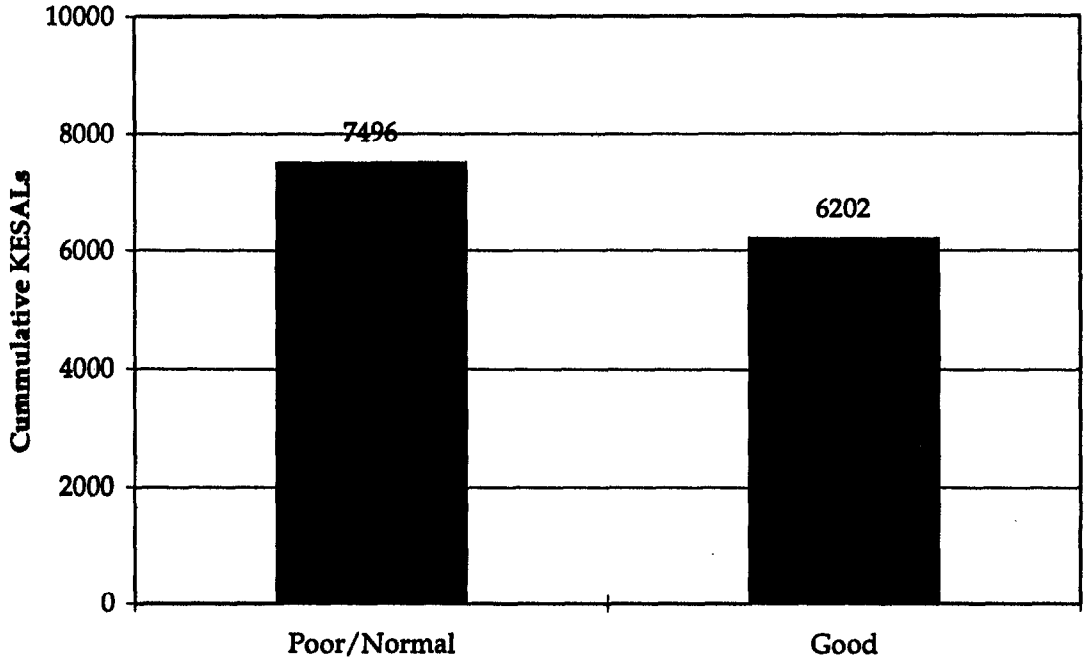

Figure 76. Effect of cumulative traffic on non-doweled JPCP faulting.

Subdrainage. Subdrainage has been cited many times as an important design feature. The overall subdrainage condition was characterized using the drainage coefficient (C_d), which is based on the 1986 AASHTO drainage coefficient.[17] This factor is a reflection of the pavement's ability to drain excessive moisture from within the structure, as well as the pavement's potential for being exposed to near saturated conditions. C_d varies from 0.7 for poor drainage to 1.2 for excellent drainage (see table 4). Figures 77, 78, and 79 illustrate the effect of drainage on non-doweled JPCP, doweled JPCP, and doweled JRCP sections, respectively. Good drainage reduces faulting for all types of pavements and designs, but especially for non-doweled JPCP.

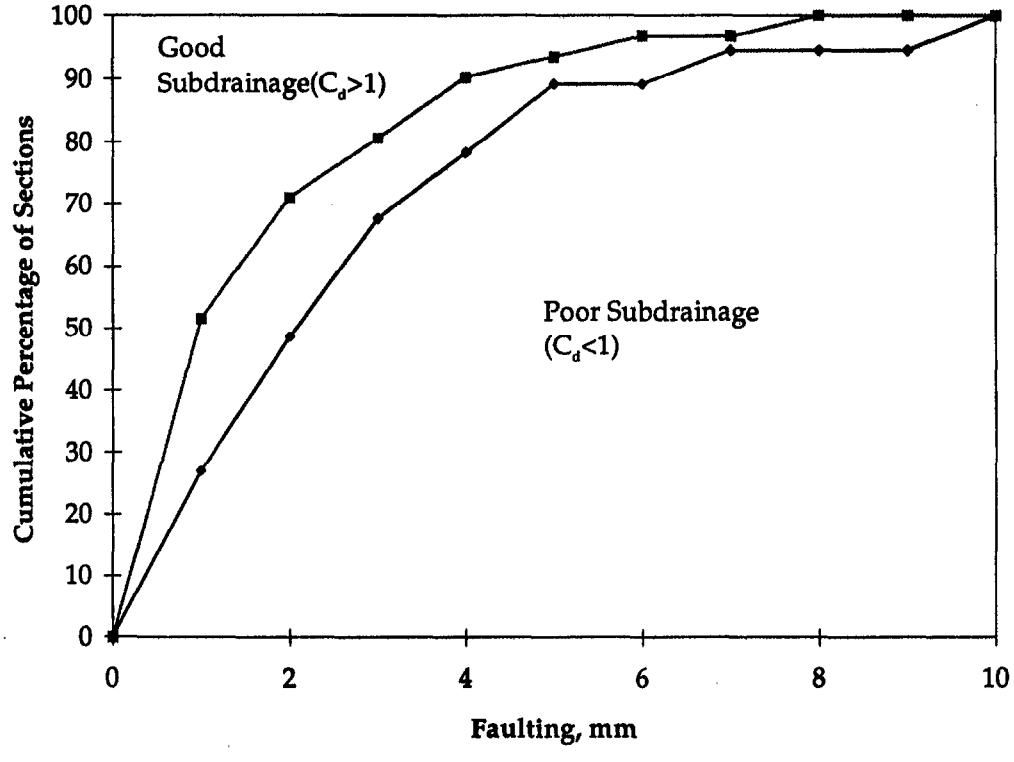

Figure 77. Cumulative frequency curves for non-doweled JPCP.

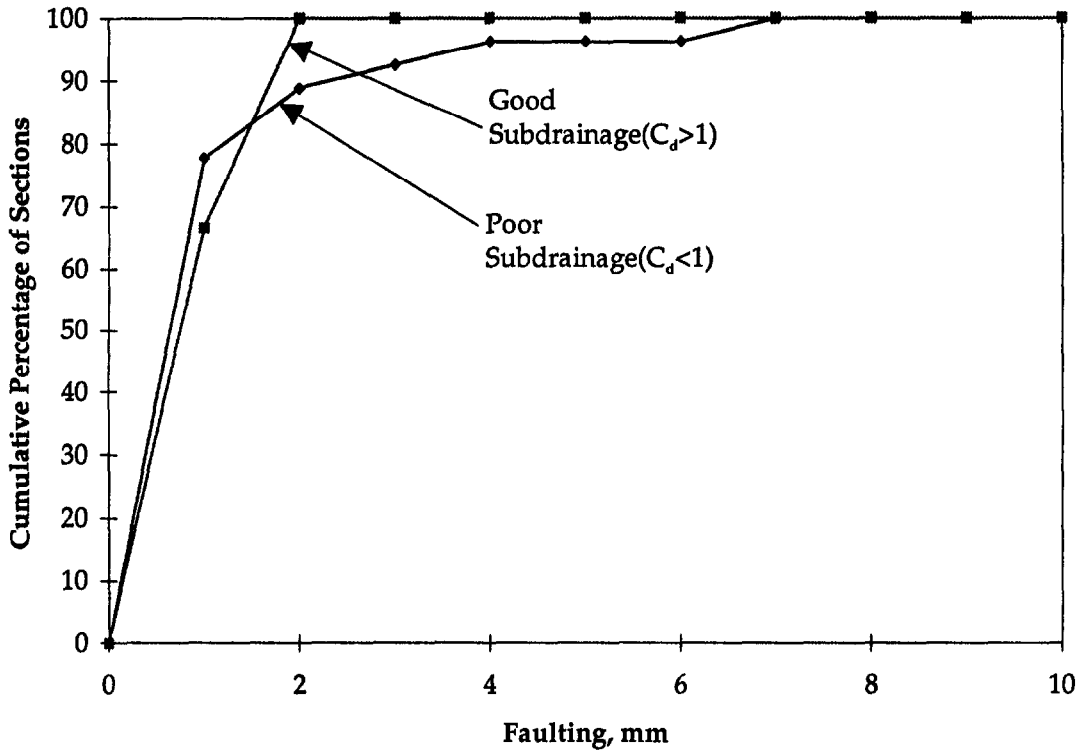

Figure 78. Cumulative frequency curves for doweled JPCP.

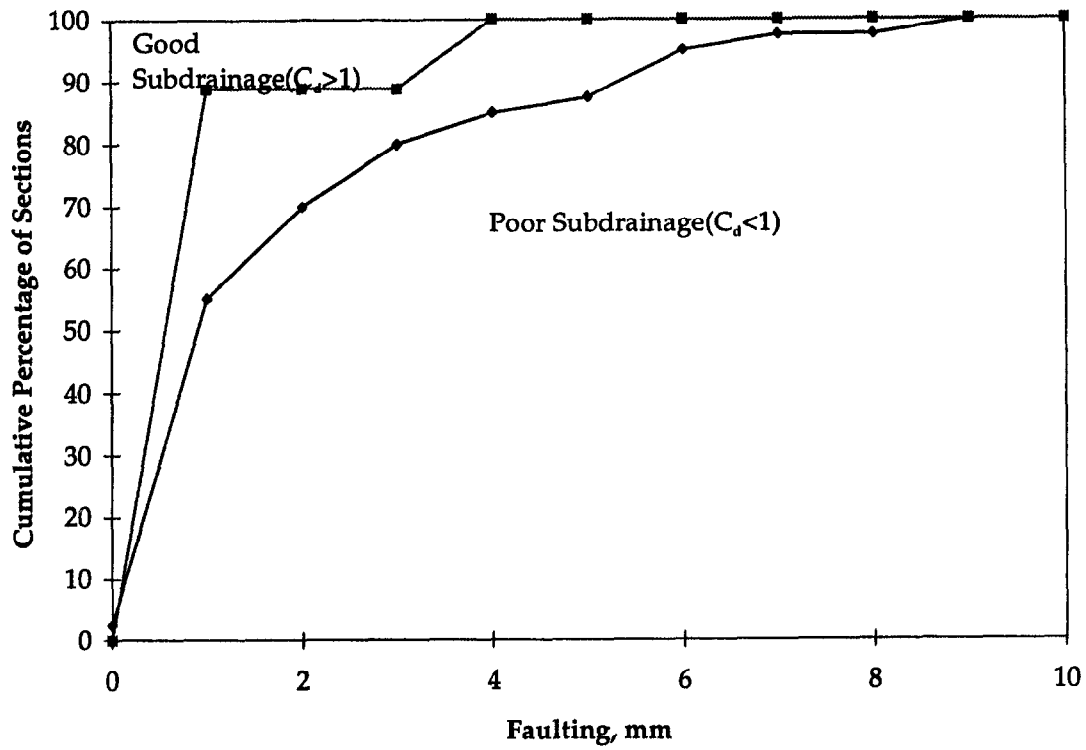

Figure 79. Cumulative frequency curves for JRCP.

Base Type. Adequate stabilization of the pavement base reduces its erodibility (note that there must be an adequate amount of stabilizer to control erodability), which leads to less faulting. Figures 80 and 81 show distributions of good and poor faulted sections for stabilized and non-stabilized bases for LTPP non-doweled JPCP and doweled JPCP/JRCP sections, respectively. It can be observed that sections with a stabilized base account for 59 percent of all good non-doweled JPCP sections and 41 percent of poor sections. A similar trend is observed for doweled JPCP/JRCP pavements, although the effect is not as pronounced as for non-doweled JPCP pavements. Stabilized bases have lower erodability than aggregate bases.

Joint Orientation. Although the practice of skewed joints has been common for many years, there exists little evidence of its benefits. A previous side-by-side comparison of pavement sections with non-doweled skewed and non-skewed joints conducted in an FHWA study demonstrated that skewed joints have approximately 50 percent lower faulting than non-skewed joints.[2] This can be explained by the reduction of impact of the wheel load from vehicles crossing the joint. The LTPP data base supports these findings. Whereas only half of the sections with non-skewed joints have shown good performance, the fraction of the good performing sections based on faulting with skewed joints is about two-thirds of the total number of the sections with skewed joints. However, LTPP results also show that perpendicular doweled joints with reasonable subdrainage will not fault; thus, it is not necessary to skew a doweled joint if proper dowel design and subdrainage are provided.

Joint Spacing

Joint spacing affects the amount of horizontal movements at pavement joints and, therefore, load transfer efficiency at the joints. Several previous studies demonstrated the importance of reducing joint spacing for improving JPCP performance in general and faulting in particular.[2,8,16] Since variability in the joint spacing is significantly higher for doweled pavements (many of which are JRCP), it is reasonable to expect that the effect is more pronounced for doweled pavements. Comparison of average joint spacing for good JRCP sections and poor/normal JRCP sections from the LTPP data base shows that the joint spacing of good sections is significantly shorter (see figure 82). The t-test confirms that joint spacing is negatively correlated with faulting for doweled pavements. Similar comparisons for JPCP sections led to similar results, although for JPCP sections the difference was not as pronounced and the t-test did not find it significant.

The influence of the joint spacing on transverse faulting might be explained by the observation that an increase in joint spacing might significantly increase temperature movements at the joints and, as a result, increase maximum joint opening and decrease effective load transfer efficiency.

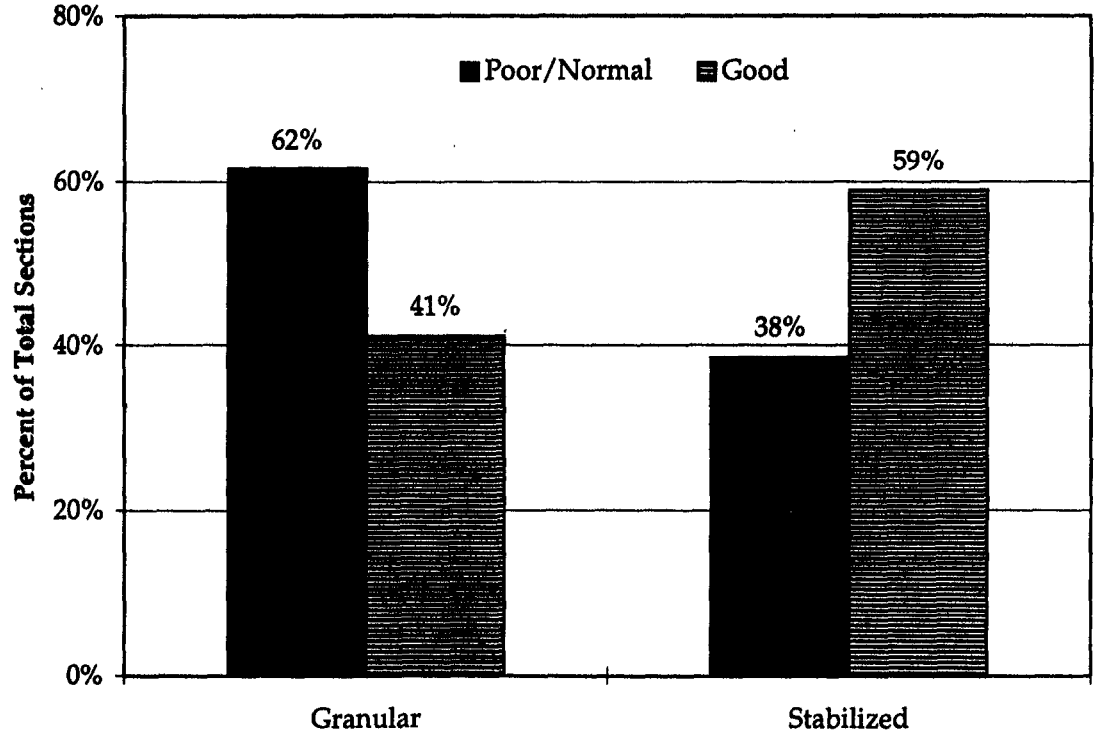

Figure 80. Effect of base-layer type on non-doweled JPCP faulting.

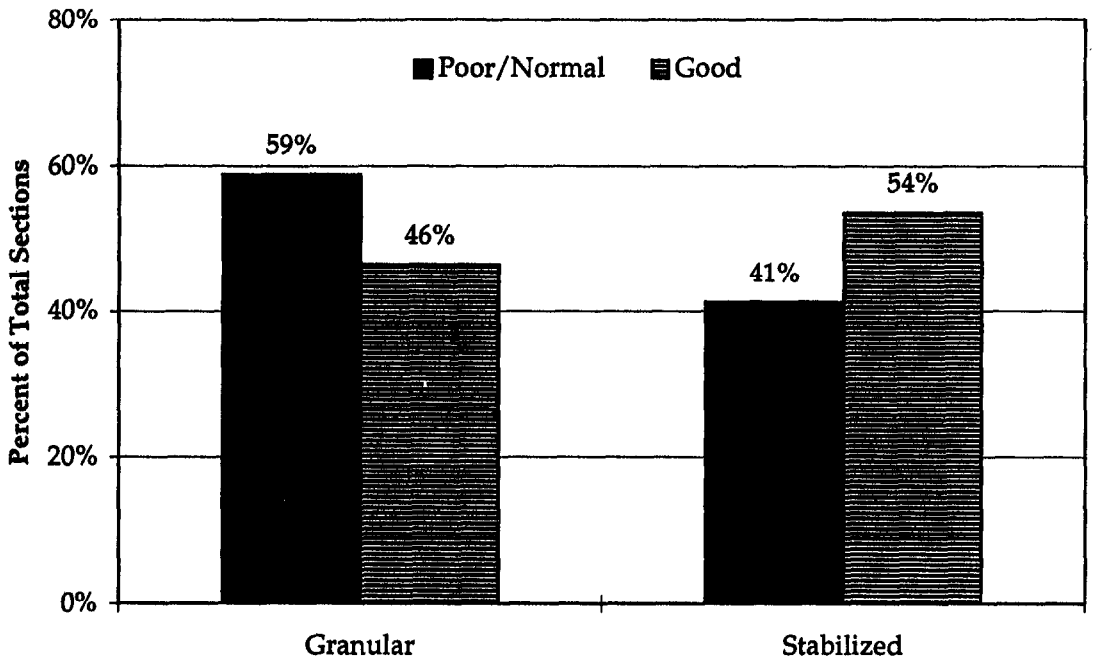

Figure 81. Effect of base-layer type on doweled JPCP/JRCP faulting.

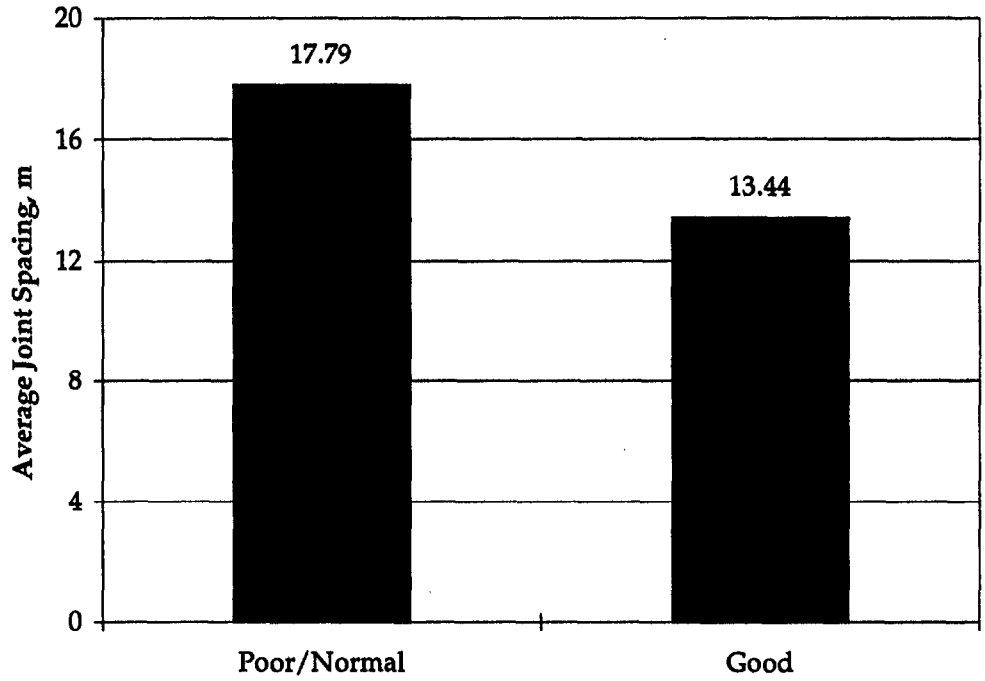

Figure 82. Effect of joint spacing on JRCP faulting.

Widening of PCC Slabs

Widened (by 0.6 m) PCC slabs (as opposed to conventional width slabs) improve faulting performance of concrete pavements by reducing the critical deflections at the corner of the slab from heavy truck axles. The result of widening effectively moves the critical corner further away from the wheel path, thereby reducing the frequency of traffic encroachment to the pavement edge. A previous limited field study showed that a widened slab reduced the amount of faulting by approximately 50 percent.[1] The LTPP data base contains information on only a few JPCP sections with widened slabs. The mean faulting for non-doweled sections not older than 10 years both with and without widened slab shows about 50 percent less faulting with a widened slab. There was no difference between doweled widened slab sections and doweled conventional slab width JPCP.

Summary of Joint Faulting Findings For JPCP and JRCP

This analysis showed that there are several site conditions and design and construction features that affect joint faulting of JPCP and JRCP over time and traffic. Faulting is an extremely critical distress since it greatly affects ride quality. The following site conditions and design/construction features were found to affect transverse joint faulting:

- **Climate/location:** No clear trend relating latitude and longitude to faulting performance was found for doweled JPCP and JRCP. However, the t-test found that average longitude for non-doweled good sections is significantly higher than for poor sections, as shown in table 38. This indicates that non-doweled JPCP in the western part of North America tends to have less faulting than in the east. One potential reason for this result is that precipitation is greater in the east than in the west as discussed in the next paragraph.

- **Precipitation:** A higher annual average precipitation and the number of annual wet days is associated with higher joint faulting for non-doweled JPCP, but not for doweled JPCP or JRCP. Doweled JPCP or JRCP has the apparent effect of negating much of the detrimental effects of increased precipitation or wet days.

- **Subgrade type:** JPCP and JRCP constructed over coarse-grained soils have less faulting than those constructed on fine-grained soils. This is likely due to increased bottom drainage of the pavement structural section.

- **Slab thickness:** No clear trend was observed relating slab thickness to transverse joint faulting in the LTPP data base. This is important in that the *AASHTO Design Guide* implies that poor joint load transfer can be adjusted for by increasing slab thickness.

- **Subdrainage:** The overall subdrainage condition was characterized using the drainage coefficient (C_d). This factor is a reflection of the pavement's ability to drain excessive moisture from within the structure, as well as the pavement's potential for being exposed to near saturated conditions. C_d varies from 0.7 for poor drainage to 1.3 for excellent drainage. Findings show that all types of JCP with good subdrainage (higher C_d) exhibit lower faulting, and especially non-doweled JPCP.

- **Base type:** The faulting of non-doweled and doweled JPCP and JRCP is lower when a stabilized base is present as compared to a granular base. The modulus of elasticity of the base layer is negatively correlated with faulting for non-doweled pavements. Stabilized bases have a greater modulus of elasticity than aggregate bases, of course.

- **Dowel diameter:** The results clearly show that doweled JPCP or JRCP with larger dowel bars have lower faulting. This is logical since larger dowel diameter reduces bearing stresses in concrete and increases long-term effectiveness of dowels in controlling faulting.

- **Skewed joints:** The LTPP data base supports the finding that non-doweled skewed joints fault less than non-doweled perpendicular joints. Whereas only half of the sections with non-skewed joints have shown good performance, the fraction of the good performing sections based on faulting with skewed joints is about two-thirds of the total number of the sections with skewed joints. However, LTPP results also show that perpendicular doweled joints with reasonable subdrainage will not fault; thus, it is not necessary to skew a doweled joint if proper dowel design and subdrainage are provided.

- **Joint spacing:** Several previous studies demonstrated the importance of reducing joint spacing for improving JPCP and JRCP performance in general and faulting in particular. Comparison of average joint spacing for good JRCP sections and poor JRCP sections from the LTPP data base shows that the joint spacing of good sections is significantly shorter. Similar comparisons for JPCP sections led to similar results, although for JPCP sections the difference was not as pronounced.

- **Widening of PCC slabs:** Widened (by 0.6 m) PCC slabs improve faulting performance of non-doweled concrete pavements by reducing the critical deflections at the corner of the slab from heavy truck axles. The percentage of reduction is approximately 50.

CHAPTER 8. PERFORMANCE OF JPCP WITH RESPECT TO TRANSVERSE CRACKING

Transverse cracking is the key structural failure mode for jointed plain concrete pavements (JPCP). The deterioration of a transverse crack in JPCP often leads to additional cracks in the slab, leading to a shattered slab that requires replacement. Slab replacement is costly and can lead to early rehabilitation of the pavement as more and more occurs.

Because this distress is the primary structural design criterion, there should not be many of these occurring in regular projects. However, the AASHTO Guide does not provide a procedure for directly checking a pavement design for transverse cracking in JPCP. Joint spacing has been found to be critical for JPCP to minimize transverse cracking, and the guide does not provide adequate recommendations.[2] Some highway agencies have built too long of slabs (for a given thickness and base) for many years (i.e., 3.6- to 5.7-m random slabs where the 5.4- to 5.7-m slabs cracked badly or 5.7 to 7.2 m where most of the slabs cracked). However, other agencies have had good success with up to 6 m joint spacing due to favorable climate and design features.

Previous Studies

Transverse fatigue cracking of JPCP has been studied in various field and laboratory investigations. In the Early LTPP Data Analysis Study, the following mechanistic-empirical model was calibrated to LTPP data:[1]

$$PCRACKED = \frac{1}{0.01 + 10*100^{-\log_{10}\frac{n}{N}}} \quad (33)$$

where

PCRACKED = percentage of cracked slabs (all severities).
n = expected number of applied edge stresses, considering ESALs.
N = number of allowable edge stress loads to 50 percent slabs. cracked (slab thickness, joint spacing, subgrade k-value, PCC. strength, PCC modulus, thermal gradients).

This model was calibrated by plotting the cumulated fatigue damage versus the percent cracked slabs for JPCP. The above model was then best fit to the LTPP data. A fairly

good relationship existed between the computed fatigue damage and measured slab cracking.

In a recent study, the following model was proposed:[2]

$$PCRACKED = \frac{100}{1 + 1.41\ FD^{-1.66}} \quad (34)$$

where

FD = accumulated fatigue damage ($\Sigma n/N$).

This mechanistic-empirical model was calibrated to the FHWA field data base by plotting the percent slabs cracked against the accumulated fatigue damage and fitting the above model to the data. A fairly good relationship existed between the computed fatigue damage and measured slab cracking.

Both models predict transverse cracking as a function of accumulated fatigue damage which is a function of the ratio of the maximum bending stress in the slab to the PCC flexural strength. The difference is in the stress calculation procedure and in the data used to calibrate the models. The design features considered in these transverse cracking prediction procedures and their effects are summarized in table 39.

Performance Criteria for Transverse Cracking

The LTPP data base contains cracking data for 109 JPCP sections. The total number of observations is 237. For some sections, time series data contain up to six observations. Other sections have only one performance record in the data base.

The data was divided into three performance categories: poor, normal, and good, based on percentage of cracked slabs and pavement age as previously described. This grouping was done to facilitate the analysis of identifying features that contribute to good and poor transverse cracking performance. This grouping was established based on the experience of an expert panel of State highway engineers. The limits that were set are shown in figure 83. The pavement section was considered to be performing good (i.e., performing better than expected) if its cracking satisfies the following condition:

Table 39. Summary of the effects of site conditions and design features on JPCP transverse cracking.

Site Condition/ Design Feature	Effect on Transverse Cracking	Reference
PCC thickness	Decreases*	1, 2
k-value	Decreases	1, 2
Joint spacing	Increases	1, 2
PCC thickness	Decreases	1, 2
Tied shoulder	Decreases	1, 2
PCC flexural strength	Decreases	1, 2
Traffic	Increases	1, 2
Stabilized base	Decreases	1
Widened PCC slab	Decreases	1, 2

* For example, as PCC thickness increases, transverse cracking decreases.

$$PCRACKED < \frac{AGE}{4} \tag{35}$$

where

PCRACKED = percentage of cracked slabs (all severities).
AGE = pavement age at the time of the observation, years.

The pavement section was considered to be performing poor if its average percentage of cracked slabs satisfies the following condition:

$$PCRACKED > \frac{AGE}{2} \tag{36}$$

where

PCRACKED = percentage of cracked slabs (all severities).
AGE = pavement age at the time of the observation, years.

Figure 83 presents a plot of all transverse cracking observations for the LTPP GPS-3 (JPCP) sections and shows designation of those sections by their performance at the time of observation. Figure 84 presents the transverse cracking as a function of cumulative 80-kN load applications.

Figures 83 and 84 show that several pavement sections developed a significant number of cracks in the first several years after traffic opening when they received only a limited number of axle loads. This indicates that serious construction problems occurred.

Since early cracking has totally a different mechanism than fatigue cracking, these sections were excluded from the analysis.

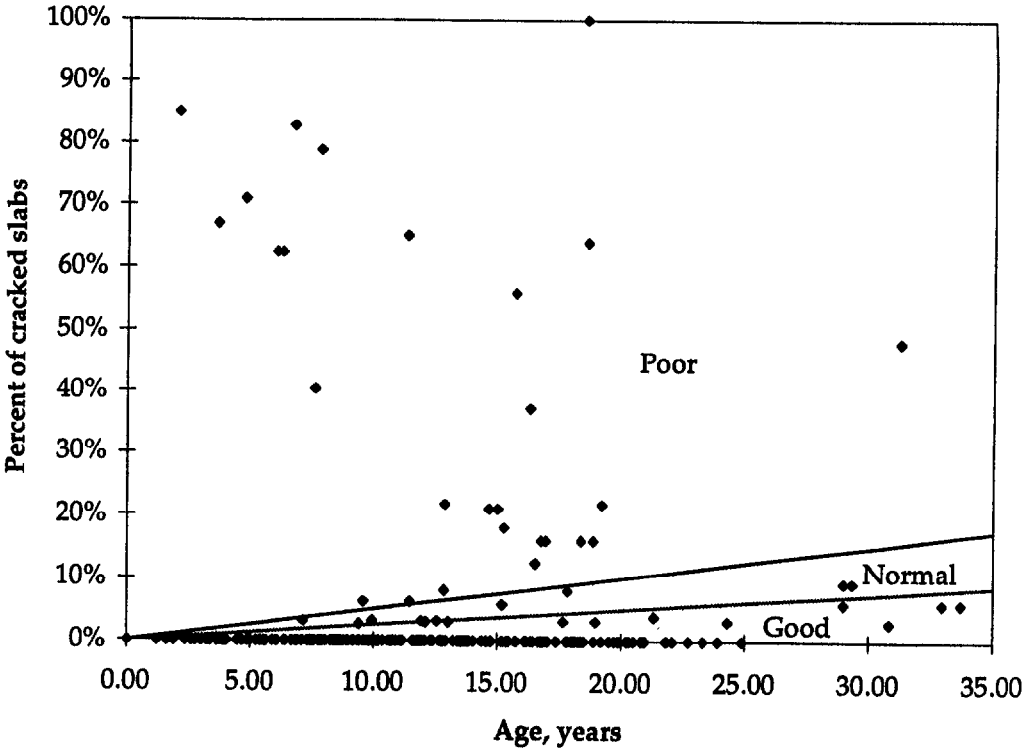

Figure 83. JPCP transverse cracking including all time-series data for each performance rating.

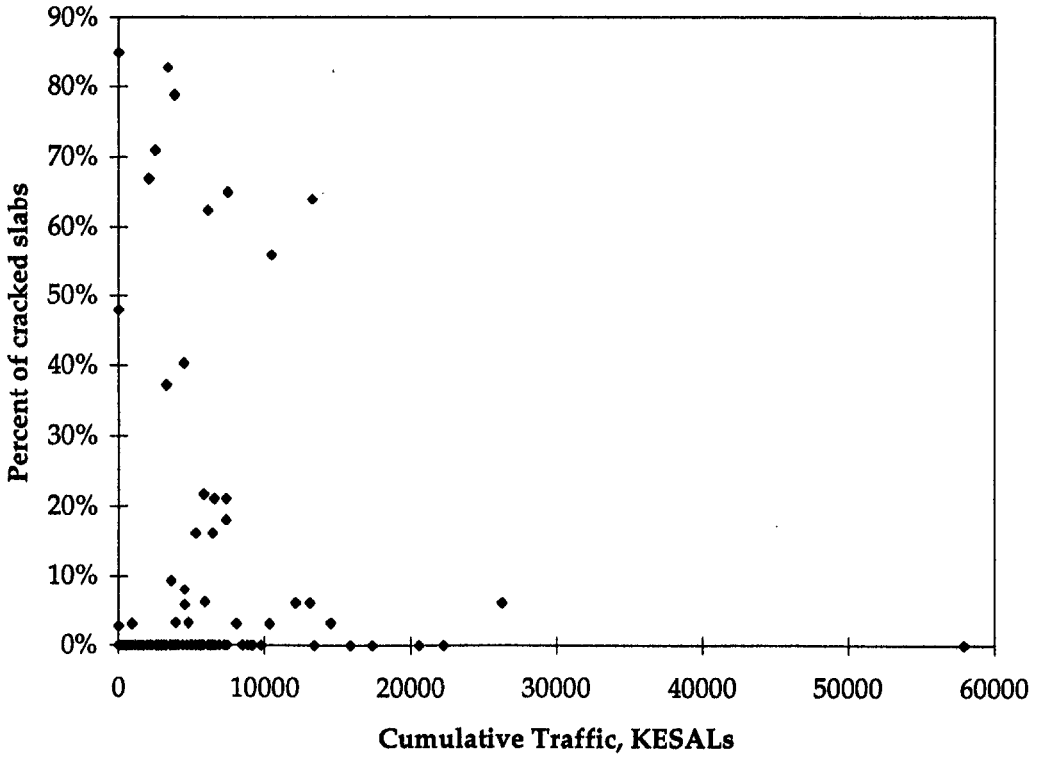

Figure 84. Effect of traffic on JPCP transverse cracking (all time-series data).

Only the last observation for each section was considered in the analysis. Figure 85 presents a plot of all sections included in the analysis with respect to transverse cracking at the time of the last available observation. Analysis of figure 85 shows that three sections 493011, 313023, and 123804 perform significantly worse than the remaining sections. These sections incorporate very stiff lean concrete or cement-treated base. These JPCP sections could have specific construction problems also.

Effect of Transverse Cracking on the Ride Quality of JPCP

Transverse cracking is a primary structural distress of JPCP. However, the occurrence of this distress is apparently not strongly related to ride quality of the pavement. Although a cracked JPCP often deteriorates rapidly and becomes rough, absence of cracks does not guarantee good ride quality due to many other factors.

To investigate the influence of transverse cracking on IRI, JPCP performance data for transverse cracking and IRI were compared. Since the measurements of these parameters were not conducted simultaneously in time, the procedure similar to that described in chapter 7 for faulting data was performed to match transverse cracking and IRI data from the LTPP data base.

Figure 86 presents IRI versus transverse cracking for JPCP sections and the results of the simple linear regression. Although sections with higher cracking, on average, have higher IRI, the relationship was not significant. The initial roughness and joint faulting both significantly affect IRI and are believed to be causing much of the scatter in results shown here. In addition, shattered slabs are usually rapidly removed to avoid the severe roughness that would occur.

Factors Considered for Transverse Cracking

Factors contributing to the development of transverse cracking of JPCP include site conditions and design/construction features. The factors studied in this analysis include those found to be significant from previous studies and others based on engineering judgment:

- **Site Conditions**
  - o Geographic/Climatic location
  - o Temperature factors
    - Freezing index
    - Freeze-thaw cycles
    - Mean annual temperature
    - Minimum annual temperature
    - Maximum annual temperature
    - Number of days warmer than 32°C
    - Number of days colder than 0°C
  - o Precipitation factors
    - Average annual precipitation
    - Average number of wet days
  - o Subgrade soil
  - o Traffic

- **Design and Construction Features**
  - o Slab thickness
  - o Concrete properties
    - Modulus of elasticity
    - Modulus of rupture
  - o Joint spacing
  - o Base type
  - o Drainage
  - o Proper joint sawing procedures

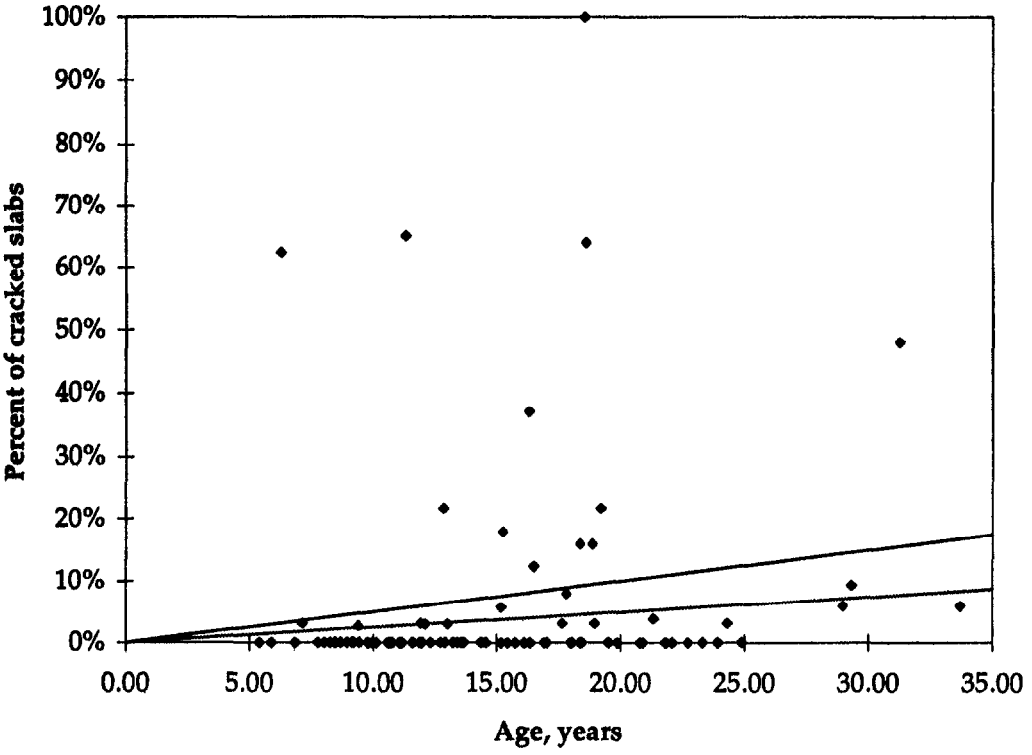

Figure 85. JPCP transverse cracking (last observation only).

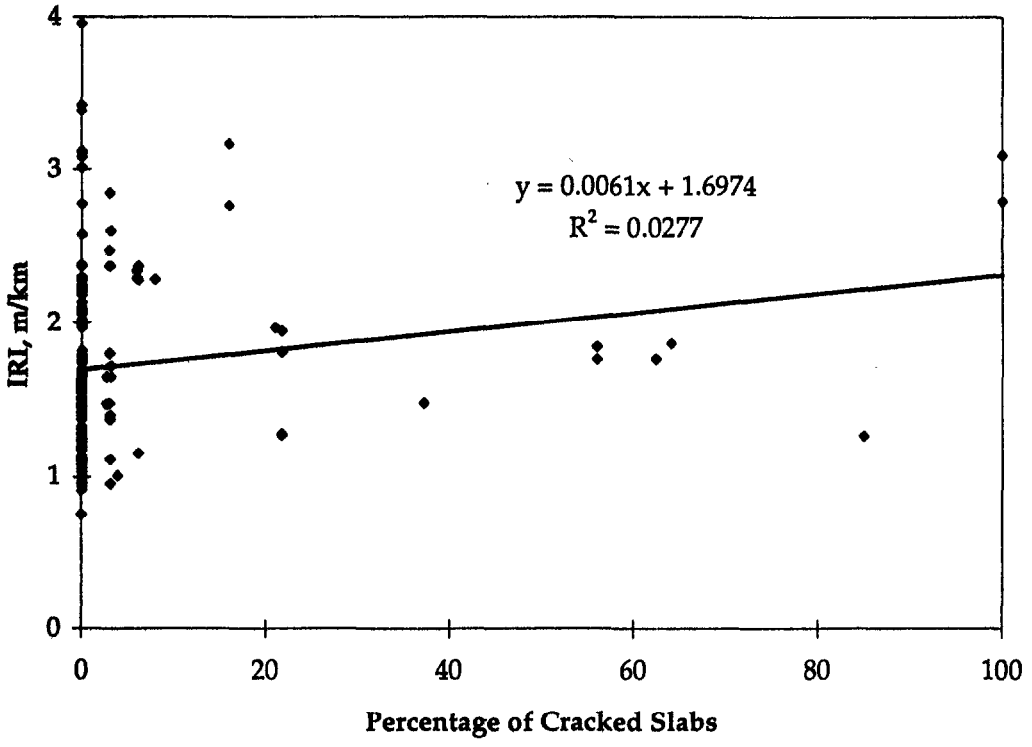

Figure 86. Transverse cracking versus IRI for JPCP.

Comparative and Statistical Analysis of IRI

Two general types of analyses were performed: a visual comparative analysis and a statistical analysis. Comparative analysis includes visual analysis of plots with a distribution of pavement sections by their performance as a function of those factors, and a comparison of average values of those factors for different groups of pavement sections. The plots can be observed and the graphical results evaluated as to significance.

The JPCP section data were partitioned into two groups based on percentage of transverse cracks observed: those that fell into the good group and those that fell into the poor/normal group (note that the poor/normal group will subsequently be called the poor group for convenience). The normal group had to be used in the analysis due to the limited number of sections available.

Statistical analyses included the t-test and Fishers's exact test to identify those site conditions and design features that contribute to good and poor JPCP performance in terms of transverse cracking.

Table 40 provides a summary of all the t-values for each comparison made for continuous variables. Table 41 provides a summary of Fisher's exact tests for discrete variables for transverse cracking of JPCP. These will be referred to during the following presentation. The significant variables at the 90 or 95 percent confidence level consist of LONG (longitude), EBASE (modulus of base), ACBASE (asphalt stabilized base), and GRANBASE (granular base). However, t-tests and Fisher's exact tests are one-dimensional and do not consider collinearity with other variables. Stated differently, the interrelationship with other variables could be masking a variable's true relationship with JPCP transverse cracking. This collinearity can only be considered through further rigorous statistical or mechanistic analyses.

In this study, two-dimensional plots of JPCP cracking with respect to various parameters were analyzed. A comparison of the mean values of those parameters and good, normal, and poor sections was performed. Although the results of this analysis are of great interest because they highlight the most significant visual trends in pavement cracking, they must be viewed with caution since the interrelationship of the variables may have a significant influence on the observed trends.

Table 40. Results of t-tests for JPCP transverse cracking.

	Mean Poor	Mean Good	t separ. var. est.	df	p 2-sided	Valid N Poor*	Valid N Good	Std. Dev. Poor	Std. Dev. Good	F-ratio variance	p variance
WIDTH	3.643	3.685	-1.892	44	0.065	18	74	0.061	0.122	2.839	0.019
FI	498.834	663.261	-0.506	38	0.616	18	74	1110.889	1654.056	2.217	0.068
FT	79.340	75.651	0.269	21	0.791	18	74	55.300	37.100	2.223	0.020
PRECIP	771.271	858.901	-0.831	24	0.414	18	74	408.940	373.380	1.199	0.574
WETDAYS	109.811	114.839	-0.464	23	0.647	18	74	42.600	35.200	1.469	0.262
LONG	101.556	93.270	1.872	22	0.075	18	74	17.600	13.300	1.741	0.108
LAT	38.389	38.162	0.165	28	0.871	18	74	5.100	5.700	1.243	0.635
TMEAN	12.874	12.412	0.346	27	0.732	18	74	5.056	5.222	1.063	0.937
DAYS32	43.743	36.640	0.842	27	0.407	18	74	31.800	33.500	1.109	0.851
DAYS0	94.834	99.755	-0.282	24	0.780	18	74	68.000	59.400	1.312	0.420
JTSPACE	5.287	5.122	0.552	23	0.586	18	74	1.190	0.976	1.460	0.269
SKEWNESS	0.432	0.391	0.557	28	0.582	18	74	0.274	0.305	1.170	0.746
KESAL	8750.938	6388.603	1.009	26	0.322	16	58	8115.300	8911.500	1.206	0.716
AGE	16.333	14.564	1.059	24	0.300	18	74	6.500	5.800	1.254	0.494
HPCC	232.689	241.783	-1.080	22	0.292	18	74	33.020	25.400	1.591	0.178
MR28	4589.333	4701.784	-0.841	24	0.409	18	74	518.128	467.142	1.232	0.525
EPCC	26661.488	27226.484	-0.794	24	0.435	18	74	2765.637	2459.907	1.264	0.481
BASETHICK	127.432	146.279	-1.653	37	0.107	18	74	40.640	58.420	2.106	0.087
EBASE	5370.372	3060.308	2.287	24	0.031	18	72	3925.805	3440.606	1.302	0.434
C_d	1.036	0.966	1.767	29	0.088	18	74	0.100	0.200	1.296	0.563
KSTATIC	48.289	46.599	0.276	22	0.785	17	69	23.301	19.693	1.398	0.339

* Poor includes both poor and normal rated sections.

where

WIDTH	= PCC slab width, m	AGE	= Pavement age, years
FI	= Freezing index, °C-days	JTSPACE	= Distance between slab joints, m
FT	= Annual air freeze-thaw cycles	SKEWNESS	= Joint skewness, m
PRECIP	= Mean annual precipitation, mm	KSTATIC	= Static elastic modulus of subgrade reaction, kPa/mm
WETDAYS	= Mean number of wet days	KESAL	= 80-kN equivalent single axle load, thousands
LONG	= Longitude location, degrees	HPCC	= Thickness of PCC slab, mm
LAT	= Latitude location, degrees	MR28	= Mean 28-day modulus of rupture, kPa
TMEAN	= Mean annual temperature, °C	EPCC	= Mean 28-day elastic modulus, MPa
DAYS32	= Annual number of days with temperature higher than 32°C	EBASE	= Mean base-layer modulus of elasticity, MPa
DAYS0	= Annual number of days with temperature lower than 0°C	C_d	= AASHTO drainage coefficient
BASETHICK	= Base thickness, mm		

Table 41. Results of Fisher Exact Tests for JPCP transverse cracking.

	Fisher Exact		
	One-tailed p	Two-tailed p	Description of variable
GRANBAS	0.025	0.033	=1, if granular base present =0, otherwise
ACBASE	0.609	1.000	=1, if asphalt stabilized base present =0, otherwise
CEMBASE	0.141	0.230	=1, if cement treated base present =0, otherwise
LEAN	0.069	0.069	=1, if lean concrete base present =0, otherwise
SUBGR	0.095	0.185	=1, if subgrade is coarse-grained soil =0, otherwise

Comparative Analysis of Transverse Cracking

Comparative analysis includes visual analysis of plots with a distribution of JPCP sections by their transverse cracking performance as a function of site conditions and design features, and a comparison of average values of those factors for different groups of pavement sections. The reader can observe the plots and evaluate the graphical results.

Climatic Site Conditions

Geographic/climatic location. Figures 87 and 88 show distribution of good, normal, and poor sections with respect to latitude and longitude of their location, respectively. Latitude and longitude are correlated with climatic factors such as precipitation, air temperature, and number of sunshine days per year. No clear trend relating latitude to transverse cracking performance was found for JPCP. The t-test found no significance of latitude on transverse cracking performance of JPCP, as shown in table 40. On the other hand, a larger number of poor sections is located in the western part of the United States and the t-test confirms that the difference is significant. This might be explained by a larger number of sunshine days in the western part of the country than in the eastern part. The number of sunshine days per year is a major factor affecting the amount of solar radiation received by the pavement surface and, as a result, maximum temperature gradient throughout the PCC slab.

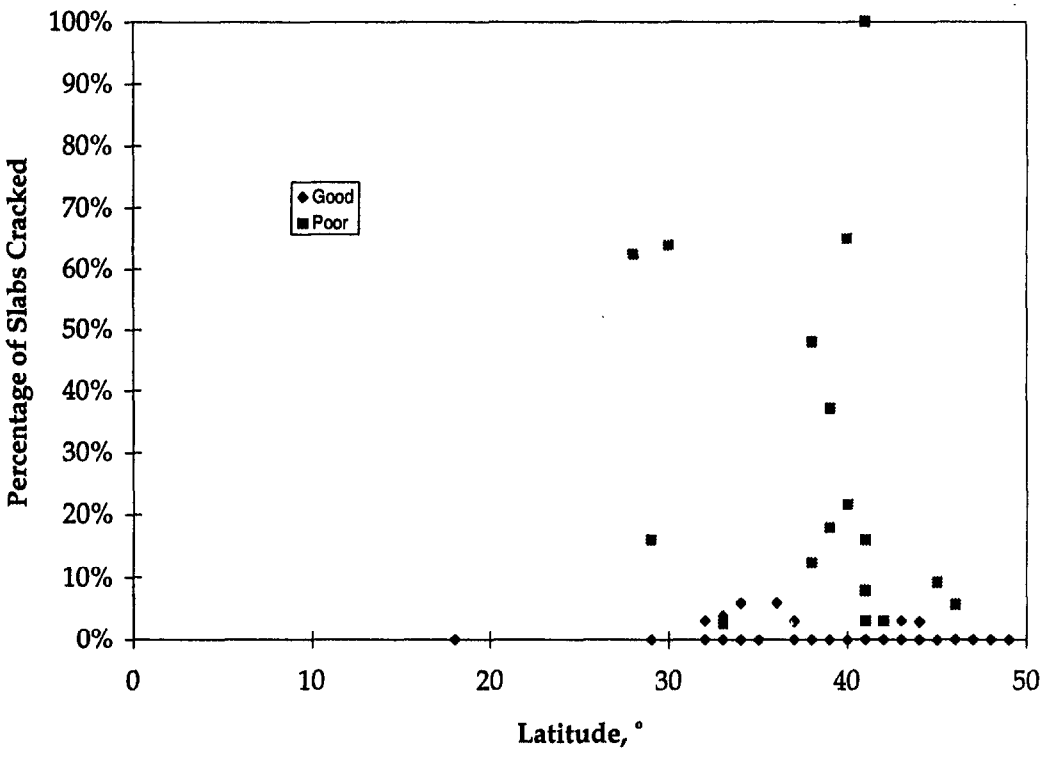

Figure 87. Latitude versus percentage of cracked slabs.

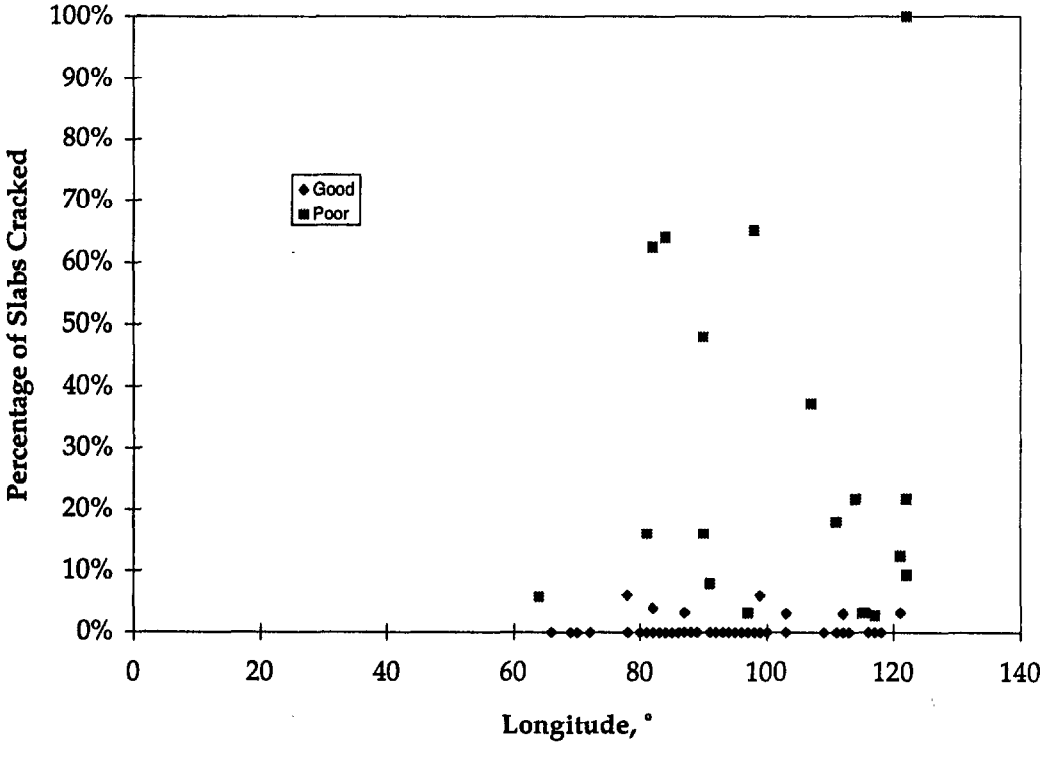

Figure 88. Longitude versus percentage of cracked slabs.

Previous theory and field studies show that temperature gradient curling dramatically affect transverse cracking. However, a comparison of temperature parameters (freezing index, number of air freeze-thaw cycles, mean annual temperature, minimum annual temperature, maximum annual temperature, number of days per year with a temperature higher than 32°C, and number of days per year with a temperature lower than 0°C) for good and poor performing JPCP sections found no clear trend relating transverse cracking with temperature factors. Figure 89 illustrates the effects of the mean annual temperature on JPCP transverse cracking. Although a significant number of poor performing sections are constructed in locations with a high mean temperature, mean annual temperatures for poor/normal performing sections is close to that for good performing sections (30.6°C vs. 30.2°C), the difference is not significant enough to derive any conclusions.

On the other hand, figure 90 shows that the average number of hot days is much higher for poor/normal sections than for good sections (43.7 vs. 36.6 days per year, respectively). This could relate to construction during hotter periods or the fact that in hotter climates, the thermal gradient is higher through the slab, which contributes to increased transverse cracking. This agrees with the LTPP and FHWA models (equations 33 and 34). It should also be noted, however, that several poorly performing sections are located in a cold climate. The statistical t-test did not confirm the significance of any of temperature parameters between good and poor sections.

Precipitation factors. Two precipitation factors were analyzed in this study: average annual precipitation and average number of wet days per year. However, no significant trend between these parameters and transverse cracking was found, and the statistical t-test did not show any significant difference in precipitation for poor and good sections.

Traffic Site Conditions

Figure 84 shows the relationship between applied ESALs and transverse cracking. It is expected that increased levels of traffic would clearly lead to an increase in transverse cracking if other design parameters and design features are equal. However, this effect is confounded by the influence of many other factors, such as climatic and design factors, so no clear trend is observed. Although poor performing pavements carried higher ESALs than good performing sections (8.8 vs 6.4 million ESALs, respectively), the difference was not found to be significant.

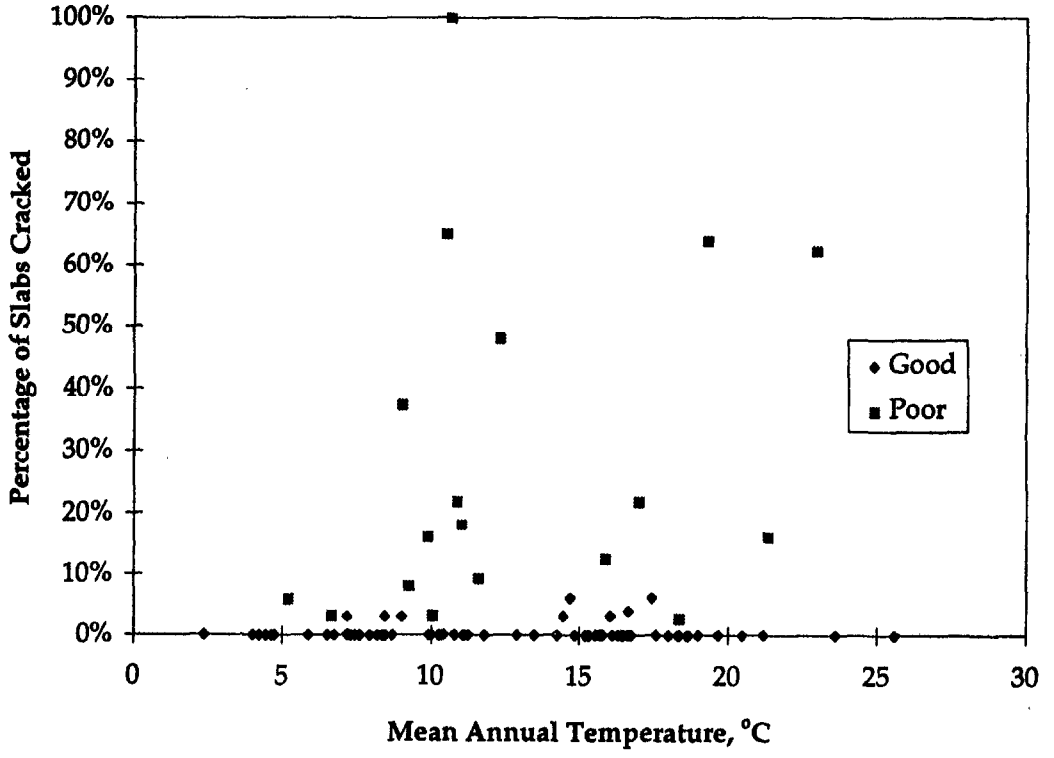

Figure 89. Average annual mean temperature versus JPCP transverse cracking.

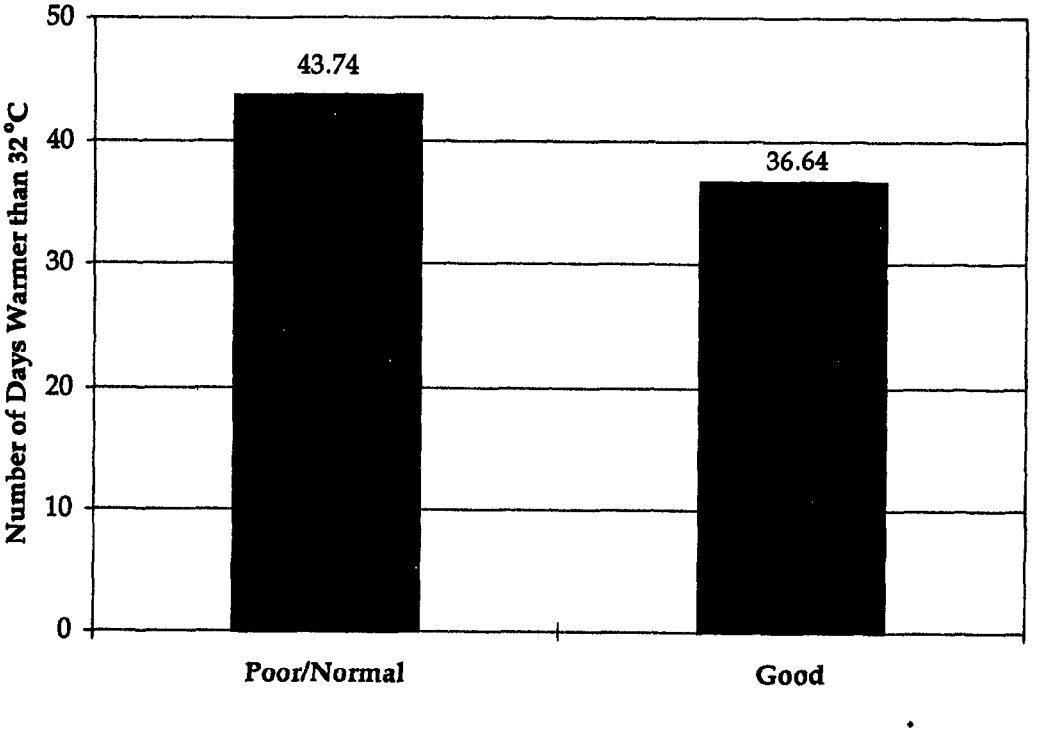

Figure 90. Effect of annual days above 32°C on JPCP transverse cracking performance.

Design and Construction Factors

Base type It is commonly believed that a stiff stabilized base increases the overall bending stiffness of the pavement structure, reducing critical bending stresses, and, therefore, reducing cracking. Field performance data, however, does not support this conclusion. Figure 91 presents the total number of sections older than 5 years and the number of sections with transverse cracks for each type of base. It can be observed that sections with a lean a stiff base (cement-treated base [CTB], soil cement base [SCB], or lean concrete base [LCB]) have a higher percentage of cracking than sections with an asphalt-treated base (ATB) or an aggregate base (AGG). The statistical t-test confirms that poor sections have statistically significant higher average base modulus of elasticity than good sections. Fishers's exact test confirmed that JPCP with asphalt treated or granular bases are less likely to exhibit poor cracking performance than JPCP with cement-treated or lean concrete bases (see table 41). A similar trend was found in a recent FHWA study, as shown in table 42.[2] This may indicate that either increased cracking is occurring during construction due to a stiff base, or that the slab and base have separated and curling stress are increased. Other factors also greatly influence pavement performance, so the causes mentioned are only tentative.

Table 42. Effect of base type on JPCP transverse cracking performance from LTPP and RIPPER study.[2]

	% JPCP sections with transverse cracks*	
Base Type	LTPP	RIPPER
ATB	8	28
AGG	22	38
SCB	38	100
CTB	42	68
LCB	56	38

* At least one crack.

Only a theoretically sound and field validated mechanistic model will be able to clarify the many aspects of influence of the base type on transverse cracking of JPCP. Other research has shown that when using a stabilized base, the joint spacing should be shorter.[2]

Joint spacing. Joint spacing affects the magnitude of bending stresses induced in the pavement by combined action of traffic loading and temperature curling at the slab edge. Several previous studies demonstrated the importance of reducing joint spacing for improving JPCP performance in general and transverse cracking in particular.[2] Comparison of the percentage of good JPCP sections for sections with the maximum joint spacing less than 4.8 m and remaining JPCP sections from the LTPP data base shows that the percentage of good sections is higher for shorter joint spacing (see figure 92). Nevertheless, the statistical t-test did not show significant difference between the average joint spacings for poor and good sections.

Figure 93 illustrates the percentage of slabs with transverse cracks as a function of the L/ℓ ratio (average joint spacing over the radius of relative stiffness). The radius of relative stiffness is defined as follows:

$$\ell = \sqrt[4]{\frac{EPCC\ HPCC^3}{12\ (1 - \mu^2)\ k}} \qquad (37)$$

The latter parameter combines the PCC slab thickness, HPCC, PCC modulus of elasticity, EPCC, PCC Poisson's ratio, μ, and the coefficient of subgrade reaction, k, into one parameter. This ratio appears to be related to transverse cracking. The percentage of sections with cracks is significantly higher for $L/\ell>6$. This indicates that the proper design of joint spacing and the PCC slab thickness, which has the greatest effect on the radius of relative stiffness, are crucial for transverse cracking control. Several sections with a large L/ℓ ratio did not exhibit any cracking. However, the risk of cracking can be seen to increase with higher L/ℓ ratio (longer joint spacing).

Widening of PCC slabs. Widened PCC slabs may improve transverse cracking performance of concrete pavements by reducing the critical edge stresses. It is achieved by moving the critical edge further away from the wheel path, thereby reducing the frequency of traffic encroachment to the pavement edge. Previous studies found that pavements with widened slabs perform well and exhibit little distress.[2] The LTPP data base contains information on eight JPCP sections with widened slabs. All of them performed well, showing no transverse cracking. However, these sections are relatively young (7 years or less). Therefore, long-term performance cannot be analyzed.

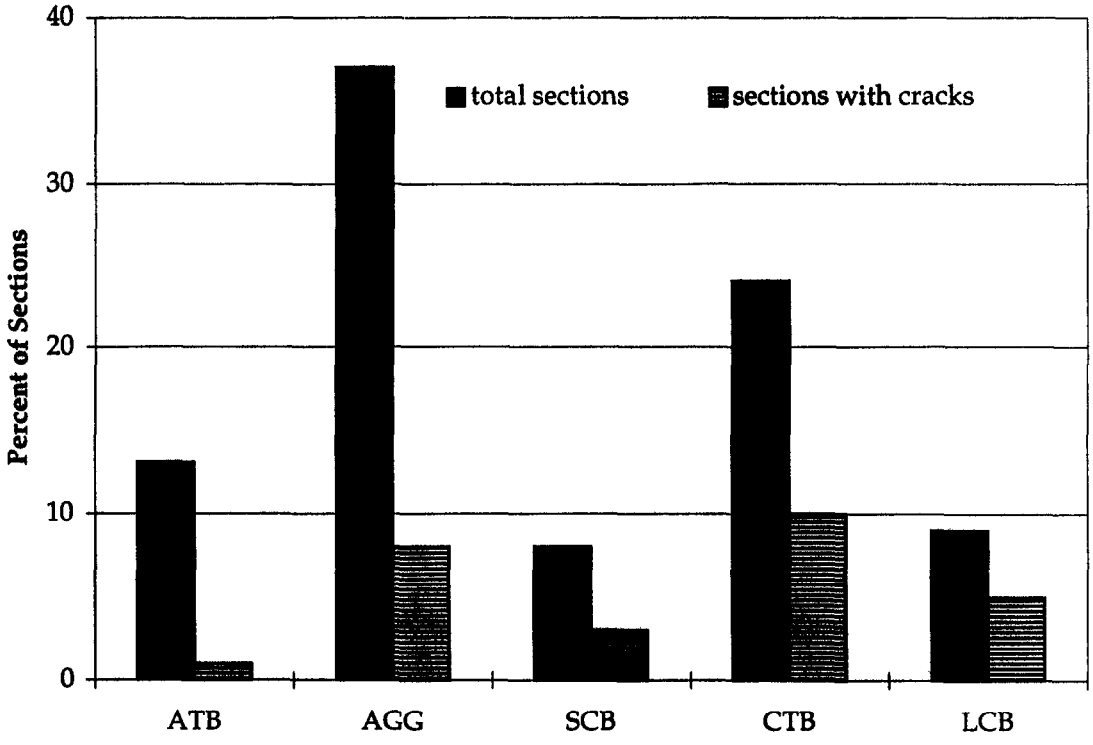

Figure 91. Effect of base type on JPCP transverse cracking performance.

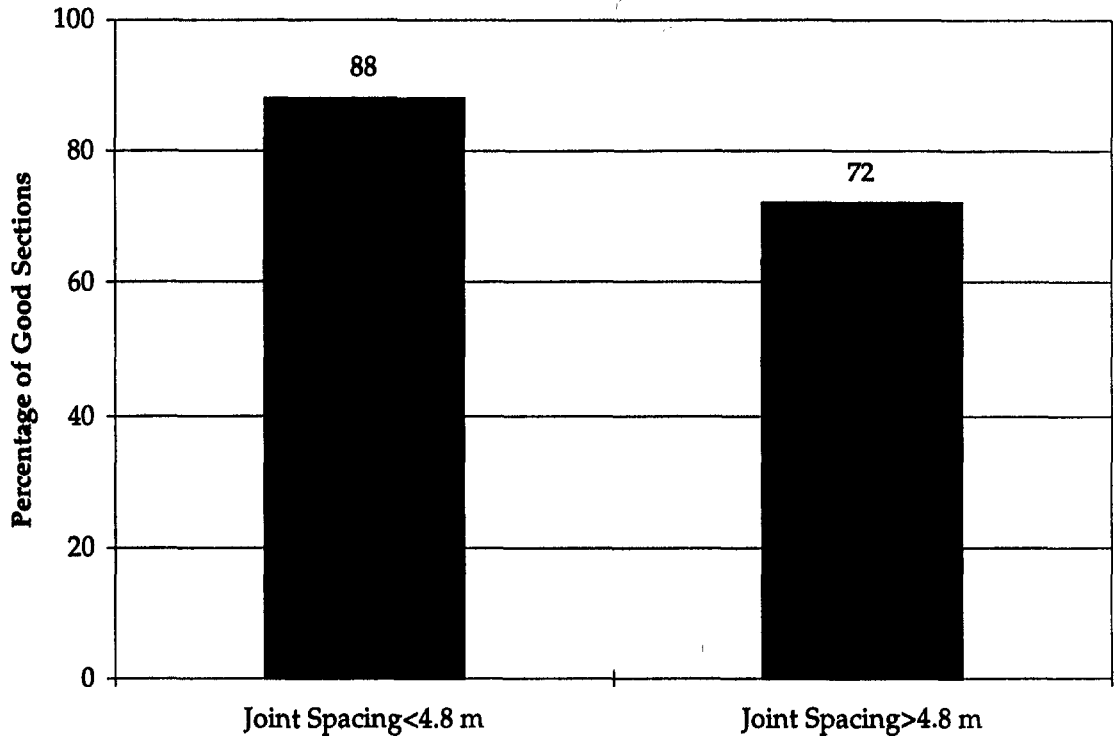

Figure 92. Effect of transverse joint spacing on JPCP transverse cracking performance

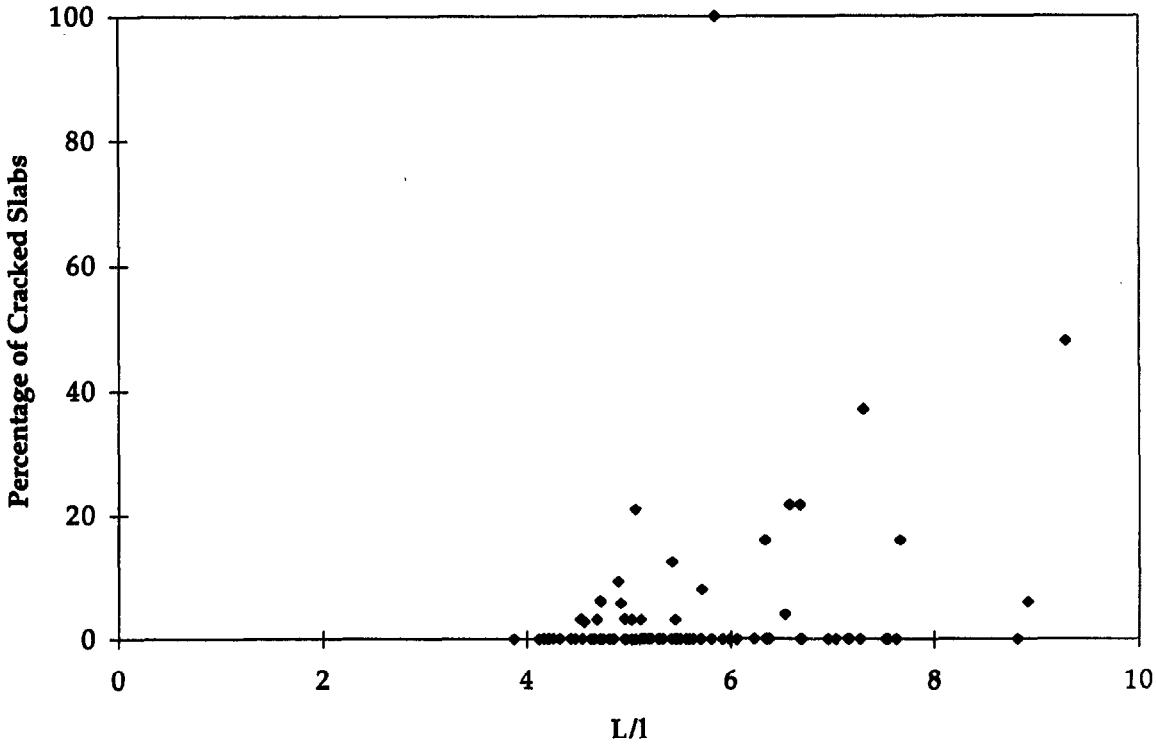

Figure 93. Effect of non-dimensional L/l ratio on JPCP transverse cracking performance.

Slab Thickness. The PCC slab thickness is identified in the previous studies as a very significant design feature.[1,2] Figure 94 shows the mean values for poor/normal and good performing JPCP sections. Although the poor performing sections have lower mean thickness, the statistical t-test did not confirm the significance of this difference. Other variables are likely confounded with PCC thickness (such as the joint spacing, the PCC modulus of rupture, and the coefficient of subgrade reaction).

PCC Modulus of Rupture. The PCC modulus of rupture is also identified in the previous studies as a very significant design feature.[1,2] In this study, an effect of estimated PCC modulus of rupture at 28 days after construction on JPCP transverse cracking performance was investigated. It was found that the poor performing sections have a lower mean modulus of rupture than good performing sections (4589 vs. 4701 MPa). However, the statistical t-test did not confirm the significance of this difference. Other variables are likely confounded with PCC modulus of rupture (such as the PCC thickness, joint spacing, and the coefficient of subgrade reaction).

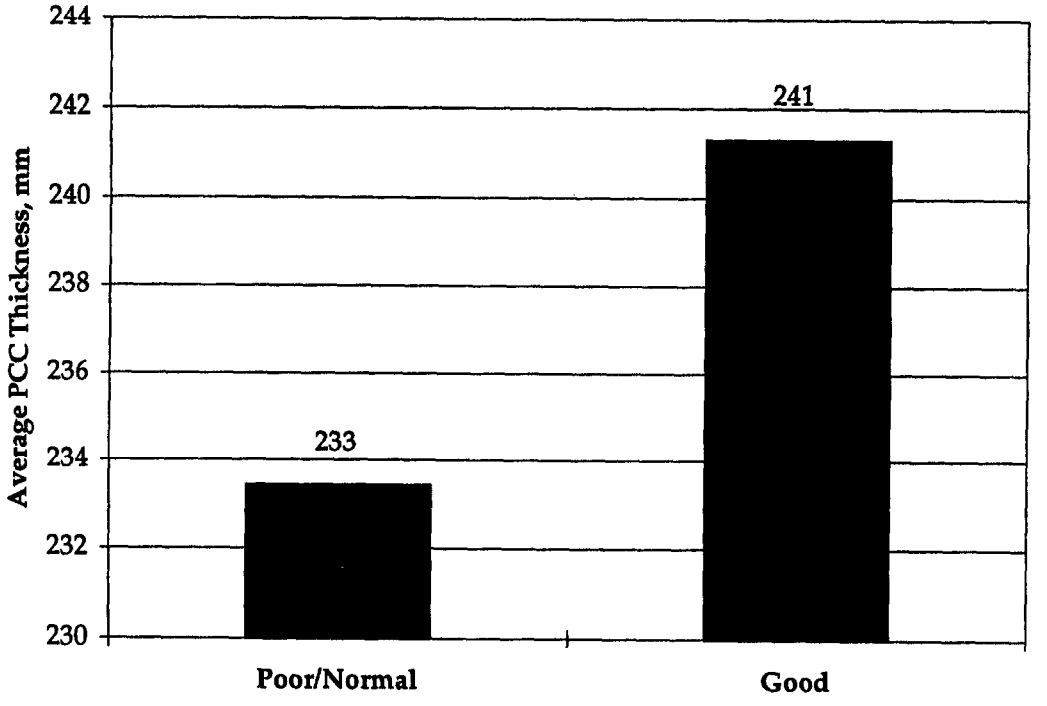

Figure 94. Effect of PCC thickness on JPCP transverse cracking performance.

Summary of Transverse Cracking for JPCP

The JPCP sections were evaluated both comparatively and statistically using the t-test and Fisher's exact test. The results of the comparative analysis and t-test comparisons were misleading in some instances due to the influence of other variables on the variable being analyzed.

This analysis showed that there are several site conditions and design/construction features that affect the transverse cracking of JPCP over time and traffic. The following site conditions were found to have an effect on transverse cracking of JPCP:

- **Climate:** Both of the referenced transverse crack prediction models include thermal gradient through the slab. Increased thermal gradients lead to increased transverse cracking. Thermal gradients vary considerably across a large geographical area like North America. They are much higher in areas with increased solar radiation (west) and lower for areas with higher cloud cover (east). It was found in this study that LTPP JPCP sections located in the western part of the United States exhibit more transverse cracking than those in the east.

- **Traffic:** ESALs are included in both of the referenced transverse crack prediction models. In this study, the poor performing pavements carried slightly higher ESALs than good performing sections, but the difference was not found to be significant.

- **Subgrade support**: The k-value of subgrade support is included in both referenced crack prediction models, but its effect is complicated. The direct t-test did not find the k-value to be a significant parameter. However, k-value could influence transverse cracking through the L/l ratio, as shown in figure 93. This is an another example of the importance of the influence of other variables on the variable being analyzed.

The following design and construction features were found to be statistically significant or to have a strong trend in preventing JPCP transverse cracking:

- **Base type and elastic modulus of the base course:** Sections with higher base modulus have a higher percentage of cracked slabs. JPCP with granular and AC bases had a significantly lower percentage of cracked sections than JPCP with cement-treated or lean concrete bases.

- **Slab thickness**: Poor performing JPCP had thinner slabs than good sections, but this difference was not found to be significant. In addition, a significant number of slabs with the ratio of the joint spacing to the radius of relative stiffness greater than 6 exhibited cracking. Therefore, the pavement thickness and joint spacing should be sufficient to keep this ratio below 6 to minimize the risk of transverse cracking.

- **Joint spacing:** Direct comparison of the mean joint spacing for poor and good JPCP sections did not show significant difference. However, it was found that the majority of poor performing pavements had a high ratio of the maximum joint spacing to the radius of relative stiffness. This indicates that the joint spacing is a critical design feature for JPCP to control transverse cracking.

- **Widened slab:** LTPP sections with widened slabs did not show any transverse cracking. However, these sections are not old enough to conclude reliably that widening of the PCC slab reduces cracking.

- **Construction:** Early cracking that appears to be related to construction problems has occurred on several of the JPCP sections. This should be studied further to see if any factors can be related to early cracking of JPCP.

- **Roughness:** Increased percent slab cracking correlated slightly with increased IRI, however, other factors such as the initial IRI and faulting cause much variation in the data.

CHAPTER 9. PERFORMANCE OF CRCP IN LOCALIZED FAILURES

A localized failure is one of the major distress types that occurs in continuously reinforced concrete pavement (CRCP). The causes and factors relating to localized failures (primarily punchouts but also steel ruptures and repairs of those distresses) in CRCP have been a topic of many investigations in past years.[11, 12, 13] Various algorithms and models have been developed in an attempt to describe the behavior of a CRCP. The main focus points of these algorithms and models are the prediction of crack spacing, crack width, concrete stress, and steel stress due to environmental changes and external wheel loads. The crack behavior as affected by the percentage of longitudinal steel reinforcement, concrete strength, aggregate type, and other environmental factors has also been analyzed by Zollinger.[14] Localized failures or punchouts are the primary mode of structural failure of CRCP. They are very critical and can lead to severe roughness if not repaired quickly.

Previous Studies

Performance of CRCP with respect to localized failures has been investigated in several studies. One localized failure model was developed for the Illinois Department of Transportation using extensive field data:[10]

$$\log_e(FAIL) = 7.27 - 5.27*10^{-5}\, HPCC^2 - 6.5858 * PSTEEL + 1.2875 * \log_e(CESAL) - 1.1408 * BAM - 0.9367 * CAM - 0.8908 * GRAN - 0.1258 * CHAIRS \quad (38)$$

where:

FAIL	=	total number of localized failures in the outer lane, number/km.
HPCC	=	CRCP slab thickness, mm.
PSTEEL	=	longitudinal reinforcement, %.
CESAL	=	cumulative ESALs, millions.
BAM	=	1 if subbase material is bituminous-aggregate mixture, 0 otherwise.
CAM	=	1 if subbase material is cement-aggregate mixture, 0 otherwise.

GRAN = 1 if subbase material is granular, 0 otherwise.
CHAIRS = 1 if chairs used for reinforcement placement, 0 if tubes used.

This model predicts localized failures as a function of site conditions and pavement design features. The cumulative ESAL is positively correlated to localized failures; that is, an increase in ESAL corresponds to an increase in localized failures. This implies that the age of the pavement is positively correlated to localized failures because, in general, the cumulative ESAL increases with the age of the pavement. This is reasonable because pavement distresses that increase the localized failures of the pavement generally tend to increase with repeated heavy axle loadings. Also, pavement features such as the slab thickness, the percent longitudinal reinforcement, and the type of the base have a logical physical influence on the localized failures.

Table 43. Summary of the effects of site conditions and design features on localized failures.[10]

Site Condition/Design Feature	Effect on localized failures over life*
PCC slab thickness	Decreases
Longitudinal reinforcement	Decrease
Traffic (ESAL)	Increases
Base type	Treated base decreases over granular base Granular base decreases over no base
Chairs vs tubes steel placement	Chairs decreases over tubes (slightly)

* For example, an increase in slab thickness results in a decrease in localized failures.

Performance Criteria for Localized Failures

This section presents an analysis of the factors that lead to localized failures of CRCP based on the measurements from the LTPP data base. The LTPP data base contains localized failures data for 69 CRCP sections. The total number of observations is 131. For some sections, time series data contain up to five observations made over 5 years. Other sections have only one performance record in the data base.

The localized failure in this study is defined as:

$$LF = PUNCH + RPATCH + FPATCH \quad (39)$$

where:

LF	=	number of the localized failures/km
PUNCH	=	number of punchouts/km at all severities
RPATCH	=	number of rigid patch/km at all severities
FPATCH	=	number of flexible patch/km at all severities

The sections were divided into three performance categories: poor, normal, and good, based on localized failures and pavement age as previously described. This grouping was done to facilitate the analysis of identifying features that contribute to good and poor performance with respect to localized failures. This grouping was established as described in chapter 2. The limits that were set are shown in figure 4. A CRCP section was considered good (i.e., performing better than expected) if its localized failures satisfied the following condition:

$$LF < 0.5 * AGE \quad (40)$$

where:

AGE	=	the pavement age at the time of the observation in year
LF	=	number of the localized failures/km

A CRCP section was considered poor if its localized failures satisfied the following condition:

$$LF > AGE \quad (41)$$

where:

AGE	=	the pavement age at the time of the observation in year
LF	=	number of the localized failures/km

Figure 95 presents a plot of all localized failure observations for the LTPP CRCP sections and shows designation of those sections by their performance at the time of observation. Because the number of observations differs among the sections, the use of all these observations in the subsequent analysis may make it biased toward the sections with a higher number of observations. To avoid this, only the maximum observation for each section was considered in the analysis. Figure 96 shows the number of sections for each performance category. According to this figure, the large majority of CRCP sections perform well relative to localized failure occurrence.

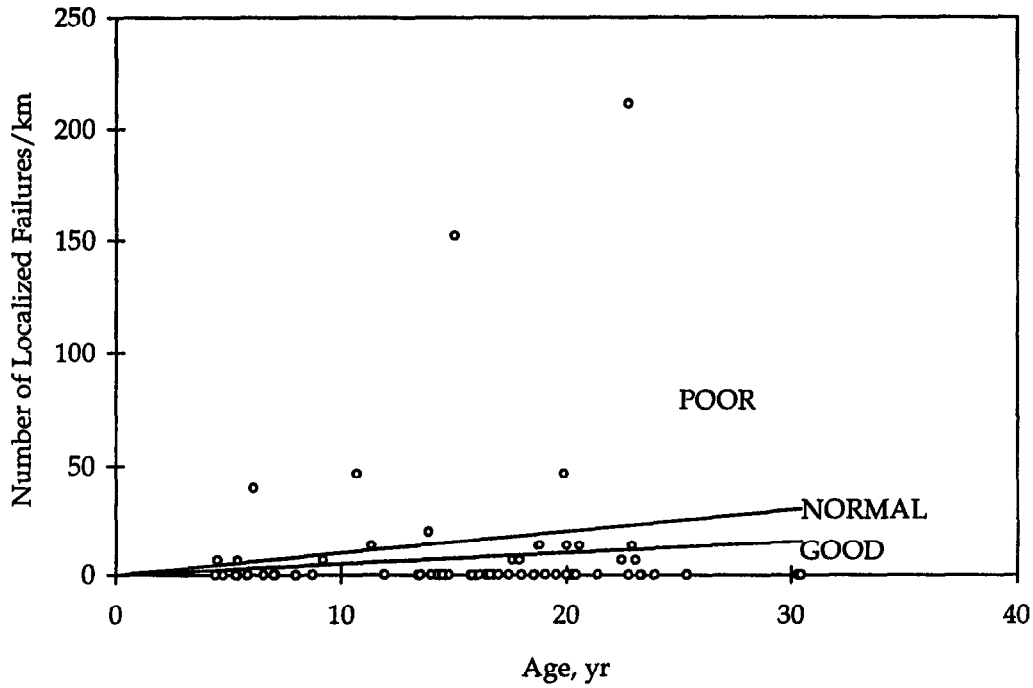

Figure 95. Localized failures for CRCP.

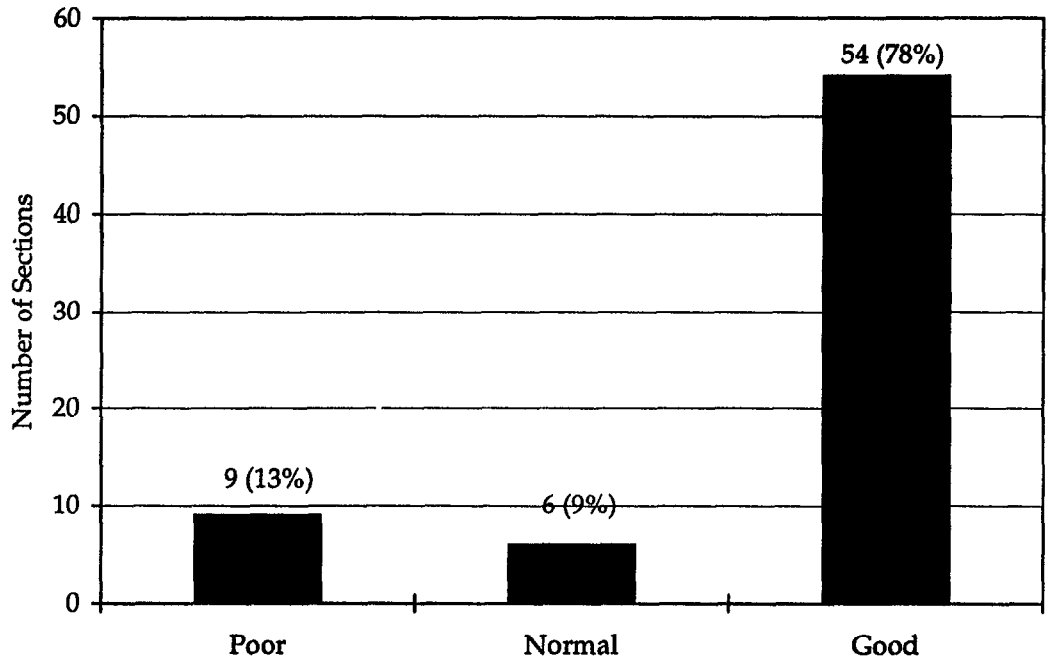

Figure 96. Localized failures for CRCP in each performance category.

Factors Considered for Localized Failures

The general types of factors affecting the localized failures of CRCP include site conditions and design and construction features. The factors studied in this analysis include those found to be significant from previous studies and others based on engineering judgment:

- **Site Conditions**
  - Geographic/climatic region
  - Temperature factors
    - Freezing index
    - Freeze-thaw cycles
    - Mean annual temperature
    - Minimum annual temperature
    - Maximum annual temperature
    - Number of days warmer than 32°C
    - Number of days colder than 0°C
  - Precipitation factors
    - Average annual precipitation
    - Average number of wet days
  - Traffic (ESALs)

- **Design and Construction Features**
  - Slab thickness
  - Percent of longitudinal reinforcement
  - Base type

Comparative and Statistical Analysis of Localized Failures

Comparative analysis includes visual analysis of plots of local failures versus each factor and a comparison of average values of each factor for good, normal, and poor groups of pavement sections.

The t-test was conducted to identify those site conditions and design features that contribute to good and poor localized failures performance. The CRCP section data were partitioned into two groups based on localized failures: those that fell into the good group and those that fell into the normal/poor group (note that the normal/poor group will subsequently be called only the poor group for convenience). The normal group had to be used in the analysis due to the limited number of sections.

Table 44. Results of t-tests for CRCP localized failures performance.

Variables		Mean Good	Mean Poor	t-value	d.o.f.	p	Valid N Good	Valid N Poor	Std. Dev. Good	Std. Dev Poor	F-ratio variance	p variance
AGE		15.584	14.654	0.480	63	0.633	54	11	5.677	6.717	1.400	0.412
KESAL		7533	8725	-0.339	63	0.736	54	11	11102	7570	2.151	0.190
Base type	Granular	0.185	0.364	-1.309	63	0.195	54	11	0.392	0.505	1.656	0.233
	Asphalt	0.463	0.455	0.050	63	0.960	54	11	0.503	0.522	1.077	0.793
	Non-Asphalt	0.278	0.000	2.025	63	0.047	54	11	0.452	0.000	0.000	1.000
Climate	Warm/Wet	0.463	0.364	0.596	63	0.553	54	11	0.503	0.505	1.005	0.903
	Warm/Dry	0.389	0.273	0.719	63	0.475	54	11	0.492	0.467	1.110	0.923
	Cold/Wet	0.074	0.273	-1.965	63	0.054	54	11	0.264	0.467	3.122	0.007
	Cold/Dry	0.074	0.091	-0.188	63	0.851	54	11	0.264	0.302	1.301	0.508
Percent reinforcement		0.611	0.603	0.345	62	0.731	53	11	0.078	0.056	1.943	0.256
Slab thickness		214.53	219.35	-0.612	63	0.543	54	11	23.93	23.47	1.038	1.000
Base thickness		116.10	124.69	-0.606	61	0.546	52	11	42.85	41.66	1.057	0.999

Table 44 provides a summary of all the t-values for each comparison made. Some sections may not be included if they do not have data for given parameters.

Climatic Site Conditions

Climatic Region. Figure 97 shows the distribution of good, normal, and poor sections with respect to four climatic zones (warm-wet, warm-dry, cold-wet, and cold-dry). Climatic regions are correlated with precipitation and temperature. There were a relatively small number of observations in the warm-dry and cold-dry regions, and no clear trend could be found relating climatic regions to localized failures. The t-test (table 44) showed that only the cold-wet climate zone shows a significant difference between good and poor groups ($p = 0.054$). Significantly more localized failures occurred in cold-wet climate.

Temperature factors. The following temperature parameters were considered in this study: freezing index (FI), number of air freeze-thaw cycles (FT), mean annual temperature (T_{mean}), minimum annual temperature (T_{min}), maximum annual temperature (T_{max}), number of day per year with a temperature higher than 32°C (DAYS32), and number of days per year with a temperature lower than 0°C (DAYS0). The t-test did not show any significance of these differences.

The distribution of localized failures vs. freezing index, FI, for each performance category is shown in figure 98. No clear trend was observed relating freezing index to localized failures in this data base. Figure 99 illustrates the effects of the annual number of air freeze-thaw cycles on localized failures. No clear trend was observed relating annual number of air freeze-thaw cycles to localized failures in this data base.

Figures 100, 101, and 102 present the effects of the mean annual temperature (T_{mean}), minimum annual temperature (T_{min}), maximum annual temperature (T_{max}), respectively. No clear trend was observed relating temperature to localized failures in this data base.

Figure 103 shows the effects of the annual days above 32°C (DAYS32) on localized failures. It is observed that DAYS32 of good and normal performing sections are almost the same, but poor performing sections have a somewhat higher value of DAYS32 than the others.

Figure 104 represents the effects of the annual days below 0°C (DAYS0) on localized failures. No clear trend was observed relating DAYS0 to localized failures in this data base.

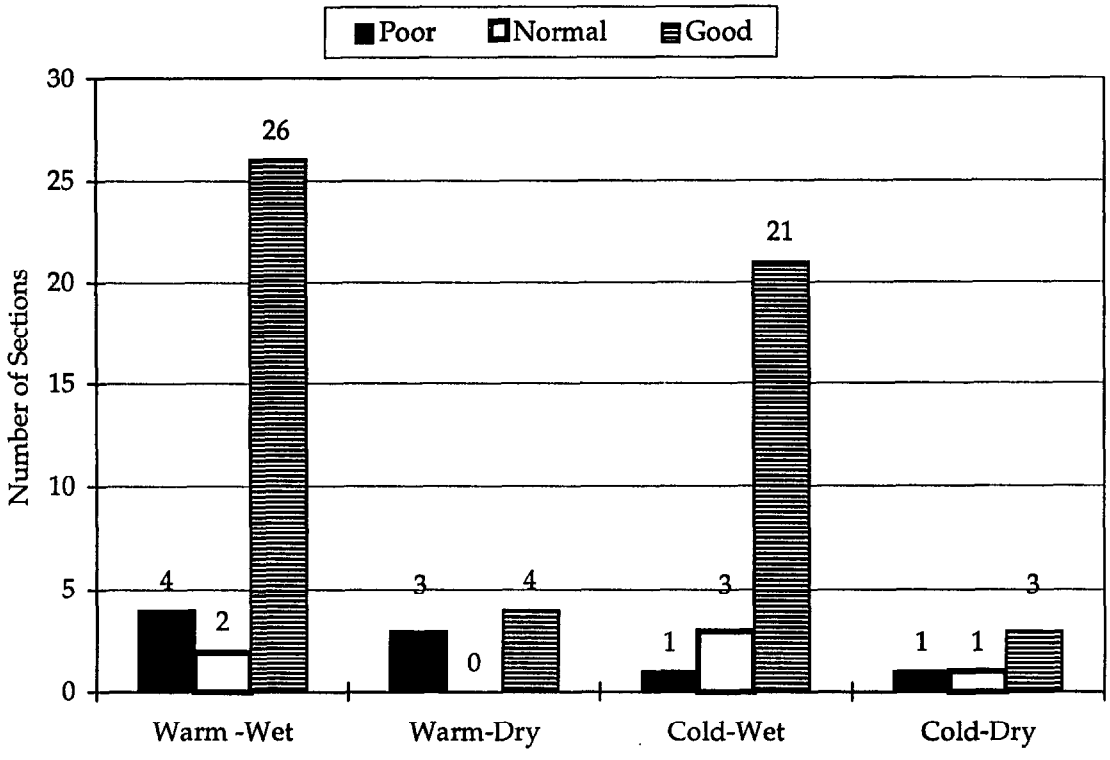

Figure 97. Effect of climatic region on CRCP localized failures.

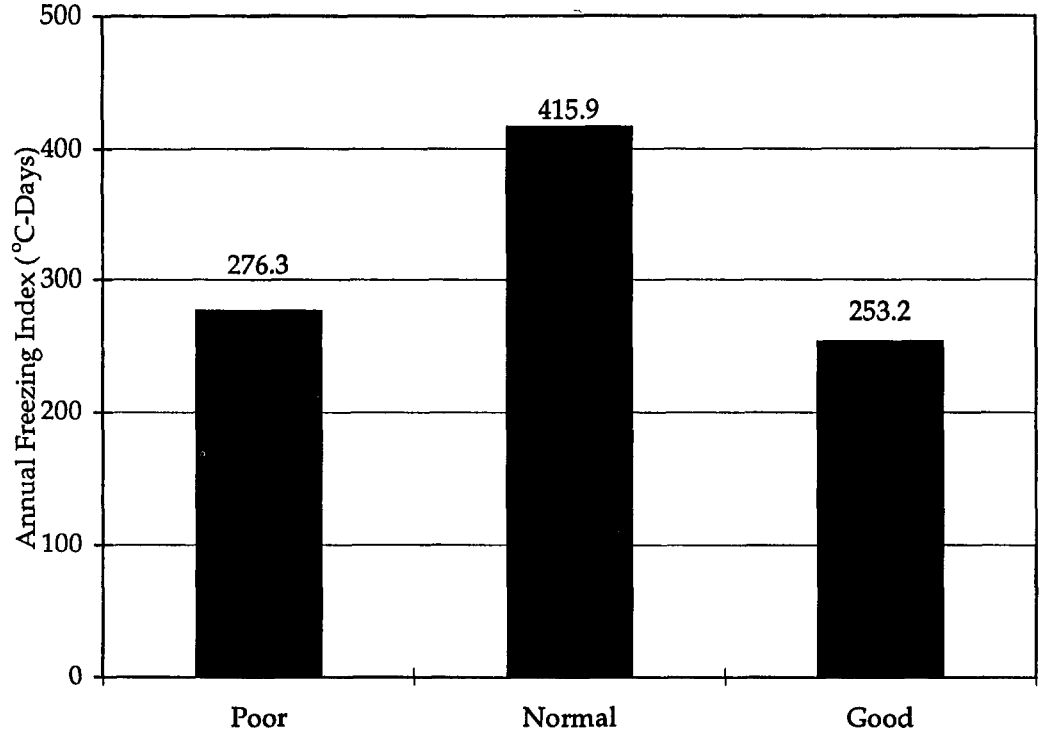

Figure 98. Effect of freezing index on CRCP localized failures.

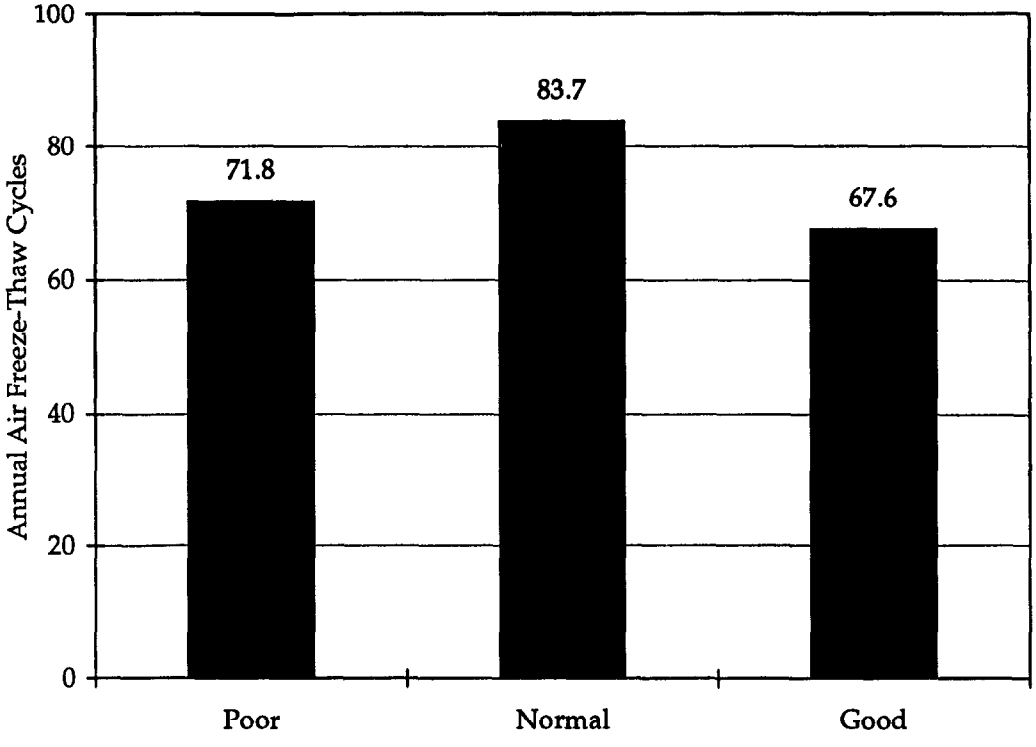

Figure 99. Effect of annual air freeze-thaw cycles on CRCP localized failures.

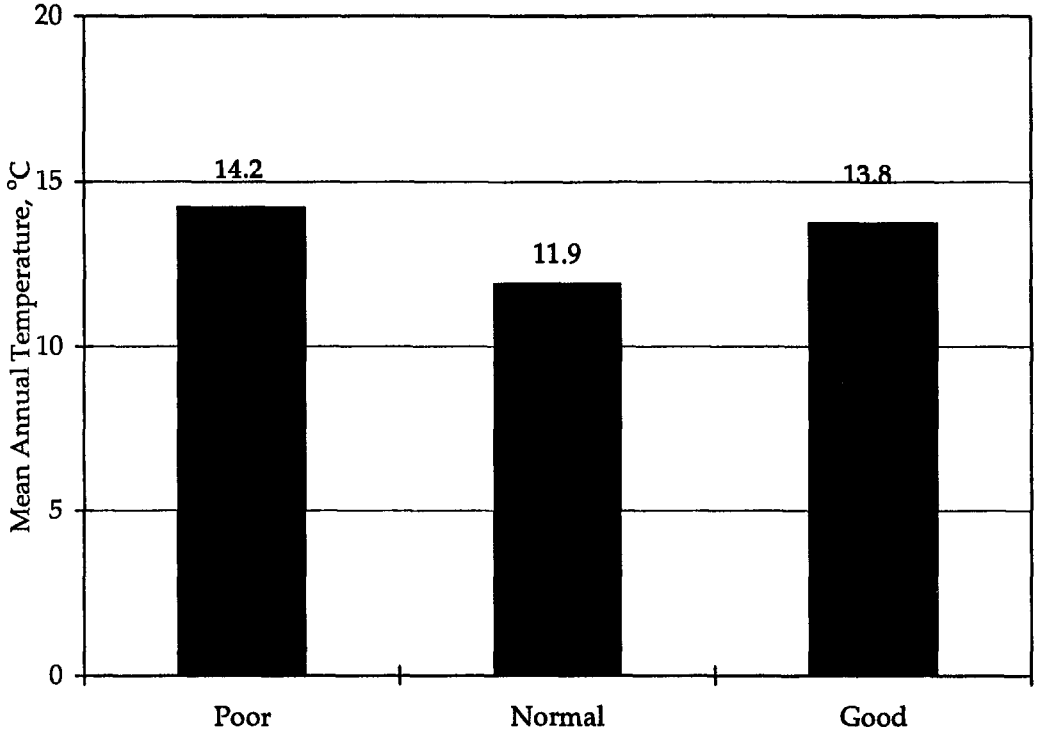

Figure 100. Effect of mean annual temperature on CRCP localized failures.

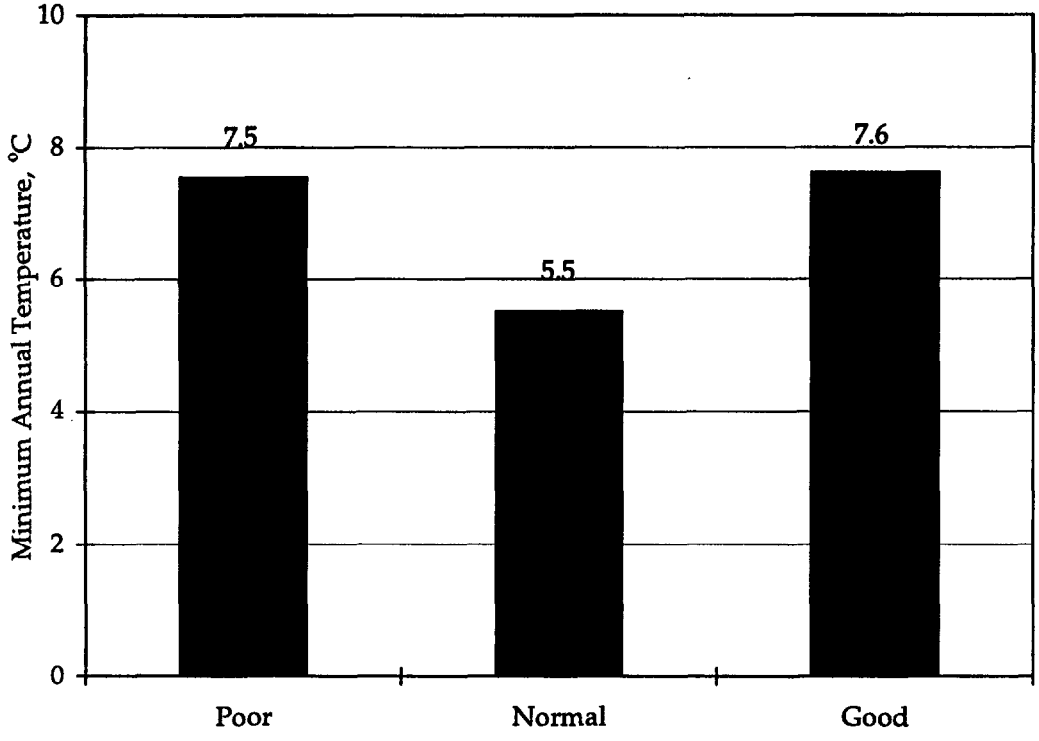

Figure 101. Effect of minimum annual temperature for CRCP localized failures.

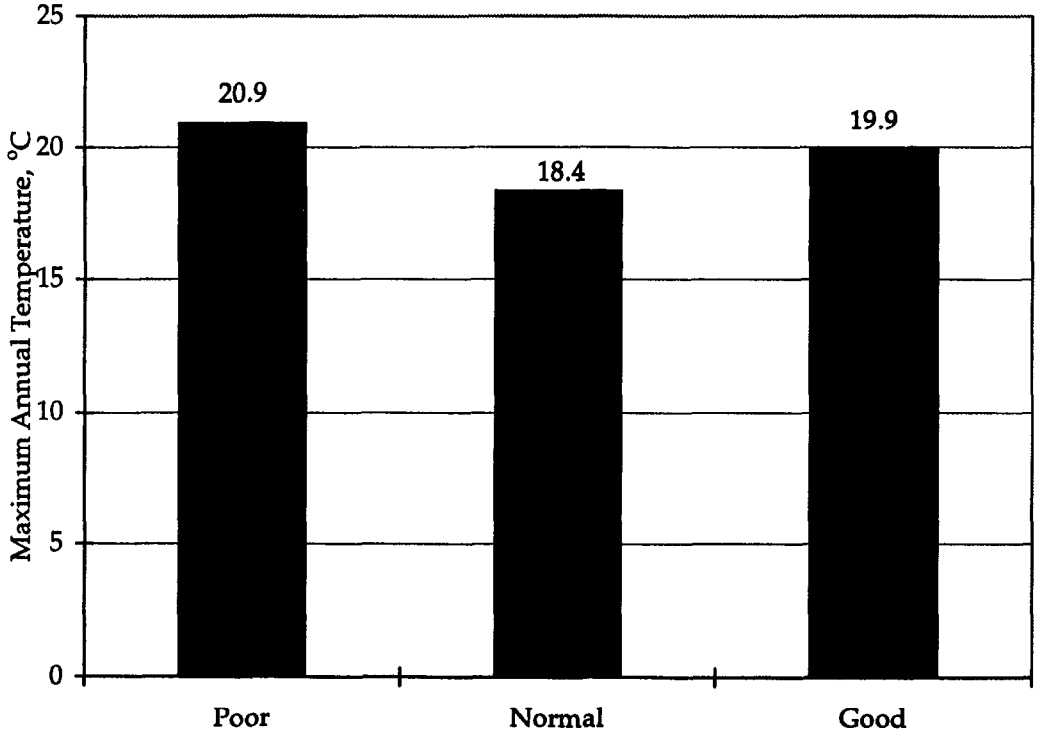

Figure 102. Effect of maximum annual temperature for CRCP localized failures.

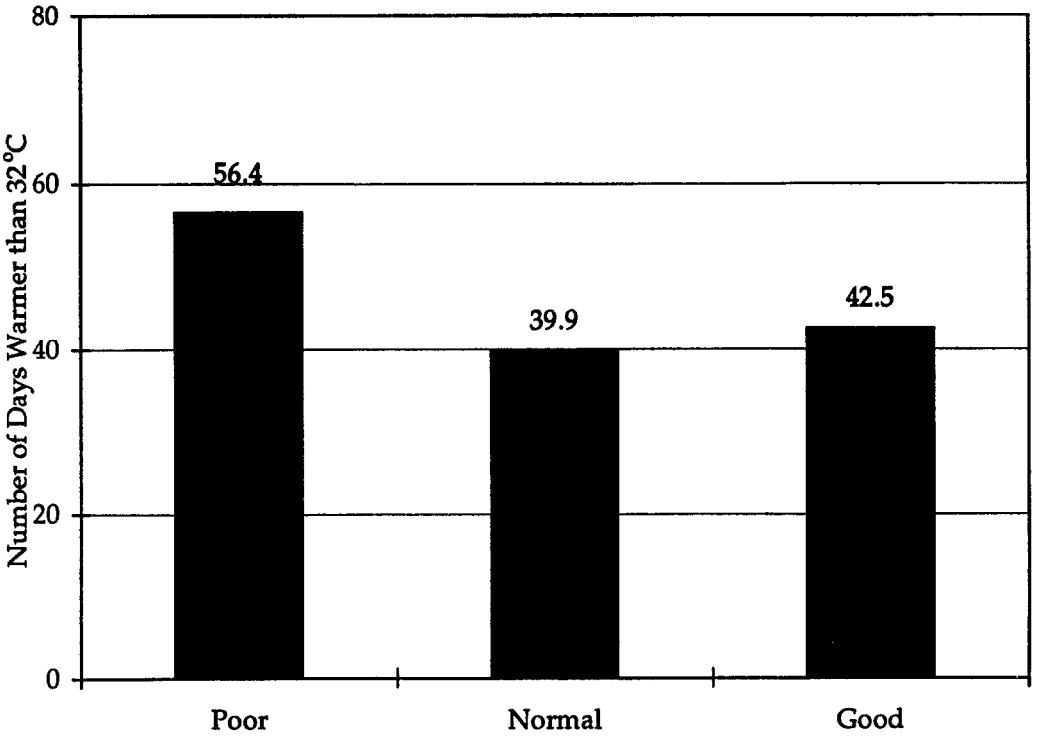

Figure 103. Effect of annual days above 32°C on CRCP localized failures.

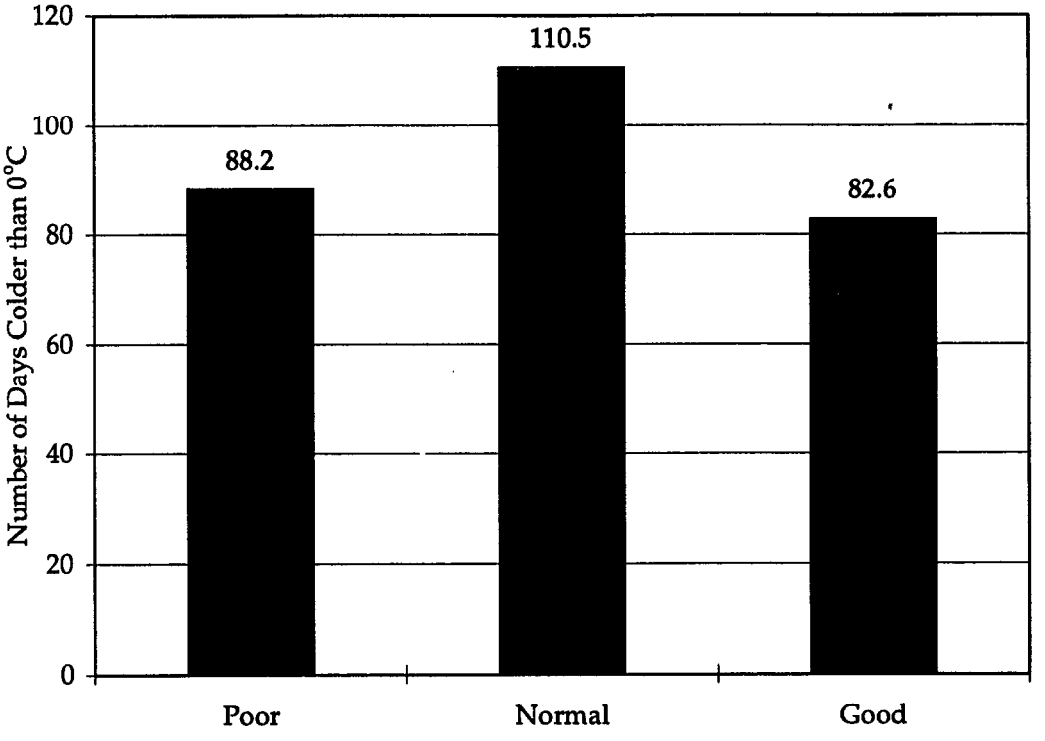

Figure 104. Effect of annual days below 0°C on CRCP localized failures.

Precipitation factors. Two precipitation factors were analyzed in this study: average annual precipitation and average number of wet days per year. No clear trend was observed relating annual precipitation levels or wet days per year to localized failures performance, as shown in figures 105 and 106. For both plots, the CRCP rated as good have a higher level of precipitation and number of wet days per year.

Traffic Site Conditions

Figure 107 shows the relationship between applied ESALs and localized failures; no clear trend was observed relating traffic to localized failures. The t-test (table 44) found that the difference between good and poor groups was not significant.

Design and Construction Factors

Slab thickness. Figure 108 shows the effects of the slab thickness on localized failures. No clear trend was observed relating slab thickness to localized failures. The t-test (table 44) showed that the difference between good and poor groups was not significant.

Longitudinal reinforcement. Figure 109 illustrates the effects of the longitudinal reinforcement on localized failures. It was observed that good and normal sections have higher percentage of reinforcement. However, the t-test (table 44) found that the difference between good and poor groups was not significant.

Base type. Figure 110 shows the effects of the base type on localized failures. Six sections were excluded because the slabs were placed directly on the subgrade. It was observed that all sections were categorized as good when the non-asphalt-treated base was used. However, it is difficult to find a clear trend relating base type to localized failures.

Summary of Localized Failures for CRCP

Localized failures are extremely important performance characteristics of CRCP because of their impact on the traveling public and on maintenance requirements. Several site conditions and design and construction features that affect the localized failures of CRCP were analyzed based on the LTPP data base. Neither the comparative analysis or the t-test comparisons showed that any of the site conditions or design features were significant with the exception of cold-wet climates showing larger failures.

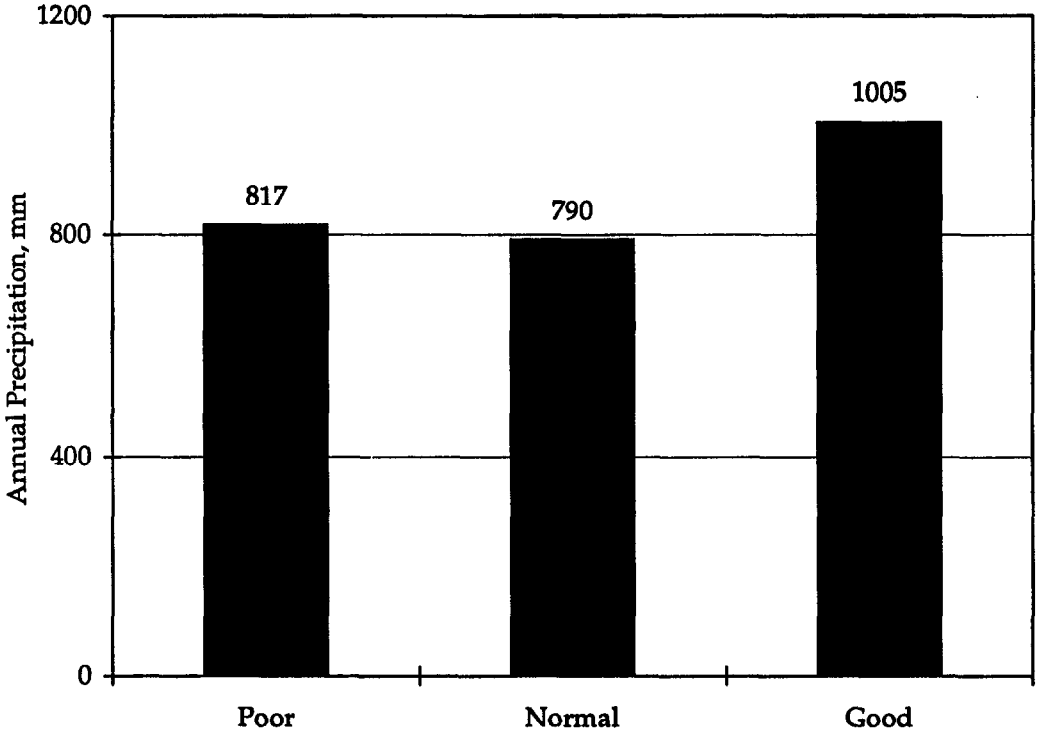

Figure 105. Effect of annual precipitation on CRCP localized failures.

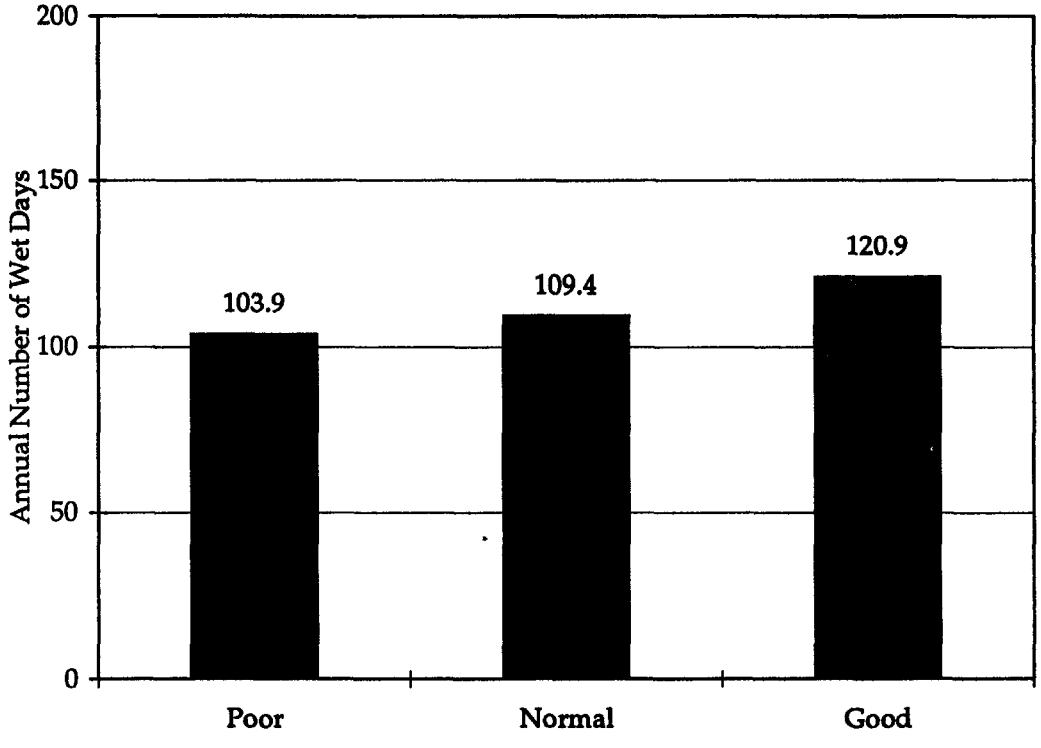

Figure 106. Effect of annual wet days on CRCP localized failures.

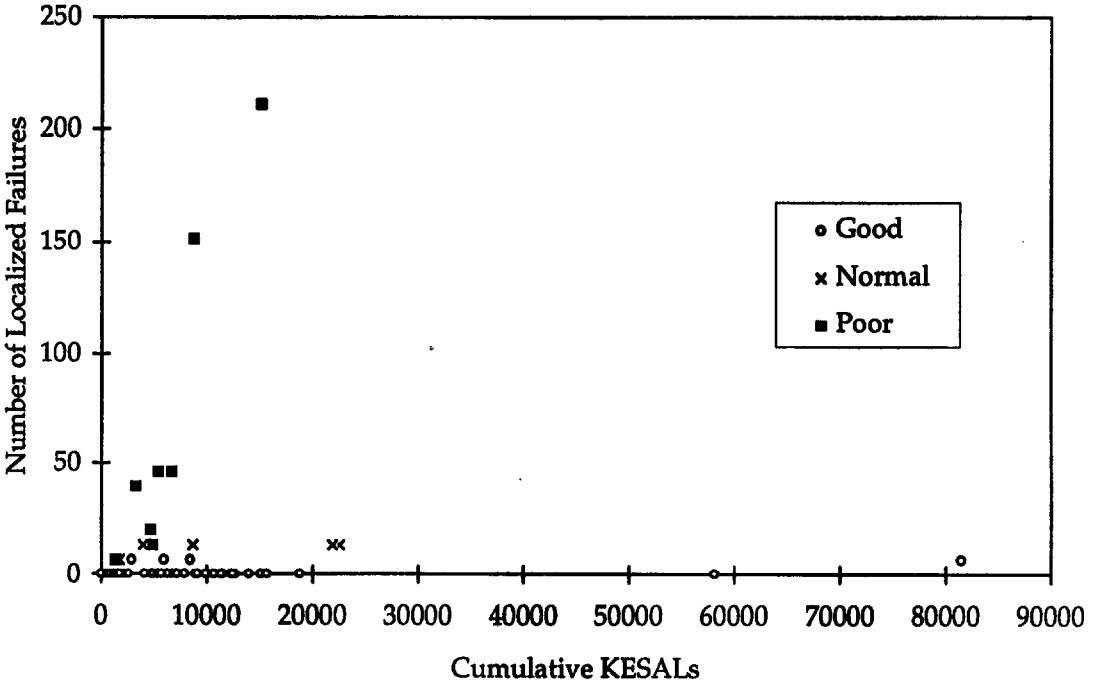

Figure 107. Effect of traffic on CRCP localized failures.

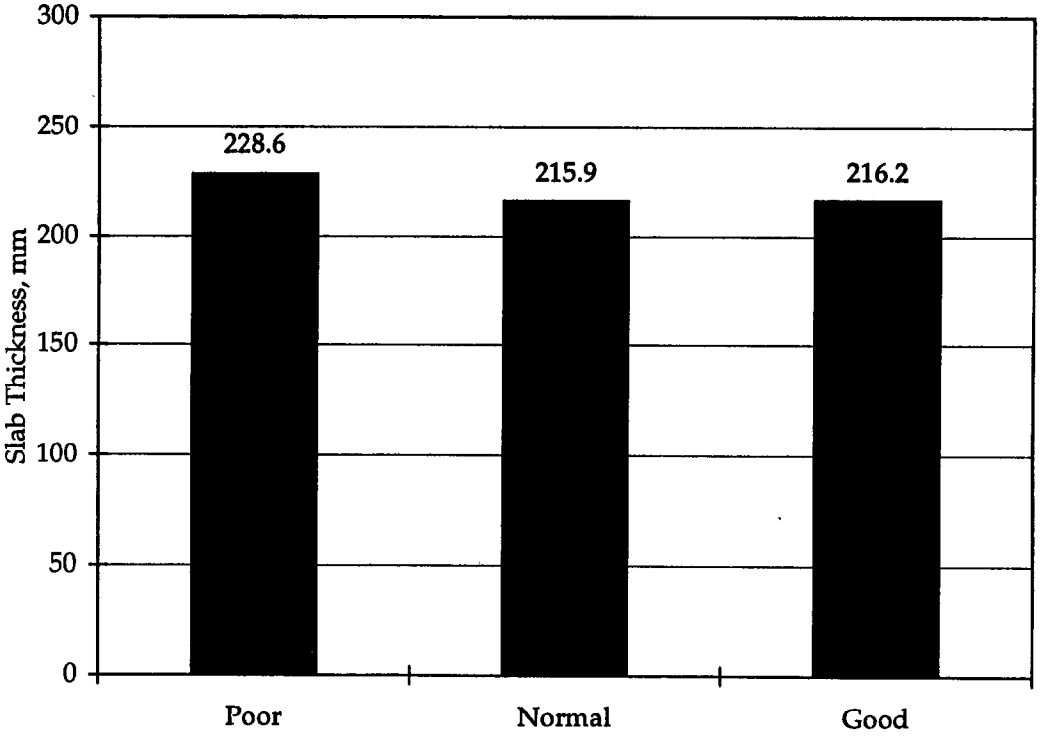

Figure 108. Effect of PCC slab thickness on CRCP localized failures.

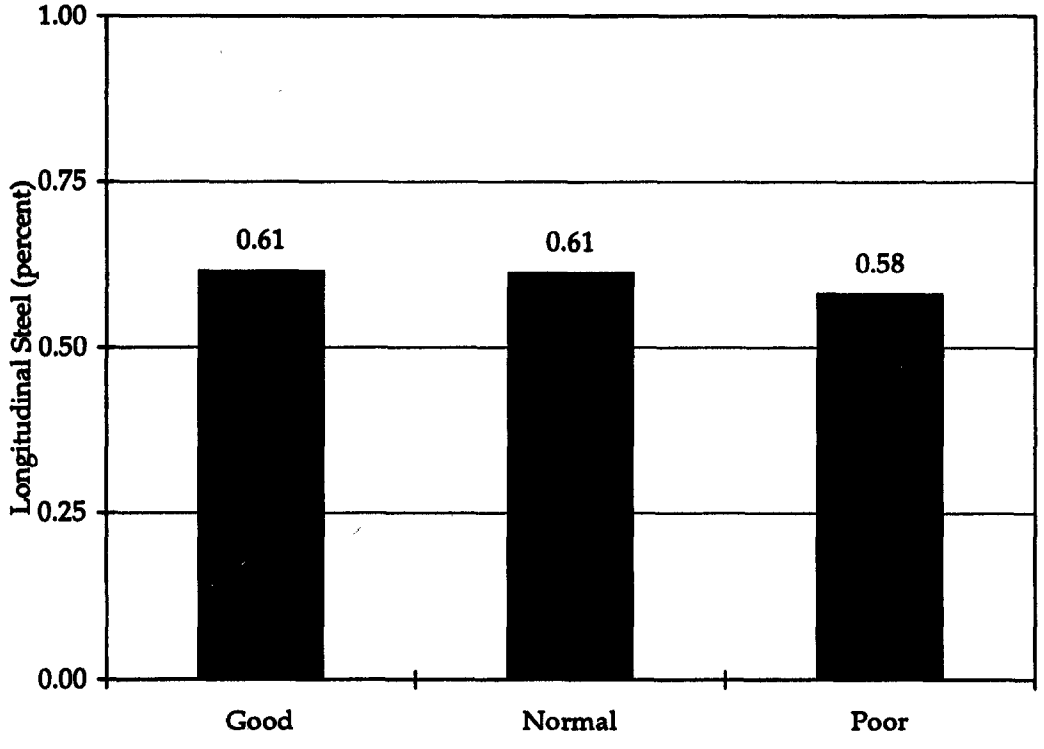

Figure 109. Effect of design steel content on CRCP localized failures.

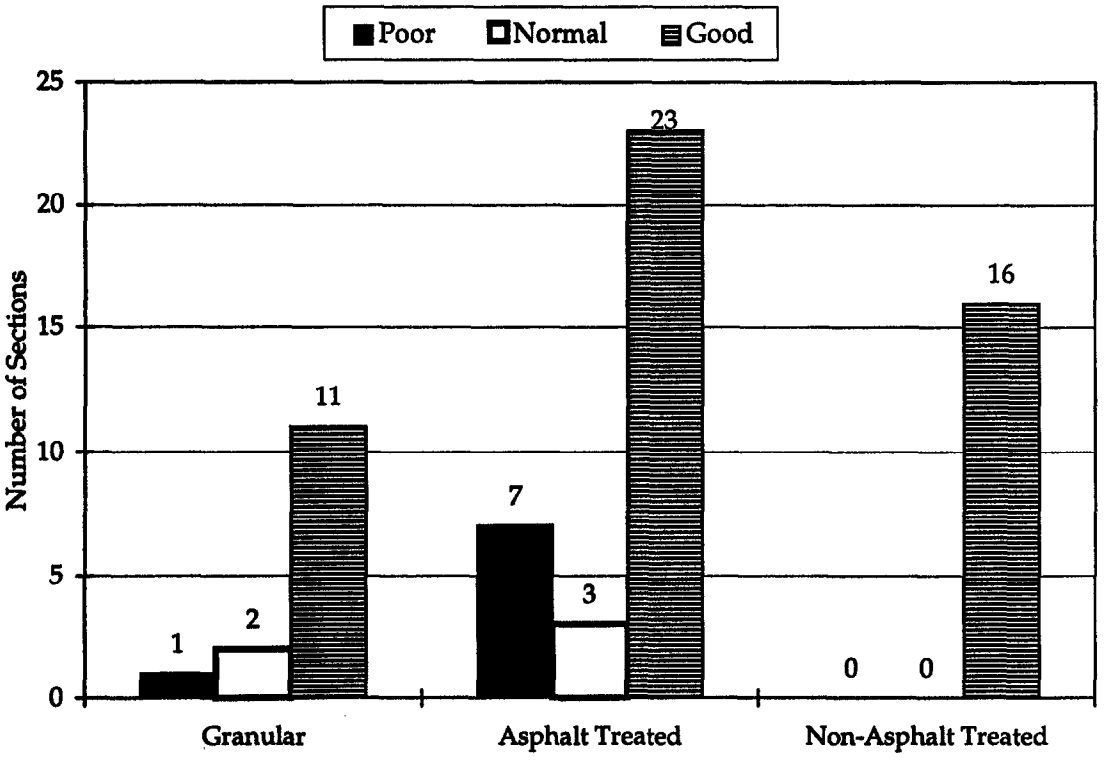

Figure 110. Effect of base-layer type on CRCP localized failures.

It is known from previous studies that traffic, climate, and structure design (slab thickness and particularly percent steel) affect the performance of CRCP in terms of the localized failures. According to this analysis, however, it is difficult to find the clear trends of relating these features to localized failures in this data base. One of the potential problems is that, in general, most of the observed sections in the LTPP data base are performing well (more than 85 percent of observed sections are in good and normal categories). The major problem is believed to be the relative shortness of the CRCP sections (150 m). Localized failures occur in various locations along long CRCP projects, and 150-m-long section is not an adequate sample for evaluating performance measured in terms of localized failures. It may be necessary to survey longer sections on either side of the official CRCP LTPP sections to achieve useful results.

CHAPTER 10. WHAT WORKS AND WHAT DOES NOT FOR PCC PAVEMENTS

This study has identified several site conditions and design/construction features that lead to good performance and poor performance of JPCP, JRCP, and CRCP. A summary of findings is provided at the end of each main chapter. The objective of this chapter is to compile these findings into an overall summary for practicing design engineers in State and provincial highway agencies to guide them in what works well and what does not work for the three major types of PCC pavements.

The designer starts out with a given set of site conditions for a project. These include primarily traffic, climate, and subgrade. Geometrics is another important site condition that usually affects the pavement and drainage design. This and related studies have shown that all of these site conditions are very important in PCC pavement performance. They cannot be controlled by the designer; however, where they are critical, the designer should take steps (i.e., modify the design features) to mitigate their adverse effects on performance.

Several design and construction features that can be controlled or specified by the designer were found to have very significant effects on performance. These are the ones to focus on to help ensure good performance. This section provides a summary of findings about the design and construction features identified as being critical to good and poor PCC pavement performance.

Although there are many similarities between JPCP, JRCP and CRCP, some of the mechanisms of their performance are very different and thus they are discussed separately.

It is important to note that not all site conditions or design and construction features were evaluated in this study. One extremely important feature not included was PCC durability. Obviously, if a non-durable PCC material is provided, the pavement could fail rapidly regardless of the other design or construction features. Another feature is variability of materials, and there are many others. This limitation needs to be kept in context when considering the following findings.

Jointed Plain Concrete Pavements (JPCP)

The key JPCP distress types considered in this study are:

- Roughness (IRI).

- Joint faulting.
- Transverse cracking.

If a designer can minimize these three (plus provide good PCC durability and other aspects), the success of the JPCP design will be maximized. Conversely, if any one of these key distress types exceeds the criteria in chapter 2, the pavement will perform poorly.

The key site conditions for JPCP that are essentially not controllable by the designer are as follows:

- Climate (moisture and temperature).
- Subgrade type (fine grained or coarse grained, k-value).
- Traffic loadings.

The key design and construction features identified in this study are as follows in the general order of impact on performance (however, a poor selection of any one of these features could lead to rapid failure of a JPCP):

- Initial constructed smoothness.
- Joint load transfer (use and diameter of dowels).
- Subdrainage.
- Base type and modulus.
- Slab widening.
- Joint spacing.
- Slab thickness.
- Slab modulus/strength.

The findings of this study along with previous findings show the following with regard to how a designer can maximize the possibility of good performance and minimize the possibility of poor performance of JPCP.

First Step—Fully Consider Site Conditions. The most critical site conditions were found to be a wet-freeze climate, fine grained subgrade, and high traffic (ESALs) over design life. Most favorable site conditions were found to be warm and dry climate, coarse grained subgrade, and lower ESALs over the design life.

The distresses affected by site conditions include joint faulting (and the subsequent roughness it creates) and slab transverse cracking.

> Climate: It is especially important to design JPCP to resist transverse joint faulting in wet-freeze climates (doweled joints seem to minimize the adverse

effect of climate on faulting) and transverse cracking in the dryer climates (western United States) where high thermal gradients exist (shorter joint spacing minimizes the adverse effect of climate).

Subgrade: Fine-grained soil subgrades showed increased joint faulting as compared to coarse-grained subgrades probably through increased erosion and reduced bottom seepage of water. Thus, placement of a thick layer of granular material beneath the base course may contribute to improved drainage and reduced faulting, especially for non-doweled pavements.

Traffic: Repeated heavy traffic loadings along with other design aspects lead to faulting and cracking. All faulting and transverse cracking prediction models include traffic loadings as an important variable. Designs should fully consider the level of traffic for a given site.

Second Step—Construct a Smooth Pavement. The results from this study clearly show the value of achieving a very smooth pavement right from the beginning. The initial smoothness appears to remain over many years (as long as the pavement does not fault or crack excessively of course). The experienced engineers provided the following levels of IRI as a guide:

Good IRI	< 0.631 m/km
Normal IRI	0.631 to 1.262 m/km
Poor IRI	> 1.262 m/km

One design feature that can help the contractor achieve the goal of building an initially smooth pavement is to provide a good foundation on which to build. The LTPP data showed that a good working platform (specifically stabilized base and granular subgrade or embankment) contributed to a smoother pavement.

The rate of deterioration of JPCP over time appeared to be highly dependent on the rating of good, normal, or poor. The following mean rates of deterioration (the slope of the IRI versus time plot) were determined:

Performance Rating	**Mean Rate of IRI Increase**
Good	0.016 m/km/year
Normal	0.040 m/km/year
Poor	0.070 m/km/year

Third Step—Minimize Future Roughness Through Selection of Design Features. Given a JPCP that has been constructed very smooth, there are several design features associated with keeping it smooth. Obviously, this means minimizing joint faulting and slab cracking among other modes of failure. The following lists the findings relative to design features found to be significant to limiting the roughness, faulting, and cracking for JPCP.

- **Joint load transfer**— Faulting correlates strongly with IRI and user ratings of ride quality and is the number one distress affecting JPCP roughness. Both the use of dowels and the diameter of dowels is important in minimizing faulting. While dowels are not required in all situations (such as low traffic level), the use of dowels clearly had a strong impact on controlling joint faulting. In critical climates, either wet or freeze climates, the use of dowels appeared to negate the effects of cold temperatures and increased moisture that lead to erosion, pumping of fines, opening of joints, and so on.

  The diameter of the dowel is also very important. The largest diameter dowel in the LTPP data base is 38 mm and faulting was low for these pavement sections (see figure 69). Smaller dowels showed increased joint faulting. Prediction models are available to help determine the need for dowels and the appropriate diameter to limit faulting for specific site conditions and design features.[1,2]

- **Subdrainage**— The effect of subdrainage was critical on both IRI and on joint faulting. JPCP with higher AASHTO drainage coefficients had lower IRI. Therefore, the use of a permeable base, edge drains, and a granular embankment or layer beneath the base course will lead to more rapid drainage and improved performance (lower faulting and IRI over time/traffic). This was particularly true for non-doweled JPCP.

- **Base type and modulus**— The effect of base type and base elastic modulus is complex. JPCP with a stabilized base performed more smoothly than an untreated aggregate base in general. JPCP with asphalt stabilized base and lean concrete base had significantly lower IRI when compared against other bases. The same was not true for cement-treated bases. On the other hand, JPCP sections with granular bases and asphalt stabilized bases had a significantly lower percentage of cracked sections than JPCP with cement-treated or lean concrete bases. This cracking did not significantly reflect itself in increased IRI however.

- **Slab widening**— Widened (by 0.6 m) PCC slabs (as opposed to conventional width slabs) improve faulting performance of concrete pavements by reducing the critical deflections at the corner of the slab from heavy truck axles. JPCP

sections with widened lanes did not show any transverse cracking. The result of widening effectively moves the critical corner further away from the wheel path, thereby reducing the frequency of traffic encroachment to the pavement edge. A previous field study showed that a widened slab reduced the amount of faulting by approximately 50 percent for both doweled and non-doweled joints.[2] The LTPP data base contains information on only a few JPCP sections with widened slabs. The mean faulting for non-doweled sections not older than 10 years both with and without widened slab shows about 50 percent less faulting with a widened slab. There was no difference between doweled widened slab sections and doweled conventional slab width JPCP. Considerable results will be obtained from the SPS-2 sections where direct comparison between conventional and widened slabs will be made.

- **Joint spacing**— Previous studies have shown that increased JPCP joint spacing increases transverse cracking greatly and to a lesser extent, joint faulting.[1,2] Analyses conducted herein were not detailed enough to show an effect. To really analyze the effect of joint spacing for JPCP, data must be obtained from each LTPP section where random joint spacing exists on the amount of cracking in each slab for each joint spacing that exists.

- **Slab thickness**— This primary design feature did not show much significance in the general data analysis. However, slab thickness is included in all previous mechanistic cracking models and has been shown to be very significant to control transverse cracking from other field tests.[1,2] Thickness is included in some faulting models, but its effect is not large. Thus, it is not possible to solve a poor joint load transfer problem with increased slab thickness. The early LTPP analysis IRI model includes JPCP slab thickness. Considerable results will be obtained from the SPS-2 studies related to slab thickness.

- **Slab modulus/strength**— Some conflicting results were obtained with regard to these design features in that some analyses show that increased modulus or strength result in increased roughness, but others show the opposite (the cause may be related to the level of initial roughness achieved during construction that is related to the workability of the concrete mix). The main distress affected by concrete strength is transverse cracking. All cracking prediction models include concrete strength and modulus and show that increasing strength is beneficial to a point in reducing transverse cracking of JPCP.

Jointed Reinforced Concrete Pavement (JRCP)

The only JRCP distress type considered in this study was roughness (IRI). Other key distress types include transverse joint faulting and transverse crack deterioration.

Although they were not included in this analysis, the data are available in the LTPP data base for future study. If a designer can minimize these distresses (plus provide good PCC durability and other aspects), the success of the JRCP design will be maximized. Conversely, if any one of these key distress types exceeds the criteria in chapter 2, the pavement will perform poorly.

The key site conditions for JRCP that are essentially not controllable by the designer are as follows:

- Climate (moisture and temperature).
- Subgrade type (fine grained or coarse grained, k-value).
- Traffic loadings.

The key design and construction features identified in this study are as follows in the general order of impact on roughness (however, a poor selection of anyone of these features could lead to rapid failure of a JRCP):

- Initial constructed smoothness.
- Joint load transfer (proper diameter of dowels).
- Subdrainage.
- Joint spacing.
- Slab thickness.

The findings of this study along with previous findings show the following with regard to how a designer can maximize the possibility of good performance and minimize the possibility of poor performance of JRCP.

First Step—Fully Consider Site Conditions. Most critical site conditions were found to be a wet climate soft subgrade (as measured by backcalculated k-value), and high ESALs over design life.

Second Step—Construct a Smooth Pavement. The results from this study clearly show the value of achieving a very smooth pavement right from the beginning. The initial smoothness appears to remain over many years (as long as the pavement does not fault or crack excessively of course). The experienced engineers provided the following IRI levels as a guide:

Good IRI < 0.631 m/km
Normal IRI 0.631 to 1.262 m/km
Poor IRI > 1.262 m/km

One design feature that can help the contractor achieve the goal of building an initially smooth pavement is to provide a good foundation on which to build. The LTPP data showed that a good working platform (specifically stabilized base and granular subgrade or embankment) contributed to a smoother pavement.

The rate of deterioration of JRCP over time appeared to be highly dependent on the rating of good, normal, or poor. The following rates of deterioration (the slope of the IRI versus time plot) were determined:

Performance Rating	Mean Rate of IRI Increase
Good	0.019 m/km/year
Normal	0.041 m/km/year
Poor	0.038 m/km/year

Third Step—Minimize Future Roughness Through Selection of Design Features. Given a JRCP that has been constructed very smooth, there are several design features associated with keeping it smooth. Obviously, this means minimizing joint faulting and slab crack deterioration among other modes of failure. The following lists the findings relative to design features found to be significant to limit roughness for JRCP.

- **Joint load transfer**— All JRCP have dowels, but the dowels must be of adequate size to control faulting in JRCP. Faulting is the number one distress affecting JRCP roughness. The largest diameter dowel in the LTPP data base is 38 mm and faulting was low for these pavement sections (see figure 69). Smaller dowels showed increased joint faulting. Prediction models are available to help determine the appropriate diameter to limit faulting for different levels of traffic and other design variables.[1,2]

- **Subdrainage**— JRCP having a high AASHTO drainage factor had low IRI and low faulting. Thus, the effect of subdrainage was critical on both IRI and on joint faulting. Therefore, the use of a permeable base, edge drains, and a granular embankment or layer beneath the base course will lead to more rapid drainage and improved performance (lower faulting and IRI over time/traffic).

- **Slab thickness**— This primary design feature showed significance in the t-tests and the multivariate analysis. However, the results show that as slab thickness increased, so did the IRI. This is of course opposite to what physically should happen. The reason for this result was found to be that the initial IRI for thinner slabs (200 to 230 mm) averaged about 1.30 m/km and that for thicker slabs averaged about 1.58 m/km. The initial roughness strongly affects the future IRI over many years to come as this so clearly shows.

Continuously Reinforced Concrete Pavement (CRCP)

The key CRCP distress types considered in this study are:

- Roughness.
- Localized failures.

If a designer can minimize these two (plus provide good PCC durability and other aspects) the success of the CRCP design will be maximized. Conversely, if any one of these key distress types exceeds the criteria in chapter 2, the pavement will perform poorly.

The key site conditions for CRCP that are essentially not controllable by the designer are as follows:

- Climate (moisture and temperature).
- Subgrade type (fine grained or coarse grained, k-value).
- Traffic loadings.

The key design and construction features identified in this study are as follows in the general order of impact on performance (however, a poor selection of any one of these features could lead to rapid failure of a CRCP):

- Initial constructed smoothness.
- Steel percentage.
- Subdrainage.
- Slab strength.
- Texture of surface.
- Base type.

The findings of this study along with previous findings show the following with regard to how a designer can maximize the possibility of good performance and minimize the possibility of poor performance of CRCP.

First Step—Fully Consider Site Conditions. The results showed that climate variables did not significantly effect the roughness but did increase localized failures in cold and wet regions.

Second Step—Construct a Smooth Pavement. The results from this study clearly show the value of achieving a very smooth CRCP right from the beginning. The initial smoothness appears to remain over many years for CRCP (as long as the pavement

does not show localized failures excessively of course). The experienced engineers provided the following IRI levels as a guide:

Good IRI < 0.631 m/km
Normal IRI 0.631 to 1.262 m/km
Poor IRI > 1.262 m/km

One design feature that can help the contractor achieve the goal of building an initially smooth pavement is to provide a good foundation on which to build. The LTPP data showed that a good working platform (specifically stabilized base and granular subgrade or embankment) contributed to a smoother pavement.

The rate of deterioration of CRCP over time appeared to be highly dependent on the rating of good, normal, or poor. The following rates of deterioration (the slope of the IRI versus time plot) were determined:

Performance Rating	**Mean Rate of IRI Increase**
Good	0.011 m/km/year
Normal/Poor	0.031 m/km/year

Third Step—Minimize Future Roughness Through Selection of Design Features. Given a CRCP that has been constructed very smooth, there are several design features associated with keeping it smooth. Obviously, this means minimizing localized failures among other modes of failure. The following lists the findings relative to design features found to be significant to limit roughness and localized failures for CRCP.

- **Steel content**— Both the Illinois predictive model for localized failures and the model from the LTPP early analysis for IRI showed that percent steel was a very significant design feature. The greater the percentage of steel, the lower the IRI and the fewer localized failures occurred. The steel content ranged from 0.51 to 0.75 percent in the LTPP data base, and the Illinois data included sections from 0.30 to 1.0 percent steel.

- **Subdrainage**— The effect of subdrainage was critical for IRI of CRCP. CRCP with higher AASHTO drainage coefficients had lower IRI. Therefore, the use of edge drains and a granular embankment or layer beneath the base course will lead to more rapid drainage and improved performance (lower IRI over time/traffic). There were no CRCP sections with a permeable base.

- **Base type**— CRCP with cement-treated bases performed with fewer localized failures than with asphalt-stabilized or untreated granular bases. The Illinois model shows that an asphalt- or cement-stabilized base has fewer localized failures than untreated aggregate bases.

- **Slab texture**— CRCP finished with a tined texture on average have higher IRI's.

- **Slab modulus/strength**— The multivariate analysis shows that the higher the flexural strength of the CRCP, the greater the IRI. This relationship does not make sense from a mechanistic viewpoint. Further analysis is needed to determine the causes of this result. This result should not be considered for implementation until further study is conducted.

CHAPTER 11. SUMMARY AND RECOMMENDATIONS FOR CONTINUED RESEARCH

The analyses reported in this document were intended to study the LTPP data and report what could be obtained on an expedited basis and reported to the highway community. This study also considered previous LTPP and other field studies.

This study used available LTPP data and results from other reports to focus on site conditions and design/construction features of PCC pavements that have a significant impact on the most common distress types. The next logical step will be to establish the relative significance of these variables to the occurrence of these distresses, so that designers can make more informed decisions. Important decisions for PCC pavements relate to the level of initial smoothness required, subdrainage design and when it should be used, when should dowel bars be used and what diameter, what type of base course, what joint spacing, and what amount of reinforcement for JRCP and CRCP.

These decisions will need to be made in terms of their impacts on the various distress types including roughness, life-cycle costs, and in consideration of the climate in which the pavement must function. What is the impact of the expected traffic? What impacts do the climatic characteristics and subgrade have on the various distress types to be considered? How do these variables interact? These are questions that are usually answered by conducting sensitivity analyses with comprehensive prediction models.

Other studies of the data are expected to contribute to identification and understanding of the various mechanisms that lead to pavement deterioration. The mechanisms will include those leading to joint faulting, transverse cracking, localized failures, and roughness. This study clearly showed the difficulties involved in empirically analyzing the data and points to the use of mechanistic concepts combined with empirical data to obtain improved comprehensive prediction models for key distress types.

After detailed studies of the data and the mechanisms involved in formation of distress, component models for individual distresses will need to be selected and/or developed. These component models can then be improved and revised through iterative testing against the measured data from LTPP. The long-term objective will be the integration of the distress models into an integrated model to be used for distress predictions, design, and alternative and strategy selection.

REFERENCES

1. Simpson, et al. (1993). *Sensitivity Analyses for Selected Pavement Distresses.* SHRP-P-393. Washington, DC: National Research Council.

2. Yu, T. H., M. I. Darter, K. D. Smith, J. Jiang, and L. Khazanovich. (1996). *Performance of Concrete Pavements: Volume III-Improving Concrete Pavement Performance,* FHWA-RD-95-111, Federal Highway Administration, 1996.

3. L. Titus-Glover, Owusu-Antwi, E., and T.E. Hoerner. (1997). *Long-Term Pavement Performance Data Analysis. Volume II: Design and Construction of PCC Pavements—Improved PCC Performance Models.* Washington, DC: Federal Highway Administration.

4. Smith, K.L., et al. (1997). *Smoothness Specifications for Pavements.* Washington, DC: National Cooperative Highway Research Program.

5. Al-Omari, B. and M. I. Darter, (1995). "Effect of Pavement Deterioration Types on IRI and Rehabilitation," *Transportation Research Record No. 1505.* Washington, DC: Transportation Research Board.

6. Sayers, M.W., T.D. Gillespie, and C.A.V. Queiroz. (1986). *The International Road Roughness Experiment: Establishing Correlation and a Calibration Standard for Measurement.* Technical Paper 45. Washington, DC: The World Bank.

7. Darter, M.I., J.M. Becker, M.B. Snyder, and R.E. Smith. (1985). *Portland Cement Concrete Pavement Evaluation System - COPES. NCHRP Report No. 277.* Washington, DC: Transportation Research Board.

8. Wu, C.L, J.W. Mack, P.A. Okamota, and R.G. Packard. (1993). *Prediction of Faulting of Joints in Concrete Pavements. Volume 2, Proceedings of the International Conference on Concrete Pavement Design,* Purdue University, Lafayette, IN.

9. Packard, R.G. (1977). "Design Considerations for Control of Joint Faulting of Undoweled Pavements," *Proceedings of the International Conference on Concrete Pavement Design,* Purdue University, Lafayette, IN.

10. Lee, Y.H., and M.I. Darter. (1994). "Development of Pavement Prediction Models," *Project IHR-529,* Illinois Cooperative Highway Research Program, University of Illinois and Illinois Department of Transportation.

11. LaCoursiere, S.A., M.I. Darter, and S.A. Smiley. (1978). *Performance of Continuously Reinforced Concrete Pavement in Illinois*, Research Report 901-1, Illinois Cooperative Research Program, University of Illinois.

12. Ma, J., and B.F. McCullough. (1977). *CRCP-2, An Improved Computer Program for the Analysis of Continuously Reinforced Concrete Pavements*, Research Report 177-9, Cooperative Highway Research Program, Texas State Department of Highways and Public Transportation and U.S. Department of Transportation, Federal Highway Administration, prepared by the Center for Highway Research, University of Texas at Austin.

13. Zollinger, D.G., and E.J. Berenberg (1988). *Thickness Design Procedure for Continuously Reinforced Concrete Pavements*, Project IHR-518-3, Illnois Cooperative Highway Research Program, University of Illinois and Illinois Department of Transportation.

14. Zollinger, D.G. (1989). "Investigation of Punchouts Distress of Continuously Reinforced Concrete Pavement," Ph.D. Thesis, University of Illinois.

15. Larson and S.D. Tayabji (1995). "Performance of Continuously Reinforced Concrete Pavements," *Proceedings*, Third International Workshop on the Design and Evaluation of Concrete Pavements (September 29-30, Krumbach, Austria), pp. 425-438.

16. Owusu-Antwi, E. et al, "Development And Calibration Of Mechanistic-Empirical Distress Models For Cost Allocation," Draft Final Report, Federal Highway Administration, 1997.

17. AASHTO *Guide for Design of Pavement Structures*, American Association of Highway and Transportation Officials, Washington, D.C., 1993.